UNIVERSITÀ DEGLI STUDI DI SALERNO

DIFARMA

UNIVERSITÀ DEGLI STUDI DI SALERNO

Dipartimento di Farmacia

PhD Program

in **Drug Discovery and Development**

XXXIII Cycle — Academic Year 2020/2021

PhD Thesis in

The role of mesoglycan in wound healing

Candidate

Emanuela Pessolano

Supervisor

Prof. *Antonello Petrella*

PhD Program Coordinator: Prof. Dr. *Gianluca Sbardella*

Preface

My Ph.D. three years course in Drug Discovery and Development at the Department of Pharmacy, University of Salerno, started in November 2017 under the supervision of Professor Antonello Petrella.

My research project has focused on studying the positive effects on wound healing promoted by mesoglycan, a natural mixture of glycosaminoglycans commonly used in vascular diseases thanks to its fibrinolytic action. My research activity has focused on achieving three main objectives:

1. Individuation of the *in vitro* molecular mechanism of mesoglycan and evaluation of its effects *in vivo*.
2. Analysis of the role of ANXA1 in the wound repair and its evaluation in association with mesoglycan.
3. Extracellular vesicles-mediated cell-cell communication in wound repair and study of the pro-angiogenic effects of mesoglycan in the healing process.

In particular, I did the third aim during the year spent at the William Harvey Research Institute, Queen Mary University of London, London, under the supervision of Professor Mauro Perretti.

My work has been preciously enriched by collaborations, in particular, the one with the laboratory of Professor De Marco, Department of Industrial Engineering of the University of Salerno, which led to the creation of two new medical devices respectively for the immediate and prolonged release of mesoglycan at the site of tissue damage.

List of publications related to the scientific activity performed during the three years Ph.D. course in Drug Discovery and Development.

- Belvedere R, Saggese P, Pessolano E, Memoli D, Bizzarro V, Rizzo F, Parente L, Weisz A, Petrella A. miR-196a Is Able to Restore the Aggressive Phenotype of Annexin A1 Knock-Out in Pancreatic Cancer Cells by CRISPR/Cas9 Genome Editing. Int J Mol Sci. 2018 Jul 6;19(7):1967
- Pessolano E, Belvedere R, Bizzarro V, Franco P, Marco I, Porta A, Tosco A, Parente L, Perretti M, Petrella A. Annexin A1 May Induce Pancreatic Cancer Progression as a Key Player of Extracellular Vesicles Effects as Evidenced in the In Vitro MIA PaCa-2 Model System. Int J Mol Sci. 2018 Dec 4;19(12):3878.
- Bizzarro V, Belvedere R, Pessolano E, Parente L, Petrella F, Perretti M, Petrella A. Mesoglycan induces keratinocyte activation by triggering syndecan-4 pathway and the formation of the annexin A1/S100A11 complex. J Cell Physiol. 2019 Nov;234(11):20174-20192.
- Pessolano E, Belvedere R, Bizzarro V, Franco P, Marco I, Petrella F, Porta A, Tosco A, Parente L, Perretti M, Petrella A. Annexin A1 Contained in Extracellular Vesicles Promotes the Activation of Keratinocytes by Mesoglycan Effects: An Autocrine Loop Through FPRs. Cells. 2019 Jul 19;8(7):753.
- Franco P, Pessolano E, Belvedere R, Petrella A, De Marco I Supercritical impregnation of mesoglycan into calcium alginate aerogel for wound healing The Journal of Supercritical Fluids Volume 157, 1 March 2020, 104711
- Franco P, Belvedere R, Pessolano E, Liparoti S, Pantani R, Petrella A, De Marco I. PCL/Mesoglycan Devices Obtained by Supercritical Foaming and Impregnation. Pharmaceutics. 2019 Nov 26;11(12):631.
- Belvedere R, Pessolano E, Porta A, Tosco A, Parente L, Petrella F, Perretti M, Petrella A. Mesoglycan induces the secretion of microvesicles by keratinocytes able to activate human fibroblasts and endothelial cells: A novel mechanism in skin wound healing. Eur J Pharmacol. 2020 Feb 15; 869:172894.
- Petrella, F.; Belvedere, R.; Labbro, V.; Apicella, A.; Bizzarro, V.; Pessolano, E.; Parente, L.; Petrella, A. A new pharmaceutical device containing mesoglycan modulates fibroblasts function in vivo. Pharmacologyonline. 2020, Vol. 1. Pag.20-30
- Belvedere R, Novizio N, Pessolano E, Tosco A, Eletto D, Porta A, Campiglia P, Perretti M, Filippelli A, Petrella A. Heparan sulfate binds the extracellular Annexin A1 and blocks its effects on pancreatic cancer cells. Biochem Pharmacol. 2020 Dec; 182:114252

- Belvedere R, Morretta E, Pessolano E, Novizio N, Tosco A, Porta A, Whiteford J, Perretti M, Filippelli A, Monti MC, Petrella A. Mesoglycan exerts its fibrinolytic effect through the activation of annexin A2. J Cell Physiol. 2020 Dec 7.
- Novizio N, Belvedere R, Pessolano E, Tosco A, Porta A, Perretti M, Campiglia P, Filippelli A, Petrella A. Annexin A1 Released in Extracellular Vesicles by Pancreatic Cancer Cells Activates Components of the Tumor Microenvironment, through Interaction with the Formyl-Peptide Receptors. Cells. 2020 Dec 18;9(12):2719.
- Davan-Wetton CSA, Pessolano E, Perretti M, Montero-Melendez T. Senescence under appraisal: hopes and challenges revisited. Cell Mol Life Sci. 2021 Jan 13.
- Pessolano E, Belvedere R, Novizio N, Filippelli A, Perretti M, Whiteford J, Petrella A. Mesoglycan connects Syndecan-4 and VEGFR2 through Annexin A1 and formyl peptide receptors to promote angiogenesis (submitted)
- Belvedere R, Pessolano E, Novizio N, Tosco A, Eletto D, Porta A, Filippelli A, Petrella F, Petrella A The promising pro-healing role of the association of mesoglycan and lactoferrin on skin lesions (submitted)

• Patent: Composition for the treatment of skin lesions WO/2020/121179, 102018000010968 University of Salerno

Table of contents

Abstract

Mesoglycan is a mixture of glycosaminoglycans able to enhance some fundamental processes in wounds repair. Particularly, it promotes the re-epithelialization through the action on keratinocytes and fibroblasts and supports angiogenesis. The mechanism of action by which the mesoglycan acts in this system is not still clear.

For this reason, one of the aims of my PhD project has been to study the molecular mechanism by which this mixture of glycosaminoglycans promotes tissue regeneration. The obtained *in vitro* data suggested that mesoglycan induced keratinocyte migration and differentiation, two important process for the correct repair of skin injury, and that some of these effects are carried out through the activation of syndecan-4/PKCα (SDC4/PKCα) pathway.

Another protein involved in a wide range of physiopathological process, including cell motility and differentiation, is Annexin A1 (ANXA1). The *in vitro* data obtained suggested that mesoglycan is able to induce the formation of ANXA1/S100A11 complex at the inner surface of the plasma membrane and that this event is mediated by SDC4 pathway. Moreover, the results showed a role for ANXA1 in mesoglycan-induced keratinocyte activation.
It is known that SDC4 participates to the formation and secretion of microvesicles (EVs) which may contribute to wound healing. ANXA1 contained in microvesicles was able to promote keratinocytes motility and differentiation by acting on Formyl Peptide Receptors (FPRs) in autocrine manner. Thus, the extracellular form of ANXA1 may be considered as a link to intensify the effects of mesoglycan. These data contribute to the identification of an interesting autocrine loop ANXA1/EVs/FPRs in human keratinocytes, induced by mesoglycan.
Furthermore, we found that EVs secreted from keratinocytes treated with mesoglycan promoted migration and invasion on fibroblasts and endothelial cells, acquiring a mesenchymal phenotype. In presence of this kind of EVs the angiogenesis appeared strongly enhanced, suggesting that EVs deriving from keratinocytes treated with the GAGs mixture, trigger a paracrine positive feedback able to further amplify the effects of mesoglycan.

The third year of the PhD program, I had the opportunity to work at the William Harvey Research Institute in London, where we have used endothelial cells isolated from Wild Type (WT) and Syndecan-4 null mice (*Sdc4*-/-) C57BL/6 mice. We demonstrate that mesoglycan promotes cell motility and *in vitro* angiogenesis acting on the co-receptor SDC4. Additionally, we characterized EVs released by HUVEC cells and assessed their effect on angiogenesis. Particularly, we focused on

ANXA1 containing EVs, since they may contribute to tube formation via interactions with FPRs and their bond stimulates the release of vascular endothelial growth factor (VEGFA) that interacts with vascular endothelial receptor-2 (VEGFR2) and activates the pathway enhancing cell motility in autocrine manner. Thus, we have shown that mesoglycan exerts its pro-angiogenic effects in the healing process triggering the activation of the three interconnected molecular axis: mesoglycan-SDC4, EVs-ANXA1-FPRs and VEGFA-VEGFR2.

Furthermore, we observed the mesoglycan ability in cell recruitment both through *in vivo* observations on C57BL/6 mice and biopsies harvested from patients affected by pressure ulcers.

Finally, in order to create a medical device that guarantees greater comfort for the patient, in collaboration with the Department of Industrial Engineering (DIIN) of University of Salerno (UNISA), we impregnated the mesoglycan on a polycaprolactone foam, obtaining a prolonged release of the drug, favouring patient compliance.

Thus, these results could encourage to consider this mixture of glycosaminoglycans as a useful pro-healing drug in skin wound care.

Abbreviations

ANXA1: AnnexinA1

b-FGF: basic fibroblast growth factor

CAA: calcium alginate

CO_2: carbon dioxide

COL1A: collagen A1

CS: Chondroitin sulfate

DLS: Dynamic Light Scattering

DS: Dermatan sulfate

ECM: extracellular matrix

EDS: EVs-depleted supernatant

EMT: mesenchymal-epithelial transition

ERK: Extracellular-signal-regulated kinases

ERM: ezrin-radixin-moesin

ESCRT: endosomal sorting complex needed for the transport

EVs: extracellular vesicles

FAK: Focal adhesion kinase

FAP1α: Fibroblast Activated Protein 1

FE-SEM: Field Emission-Scanning Electron Microscope

FGF: Fibroblast growth factor

FPR: Met-Leu-Phe formylated peptide receptor

Gal: galactose

GalNAc: N-acetyl-β-D-galactosamine

Glc: glucose

GlcA: β-D-glucuronic acid

GlcN: glucosamine

GlcNAc: N-acetyl-glucosamine

HA: hyaluronic acid

HIF1: hypoxia inducible factor-1

Hp: Heparin

HS: Heparan sulphate

HSP: Heat shock proteins

HSPG: Heparin sulfate proteoglycans

IdoA: α-L-iduronic acid

IHC: Immunohistochemical

ILVs: intraluminal vesicles

KS: Keratan sulphate

MAPK: mitogen-activated protein kinase

MHC class II: histocompatibility complex class II

MMP: metalloproteinases

MMPs: matrix metalloproteinases

MVB: multivesicular body

MVs: Microvesicles

NO: nitric oxide

p38MAPK: p38 mitogen-activated protein kinases

PCL: polycaprolactone

PDGF: platelet derived growth factor

p-FAK: Focal adhesion kinase phosphorylated

PG: proteoglycans

p-HSP27: heat shock protein 27 phosphorylated

PIP2: phosphatidylinositol 4,5 bisphosphate

PKCα: protein kinase Cα

PLA2: phospholipase A2

$scCO_2$: supercritical carbon dioxide

SDC1: syndecan-1

SDC2: syndecan-2

SDC3: syndecan-3

SDC4: syndecan-4

siRNA: small interfering RNA

SS: conditioned medium

TNF-a: tumour necrosis factor alpha

TSG101: tumour-susceptibility protein

UA: uronic acid

VE-cadherin: Vascular Endothelial cadherin

VEGF: vascular endothelial growth factor

αSMA: α-smooth muscle actin

1. Structure and function of the skin

The skin provides a life-protective barrier between the body and the external environment against physical damage, pathogens, fluid loss, and has immune-neuroendocrine functions that contribute to the upkeep of body homeostasis [1].

The structure of the skin is composed of two layers: the epidermis and the dermis.
The epidermis hosts resident cells such as keratinocytes, melanocytes, dendritic cells, Langerhans cells and other immune cells, sensory axons and epidermal-dermal basement membrane [2]. The dermis includes skin appendages, mast cells, fibroblasts, antigen presenting dermal cells, resident and circulating immune cells [3]. In addition, the dermal layer contains extracellular matrix (ECM) complex that gives support for intercellular connections, cell movement, and regulate the cytokines and growth factors.

The blood circulation in the skin comprises parallel arterial-venous temperature-regulated and is controlled by tonic adrenergic sympathetic vasoconstrictors and vasodilator nerves, which originate from the subepidermal capillary network, which supplies oxygen and nutrients to the epidermis and remove and waste CO_2 [4].

Is fundamental to maintain the integrity of our biggest organ, the skin, and for this reason, losing its entirety represents a relevant clinical problem and their eventual complications may feature cause of pathological states, sometimes even fatal. A wound is defined as an interruption within the continuity of the skin or mucosa, due to damage or destruction of normal anatomical structures and their functions. The damages can range from a simple injury of the skin's epithelial integrity to a deep injury that extends it to the subcutaneous tissue with damage to other structures: tendons, muscles, vessels, nerves, resulting from physical or thermal damage. Wounds can be classified according to several criteria, such as appearance, duration of repair process, and affected area. Depending on the appearance of the wounds, they may be necrotic, sloughy, granulated, epithelial, or infected. Necrotic wounds comprise an accumulation of dead cells, tissue, and cellular debris. Sloughy wounds are characterised by wet and rehydrated necrotic tissue. Granulating wounds contain abundant granulation tissue with the production of excessive exudate. Instead, the new epidermis formation characterises the epithelial wounds. Finally, infected and malodorous wounds are typical of contamination with microorganisms, inflammation and pus formation [5].

Depending on the duration and nature of the skin lesion, the wounds can be divided into acute and chronic [6], [7]. Acute wounds are skin injuries that occur suddenly due to accidents or surgical procedures. It usually heals within a predictable time frame of 8-12 weeks, depending on the size, depth, and degree of damage of the skin epidermis and dermis layer [7], [8]. On the other hand,

chronic wounds cannot progress during the normal healing phase, nor can they be repaired in an orderly and timely manner. Chronic wounds are usually caused by bedsore ulcers, leg ulcers and burns [7]. Often chronic wounds begin with minor traumatic injuries in patient underlying pathologies (such as diabetes-induced and non-diabetic neuropathy). Indeed, penetrating injuries, insect bites or even simple abrasions of dry skin can that usually heal within a few days/weeks, leads these patients with to wound that cannot heal [9].

The Wound Healing Association classifies chronic wounds into 4 major categories: pressure ulcers, diabetic foot ulcers, venous ulcers and ulcers with insufficient arterial blood supply. These wounds cannot progress through timely repair, without restoring anatomical and functional results. Some common characteristics shared among the chronic injury include long-term or excessive inflammation, persistent infection, the formation of a biofilm of resistant microorganisms, and the inability of dermal and/or epidermal cells to respond to repairing stimuli [10]. Overall, these pathophysiological phenomena prevent these wounds from healing. However, the underlying pathology varies between different types of chronic wounds.

1.1 Physiologic wound healing process

Skin wound healing is an essential, natural, and physiological reaction to tissue injury. It is a dynamic and interactive process that begins at the moment of wounding and involves the synergy of many cell types, including their products as soluble mediators and the production of the ECM [11]. Wound repair is not a simple linear process, but it has been organised into three sequential and overlapping phases over time: the haemostasis and inflammatory phase, the proliferative phase, and therefore the remodelling phase.

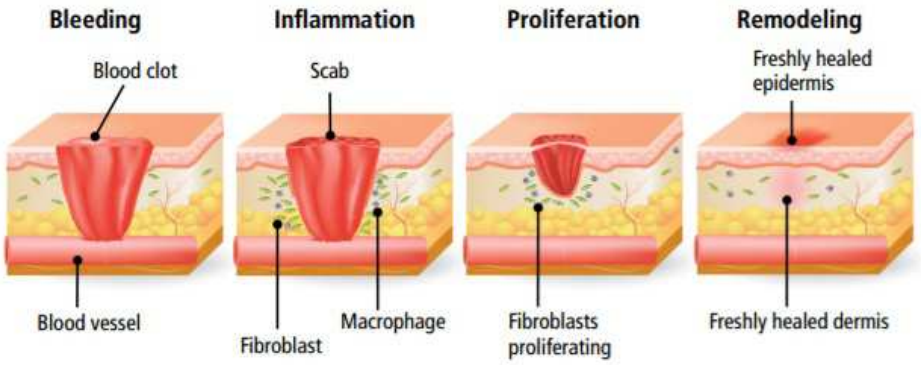

Fig.1.1: Stages of wound healing

The inflammatory stage starts with haemostasis. This first event sets up in the first few seconds after the injury and lasts about 1 hour. Then, neutrophils are quickly recruited into the injured tissue within the first 24 hours, and after declined backward in the following week. The gradual infiltration

of inflammatory monocyte macrophages into the wound starts on the second day after the trauma and continued to increase. It reaches the greatest during the proliferative phase and decline in the next two weeks. On the 4th day after the injury, circulating lymphocytes migrate to the skin, their presence persists for two weeks, and then declined. The last phase begins the second week after the injury and includes remodelling the tissue formed during the proliferation phase and restore skin integrity. The ultimate stage may last several months [8]. The degree of any single process involved in the repair process is variable and depends on the characteristics of the wound.

1.2 Inflammatory phase

Immediately after the skin injury, when the structural integrity is damaged, the response signal, which is both chemical and mechanical, begins. Damaged and stressed cells at the edge of the wound activate multiple "stress signal" pathways in a few minutes to respond to the injury. One of the earliest responses is promoted from the damage to local blood vessels, because is necessary to stop local haemorrhage immediately. The **platelets** begin a haemostatic reaction trough the adhesion to damaged blood vessels and give rise to a blood-clotting cascade that prevents excessive bleeding and provides provisional protection for the wounded area. In normal physiological conditions, platelets do not interact with the endothelial cell surface because the glycocalyx barrier prevents their contact. Vascular injury exposes basement membrane proteins and large molecules of the ECM. The receptors on the surface of the platelet membrane join with the collagen to activate the platelets and produce thrombin, catalysing the initiation of the coagulation cascade [12]. Moreover, platelet integrin, which binds to fibrinogen, is a source of fibrin [13]. Fibrin accumulates with interstitial collagen, capturing neutrophils, red blood cells, and other blood components that form clots [14]. The formed blood clots can also serve as a temporary matrix to which growth factors, can bind and allow cells to migrate [15]. The temporary ECM is composed by fibrin monomers that form fibrin fibrils, which are stabilised by intermolecular connections through the action of factor XIIIa. Subsequently, this initial matrix is used by fibroblasts and endothelial cells to migrate and promote the secretion of the ECM protomyofibroblast-mediated [16]. Then, the ECM is remodelled by metalloproteinases released by fibroblasts and macrophages to support the migration of neutrophils and monocytes [17]. Moreover, activated platelets are themselves an important source of growth factors including platelet derived growth factor (PDGF), basic fibroblast growth factor (b-FGF), transforming growth factor-β (TGFβ) and vascular endothelial growth factor (VEGF) that interact with endothelial cells, neutrophils monocytes, dendritic cells, B and T cells, and natural killer cells, promoting neutrophil activation, pathogen detection, trapping, and modulation of the innate and adaptive immune responses [18], [19]. It is known that the release of this growth factors promotes various aspects of the repair process, including angiogenesis, inflammation, and migration of keratinocytes and fibroblasts. The release of

TGF-β from the degranulation of alpha granules of the platelets acts as an important chemoattractant for the recruitment of various types of immune cells, such as white blood cells, neutrophils and macrophages to the site of damage [13].

The inflammatory response to the wound continues with the passive loss of circulating **leukocytes** from the damaged blood vessels in the injured area. Neutrophils are activated and recruited in a wound in minutes and they are involved in this phase [20]. Neutrophils follow platelets as the main effector cells at the beginning of the inflammatory phase and declines 4 days later. Their recruitment is initiated by growth factors and chemokines released by activated platelets in the blood clot [21]. Neutrophils exploit integrins present on their cells surface such as CD11a/CD18 (LFA-1); CD11b/CD18 (MAC-1); CD11c/CD18 (gp150, 95); CD11d/CD18 [22]. Moreover, these cells can bind the endothelium via adhesion receptors such as selectins/selectin ligands and integrins (endothelial P- and E-selectins and Intercellular Adhesion Molecule 1 and 2) to promote the leukocyte recruitment cascade: rolling, adhesion, crawling, and migration to the inflamed tissue [23]. Once in the lesion site, neutrophils activate a loop to produce neutrophil chemoattractants, which continue to recruit other neutrophils. The increased number of neutrophils in this stage is also in response to the activation of the complement system, platelet degranulation, and bacterial degradation products. In this way, the number of neutrophils in the wound increases exponentially in the first 24 hours up to two days later, becoming the most abundant cell line in the site of tissue damage [20]. They have a crucial role in the clean-up of the tissue and kill invading microorganisms via a variety of strategies. Indeed, neutrophils are known for expressing many pro-inflammatory cytokines and antimicrobial substances, including reactive oxygen species (ROS), cationic peptides, and proteases at the location of the lesion [7]. These cells can also influence many other aspects of wound healing, such as resolution of the fibrin clot and temporary ECM, promotion of angiogenesis, and re-epithelialization [24]. In addition, neutrophils take part in cell crosstalk through cell-to-cell contact trough cytokines, chemokines, and angiogenic factors activate resident hematopoietic cells, macrophages, dendritic cells, B cells, T cells, and natural killer cells regulating innate and adaptive immune responses [24].

Neutrophils and **monocytes** macrophages cooperate in time and space during the inflammatory phase [22]. Without stimuli, the neutrophil infiltration stops after a few days, and they are phagocytosed by macrophages, which are present at the wound site within 2 days after injury. Most macrophages it the injury area are recruited from the blood in response to chemotactic products, ECM protein fragments, TGF-β, protein 1 chemotactic for monocytes MCP-1 [25]. The migration of monocytes to the wound is also regulated by the interaction of α4β1 integrin with endothelial vascular cell adhesion molecule 1. After 48 hours from the beginning of the lesion, other monocytes from adjacent blood vessels infiltrated into the lesion area. In the blood coexist three subpopulations of

monocytes with different phenotypes in size, morphology, and transcriptional profiles: CD14++ CD16- or classical monocytes capable of migrating and entering tissues, CD14++ CD16+ or intermediate monocytes able to increase angiogenesis and antigen processing and presentation activities, and CD14+ CD16++ or non-classical monocytes that can patrol blood vessels through endothelial and tissue monitoring functions [26]. Circulating monocytes contribute to the formation of skin tissue monocyte-macrophage populations [27]. Monocytes release molecules as cytokines and chemokines [21] to recruit neutrophils into the wound. The intervention of neutrophils granule contents promotes the further recruitment of inflammatory monocytes that mature into macrophages. In this way, monocyte-macrophage becomes the most abundant population in the wound that can act as cells that present antigens and that aid neutrophils in phagocytosis. Then, when monocytes come out of blood vessels, they are activated and differentiated in **macrophages**, and gene expression changes significantly. Based on these differences, macrophages can be divided into classical activation (M1 pro-inflammatory) and alternative activation (M2 anti-inflammatory and pro-angiogenesis) [28]. After the wound is cleaned, neutrophils will cooperate with macrophages to coordinate the resolution of the inflammation stage [29]. This phase begins a day or two after neutrophils reach the inflamed tissue. The restoration of the homeostasis begins with neutrophils releasing microparticles containing pro-resolving protein as annexin A1 and lipid mediators. Apoptotic neutrophils expose phosphatidylserine on the surface, targeting them for efferocytosis. In this process, neutrophil microparticles transfer their molecules to macrophages, thereby improving the biosynthesis of lipoxins, resolvins, protectins, and maresins that are released into the wound tissue [30]. This efferocytosis of apoptotic neutrophils, stimulates the synthesis of miR-21, thereby promoting the anti-inflammatory phenotype of macrophages: M2 population [31]. This cell population release IL-10 and inhibit the production of IL-1β and TNF-α. Anti-inflammatory activity is also promoted by reducing the damage caused by the long-term activation of M1, which instead has a pro-inflammatory phenotype [32]. In addition to being antigen-presenting cells and phagocytes during wound repair, macrophages are also thought to synthesise many effective growth factors such as TGF-β, TGF-α, basic fibroblast growth factor, platelet-derived growth factor and vascular endothelial growth factor. These molecules can stimulate cell proliferation and synthesis of ECM molecules [28]. An orderly and well-controlled inflammatory phase is essential for proper wound repair and for continuing with remodelling [33].

1.3 Proliferative phase

The proliferative phase begins about 4-21 days after the initial injury, follows and overlaps with the inflammatory phase. The purpose of the proliferative phase is to reduce the area of injured tissue through contraction and fibrosis, thereby reestablishment of the epithelial surface to activate

keratinocytes and revascularization of the damaged area. This stage includes fibroplasia, re-epithelialisation and angiogenesis. All these processes are mediated through the effects of the local microenvironment, within the first 48 hours, and can be extended to the next 14 days. In the proliferation stage, as seen before, the macrophage M2 are the most abundant populations coordinating the interaction with fibroblasts, ECM keratinocyte and endothelial cells, [34].

Among the protagonist cells of the proliferative phase there are **fibroblasts**, recruited from the dermis on the edge of the wound. These cells, can respond to IL-1, tumour necrosis factor alpha (TNF-a), TGF-β1, PDGF, EGF, and FGF-2 released by platelets and macrophages in the previous stage [35] and then by the fibroblasts themselves. These soluble extracellular signals activate fibroblast proliferation and regulate the production of metalloproteinases and metalloproteinase inhibitors [34] because to migrate into a cross-linked fibrin clot is required the active proteolysis to permit the opening of a path for the migration. The term "proto-myofibroblast" distinguishes activated fibroblasts from quiescent fibroblasts, which do not have any contractile devices in most intact tissues. These fibroblasts, come from the deep layers of the reticular dermis, migrate into injured tissue and bind to the fibronectin of the blood clot through the receptors of the integrin superfamily. After the migration to the wound site, the migratory phenotype of the fibroblasts is replaced by the fibrotic phenotype. This change is characterized by a reduced expression of the α3β1 and α5β1 integrin. Instead, there is the exhibition of a greater expression of the α2β1 collagen receptors, a rich rough endoplasmic reticulum, and a Golgi apparatus full of collagen. Thus, the fibronectin-rich temporary matrix is gradually replaced by a collagen matrix [36]. Indeed, once in the wound, the fibroblasts start the collagen synthesis, and replace the fibrin temporary matrix stablished during the inflammatory phase [35]. The connective tissue matrix formed by fibroblasts is composed by fibronectin, HA, sulfated PGs and collagens and provides the migration of macrophages, new blood vessels and fibroblasts. During this initial stage of repair, the type III collagen is predominant component of this matrix, and it is eventually replaced by stronger type I collagen. The uninjured dermis contains about 80% type I collagen and 20% type III collagen. Instead, acute wound granulation tissue expresses about 40% of type III collagen. Once a large amount of collagen matrix is deposited in the wound, fibroblasts stop the production of collagen.

Fibroblasts also synthesize and release glycosaminoglycans and proteoglycans as a part of the new granulation tissue which is characteristic of the proliferative phase. The hyaluronic acid-proteoglycans complex binds water, thereby expanding the extracellular space, thereby promoting the migration of fibroblasts. Granulation tissue began to form about four days after the lesion and is named for the granular appearance.

Fibroblast density in acute wounds reaches a maximum 7 to 14 days after injury. At this point, an inhibition of cell-cell contact occurs, the intracellular polymeric chains of actin condense in stress fibers containing α-smooth muscle actin. These mature fibroblasts are named myofibroblasts and exhibit contractile properties, playing a major role in the contraction of the tissue. In the process of physiological wound healing, the contractile activity of myofibroblasts is terminated after the tissue is repaired. Then, the expression of α-SMA decreases and fibroblasts disappear due to apoptosis [37].

Reepithelialisation is a term used to describe new epithelium resurfacing skin wounds. It starts from 16-24 hours after injury and continues until the remodelling stage of wound repair for two to three weeks. This step is facilitated by the underlying contractile connective tissue which, shrinking, brings the edges of the wound closer together. Reepithelialisation develops from the surrounding wound edge to the centre, forming a continuum in the regeneration of differentiated epidermis. Reepithelialisation of human partial-thickness wounds mainly occurs from the stem / progenitor cells of the exocrine sweat gland and sebaceous gland units. In full-thickness wounds where these accessory structures are destroyed, re-epithelialization must originate from epidermal cells at the wound edge [38]. The purpose of this process is to restore the epidermis which is mainly composed of **keratinocytes** and is continuously renewed through the proliferation of stem cells and the differentiation of their progeny. These stem cells undergo terminal differentiation when they leave the basal layer and move up to the surface to die and fall off [39]. The formation of a temporary wound bed matrix formed from an insoluble protein exudate, as discussed above, is essential for the migration of epidermal keratinocytes, their proliferation is necessary for the advancement of the epithelial tongue, the stratification and differentiation of the new epithelium. Growth factors, chemokines and cytokines produced by cutaneous cells are responsible for the activation of keratinocytes which involves a phenotypic change in cytoskeletal network and cell surface receptors.

Activated keratinocytes proliferate more, migrate, change their cytoskeleton, and enhance the level of cell surface receptors. However, a day or two after the injury, keratinocytes must proliferate, to provide the cells needed to support re-epithelialization. The lack of adjacent cells at the edge of the wound can trigger epithelial cell proliferation and migration. In support of this thesis, studies have shown that epidermal desmosomes lose high adhesion and cadherin changes from E-cadherin to P-cadherin at the wound edge [40]. Intercellular communication provides a signal for advancing the epithelial layer, but the exact mechanism is unclear. One of the proposed mechanisms is the sliding model according to which the cells responsible for movement are mainly basal cells. They first release their attachment to the basal layer, migrate from both the margin until they meet and actively spread, while the cells in the upper layer are passively carried. Other proposed method is a model in which the superior basal cells dedifferentiate and participate in the reconstruction of new human epithelial

cells together with the basal cells. This second method is supported by the fact that in response to the injury, the upper basal keratinocytes undergo adaptive changes, such as inducing K16, down-regulating K10 and up-regulating K14 obtaining a migration phenotype [41].

Regardless of the mechanism, keratinocytes to migrate must undergo the mesenchymal-epithelial transition (EMT), characterized by the phenotypic transformation.

Keratinocytes in the healed wounds polymerize the cytoskeletal actin fibers and form new adhesion complexes. Cell surface receptor integrins (integrin αvβ5, αvβ6, and α5β1), plasminogen and matrix metalloproteinases, ECM components, growth factor receptors and proteoglycans transmit intracellular signals [42]. Keratinocytes to migrate do not express integrin αvβ3, which is a receptor for fibrinogen / fibrin, therefore, they do not have the ability to interact with these matrix proteins [43]. Instead, it migrates along the type 1 collagen-rich wound edge through the α2β1 receptor until it encounters fibronectin-rich granulation tissue, and then migrates on the newly formed tissue through the α5β1 receptor [44]. Once the surface of the lesion is covered, the suprabasal cells initiate differentiation procedures on the outer layer of the repaired skin. Indeed, the transcription factors that regulate the expression of keratin genes are activated and the cells can differentiate, to generate the newly stratified epidermis. Indeed, the keratinocytes that migrate to the site of damage have high levels of keratins K6, K16 and K17, differentiating itself from keratinocytes expressing K5 and K14 which are expressed in the basal layer or K1, K2 and K10 present in the differentiating cells [45].

Keratinocytes produce autocrine signals for the other surrounding keratinocytes but also paracrine signals for the other cells present in the wound and this is essential for creating a communication network [45]. In fact, as reported in the literature, keratinocytes stimulate fibroblasts to synthesize growth factors. While the latter in turn stimulate the proliferation of keratinocytes in a paracrine way [46].

In this phase, there is decreased blood supply because of vessel disruption and accelerated metabolism of the cells involved in the tissue repair. These two characteristics play together in forming a hypoxic environment, that stimulates the synthesis of hypoxia inducible factor-1 (HIF1) in various cell lines such as in macrophages, fibroblasts, vascular endothelial cells, and keratinocytes [47]–[50]. Hypoxia also causes endothelial cells to produce nitric oxide (NO), that promotes vasodilation and angiogenesis, improves local blood flow. The hypoxic condition is the main stimulus for angiogenesis.

Angiogenesis is an organised process that includes proliferation of **endothelial cells**, rupture and rearrangement of the basement membrane, migration and association of tubular structures and recruitment of perivascular cells.

As mentioned above, wound repair is composed of a series of processes overlapping each other over time. The growth factors released in the inflammatory phase by the platelets and then by the cells as macrophages and monocytes residing in the wound bed are all central mediators of the injury-induced angiogenic induction. There is a physiological balance between stimulators and inhibitors of blood vessel growth, angiogenesis reflects this change in regulatory balance, which is temporarily conducive to angiogenesis stimulation. In particular VEGF, (FGF-2), TGF-β1 and PDGF are sequestered within the ECM and initiate angiogenesis, stimulating endothelial proliferation, migration and tube formation [51]. The expression of PDGF is detected on the vascular endothelium of damaged skin, while is rarely present in normal intact skin. Between 3 and 7 days after the injury, VEGF reached a peak, which is consistent with the clinical manifestation of granulation tissue. From the day 5, b-FGF is expressed at its peak level, and by day 7, it returns to baseline level.

Moreover, the thrombin produced by platelets, essential for coagulation, also plays an important role in upregulating VEGF [52]. Endothelial cells exposed to thrombin also release MMP-2, thereby promoting local dissolution of the basement membrane, which is a necessary early step in angiogenesis [53]. The protease that breaks the damaged tissue matrix further releases angiogenesis stimuli. The digestion of fibrin produces fibrin fragment, which directly stimulates angiogenesis and enhances the effects of VEGF and b-FGF [54].

At this stage, the migration of endothelial cells to chemical attractants and their continued proliferation promoted the sprout extension. Capillary tips and sprouts together form a new blood vessel network, which then supplies oxygen to the wound, thereby improving tissue ischemia, hypoxia and providing nutrients for facilitating further healing [55]. To better explain this process, it is important to clarify that in intact tissues the blood vessels are in a state of quiescence that have aligned endothelial cells, and the tight intercellular adhesion can form a barrier that helps maintain blood flow [56]. This mature blood vessels are surrounded by a basement membrane composed of collagen IV and laminin [57]. They are also coated with pericytes, which can promote the survival of endothelial cells and help maintain the stability of blood vessels. When the quiescent vessels are exposed to a proangiogenic stimulus, as in the case of growth factors, endothelial cells inside the blood vessels activate and lose their cell-to-cell contact. In addition, detachment of pericytes and enzymatic degradation of the basement membrane provide for the development of new blood vessel germination. Adjacent endothelial cells proliferate and migrate to prolong the germinal vessels. After this process, the blood vessel returns to a resting state and a new basement membrane is formed, and the and endothelial cells release PDGF recruiting pericytes which express receptor β (PDGF-Rβ) and cover the new vessels [56]. The whole process of angiogenesis is controlled by changes in the levels of proangiogenic and antiangiogenic molecules present in the injury microenvironment. At the end

of the process, the number of blood vessels returned to normal and returned to a level close to that of uninjured skin. Finally, fibroblasts synthesize and deposit new ECM to support cells and new blood vessels [35].

1.4 Remodelling phase

Two or three weeks after the start of the injury starts the remodelling phase which may extend to a year or more. This final phase attempts to restore the normal structure of the tissue, the granulation tissue gradually remodelled, reducing cells and blood vessels and deep changes in the ECM. Myofibroblasts and excess newly formed blood vessels disappear, undergoing apoptosis, mediating the transition from granulation tissue to scars [37]. In addition, excessive accumulation of collagen fibers are digested at this stage. The activation of tissue collagenase (MMP) and other enzymes (such as hyaluronidase, bacterial collagenase, and lysosomal proteases) can reshape granulation tissue. TGF-β1 and FGF control the degradation of type III collagen and the synthesis of type I collagen. The collagen fibers become thick and placed in parallel, thereby enhancing the tensile strength of the tissue. Throughout the remodelling process, fibronectin and hyaluronic acid are degraded by cells and MMP [58] slowly replacing the granulation tissue with a fibrotic scar. Indeed, as seen in the previous stages of wound healing, fibroblasts stimulated by various soluble factors, synthesize, and degrade collagen. However, if the balance between synthesis and degradation is altered, scars are formed. Hypertrophic scars remain as if to cover the original wound and may regress over time for the reduction of excessive collagen.

1.5 When wound repair fails

The tissue damage repair mechanism just described involves a cascade of concatenated and consequential cellular events. If such events are disrupted is produced excessive scarring or failure to heal entirely. These injuries are named as chronic wounds. When the normal wound healing process is in overdrive, it will produce pathological scars such as keloids and hypertrophic scars, resulting in excessive disordered collagen deposition. Scar formation after wound healing can result from accidents, surgery and even acne. The resulting changes in appearance can have a negative impact on body image and self-confidence, and the shame and aggression that can cause stress in social interactions reducing the quality of life of the individual [59]. Besides the aesthetic point of view, scars represent a serious problem, since they involve a loss of the functionality, lack of skin appendages and limitation of the movement of the tissues.

It is known that aged and diabetic mammals skin are more predisposed to injury, because of the altered skin barrier and the loss hydration of the tissue [60]. Ageing and diabetes lead to the loss of dermal matrix, with consequent changes in tissue mechanics and more susceptibility to damage [61].

A main factor implicated in aged and diabetic wound pathology is cellular senescence [62]. Indeed, mitotic cells become senescent and non-proliferative as reaction to several intrinsic and extrinsic factors. These senescent cells acquire an hypersecretory capability secreting several pro-inflammatory cytokines and proteases and the chronic wound environments are perfect for the induction of these cells thanks to the high levels of inflammation and oxidative stress [63].

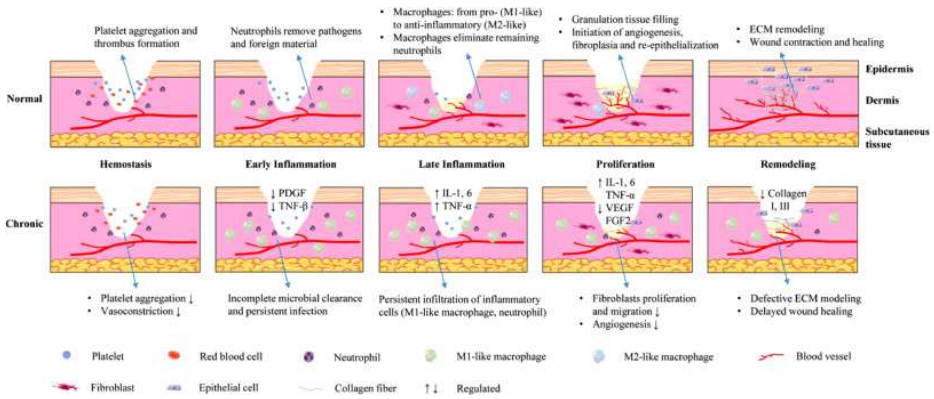

Fig. 1.2: Differences in normal and chronic wound healing stages [64]

Main actor of chronic wound is the excessive inflammation, that is responsible of the chronicity due to the continued destruction of tissue. In chronic wounds, neutrophils produce an excessive neutrophil extracellular traps resulting cytotoxic for the cells and delay the wound healing [65]. Other cells abundant in chronic wounds are macrophages that loss their ability to efferocytosis of apoptotic cells, phagocytose bacteria and ability to polarize to an anti-inflammatory state [66]–[68]. Taken together these information show that immune cells in chronic wound inhibit the shift from inflammation to resolution and increase the susceptibility to infection.

Another critical step for the correct heling is the remodelling phase. Non-healing wounds are characterized by keratinocytes that at the edge of the injuries show an abnormal nuclear presence of β-catenin and c-myc, that delays the motility obstructing the healing [69]. Moreover, the edge of the chronic wound is characterized by a dysregulation of cell cycle, desmosomal markers and growth factor receptor signalling. In the same time, fibroblasts are highly senescent compromising ECM deposition [70].

The presence and the persistence of wound infection is another obstacle for the correct healing of a skin wound and it is one of the responsible for the chronicity [71]. *Staphyloccoccus aureus* and *Pseudomonas aeruginosa* are the most common wound pathogens in chronic wounds, that often develop into polymicrobial aggregates (biofilms) in a protective matrix that grant resistance to the traditional antibiotics [72].

1.6 Scar-Free Skin Wound Healing

Therefore, one of the most compelling challenges in the scientific world is the ability to restore the skin to its original state.

As early as 1979 was observed that the foetus has an extraordinary ability to heal skin wounds in a regenerative way without leaving scars [73]. It would be very interesting to reproduce foetal healing. Therefore, it is interesting to deepen this process, to compare it to what happens in adults and lead to the development of new regenerative strategies.

This regenerative capacity is not only due to the sterile, warm, and rich in growth factors environment or amniotic fluid, because this regeneration ability will be weakened during the third trimester.

The most obvious difference is a cellular event: the absence of acute inflammation.

The acute inflammatory infiltrate of foetal wounds is mainly made up of macrophages and almost devoid of leukocytes and lymphocytes, with reduced degranulation and platelet aggregation. There is a reduced phagocytic activity, and only a few neutrophils reach the wound [74]. Thus, macrophages and fibroblasts deal with the removal of debris from the devitalised tissue [75]. In foetal wounds, cytokines also play an important role. In fact, pro-inflammatory cytokines are reduced, as with IL-8. Instead, anti-inflammatory cytokines such as IL-10 are highly expressed [76].

Another distinction between foetal and adult wounds is in the activity of fibroblasts. These dermal cells in foetuses have a synthetic and secretory phenotype that allows them to have a more coordinated ECM deposition which is more regenerative. In this there is an increase in proteoglycans and glycosaminoglycans such as hyaluronic acid (HA) which makes the matrix more flexible, promotes both cell proliferation and migration [77].

The deposition of the collagen type also varies between the adult and the foetus in the repair of tissue damage. In foetal wounds there is excess type III collagen over type I collagen, and the new collagen settles in a fine reticular pattern very similar to intact skin [78].

In adult wounds, there is a relative increase in the expression of TGF-β1 and TGF-β2 compared to TGF-β3. Opposite situation in foetal wounds, which express more TGF-β3. In fact, low levels of TGF-β1 are associated with a reduction of scars [79].

This information provided cellular and molecular insights that can be modulated to target a pro-regenerative response without scarring.

2. Extracellular vesicles

Intercellular communication is a key characteristic of multicellular organisms and can be mediated through direct cell-cell contact or transfer of secreted molecules. A new mechanism for intercellular communication has emerged in recent decades, involving the intercellular transfer of extracellular vesicles (EVs). The EVs serve a variety of purposes, in addition to their functions in communication, they are involved in transfer of genetic information, removal of dangerous substances and unnecessary metabolites such as chemotherapeutics or oxidised lipids from cells [80]. It is not sure if the process of vesicle secretion belongs to all the eukaryotic cells, but for those that do, it seems to be maintained throughout the evolution timeline. Different types of cells can release distinct types of vesicle. Moreover, from a single cell may be released EVs of varying size, biogenesis, and cargo, which can change with the physiological state of the cell. Several number of EVs subtypes have been identified, and common distinction of EVs rely on size. The smallest diameter of the phospholipid vesicles can be between 10 and 20 nm, while the upper limit of the EVs is not known. It is known that the size of apoptotic bodies and "oncosomes" is in the order of microns (1-to 10-μm in diameter), while mammalian platelets are approximately 2 μm in diameter. For this reason, many studies therefore concentrate on EVs with a diameter of 1 micron or less. Depending on the size and their biogenesis, the EVs are divided into three broad classes. The vesicles with the largest diameter are included in the apoptotic bodies group. They are heterogeneous diameter vesicles, which vary from 200 nm to 5 μm in diameter and are released from the plasma membrane of cells during programmed cell death. Instead, microvesicles or ectosomes have a diameter of 100-800 nm and are known to be released from the plasma membrane of viable cells. Finally, the exosomes represent the smallest group of vesicles, they have a size of 30-150 nm. They are formed when MVBs merge with the plasma membrane and expel their intraluminal vesicles which are released into extracellular space [81].

These three big groups of EVs, comprise subgroups further divided according to the size of the particles, biogenesis and biomarkers.

Oncosomes or large oncosomes are large EVs released by highly aggressive cancer cells (1000–10,000 nm) [82].

Migrasomes (up to 3000 nm) are oval-shaped microvesicles containing small vesicles. the cells that secrete migrasomes from tips of their retraction fibers. These vesicles are formed and released in migration-dependent manner [83].

Microvesicles or MVs (100–1000 nm) are released from the surface of cells. MVs share some biomarkers with exosomes, such as CD63, and both the vesicles transport bioactive cargos between cells [84].

Exosomes are vesicles (30–100 nm), this group includes three subpopulations of exosomes: large exosomes (Exo-L, 90–120 nm) and small exosomes (Exo-S, 60–80 nm) and non-membranous smaller nanoparticle named “exomeres” (< 50 nm) [85].

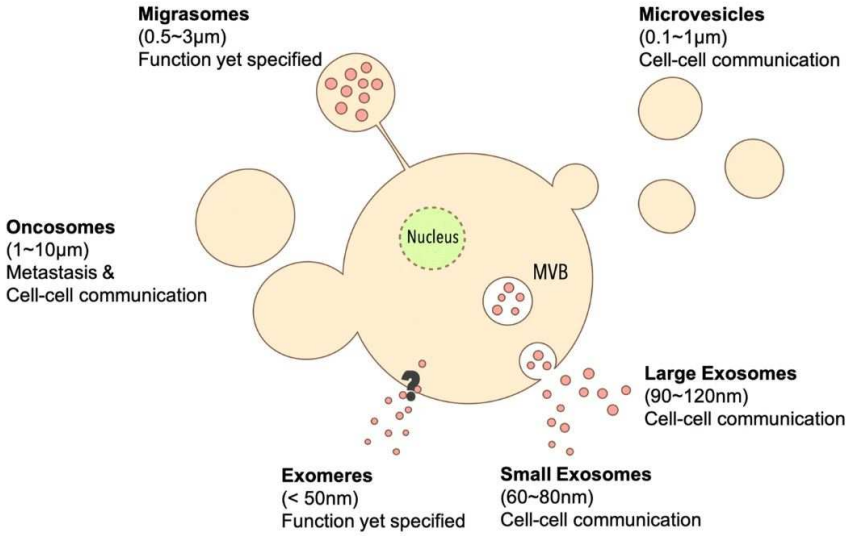

Fig. 2.1: EVs subpopulation

[86]

2.1 Shape of the vesicles

It was assumed, for a long time, that all EVs were circular in nature, but trough Cryogenic Electron Microscopy (cryo-TEM), a technique that allows to see the vesicles retaining their natural state, it has been observed that the morphology of the vesicles was much more diverse [87]. It was interesting to observe how a single cell has the capacity to release EVs with many different morphologies and which further increases the diversity of EVs [88]. By comparing studies carried out from vesicles released by different human fluids, such as human ejaculate [89] or plasma [90], or from cell cultures [88], it is confirmed that EVs can have various morphologies. Indeed, unlike the classic circular shape that was expected, it has been seen that the vesicles can have the shape of membranous tubes. Or they can be enclosed in a single larger membrane vesicle that contains several smaller vesicles.

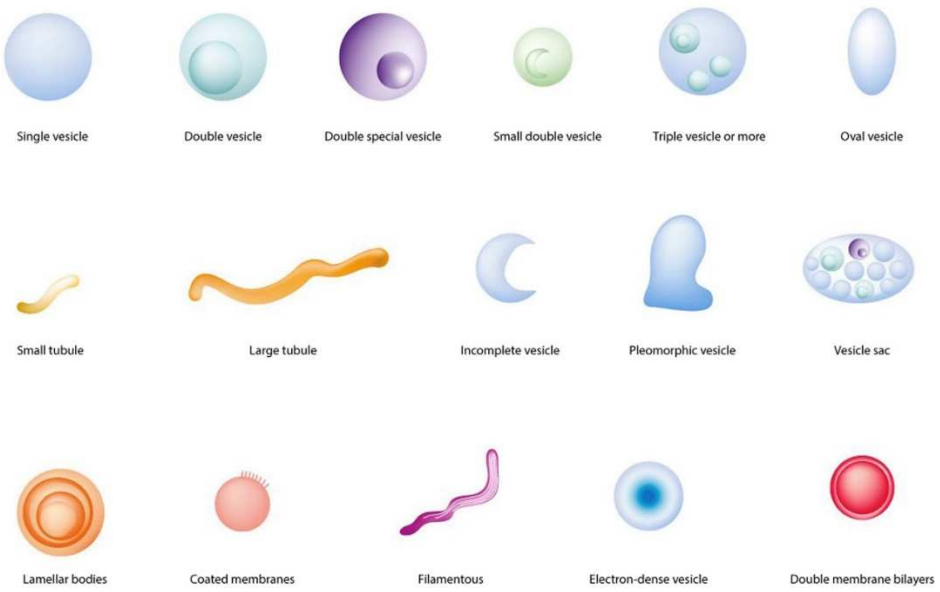

Fig. 2.2: Extracellular vesicles differences based on morphology [91]

2.2 MVs biogenesis

Only recently started to emerge the processes involved in the secretion of microvesicles from the plasma membrane. This biogenesis requires rearrangements of the plasma membrane, including changes in lipid components, protein composition and calcium levels.

Calcium-dependent enzyme machinery includes aminophospholipid translocases (flippases and floppases), scramblases and calpain that promote membrane bending and rearrangement of the underlying actin cytoskeleton to facilitate membrane sprouting and thus vesicle formation [92].

2.3 Exosome biogenesis

Exosomes and MVs have different type of biogenesis, in distinct sites within the cells. However, the biogenesis of both entities involves common intracellular mechanisms and sorting machines. Exosomes are formed from late endosomes induced by the inward budding of the multivesicular body (MVB) membrane. Invagination of late endosomal membranes contributes to the formation of intraluminal vesicles (ILVs) in broad MVBs [93].

2.4 ESCRT-dependent mechanisms

One of the most approved mechanisms for the creation of MVBs and ILVs is the endosomal sorting complex needed for the transport (ESCRT) function. This protein machinery comprises four complexes (0 through III) and work with other associated proteins such as VPS4, VTA1, ALIX also called PDCD6IP [94]. More in detail, the subunit ESCRT-0 consists of HRS that can bind clathrin coats and create a protein network on endosomal membranes, collects ubiquitinated cargo proteins and starts their sorting through the MVB pathway. HRS recruits the tumour-susceptibility

protein (TSG101) of ESCRT-I subunit and ubiquitinated cargo proteins and interacts with ESCRT-II [95]. ESCRT-I is then involved in the recruitment of ESCRT-III via ESCRT-II or ALIX. Indeed, this starting complex is important in initiating ESCRT-III recruitment and assembly. Unlike the other ESCRT complexes, ESCRT-III does not form a stable cytoplasmic complex, but consists of four core subunits: Vps20, Snf7, Vps24, and Vps2. Some of these subunits form linear polymers that have been implicated in cargo trapping, membrane deformation and vesicle abscission. At this step, intervene the AAA-ATPase VPS4 which is involved in the scission of the forming vesicle and also for the recycling of the ESCRT machinery for subsequent rounds of sorting [96]. It was demonstrated that ESCRT-III-associated protein ALIX facilitate intraluminal budding of vesicles in endosomes and thus exosome biogenesis, following association with syntenin, the cytoplasmic adaptor of heparan sulphate proteoglycan receptors. Syndecan (heparan sulphate proteoglycan receptors) cargo creates syndecan assemblies that can recruit syntenin–ALIX. Syntenin interacts directly with ALIX through LYPX(n)L motifs, supporting the intraluminal budding of endosomal membranes [97].

2.5 ESCRT-independent mechanisms

Moreover, concomitant inactivation of four proteins of the four separate ESCRT complexes does not preclude the development of MVBs, indicating that MVBs and ILVs that can develop in the absence of ESCRT activity [98]. Indeed, recent research favours an alternative mechanism for sorting exosomal cargo into MVBs in an ESCRT-independent manner, which appears to rely on raft-based microdomains for lateral segregation of cargo inside the endosomal membrane. Such micro-domains that contain high concentrations of sphingolipids from which ceramides are produced. Ceramide may cause the agglomeration of small micro-domains into larger domains that facilitate domain-induced budding [99]. This ceramide-dependent mechanism highlights the main role of exosomal lipids as well as tetraspanins in exosomal biogenesis. Tetraspanin CD81, for example, plays a crucial role in sorting target receptors and intracellular components into exosomes. However, CD81 acts with tetraspanin-enriched microdomains (TEMs) as ubiquitous complex membrane sites for the compartmentalization of receptors and signalling proteins in the plasma membrane [100].

Over CD81, there are identified other tetraspanins such as CD82 and CD90 to play a role in the development of microdomains and exosome cargo sorting [101]. These proteins may aggregate and create rafts with other tetraspanins or other cytosolic proteins, resulting in cytoskeletal remodelling and micro-domain creation [102].

2.6 Release of the vesicles

Once the microvesicles are formed, EVs and the exosomes are released in different ways and times. Microvesicles come out of the plasma membrane faster and in a way dependent on the interaction

between actin and myosin fibers with a subsequent ATP-dependent contraction [103]. Instead, exosome secretion is a longer process in which the transport and apposition of MVBs onto the plasma membrane is necessary to merge and release ILV into the extracellular environment. The formed MVBs can either fuse with lysosomes or after incorporation with the plasma membrane are released in an extracellular environment as exosomes. The transfer of these vesicles through the cells to cell membrane depends on the interaction with the cytoskeleton and it is regulated by several proteins. This machinery of the scission/release of MVs includes cytoskeleton (actin and microtubules), related molecular motors (kinesins and myosins), molecular switches (small GTPases) and fusion machines (Soluble NSF Attachment Protein Receptor (SNAREs) and tethering factors). Among the GTPase proteins Rab family is particularly important, even if their involvement seems cells specific. Rab27a and Rab27b are involved in the release of exosomes from HeLa cells. In detail, Rab27b regulates the motility of MVBs towards the cell membrane, while Rab27a promotes their fusion [104]. Instead, other proteins of the Rab family are involved in the release of exosomes in other cell structures, as in the case of Rab35 in the Oli-neu cells (oligodendroglial cell lines) [105] and Rab11 in the K562 cells (chronic myeloid leukemic cells of the bone marrow) [106].

The proteins of the SNARE family play a key role in the final step of the membrane fusion process and release of exosomes. It is necessary that three or four elements of the SNARE family form a complex. The members of this protein family are known also as R- or Q-SNARE. The formation of this complex requires one R-SNARE (usually v-SNARE) and three Q-SNAREs (usually t-SNAREs) [107]. Their activity is determined partly by the state of phosphorylation of these proteins, which influences their localisation and their interaction with SNARE partners, thus leading to the release of regulated exosomes [108].

The release of EVs from the plasma membrane is induced by stimuli leading to an increment of intracellular calcium and cytoskeleton remodelling [109]. In comparison to plasma membrane derived EVs, the exosome secretion is typically studied in the absence of a signal established to cause this secretion, indeed the intracellular signals involved are not known.

2.7 EVs composition

During their biogenesis, the vesicles incorporate material belonging to the “mother cell”, including cell-specific proteins, lipids, RNA or even DNA as a "molecular signature". Indeed, by studying the pools of vesicles from samples composed of various types of cells (as in the case of blood) it is possible to discriminate the cell of origin of a vesicle on the basis of its content. Despite the selective proteins, particularly in exosomes, there are omnipresent proteins that are most likely related to biogenesis or exosome functions. Among those always present, there are cytoskeletal proteins such as tubulin, actin and actin-binding proteins, proteins involved in intracellular membrane fusions and

transport such as annexins and Rab, heat shock proteins, such as the constitutive isoforms of HSP70 and HSP90, tetraspanins such as CD9, CD63, CD81 and CD82 and metabolic enzymes.

Even on the basis of the origin of the vesicles their content can change, indeed exosomes derived via the endolysosomal compartment appear to be most enriched with histocompatibility complex class II (MHC class II) and CD37, CD53, CD63, CD81, and CD82 histocompatibility complexes [110]. As described before, the use of the ESCRT complex for biogenesis requires accessory proteins. Therefore, regardless of the cell of origin, the exosomes generated in an ESCRT dependent manner contain proteins ESCRT, Alix, TSG101 and chaperones, such as Hcs70 and Hsp90 [111]. Then, MHC II, tetraspanine, ESCRT, Alix, TSG101 and heat shock proteins that we find in all exosomes regardless of the type of parent cell, can be considered exosomal markers [111]. Instead, MVs compared to exosomes contain more proteins with post-translational modifications, such as glycoproteins or phosphoproteins [112]. By isolating EVs through a differential centrifuge, mitochondrial proteins such as Aconitase, Golgi apparatus such as GM130, endoplasmic reticulum such as Calreticulin and some cytoplasmic proteins such as α-tubulin have not been found. For this reason the purity of EVs can be confirmed by checking the absence of these proteins [113]. Through spectrometric analysis, the content of vesicles from ovarian cancer cells was analysed. These EVs are enriched in proteins that undergo acetylation and phosphorylation such as phosphatidylinositol-3-kinase, mitogen-activated protein kinase (MAPK). The presence of kinases which are key signalling molecules can probably explain the ability of these EVs to affect recipient cells [113]. Exosomes derived from tumour cells and oncosomes are characterized by MMP inside them. These enzymes are necessary to digest the ECM and improve tumour invasiveness and therefore can carry signalling messages from the cells of origin to the receiving cells [114].

EVs, like cells, are covered with a double-layer phospholipid which, however, is enriched with sphingomyelin, gangliosides and unsaturated lipids, that suggest a more stable casing than cell membranes. Instead, their amount of phosphatidylcholine and diacylglycerol is decreased relative to the membranes in their cells of origin [115].

As with the previous EVs components, the RNA content also varies according to the cell of origin. The RNA carried by EV is generally less than 200 nucleotides, therefore shorter. In the vesicles there are both coding and non-coding RNA (miRNA, tRNA, rRNA, small nuclear (snRNA), small nucleolar (snoRNA) and interacting RNA with piwi (piRNA)) [116]. The RNA transported by EVs can be released to the acceptor cells [117], and it is interesting to note that, for example, transported miRNAs can regulate the translation of the target mRNAs in the receiving cells. This process that can be crucial in tumour progression [118].

Finally, among the material contained in EVs there is also DNA in size from 100 base pairs (bp) to 2.5 kilobase pairs (kB). The information deriving from the analysis of the genetic material contained in the vesicles can be exploited as a circulating biomarker in the early diagnosis of tumours and in the monitoring of the response to treatment [119].

2.8 EVs interactions with cells

Once released into the extracellular space, the EVs reach the extracellular environment and can influence the function of the target cells with their content [120], [121]. The messages that these vesicles carry within them can influence the physiology of the receiving cells, promoting physiological or pathological changes. However, the process responsible for EVs cell internalisation has generated a lot of controversy in the literature, because various types of mechanism can be applied for this communication. EVs can deliver their message in the extracellular space through the physical bond of the vesicles to the cell surface, or through the fusion with the plasma membrane.

2.9 Protein interaction

The uptake mechanisms of EVs involve protein interactions that facilitate subsequent endocytosis [122], [123]. The list of specific protein-protein interactions that mediate EVs attachment and absorption in cells is continuously updated in the literature.

Tetraspanins, as seen above, are very abundant in EVs and play a role in cell adhesion. Based on this evidence, they could also have a function in EVs uptake [124]. To support this, studies conducted using antibodies against tetraspanins CD81 or CD9 have reduced the internalization of vesicles by dendritic cells [125]. Another class of proteins involved in cell adhesion, and therefore potential promoters of uptake are integrins. Using antibodies that mask the binding sites of αv (CD51) and β3 (CD61) integrins on the cell surface, results a reduced absorption of EVs in dendritic cells [125].

Heparin sulfate proteoglycans (HSPG) are highly glycosylated proteins that act as co-receptors in cells. They are used by viral particles and lipoproteins to enter in the cells. To understand whether they are also able to promote the entry of EVs into cells, studies have been conducted by marking both the vesicles and the membrane proteoglycans (syndecan and glypican) of the receiving cells with fluorescent probes. From this studies a co-localization of both fluorescent signals was observed, suggesting that HSPG are needed on the cell surface for efficient internalization of EVs [122].

2.10 Endocytosis

The most accredited method for uptake of EVs is endocytosis [126], [127], which can be rapid up to 15 minutes after exposure [128]. It is also a process that requires energy from cells, indeed the ability to internalise EVs at 4°C is drastically reduced [122], [126]. Besides requiring energy, EVs requires a functioning cytoskeleton. Treating cells with cytochalasin D (metabolite that

depolymerizes actin filaments with inhibition of endocytic pathways) there is a significant reduction of EVs internalization in a dose dependent manner [123], [126].

The term endocytosis encompasses several mechanisms including clathrin-mediated endocytosis (CME), phagocytosis, macropinocytosis and plasma or endosomal membrane fusion that are involved in the uptake of EVs.

- Clathrin-mediated endocytosis: it is also called receptor-mediated endocytosis. EVs have transmembrane molecules on their surface that interact with molecules on cell membranes. Following this ligand-receptor interaction, the cells internalize molecules by invagination of the plasma membrane which collapses into a vesicular bud, matures, and pinches. The resulting intracellular vesicle is covered with clathrin and then merges with the endosome where it deposits its contents. In ovarian cancer cells [126] and in phagocytic receptor cells [128] has been observed that the use of chlorpromazine prevents the formation of clathrin-coated pits on the plasma membrane, reducing the absorption of EVs by the receiving cells.
- Caveolin-dependent endocytosis: caveolae are tiny cave-like invaginations in the plasma membrane that may be internalised into the cell. Caveolin-1 is a protein necessary and sufficient for the formation of caveole. A specific knockdown of the CAV1 gene leads to a reduction of the caveolin-1 protein and to a reduced absorption of EVs, highlighting its importance [129]. At the same time, the precise role of this path can vary between cell types and EVs, as with CAV1 knockout in mouse embryonic fibroblast cells which instead leads to an increase in the absorption of EVs [123].
- Macropinocytosis: the EVs may be internalised through macropinocytosis, where the membrane protrusions stick out from the cell, wrapping up the EVs and enclosing them to the lumen of the macropinosome. Or, if EVs are stucked in membrane ruffles, are macropinocytosed. This mechanism requires Na +/H+ exchanger activity and it is also rac1-, actin- and cholesterol-dependent [130]. In microglial, the macropinocytosis of EVs derived from oligodendrocytes has been abrogated through different approaches. Significant reduction in uptake occurred by inhibiting the Na + / H + exchanger. Even using the molecule NSC23766, small molecules used as inhibitor of rac1, the absorption of EVs by the microglia was reduced [131]. Instead, other studies using inhibitors did not reduced macropinocytosis in EVs uptake [122], [128], [129].
- Phagocytosis: this method is generally used by macrophages and is able to internalize both small molecules (such as exosomes) and larger molecules. Phosphoinositide 3-kinase (PI3K) plays a key role in phagocytic processes in facilitating membrane incorporation in phagosome creation. To study the involvement of PI3K in phagocytosis, PI3K inhibitor such as wortmannin and

LY294002 were administered to macrophages. Both molecules blocked EV uptake in a dose-dependent manner [128].

- Involvement of lipid rafts: the composition of the plasma membrane is not the same in all its regions, there are regions morphologically represented by accumulations of particular proteins and lipids. For these lipid accumulations in some areas of the membrane, it appears thicker. To study the involvement of lipid drafts in EVs uptake, inhibitors of components belonging to these areas of the plasma membrane were used. Fumonisin B1 and N-butyldeoxynojirimycin hydrochloride, molecules that decrease the glycosphingolipidic composition in the plasma membrane were administered to dendrid cells by preventing its biosynthesis. Resulted the evidence that the internalization of EVs has been significantly reduced, suggesting that sphingolipids play an important role in endocytosis [132]. Protein from these areas of the membrane can also play a key role in the EVs uptake. Annexin II may have a role to play in the anchoring of EVs to the plasma membrane lipid raft domains, whereas Annexin-VI may lead to the trafficking of EVs to the late endosomal compartment [133].

2.11 Cell surface membrane fusion

The fusion is the process whereby two distinct membranes (one of EVs and the other of the plasma membrane) merge. When the lipid bilayers are close together, they have the outer leaflets in direct contact. This leads to the formation of a hemi-fusion stalk in which the outer-leaflets are fused. Subsequently, the expansion of the stalk produces the double layer of the hemi-fusion diaphragm from which a fusion pore opens. It can be promoted by several factors, such as acid pH, wich in the extracellular environment has been shown to improve fusion [134].

2.12 Roles of EVs in wound healing

Thanks to their rich composition, EVs can transport many molecules belonging to the cell of origin, allowing to transport the physiological and pathological messages even where the cells cannot reach. The lipid membrane of EVs protects their content from degrading enzymes present in body fluids during travel [135]. EVs take part in many biological processes, permitting cells from different tissues to communicate, and this ability can play in favour of complex processes such as wound repair. Wound healing process requires several cell types from a variety of distinct compartment where each reacts and produces a set of signals at various times. A considerable amount of literature has been published on EVs that can take part in tissue damage repair processes [136]–[141].

2.12.1 Coagulation

Transported molecules of the EVs content can modulate a series of intracellular signalling pathways in the receiving cells. Tissue factor (TF) circulates in the plasma and plays an important

role in blood clotting processes. TF is a transmembrane protein that has an important role in converting the FX zymogen to its active form FXa, which then converts prothrombin to thrombin. TF can therefore be considered the initiator of the activation of coagulation and has been found on the plasma membranes of EVs secreted by monocytes [142] and platelets [143]. EVs secreted by monocytes and rich in TF, can interact with the platelets and transfer their contents, activating the extrinsic coagulation cascade and promoting the formation of thrombin and fibrin clots within minutes [142].

2.12.2 Inflammation

The administration of EVs derived from human umbilical cord mesenchymal stem cell regulate the inflammatory reaction by moving miR-181c, which prevents the translation of TLR4 (a critical regulator in wound inflammation) from its mRNA. Indeed, this modulation is identified by increasing the number of leukocytes and pro-inflammatory cytokine concentrations such as the tumour necrosis factor alpha and IL-1β. While anti-inflammatory cytokines such as IL-10 increase following treatment with EVs [141].

According to signals in the microenvironment, the polarization of macrophages from an M1 (pro-inflammatory) to M2 (anti-inflammatory) phenotype is necessary in wound healing to avoid a prolonged inflammatory state that characterizes chronic wounds [144]. Mesenchymal stromal cells preconditioned by LPS secrete EVs capable of having paracrine effects that lead to improved regenerative and reparative properties. These vesicles can induce the promotion of M2 macrophage activation [145].

2.12.3 Cell Proliferation

Cell proliferation is a necessary process for different cell types during the repair of tissue damage. It is interesting to note that cell proliferation can be stimulated by EVs of various cells such as mesenchymal stem cells [139], myofibroblasts [146] and endothelial progenitor cells [138]. ERK 1/2 and Stat3 pathways are considered to play important roles in wound healing, including functions in cell proliferation [147], [148]. EVs can activate these pathways by stimulating proliferative processes in recipient cells [136], [149], [150]. ERK1/2 signalling can activate cell proliferation by controlling the transcription of key cell cycle regulators such as c-myc and the cyclines A1, D2 [136], [149].

Moreover, EVs can promote cell proliferation by activating signalling pathways not only directly by stimulating the cell cycle, but also by stimulating the expression of growth factors. Growth factors can create loops that further simulate cell growth responses, either paracrine or autocrine. Mesenchymal stem cells (MSC) exosomes induce both normal fibroblasts and fibroblasts from diabetic wounds to express a number of growth factors such as hepatocyte growth factor (HGF), a

growth factor similar to insulin-1 (IGF1), nerve growth factor (NGF) and stroma-1 derived growth factor (SDF1) [149]. This represents an interesting result, since in chronic wounds where healing is compromised there is the presence of dysfunctional fibroblasts with defects in the migration, proliferation, and secretion of growth factors, which lead to non-healing [70].

2.12.4 Cellular migration and invasion

In wound healing and tissue regeneration, cells move from the periphery to reach the site of the injury. Then keratinocytes, endothelial cells and fibroblasts migrate to the lesion area where they stimulate the secretion of growth factor, the synthesis of the ECM, angiogenesis and collaborate for the closure of the wound. All these cell types are recruited following different stimuli, EVs can play a role in this process and in promoting migration. In addition, EVs can encourage migration and invasion by interacting with the ECM. As previously analysed, the binding of EVs to the ECM components of the recipient cell can be based on ligand-receptor interactions. EVs can have integrins on their membrane, facilitating adhesion. Indeed, the integrins α6β4 and α5β1 on EVs can bind the molecules of the laminin-332 matrix and fibronectin [151]. Furthermore, matrix metalloproteinases (MMPs) transported by EVs, can degrade the ECM by increasing invasion and migration especially of cancer cells [152].

It is known that in electric vesicles it is possible to find members of the family of Heat shock proteins (HSP) such as HSP-70 and HSP-90. These proteins can promote several biological activities including cell motility induction [153], [154]. Analysing the structure of HSP90α we know that it is made up of four domains. There is an N-terminal domain, a central sequence next to the N-terminal, an intermediate domain and finally a C-terminal domain [155]. The pro-motility activity resides in the intermediate domain, that forms a highly conserved surface loop. The secreted HSP90α promotes cell migration through the LRP-1 (LDL receptor-related protein 1) / CD91 surface receptor. Indeed, administering to fibroblasts the EVs isolated from keratinocytes and rich in HSP90, these vesicles can stimulate the migration [156]. Furthermore, in a different study in which vesicles released from keratinocytes and mesenchymal stem cells were administered to fibroblasts, not only was observed the increase in migration speed, but also the promotion of the expression of important genes involved in the ERK1/2 signalling pathway (which has roles in both cell proliferation and migration), such as TGF-β, type I collagen, type III collagen, N-cadherin, MMP -1, MMP-3 and IL-6 [157], [158].

2.12.5 Angiogenesis

Angiogenesis, is the formation of new vessels, requires the proliferation of endothelial cells, the evasion of the ECM and the formation of tubular structures. These processes require not only the interaction between endothelial cells, but also angiogenic factors including the growth factors VEGF

and FGF. The treatment with exosomes promote a greater number of blood vessels [136], [159]. EVs play an important role in transporting growth factors, miRNAs and other molecules able to promote angiogenesis through the proliferation and migration of endothelial cells to the wound site [136], [160]. VEGF, FGF and PDGF are secreted following platelet activation and are contained in the EVs released by the platelets. By treating endothelial cells with EVs secreted by platelets, we assist to the promotion of proliferation, migration and the formation of capillary structures *in vitro* [161]. Hence, these EVs can promote the development of new blood vessels, as also observed *in vivo*. Mice experiments show that after injection of platelet-derived EVs into the ischemic heart muscle, the revascularization increases [162]. In angiogenesis process the ERK1/2 signalling pathway is enormously involved. Following the administration of EVs various pro-angiogenic genes are up-regulated, such as IL-6, IL-8, angiopoietin-1, E-selectin and FGF2, molecules that activate ERK1/2 pathway. Likewise, after treatment with EVs, the target downstream of the ERK1/2 pathway as inhibitor of DNA 1 binding, cyclooxygenase 1, VEGFA, VEGFR-2, c-Myc and cyclin-D1 also increased [136], [138].

EVs derived from endothelial cells contain MMP-2, MMP-9 and MT1-MMP which promote matrix degradation by stimulating the formation of new blood vessels [163].

Besides pro-angiogenic characteristics, EVs can also have anti-angiogenic effects. This is the case in which these vesicles can stimulate the production of reactive endothelial oxygen species (ROS). For example, lymphocytic EVs *in vitro* generate a reduction in nitrite oxide (NO) after treatment with actinomycin D and increase ROS production by inhibiting angiogenesis [164].

2.12.6 ECM Remodelling

The formation of granulation tissues is an essential step in wound healing. It provides a track for migration of cells from the wound edges, helping the wound closure.

Bone marrow-derived mesenchymal stem cells improve wound repair in paracrine manner. In hypoxic conditions (typical of wound healing because of decreased blood flow) the cells express and secrete high quantities of bFGF, VEGF-A, IL-6 and IL-8. These mesenchymal stem cells can promote wound healing through hypoxia-enhanced paracrine activity. Indeed, soluble factors present in the conditioned medium derived from these cells in the hypoxic environment significantly improved the proliferation and migration of keratinocytes, fibroblasts, endothelial cells and angiogenesis *in vitro*. [165]. Fibroblasts are the main cell types that comprise granulation tissue, they secrete elastin and type I and III collagen, which are the essential components of the ECM. In another study, the exosomes derived from mesenchymal stem cells through a paracrine mechanism stimulate the fibroblasts in the secretion of collagen and elastin provide resistance of the tissues. Among the components of the ECM there is fibronectin which promotes the migration of fibroblasts. Fibronectin

increases its levels following the administration of exosomes derived from mesenchymal stem cells. Hence, these vesicles can contribute in a paracrine way to the contraction of the wound and the maturation of collagen during the healing process [159]. *In vivo* experiments also underline the potential of exosomes secreted by stem cells on fibroblasts. Indeed, exosomes secreted by human adipose mesenchymal stem cells were administered intravenously in mice in which a soft tissue wound was produced. From histological examinations, a high production of collagen I and III was observed in the initial phase, promoting the first stages of wound healing by shortening the healing time. Instead, in the advanced phase of wound healing the administered exosomes inhibited the expression of collagen to reduce scar formation [157].

Finally, it has been shown that EVs also play an important role in improving the aesthetics and functionality of injured skin, reducing scar formation. Vesicles derived from umbilical cord-derived mesenchymal stem cell transfer miRNA derivatives such as miR-21, miR-23a, miR-125b and miR-145, which prevent activation of TGF-β / Sma and Mad related protein 2 pathways (SMAD2), thus inhibiting the differentiation of myofibroblasts and the production of collagen [137].

3. Glycosaminoglycans

Among the most important chemical constituents of the fundamental substance of the connective tissues, there are a heterogeneous class of substances called glycosaminoglycans (also known as GAGs or mucopolysaccharides) which, by binding to proteins, form large protein-polysaccharide complexes called proteoglycans (PG). GAGs are among the major constituents of the cell-ECM interface in animal tissues, taking part in many physiological events. They play crucial roles in cell growth, cell differentiation, morphogenesis, cell migration and both bacterial and viral infections [166].

Their basic structures comprise repetitive disaccharide blocks composed of alternating uronic acid (UA) and exosamine units.

UA units may be β-D-glucuronic acid (GlcA) or its epimer, α-L-iduronic acid (IdoA).

Amino saccharides (characterised by an amino-functional group (-NH2) instead of a simple hydroxyl functional group (-OH) in a monosaccharide) may be based on glucose (Glc) (α- D - or β-D - glucosamine, GlcN) or galactose (Gal), such as N-acetyl-β-D-galactosamine (GalNAc).

GAGs are distinguished by a significant degree of structural variation through substantial modifications that involve the degree of sulfation and epimerization of uronate.

Chondroitin sulfate (CS) and dermatan sulfate (DS) are both GalNAc-containing, but the second sugar is GlcA for CS and IdoA for DS [167]. Heparan sulphate (HS) and heparin (Hp) contain both GlcN, they also have GlcA in HS and IdoA in Hp respectively [168]. Keratan sulphate (KS) does not include UA but alternates N-acetyl-glucosamine (GlcNAc) with Gal [169]. Instead, hyaluronic acid (HA) alternates GlcNAc with GlcA [170], it appears without the core protein.

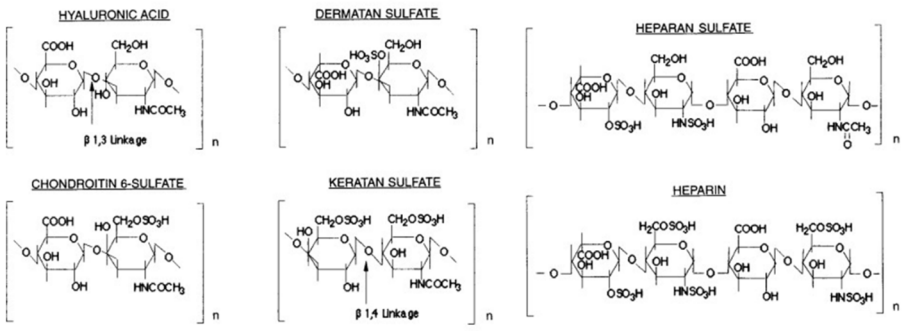

Fig.3.1: GAGs structure

3.1 Chondroitin sulfate

Chondroitin sulfate are GAGs sulphates, composed of an alternating chain of sugars (GalNAc and GlcA), there can be more than 100 sugars in each chain, each of which can bind sulphate ions. They

are also found in tissues as components of PGs. CS is one of the main components of the ECM in connective tissues, including cartilage, bones, skin, ligaments, tendons, and is responsible for important biomechanical properties, such as strength and elasticity. Moreover, it have an anti-inflammatory, anti-catabolic and anti-apoptotic effect and antioxidant properties [171].

3.2 Dermatan sulfate

The DS has a similar structure to the CS, it is made up of repeated disaccharide units of GalNAc sulphated in C-4 and IdoA (a stereoisomer of glucuronic acid) joined by α-1,3 bond. because there is a reversal in the epimeric form.

DS represents the most present GAG in the skin and, like Hp and HS, acts as a stabilizer, cofactor and/or co-receptor for growth factors, cytokines and chemokines. Therefore, it can regulate enzymatic activity, mediate cellular response to damage, such as wounds, infections and carcinogenesis, and finally can bind bacterial and viral virulence factors involved in invasion and escape from the immune system [172].

3.3 Heparan sulfate and heparin

From a structural point of view, HS and Hp are the most complex members of the GAGs family.

HS has many N-acetylated glucosamine residues and few N-sulphate groups. It is a ubiquitous component of the cell surface as PG.

Hp is constituted of a disaccharide unit composed of glucosamine and a residue of uronic acid, which can be both IdoA and GlcA. Most of the amino groups carry an N-sulfate group although a small part of the glucosamine residues is N-acetylated. The Hp has an endocellular location (such as in mast cells and basophilic granulocytes) and can be released in response to various stimuli.

HS is also synthesized as PG however, unlike Hp, it is not only produced in mast cells, but in most other cells and is localized on their surface and in the ECM. Hp is recognized for its anticoagulant activity, which is why it has been widely used in the clinic. It also induces the release of lipoprotein lipase and liver lipase, inhibits complement activation, angiogenesis and tumour growth. Through binding to different proteins including growth factors, HS mediates various biological functions, including cell adhesion, cell growth and proliferation regulation, inhibition of clotting and binding of the cell surface to lipoprotein lipase and other proteins. It also plays a fundamental role in angiogenesis, viral infections and tumour metastasis [173].

3.4 Keratan sulfate

There are two types of KS: type I is located exclusively in the cornea; type II is always found together with the CS in the skeleton, cartilage, bones and in corneal structures such as nails and hair. KS are more similar to glycoproteins than to PGs in that the repeating disaccharide (galactose-

glucosamine) is similar to that found in many glycoproteins. In addition, KS contains sialic acid, fucose and mannose (which are the carbohydrates found in glycoproteins). It is also synthesized in the central nervous system, where it participates in the development and formation of a scar tissue and the glial scar, following damage. At the level of the cornea, where it is associated with various proteins forming different proteoglycans (lumicano, keratokane and mimecano), the abundance of KS contributes to maintaining the correct level of hydration. This activity is also carried out in other tissues, such as cartilage, in which aggrecane (proteoglycan that contains KS) confers resistance to physical stress [174].

3.5 Hyaluronic acid

Unlike the other GAGs, HA does not contain sulphate groups and does not give rise to proteoglycans by binding protein cores. It consists of an unbranched polysaccharide chain produced by the condensation of thousands of disaccharide units formed by residues of GlcA and GlcNAc, linked, alternately, by β1.4 and β1.3 glycosidic bonds and intramolecular hydrogen bonds, which stabilize its conformations. Despite comprising a single polysaccharide chain, it can reach a significant molecular weight, from 105 to 107 Da. HA is present in large quantities during embryonic development, and, in adults during the wound healing phase and in some specialized tissues such as cartilage, vitreous humor of the eye, umbilical cord and synovial fluid. The hydrophilic groups of HA attract water, contributing to the hydration of the tissues and the lubrication of the joints. For this reason, in the connective tissue the HA takes care of maintaining its degree of hydration, turgidity, plasticity and viscosity, since it is arranged in space in an aggregate conformation thus forfeiting a significant number of water molecules. It is also able to act as a cementing substance and as an anti-shock molecule as well as an efficient lubricant (e.g. in synovial fluid) preventing damage to the tissue cells from physical stress [175].

3.6 Biosynthesis

We can divide the path leading to the formation of the GAGs into three phases. The first phase comprises the activation of the individual monosaccharides in the diphosphate nucleoside sugars. This stage takes place in the cytoplasm and is important for the formation of the 3'-phosphoadenosine 5'-phosphosulfate sulphate. Then, in the second phase, the compartments involved are the endoplasmic reticulum and the Golgi apparatus in which the sugar residues are transferred. The lasts sugars are incorporated into the polysaccharide chain found in the Golgi apparatus. Each saccharide is added thanks to the work of β-glycosyltransferase. Once the tetra saccharide is completed, the addition of the fifth sugar residue determines the type of GAG that is in formation. Indeed, the addition of GalNAc will form CS or DS by the enzyme β-N-acetylgalactosaminyltransferase. Instead,

α-N-acetylglucosaminyltransferase leads to the addition of GlcN with the consequent formation of HS or Hp. Finally, the polymerization continues with the addition of the sixth sugar residue and the enzyme involved have a N-acetylgalactosaminyltransferase and glucuronyltransferase activity. As an alternative to this latter enzyme, the activity of a heterodimer with N-acetylglucosaminyltransferase and glucuronyltransferase activity may be involved. Then DS and Hp will present IdoA while CS and HS will have GlcA [176].

The disaccharidic repeated in HS can be modified both as N and O sulphated (glucosamine 6-O- and 3-O-sulfation and uronic acid 2-O-sulfation) and with the epimerization of GlcA and IdoA. Instead, the repetitive unit of disaccharide in CS can be changed by the 4-O-and 6-O-sulfation of GalNAc, by the 2-O-and 3-O-sulfation uronic acid and also by the epimerization of GlcA. Five sulfotransferase enzymes complete the O-sulfation of CS and DS at specific positions on GalNAc, GlcA and IdoA [177]. Also the biosynthesis of HS and Hp is provided with O-sulfation in various positions of the disaccharides, three sulfotransferase enzymes are managed by this process [178]. In addition, the biosynthesis of KS begins in the cytosol thanks to the activation of sugars through the bond with the nucleotide diphosphate. Then its synthesis continues in the endoplasmic reticulum and in the Golgi apparatus, as well as for the previous GAGs analysed. While the cellular compartments involved are the same, the path that follows is different. Indeed, the first step involves the synthesis of three possible linkers, and not four as in the previous GAGs. These three linkers are N-linked to asparagine or are O-linked to serine or threonine residues. Another difference with the CS, DS, HS and Hp tetrasaccharide liker is that with KS each of the three linkers can polymerize the GAG. The polymerization of KS is carried out by two glycosyltransferases, which alternately add N-acetylglucosamine and galactose. Instead, the O-sulphation of both sugars occurs thanks to two different sulfotransferases [179].

3.7 Mesoglycan

Mesoglycan is a natural GAGs mixture, it is extracted from the porcine intestinal mucosa and is composed of HS (52%), DS (35%), Hp (8%) and CS (5%). Mesoglycan has positive effects on the fibrinolytic system, on macroreological and microreological parameters, and also restores the electronegativity of the vascular endothelium in case of damage [180]. Data relating to mesoglycan showed its anti-thrombotic and pro-fibrinolytic activities, for this reason, mesoglycan may be useful in the treatment of vascular diseases when combined with antithrombotic and vasodilator drugs, in patients with chronic peripheral arterial disease. Indeed, mesoglycan can inhibit platelet adhesion, stimulation of lipoprotein lipase and inhibition of smooth muscle cell proliferation. The anti-thrombotic effects with the activation of anti-thrombin III, heparin cofactor II and the pro-fibrinolytic action are due to HS and DS, fundamental constituents of the vessel wall [181]. Mesoglycan can also

restore the physiological properties of the capillary endothelium with anti-edema activity. In humans, the administration of mesoglycan reduces the number of micro-haemorrhages, micro-aneurysms and exudates in patients with diabetic retinopathy and promotes fibrinolysis for the healing of ulcers in patients with chronic venous insufficiency.

The role of mesoglycan in tissue damage repair process was also recently investigated. Through *in vitro* experiments, PGs have been shown to bind to multiple components of the cellular microenvironment. *In vivo*, on the other hand, abundant PGs are released during wound repair such as DS which, in the wound fluid, assists FGF-2, to signal cell proliferation [182].

Our group for the first time has highlighted the effects of mesoglycan on cell population involved in wound healing. In [183] experiments conducted on human epidermal keratinocytes and dermal fibroblasts showed that mesoglycan is able to promote their migration and proliferation process *in vitro,* two important steps for the re-epithelialization of the wound. Upon migrate to the temporary wound matrix, epithelial cells can degrade the provisional matrix while depositing collagen and other ECM components. Both cell-matrix and cell-cell adhesions need to be disrupted by MMP-mediated proteolysis, or disassembled to allow cells to migrate forward freely [184]. Mesoglycan promote the release by the fibroblasts of two metallogelatinase, MMP2 and MMP9, that play important role in cell migration and re-epithelialization [185]. To migrate the keratinocytes need to loss the contact inhibition and cell adhesion structures, this is the stimulus for the reorganization of the cytoskeleton driving motility [186]. After the treatment with mesoglycan, keratinocytes exhibited a significant decrease of E-cadherin levels and a strong F-actin reorganization. Investigating the mechanism of this enhanced motility and cytoskeleton modification, it is found that mesoglycan increase the CD44 receptor expression and the consequent activation of the ERM complex (ezrin-radixin-moesin) that linked the receptor with actin filaments [187]. Contemporary, the activation of mesenchymal phenotype of fibroblasts was confirmed through the high vimentin expression following the stimulation with mesoglycan and the well-defined cytoskeleton, supporting the functional behaviour observed.

At the same time, was investigate the effects of mesoglycan on endothelial cells to verify the new blood vessel formation response, a key process in wound healing. Mesoglycan promoted the motility of these cells both in terms of migration and invasion. Endothelial cells in presence of mesoglycan increased the pro-angiogenic effects evaluated through the increased number of branches and the length of new formed vessels on coating of matrigel and the number of cells spread from mice aortic fragments. In addition to the high expression of CD44, other several markers were enhanced in presence of mesoglycan proving the induction of EndMT. For example, following the treatment with the mixture of GAGs, endothelial cells showed a well-organized filaments of α-SMA [188], high

expression of N-cadherin, a membrane protein typically expressed by cell with an highly invasive phenotype [189] and in opposition the loss of the adhesion molecule VE-cadherin suggesting the high impact of the mesoglycan on angiogenesis promotion.

3.8 Proteoglycans

GAGs can bind various proteins through their sulfated parts and/or portions of oligosaccharides connected to O- and N- that bind the protein core. Generally, the tetrasaccharide linker is coupled to the protein nucleus through an O-glycosidic bond with a Ser residue in the protein, forming proteoglycans (PG). In the case of KS, the attack between sugar and the core protein can take place either through O-linkage or through N-linkage. Furthermore, since there are two main types of KS (KSI and KSII), PGs containing KSI via N-linkage and PGs containing KSII formed via O-linkage can be formed.

Cell surface PGs are involved in anchoring cells to the matrix fibres. Membrane-associated PGs generally comprise heparan-sulfate chains and they can be transmembrane or glycosylphosphatidylinositol (GPI) -anchored.

3.8.1 Syndecans

Syndecans (SDC) are a family of transmembrane PGs consisting of a protein core and one or more chains of GAGs covalently. The basic structure of syndecans is composed of three distinct domains: an extracellular domain with N-terminal polypeptide in which specific serine residues can bind GAGs, a transmembrane domain and C-terminal cytoplasmic domain.

The extracellular portion of syndecans across GAGs chains mediates both cell-cell and cell-matrix interactions. The part of the syndecans that contains the GAGs attachment sites is the ectodomain, that binds HS, characterizing the family as heparan sulfate proteoglycans (HSPG). Sometimes this portion can also bind chains of CS, producing the variability in syndecans family. Indeed, there are 4 different syndecans belong to this family, syndecan-1 (SDC1) and syndecan-3 (SDC3) which both have the chains of HS and CS, and syndecan-2 (SDC2) and syndecan-4 (SDC4) whose ectodomains bind only HS [190].

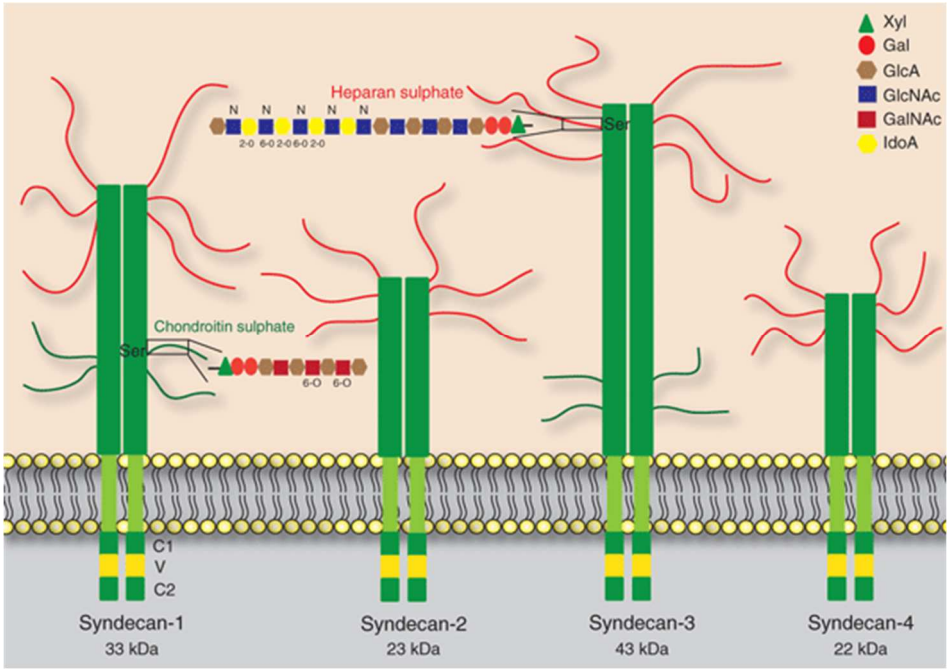

Fig. 3.2: schematic representation of the four syndecans [191]

SDC1 is present in leukocytes and in various epithelial tissues, SDC2 is found in mesenchymal cells, in the endothelium and in fibroblasts and in smooth muscle, SDC3 is widespread in neuronal tissues and, finally, SDC4 is abundant in many cell types and therefore present in most tissues [192].

The extracellular domain also contains cleavage sites for metalloproteinases [193], for proteins containing the disintegrin domain and metalloproteinases [194], and in SDC1 and SDC4 also for plasmin and thrombin [191]. Through these cutting sites, SDC are subjected to proteolytic cleavage, in a process known as shedding which is generally regulated by external stimuli, cell differentiation and inflammation. Among the extracellular stimuli that can promote SDC shedding there are growth factors [195], chemokines [196], heparanases [197] and cellular stress [198]. However, the mechanism by which they promote release is still unclear. When the complete structure loses its extracellular domain, signal transduction can be compromised. Instead, the released extracellular portion can bind the extracellular ligands, resulting as a competitor for the SDC remained intact [199]. Soluble forms of both SDC1 and SDC4 can often be found in skin wound fluids [195]. In particular, the soluble form of SDC1 can maintains the proteolytic balance of the wound fluids. This is allowed because it binds cathepsin G and inflammation-related neutrophil elastase [200]. At the edge of the wound, keratinocytes and endothelial cells engaged in proliferation express SDC1 [201]. Subsequently, this expression is significantly reduced in keratinocytes following the promotion of EMT [200]. In epithelial cells following an injury, SDC1 is cut mainly by MMP-7. Thanks to studies carried out on mice without MMP-7, it has been observed that they show a reduced re-epithelialization. This demonstrated that the release of SDC1 facilitates wound closure, regulating

inflammation and repairing lung epithelial lesions in mice [202]. Instead, a different study conducted on mice that overexpress SDC1, it was seen that the soluble form of this PG leads to a delay in wound healing [203], showing that the function of these HSPGs can be tissue specific.

The transmembrane domain of SDC is conservative. This portion is necessary for the dimerization of the core protein in homodimers, which is important for their functions [204]. The interactions of aromatic amino acids (phenylalanine, tyrosine and tryptophan) in particular a residue of phenylalanine of the transmembrane domain of SDC, regulates intermolecular interactions between these HSPGs that form both homodimers and heterotrimers [205].

Instead, the cytoplasmic domain of SDC comprises two different conserved regions called C1 and C2. At the centre of these two conservative regions is a variable region (V) which is typical of each individual family member [192].

The membrane proximal common region C1 can be involved both in interactions with the cytoskeleton and in endocytosis. Indeed, the ERM complex proteins bind this region in SDC2 by connecting directly with the actin cytoskeleton [206]. In SDC1, the C1 region is fundamental for endocytosis. Indeed, the activation of this HSPG triggers the phosphorylation of this working portion of an ERK-regulated kinase and influences the dissociation between SDC1 and α -tubulin, a molecule that can act as an anchor to the plasma membrane. In addition, Src family kinases-mediated phosphorylation that recruits an efficient actin-dependent endocytosis mediator: cortactin [207] which interacts with the microfilaments and microtubules of the cytoskeleton. The C1 region of SDC2 can bind ezrin, that serve as connection between the SDC and the actin cytoskeleton. This protein connects membrane receptors, which are bind through basic amino acid sequences, to the cortical actin network [208]. Only the C1 conserative region of SDC4 can interact with the syndesmos protein. This difference is because the syndesmos protein, besides binding the C1 portion, also binds the V region, which being variable makes the interaction exclusive for syndcan-4 [209]. V region modifies the configuration of the C1 region to favour interaction with this ligand. Instead, the previous proteins interacted only with C1, which being a highly conserved domain, the interaction can also be expected to occur with other members of the HSPG family.

Portion V are different between members of the SDC family, determining specific biological roles. There are few ligands for this region, but in the case of SDC4 both phosphatidylinositol 4,5 bisphosphate (PIP2) and the catalytic domain of the serine/threonine protein kinase Cα (PKCα) can be bound [210]. The V region of SDC4 to activate PKCα must oligomerize, also, PIP2 stabilizes the dimerization. PIP2 is involved in cytoskeletal organisation. Indeed, can control the polymerisation of actin by modulating profilin, gelsolin and actin, proteins that bind the actin itself. Among the proteins with which it acts there are actinin and vinculin causing their association with the cytoskeleton [211].

PIP2 can be part of several signal transduction pathways, it can be phosphorylated by the enzyme phosphatidylinositol 3-kinase generating 3,4,5-triphosphate phosphatidylinositol (PIP 3), which is further known as a molecule capable of promoting cytoskeletal organisation [212] and vesicle trafficking [213]. On the contrary, PIP2 can also be dephosphorylated to phosphatidylinositol 4-phosphate from the enzime 5-phosphatase [214]. Finally, the phospholipase Cγ can hydrolyse PIP2, giving rise to two different intracellular messengers: inositol 1,4,5-triphosphate, which mobilises Ca^{2+}, and diacylglycerol, which can activate PKC. But even PIP2 itself can directly activate PKC, even more strongly than diacylglycerol [215]. The cytoplasmic domain of SDC4, with the single portion (LGKKPIYKK) can interact with the catalytic domain of PKC to directly regulate its location and activity [216].

The C2 region of all SDC shows a conserved tetrapeptide sequence Glu-Phe-Tyr-Ala called EFYA. This C-terminal sequence can bind to the postsynaptic density protein, disks large, *zona occludens* (PDZ) domain present in specific proteins that are able to recruit signalling and cytoskeletal proteins. The proteins containing the PDZ domains are characterised by 80-90 amino acids that bind their target's canonical peptides, often present at the C-terminal [217]. The SDC-PDZ protein binding can promote a series of events that lead to cytoskeletal rearrangements but also to cell adhesion and migration. Among these protein-containing PDZ domains are syntenin, synectin, and Ca2 + / calmodulin-associated serine / threonine kinase (CASK). Syntenin is a cytosolic protein containing two PDZ domains between an N-terminal and a C-terminal domain [218]. The two PDZ domains can bind SDC but can also work as a connection among SDC and other proteins or as a SDC cross-linker. Syntenin controls the endocytic recycling of SDC through the interaction between its PDZ domains and PIP2. In this way, it can also control the molecules associated with SDC such as growth factors [219]. SDC, syntenin and ALIX come together in a key complex for the formation and composition of exosomes. The three proteins are not only present in the exosomes, but it is estimated that they control about 50% of the secreted vesicles, working together to control their exosomal release [97].

CASK instead contains a single PDZ module can bind the C-terminus of SDC2 and SDC4 monomeric. CASK forms a complex with SDC and protein 4.1, connecting the extracellular membrane and the cytoskeleton in the epithelial cells [220].

In fibroblasts after the binding with extracellular ligands, SDC4 can undergo phosphorylation of the cytoplasmic tail. This HSPG contains three tyrosines, one serine and one threonine in the intracellular portion. Phosphorylation was highlighted in serine^{183} [221].

SDC are very involved in cell adhesion and migration, and their activation is due both to their HS tails and to the cytoplasmic domain. HS tails can interact with extracellular ligands that activate signalling and cytoskeletal activation pathways. But even the cytoplasmic domain can interact with

many molecules. Experiments on SDC4 described how this HSPG regulates focal adhesion and stress fiber formation. Change cells devoid of region V, it is seen how this reduces the formation of focal adhesion, highlighting how SDC4 influences both morphology and cell migration [222].

Among the cell surface receptors, there are two families engaged in cell-ECM adhesion, they are SDC and integrins. Integrins are transmembrane glycoproteins that combine into heterodimers, 24 different transmembrane receptors may exist. The extracellular portion of the integrins can interact with the ECM glycoproteins while the cytoplasmic domains interact with the cytoskeleton. The modulation of cellular responses can involve cooperation between families of integrins and SDC. For example, the integrins α5β3 and α5β5 cooperate with SDC1 during adhesion to vitronectin [223], [224]. Instead, integrins α2β1 and α6β4 collaborate with SDC to adhere to laminin [225], [226]. In particular, the involvement of SDC on the cell surface, coordinated with the signalling mediated by integrin [227]. SDC4-induced PKCα activation requires α5β1 integrin and not α4β1 integrin, which is independent of SDC. The synergy of α5β1 integrin and SDC4 generates focal adhesion formation and therefore modulates cell migration [228]. A study helps to better understand the mechanism by which integrin α5β1 and SDC4 promote the cell migration of cell-ECM adhesion promoted, a study has suggested that integrin α5β1 stimulates the phosphorylation of p190Rho-GAP through Src kinases and this results in a downregulation transient level of GTP-RhoA. This phosphorylation is independent of SDC4, it is instead responsible for the distribution of p190Rho-GAP in specific membrane domains. This explains the coordination between α5β1 integrin and syndecan-4 in the formation of focal adhesion [229]. Furthermore, SDC4 and integrin α5β1 can form in the presence of thy-1 a trimer responsible for mechano-signalling in melanoma cells [230].

3.8.2 Syndecan-4 and wound repair

SDC4 can be found in the epidermis of injured skin. Indeed, it is upregulated in the granulation tissue on endothelial cells and fibroblasts. Keratinocytes at the edge of the wound are hyperproliferative and are characterized by high levels of SDC4 compared with the once that migrate across the fibrin clot [231]. Wound closure in null mice was slower opposed to the wild type. This delay was significant between days 3 and 6, while the complete wound closure occurred on day 12 in all three genotypes. Three days after injury, the knock-out animals exhibited reduced granulation tissue and wound contraction compared to wild types. The wound bed was filled in both the type of mice with granulation tissue after 7 days, but the skin of wild animals was more vascularized. *In vitro* migration assays of dermal fibroblasts from these mice revealed delayed migration of knock-out cells compared to the wild-type. These findings demonstrate the complex but essential role of SDC4 in wound healing and angiogenesis [232].

4. Annexin A1

Annexin A1 (ANXA1) is the first characterised member of the annexin family. It binds membrane phospholipids in a calcium-dependent manner. Annexin A1 has been found in different tissues and is involved in many physiological events such as hormone secretion, vesiculation, inflammatory response, apoptosis and differentiation.

4.1 Annexins family

Annexins are ubiquitous cytosolic proteins that share the property of calcium-dependent binding of membranes containing negatively charged phospholipids. The term annexin derives from the Greek "annex", which means "to hold together", and was chosen to describe the main characteristic of all or almost all annexins, that is to bind and hold together certain biological structures, in particular membranes. Initially, from the data of their discovery between the 70s and 80s, the annexins were given different names that referred to their biochemical properties, such as sinexin, chromobindins, calcimedins, lipocortins and calpactins. Subsequent studies have led to the conclusion that these proteins share fundamental biochemical properties, as well as gene structure and sequence characteristics [233]. Over 100 annexins have been identified in many species. Twelve proteins have been identified in humans, conventionally referred to as annexin A1-13. The letter "A" denotes their presence in vertebrates, the "B" in invertebrates, "C" indicates their presence in fungi and in some groups of unicellular eukaryotes, "D" in plants, finally "E" in protists [234]. Annexins are involved in many processes regulated by calcium within the cell. The C-terminal portion is evolutionarily conserved and contains the calcium binding sites, while the N-terminal tail is unique and allows the protein to interact with distinct cytoplasmic partners. Calcium ions are coordinated in defined type II or type III binding sites. At low intracellular calcium levels, annexins are diffusely distributed in the cytosol or can be located in specific regions or structures of the cell. After stimulation, each assumes a distinct position in cell membranes. Annexin A2 is involved in the movement of intracellular vesicles and is associated with an endosomal function. An endosomal localization has also been reported for annexin A1. Annexin A5, which is widely used as a tool to identify apoptotic cells, is associated with the Golgi apparatus, vacuolar membranes and endoplasmic reticulum [235]. Although a clear *in vivo* role for annexins has not yet been determined, a broad category of biological functions has been attributed to them, including aggregation and fusion of membranes and involvement in endocytosis and exocytosis, inhibition of phospholipase A2 and therefore anti-inflammatory effects on due to blocking the release of arachidonic acid, anticoagulant effects, interaction with cytoskeletal proteins and an enzymatic role in the metabolism of inositol phosphate. Some members of the annexin family are substrates of cellular kinases *in vivo*. Phosphorylation occurs at the N-terminus and can

modulate the properties of the annexins. For example, phosphorylated annexin A2 requires higher calcium concentrations for binding to phospholipids than the non-phosphorylated form, while phosphorylation of annexin A1 produces the opposite effect and increases degradation by proteolysis. Phosphorylation of annexin A1 and A2 regulates their ability to cause the aggregation of lipid vesicles. Further post-transcriptional modifications include glycosylation of annexins A1 and A2 and N-myristylation of A13 [236].

4.2 Annexin A1 structure

Each annexin is made up of two main domains: the N-terminal tail, different in length and sequence, and the C-terminal. The latter includes four homologous segments (except for annexin A6 which contains eight), numbered from I to IV and each consisting of five helices, called A, B, C, D, and E. The helices A and B, and the helices D and E form two parallel helix-loop-helix motifs. The helix C connects the C-terminal of the helix B with the 'N-terminal of helix D. The four domains together form a disc with a slight curvature. All the loops of the helix-loop-helix motifs are on the convex side of the disc, while the four C helices with the connecting loops are on the concave side. The four domains also form a hydrophilic channel [237]. Type II and type III calcium binding sites are in the loops of the helix-loop-helix motifs on the convex side of the molecule. Calcium ions bind to this surface of the protein core by simultaneously coordinating the carbonyl and carboxyl groups of annexin and the phosphate groups of glycerol belonging to the membrane phospholipids. In this way, the convex side of the disc is towards the membrane when annexin is associated with phospholipids [238]. The N-terminal domain of ANXA1 contains 41 residues and folds to form a unit structurally separate, probably on the concave side of the protein core. The first 26 amino acid residues of the N-terminal domain form two α-helices, which are inclined by 60 ° with respect to each other at the level of the amino acid Glu17. The α-helix between residues 26 and 18 interacts with the surface of segment IV of the central domain, while the other points towards the convex portion of the molecule. In absence of calcium, the latter partly occupies the position of the helix D of segment III within the protein, which extrudes from the surface. When the N-terminal domain is hidden within the core protein of ANXA1, it represents the inactive form of the molecule. Following calcium-mediated binding of annexin to the membrane, the segment III D helix acquires the appropriate conformation to bind calcium, forming a type II binding site. During this process, the N-terminal domain is expelled from the hydrophobic pocket and becomes accessible from the concave side of the molecule.

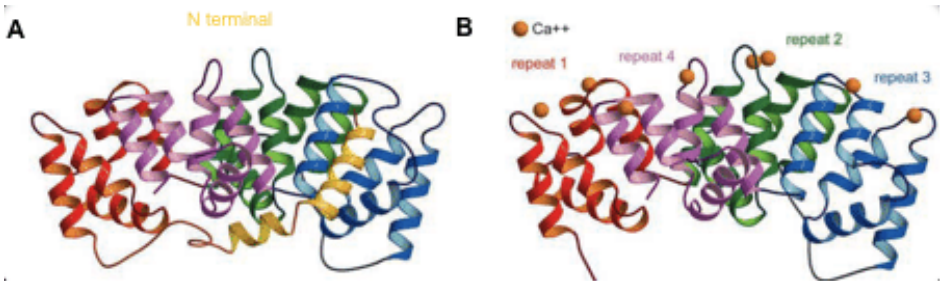

Fig.4.1: Molecular structure of Annexin A1

It can interact with specific molecules causing aggregation of membranes through various mechanisms: the interaction of the N-terminal helix with a second bilayer, the dimerisation of two annexin molecules through the N-terminal helices, or the binding of the concave sides of two annexins mediated by a dimer of the S100A11 protein, molecular partner of ANXA1. The N-terminal domain also contains the EGF phosphorylation site (Tyr21). It is located in the second α-helix and, when the protein is in the inactive state, this residue is hidden inside a hydrophobic pocket. In absence of calcium, therefore, annexin cannot be phosphorylated [239].

4.3 Role of the intracellular ANXA1

The different annexins show a different subcellular distribution, both at the cytosolic level and in association with the membranes, which changes according to the calcium concentration. The membranes that are linked by the various annexins are mainly represented by the plasma membrane and by membranes involved in biosynthesis or endocytosis. The N-terminal domain plays a fundamental role in the localisation of ANXA1: its proteolytic cleavage causes a redistribution of this protein from multivesicular endosomes to late endosomes, as occurs in the internalisation of the EGF receptor. ANXA1 together with S100A11 participates in the internal vesiculation process that generates multivesicular endosomes starting from early endosomes, as this complex is able to connect the membrane surfaces as previously described [239]. Once the forming vesicles evolve through the final fusion process, ANXA1 is phosphorylated by internalized EGF receptors intended for degradation. Phosphorylation makes this protein susceptible to proteolysis of the N-terminal domain: in this way not only the sequence required for the localisation of annexin in early endosomes is eliminated, but also the binding site with S100A11. As a result, the S100A11 dimer is released, along with the N-terminal sequence of ANXA-1, in a process that accompanies actual membrane fission and internal vesicle release. This annexin involvement may not be essential for endosome maturation and transport, but it may facilitate kinetics by providing a support structure for membranes [233]. By acting as a substrate for the tyrosine kinase domain of the EGF receptor, ANXA1 inhibits EGF-mediated proliferation. It can bind the Grb2 protein, which is located upstream of the MAPK signal cascade [240]. ANXA1 exerts a negative regulation of proliferation in different cell types through

sustained activation of the ERK cascade. This involves an anomalous organisation of the actin cytoskeleton which, together with the inhibition of cyclin D1 mediated by annexin, causes a block of proliferation [241]. ANXA1 is phosphorylated by various kinases, such as those associated with the PDGF receptor, the hepatocyte growth factor receptor and protein kinase C, thus contributing to its importance in proliferation [240].

4.4 ANXA1 extracellular role

In addition to its intracellular role, ANXA1 can be released and act on specific cells in an autocrine or paracrine manner. Most times, the protein is externalised during cell activation or due to stimulation by glucocorticoids. Indeed, they lead to an increase in the synthesis of ANXA1 in different cell types: a treatment with glucocorticoids causes a rapid exocytosis of annexin both in peripheral and central tissues. They can also induce phosphorylation of this protein and translocation to the membrane. It is not always completely clear how ANXA1 is released from cells. In the case of polymorphonuclear cells, the extrusion of the granules leads to an enrichment of annexin on the cell surface, but in cells where this protein is not stored in granules, the secretion is mediated through a different mechanism. ANXA1 does not contain a sequence or other secretory signal, but the involvement of the ABC-A1 protein, a transmembrane transporter, has been shown. Furthermore, since it has amphipathic properties, another possibility could be in passing through pores or channels. In recent years, the importance of Ser27 residue phosphorylation as a secretion signal has become evident. This post-transcriptional modification is commonly observed prior to the appearance of ANXA1 outside the cells [242]. Originally described as an inhibitor of phospholipase A2 (PLA2), ANXA1 can affect several components of the inflammatory response, as well as the metabolism of arachidonic acid. Initially, the inhibition of PLA2 activity was attributed to a binding of annexin to the substrate rather than to a direct interaction with the enzyme. This idea has been reconsidered as both a secreted form and a cytosolic form of this enzyme have been discovered. Cytosolic PLA2 is sensitive to calcium and shows a predilection for arachidonyl-containing phospholipids. This enzyme is mainly involved in the production of lipid mediators of inflammation, and the activation of arachidonic acid and PLA2 represents a limiting step in the synthesis of these molecules. ANXA1 has been shown to inhibit the activity of this enzyme directly, rather than through substrate depletion. However, the interaction between PLA2 and ANXA1 is unclear and occurs in specific cells [240]. ANXA1 has also been found in plasma, particularly during inflammatory events such as myocardial infarction. It specifically inhibits the trans-endothelial migration of leukocytes, limiting inflammation. The regulation of leukocyte extravasation by ANXA1 is mediated by the interaction of this protein with receptors present on neutrophils and monocytes, which belong to the receptor family of the Met-Leu-Phe formylated peptide (FPR). FPRs are G-protein-coupled receptors initially

identified as targets for bacterial peptides. The latter direct leukocytes as they migrate to the site of infection, activating a signal cascade mediated by FPR that leads to a reorganization of the cytoskeleton necessary for cell movement.

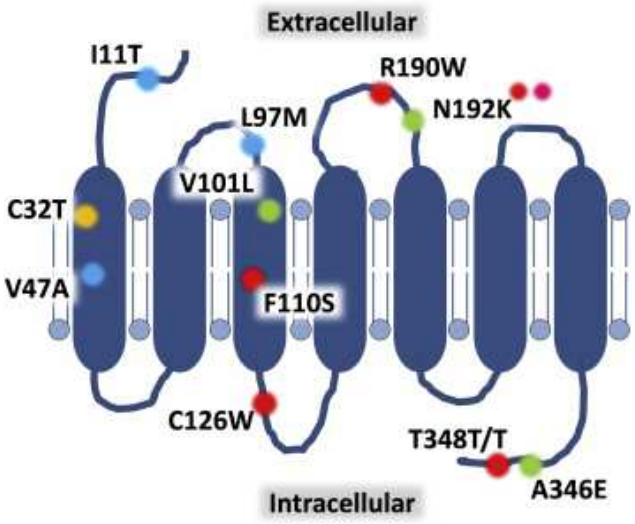

Fig.4.2: Structure of the FPR1

ANXA1 also binds the FPR2 receptor, also defined ALXR or receptor of lipoxin A4; in any case, the interaction is mediated by the N-terminal portion (the first 25 residues), which is found in a free form at the infection sites. The receptor activation also induces the loss of L-selectin from the leukocyte surface and the detachment of the attached leukocytes from the activated endothelium. Therefore, through the activation of members of the FPR family, ANXA1 can act as a regulator of leukocyte migration and as an endogenous anti-inflammatory protein. Furthermore, since the presence of FPR is not limited to leukocytes only, the interaction between these receptors and ANXA1 can regulate the migratory activity of other cell types, such as dendritic cells, hepatocytes, astrocytes and type II alveolar cells [243]. In general, ANXA1 exerts a powerful suppressive effect on the innate immune system, acting on granulocytes (PMN), monocyte-macrophages and mast cells, along with other different cell types. Polymorphonuclear leukocytes contain an abundant amount of annexin stored in granules. When PMNs are activated, the protein is immediately mobilised to the plasma membrane, where it acts negatively on the FPR2. The action of the protein at this site is terminated in a few minutes by the action of a membrane-bound enzyme, which cuts the annexin between residues 29 and 33. ANXA1 is also involved in the apoptosis of neutrophils, limiting the inflammatory response [244]. As with granulocytes, ANXA1 is released by macrophages and binds to FPR2, reducing the activity of these cells, including the release of eicosanoids and superoxide radicals. Mast cells represent a site of intense synthesis of ANXA1, which is on the granules, or within

them, and in other compartments, including the cytoplasm and the nucleus. Through interaction with the FPR2 membrane receptors, annexin leads to the reduction of histamine secretion and the production of prostaglandin D2 [242]. ANXA1 exhibits a different distribution and function in the cells of the adaptive immune system: lymphocytes contain a small amount of ANXA1 and do not bind this protein in the same way as monocytes / macrophages. In baseline conditions, both annexin and FPR2 are present on the membrane of T cells. Stimulation of T cells through TCRs leads to the externalisation of FPR2 and the release of ANXA1. The activation of this receptor by annexin modulates the strength of the signal mediated by TCR, increasing the levels of transcription factors such as AP-1, NF-κB and NFAT. An additional anti-inflammatory role of ANXA1 is in its ability to mediate the action of glucocorticoids, as it is involved in the antipyretic effect of these molecules and in blocking the hyperalgesic effect mediated by COX-2 [245]. Besides intervening in inflammatory processes, such as glucocorticoids, ANXA1 is involved in the regulation of hormonal secretion, suppressing the release of corticotropin and vasopressin, respectively, from the adenohypophysis and hypothalamus. It also contributes to the regulating action of glucocorticoids on other pituitary hormones, such as prolactin, thyroid stimulating hormone, luteinizing hormone and growth hormone. ANXA1 appears to mediate the *in vitro* glucocorticoid-induced reduction in testosterone production in the testis, and to exert positive effects on glucose-mediated insulin release from pancreatic cells [245]. In addition to the role of mediator of the action of glucocorticoids, ANXA1 is involved in the regulation of apoptosis: in some cases for its pro-aptotic effect, in others a link between ANXA1 and cell resistance to apoptosis has been observed. The reason for this difference could be due to the cell type or the state of differentiation [240].

4.5 ANXA1 externalisation

The proteins secreted by eukaryotic use an N-terminal signal peptide to direct their co-translation to the ribosome of the rough endoplasmic reticulum. Subsequently, they progress to the Golgi apparatus and, finally, through secretory vesicles, they are directed to the cell surface or to the extracellular environment [246]. Studies conducted on ANXA1 revealed that this protein lacks the N-terminal signal peptide necessary for the classic protein externalization; this suggests that ANXA1 could be externalised through different secretory pathways [247]. Furthermore, it has been observed that, after its externalization, ANXA1 undergoes a proteolytic cleavage on the N-terminal [248].

Thanks to various studies, it has been deduced that ANXA1 can be externalised through five mechanisms: The first way for ANXA1 externalisation may depend on a myristylation process. Indeed, the protein sequence has potential sites for this modification, and PKC can target its myristylated substrate to the plasma membrane. The passage of ANXA1 across the plasma membrane

could be facilitated by lipidization [249]. The second proposed mechanism, includes the inhibition of ATP-Binding Cassette ABC-A1, a transporter involved in ANXA1 secretion, but it can only partially suppress the protein's externalisation, suggesting that other mechanisms may contribute to its release [250]. The third way was highlighted PMNs in adhesion to endothelial cells, the granules fuse with the plasma membrane and, during degranulation, release ANXA1 in the extracellular compartment [251]. The fourth mechanism is by activating flippase and scramblase, the lipid bilayer orients itself outward exposing the phosphatidylserine. Since ANXA1 has a great affinity for acid phospholipids (in particular phosphatidylserine), it has been hypothesised that this protein is exposed on the surface of microparticles, for example, released by PMNs [252]. Finally, the fifth way for ANXA1 secretion involves the fusion of small vesicles, called exosomes, with the plasma membrane. All the proteins associated with these nano-vesicles could be externalised, including ANXA1 [253].

Studies conducted by [254] highlight the role of EVs containing ANXA1 in the intestinal inflammatory process and in intestinal epithelial lesions. Patients with inflammatory bowel disease, compared to healthy donors, showed elevated levels of EVs containing ANXA1 in serum. Thus, these micro-vesicles are likely to be present in response to the inflammatory process and could serve as a biomarker of inflammation in the intestinal mucosa. Furthermore, EVs containing ANXA1 mediate tissue wound repair processes: their role in colonoscopy-induced lesions of the murine intestinal mucosa was studied by [254]. The repair was investigated using synthetic nanoparticles (NP) containing Ac2-26, capable of simulating the pro-restorative effects of ANXA1 released by EVs. The repair was accelerated following the administration of the latter intramucosally. Our studies in [255] investigated the role of ANXA1 in promoting the secretion of EVs and their involvement in the processes of metastasis, in particular in the process of angiogenesis underlying the development of metastases. The exosomes can induce the formation of new vessels that guarantee an adequate supply of nutrients and oxygen to the tumour [256].

4.6 ANXA1 in differentiation and motility cell processes

ANXA1 acts as an inhibitor of proliferation in lung cancer epithelial cells A549: when these cells are treated with glucocorticoids to induce them to differentiate, they increase the levels of ANXA1, together with the expression of CD26, a marker of epithelial cell differentiation [257]. In thyroid cancer cell lines, ANXA1 expression varies according to the stage of differentiation: papillary thyroid cancer cells and follicular cells show high amounts of ANXA1, while the protein levels are very low in undifferentiated tumour forms [258]. Also in the case of cervical neoplasms, an association has been observed between the expression of ANXA1 and cell differentiation in invasive squamous cell carcinoma [259]. In biopsies of patients with nasopharyngeal carcinoma and in biopsies of patients

with lymph node metastases of the cervix, a reduction in the expression of ANXA1 was shown compared to normal nasopharyngeal tissue. The reduction of ANXA1 correlates with a poor histological differentiation and with an advanced stage of the disease, suggesting a possible use of this protein as a biomarker of the differentiation stage of nasopharyngeal carcinoma [260]. The same expression profile has been found in gastric cancer: low protein levels are associated with an advanced neoplastic stage, the formation of lymph node metastases and inadequate histological differentiation [261]. Studies on the differentiation of murine C2C12 myoblasts show that the expression of ANXA1 increases during this process and that a negative regulation of the protein inhibits differentiation [262].

ANXA1 is highly expressed in human keratinocytes: it has been observed in the cytosol of the lower layers of the epidermis, beyond which it is involved in the formation of the horny envelope. This change in cellular localization demonstrates its involvement in keratinocyte differentiation [263]. ANXA1 is soluble in the keratinocytes of the basal layer and subsequently moves towards the internal cytoplasmic surface with increasing calcium levels during progressive differentiation. Once at the plasma membrane, the annexins are bound to each other and probably to other proteins, via the N-terminal domain. In basal cells, it can act as a signal transduction protein, or it can anchor the cytoskeleton to the cell membrane. In differentiated cells, ANXA1 is a substrate of transglutaminase-1. Although all annexins interact with membranes, ANXA1 is the only member included in the stratum corneum, and this demonstrates a role of this specific annexin in the assembly of this structure [264].

Numerous examples are reported in the literature concerning the effects of ANXA1 on the process of cell migration and invasion. Both in cells deriving from colorectal adenocarcinoma [265] and in melanoma cell lines [266], the suppression of ANXA1 causes a reduction in the degree of invasiveness, while in BLBC cells there is a change in the cellular phenotype: they become similar to mesenchymal cells of the epithelium, with a low migration rate. Triple negative breast cancer (TNBC) cells equally transfected in order to reduce the expression of ANXA1 show a reduction in the invasion rate [267]. Even in the case of pancreatic ductal adenocarcinoma cells, the shutdown of ANXA1 expression led to a loss of migratory and invasive capacity [268]. Another tumour line in which the effects of ANXA1 have been evaluated is non-small cell lung cancer cells, in which the shutdown of annexin expression resulted in a loss of migratory and invasive capacity [269]. In esophageal squamous cell carcinoma cells, an increase in the expression of ANXA1 induced by transfection is associated with a greater invasive and migratory capacity than in wild type cells [270].

5. Aim of the work

Mesoglycan is a mixture of glycosaminoglycans able to enhance some fundamental processes in wounds repair. Particularly, it promotes the re-epithelialization through the action on keratinocytes and fibroblasts and supports angiogenesis. The mechanism of action by which the mesoglycan acts in this system is not still clear.

The general aim of this PhD project has been to study the molecular mechanism by which this mixture of glycosaminoglycans promotes tissue regeneration. The *in vitro* approach, based on the use of different cell type such as keratinocytes fibroblasts and endothelial cells, allowed to focus the attention on several aspects of wound repair, including migration, invasion and angiogenesis. Prisma® Skin, a new pharmaceutical device developed by Mediolanum Farmaceutici S.p.a. which includes alginates, hyaluronic acid and mainly mesoglycan, has allowed to evaluate the effects *in vivo* on patients suffering from chronic ulcers.

Another aim was to develop a new medical device containing mesoglycan in order to promote a better compliance for the patients in the administration and release of the drug.

6. Material and methods

6.1 Cell cultures

HaCaT cell line (human immortalized keratinocytes spontaneously established from a transformed human epithelial cell line of adult skin) was purchased from CLS Cell Lines Service GmbH (Eppelheim, Germany) and was maintained in Dulbecco's modified Eagle's medium (DMEM, Euroclone, Milan, Italy) with 10% fetal bovine serum (FBS, Euroclone, Milan, Italy).

BJ cell line (Human immortalized fibroblasts) was purchased from ATCC (American Type Culture Collection) (ATCC® CRL2522™) and was maintained in Eagle's Minimum Essential Medium (MEM) with 10% FBS, 1% L-glutamine, 1% Sodium Pyruvate, 1% NEAA (Non-Essential Amino Acids).

HUVEC cell line was purchased from American Type Culture Collection (ATCC, Manassas, VA, USA) (ATCC® PCS-100-010™) and cultured in endothelial growth medium (EGM-2) medium contains EBM-2 medium (serum free, growth-factor free), supplemented with 2% fetal bovine serum (FBS), human fibroblast growth factor-B (hFGF-B), human epidermal growth factor (hEGF), human vascular endothelial cell growth factor (hVEGF), long R insulin-like growth factor-1 (R3-IGF-1), ascorbic acid, hydrocortisone, and heparin (Lonza). Cells cultured until passage 10. All the media were supplemented with antibiotics (10000 U/ml penicillin and 10 mg/ml streptomycin). Cells were maintained at 37 °C in 5% CO_2 −95% air humidified atmosphere and were serially passed at 70–80% confluence.

MLEC WT and SDC4-KO were isolated form Wild-type and syndecan-4-null C57BL6 mice (4–6 week-old females) obtained from Charles River Laboratories (UK), and kept under pathogen-free conditions in the Animal Facility of the Queen Mary University of London for 7 days of acclimatisation. All experiments were approved in accordance with UK Home Office regulations, under the UK legislation for the protection of animals. Wild-type and syndecan-4-null mice were sacrificed by cervical dislocation and lungs were excised and minced with a scalpel for 5 minutes. The lung fragments were digested with collagenase (Life Technologies, Carlsbad, California, USA) for 1 hour at 37◦C. then transferred in a petri dish containing 10mL of MLEC medium (40% Dulbecco's modified Eagle's low glucose medium (DMEM, Life Technologies, Carlsbad, California, USA), 40% Hams F-12 Medium (Life Technologies, Carlsbad, California, USA), Endothelial Growth Supplement (Sigma Aldrich, St. Louis, MO, USA) and 20% of heat inactivated foetal calf serum (Invitrogen, Carlsbad, California, USA). The resulting solution was disaggregated by aspiration through a 19.5-gauge needle for 4 times. The resulting cell suspension was filtered with a 70 μm filter and then centrifuged at 1200 RPM for 5 minutes. The resultant cell pellet was resuspended in MLEC

medium and plated on flasks coated with a mixture of 0.1% gelatin (Sigma Aldrich, St. Louis, MO, USA), 10 mg/ml fibronectin (Millipore, Burlington, Massachusetts, USA) and 30 μg/ml collagen (Advanced Biomatrix, Sea Lion Pl, Carlsbad, CA, USA). After 24 hours the media was refreshed. After one week the endothelial cells were purified by a positive (ICAM-2; BD Pharmingen, Franklin Lakes, NJ, USA) cell sort using anti-rat IgG-conjugated magnetic beads (Dynal, Wiltshire, UK).

6.2 Preparation and seeding of mesoglycan

Powder of sodium salt mesoglycan is composed of heparin (40% low molecular weight from 6.5 to 10.5 kDa and 60% less than 12 kDa, sulphurylation degree 2.2–2.6), HS (UFH-unfranctioned heparin- from 12 to 18 kDa up to 40 kDa; sulphurylation degree 2.6), dermatan sulfate deriving from epimerization of glucuronic acid of chondroitin sulfate (molecular weight 18–30 kDa, sulphurylation degree 1.3) with a total sulphurylation degree of 9.1. The manufacturing of the drug complied with the pharmaceutical quality standard required for active substances of biological origin approved in the EU, including those concerned with viral and BSE safety. It was kindly provided by Mediolanum Farmaceutici S.p.a. (Milan, Italy) and dissolved in the cell medium at an initial concentration of 1 mg/ml. After dose-effect curve results performed in our previous works [183], [271], mesoglycan administration was established in a dose of 0.3 mg/ml for all performed experiments.

6.3 Confocal microscopy

After the specific time of incubation, HaCaT, BJ, HUVEC or MLEC cells were fixed in p-formaldehyde (4% v/v with PBS; Sigma-Aldrich) for 5 min, permeabilized in Triton X-100 (0.5% v/v in PBS; Sigma-Aldrich) for 5 min, and then incubated in goat serum (20% v/v PBS; Lonza, NJ) for 30 min. Then, the cells were incubated with anti-E-cadherin antibody (mouse monoclonal; 1:500, BD Transduction Laboratories, San Jose, CA), anti-CK6 (rabbit polyclonal; 1:500; Flarebio Biotech LLC., MD), anti-CK10 (rabbit polyclonal; 1:500; Flarebio Biotech LLC.), anti-phospho PKCα (rabbit polyclonal; 1:100; Thermo Fisher Scientific, IL), anti-SDC4 (rabbit polyclonal; 1:100; Thermo Fisher Scientific), anti-integrin β1 (mouse monoclonal; 1:250; Santa Cruz Biotechnologies, CA), anti-phospho paxillin (mouse monoclonal; 1:100; Santa Cruz Biotechnologies), anti-ezrin (mouse monoclonal, 1:100, Santa Cruz Biotechnologies), anti-ANXA1 (rabbit polyclonal; 1:100; Invitrogen Thermo Fisher Scientific), anti-S100A11 (mouse monoclonal; 1:100; Santa Cruz Biotechnologies), anti-involucrin (mouse monoclonal; 1:250; Santa Cruz Biotechnologies, CA, USA), anti-vimentin (1:500; Santa Cruz Biotechnologies; CA, USA), anti- COL1A (1:100; Santa Cruz Biotechnologies, CA, USA), anti-fibronectin (1:100; Santa Cruz Biotechnologies, CA, USA), anti-VE cadherin (1:200; Santa Cruz Biotechnologies, CA, USA), rabbit polyclonal antibodies anti-FAPα (1:250; Santa Cruz Biotechnologies, CA, USA), anti-αSMA (1:100; Cusabio Life Science, College Park, MD, USA),

anti-VEGF (rabbit polyclonal, 1:100; Santa Cruz Biotechnologies, CA, USA), anti-FGF-2 (1:100; Santa Cruz Biotechnologies, CA, USA), anti p-VEGFR2 (rabbit monoclonal; (Tyr951); 1:100; Cell Signaling Technology, Danvers, Massachusetts, USA); FAK (rabbit monoclonal; 1:1000; Cell Signaling Technology, Danvers, Massachusetts, USA) overnight at 4°C. F-actin was evaluated by 5 µg/ml of Phalloidin-FITC (Sigma-Aldrich; Saint Louis, MO, USA) for 30 min at RT in the dark. After two washing steps, the cells were incubated with antirabbit and/or antimouse DyLight (488- and/or 550-conjugate; 1:1,000; ImmunoReagents Inc., NC) for 2 h at RT. To detect nucleus, Hoechst 33342 nucleic acid stain (1:5,000; H1399, Molecular Probes, Thermo Fisher Scientific) was used and samples were excited with a 458 nm Ar laser. A 488 nm Ar or a 555 nm He-Ne laser was used to detect emission signals from target stains. The samples were vertically scanned from the bottom of the coverslip with a total depth of 5 µm and a 63 × (1.40 NA) Plan-Apochromat oil-immersion objective. Images and scale bars were generated with Zeiss ZEN Confocal Software (Carl Zeiss MicroImaging GmbH, Jena, Germany). For immunofluorescence analysis and quantification, final images were generated using Adobe Photoshop CS4, version 11.0. If suitable, quantifications were performed from multichannel images obtained using a 63 × 1.4 NA objective and using the ImageJ software (NIH, Bethesda, MD), as follows. Briefly, 10 field images from a single coverslip from n = 3 biological repetitions were randomly selected and registered for each experimental condition identifying 10 distinct cells by Hoechst 33342 nuclear staining. Then, the individual cell total area was selected using the area selection tool, the fluorescence intensity value was measured and expressed as Arbitrary Unit (A.U.; the ImageJ software) subtracting background. The obtained mean value was used to compare experimental groups.

6.4 Western blot

Protein expression was examined by SDS-PAGE, as described previously [272]. Briefly, total intracellular proteins were extracted from the cells by freeze/thawing in lysis buffer containing protease inhibitors. Protein content was estimated according to Biorad protein assay (BIO-RAD). A total of 20 µg of proteins were visualized using the chemioluminescence detection system (Amersham biosciences; Little Chalfont, UK) after incubation with primary antibodies against anti-E-cadherin antibody (mouse monoclonal; 1:5000, BD Transduction Laboratories, San Jose, CA); anti-CK6 (rabbit polyclonal; 1:1000; Flarebio Biotech LLC., MD); anti-CK10 (rabbit polyclonal; 1:1000; Flarebio Biotech LLC.); anti-phospho PKCα (rabbit polyclonal; 1:1000; Thermo Fisher Scientific, IL); anti-SDC4 (rabbit polyclonal; 1:1000; Thermo Fisher Scientific); anti-integrin β1 (mouse monoclonal; 1:1000; Santa Cruz Biotechnologies, CA); anti-ezrin (mouse monoclonal, 1:1000, Santa Cruz Biotechnologies); anti-ANXA1 (rabbit polyclonal; 1:10000; Invitrogen Thermo Fisher Scientific); anti-S100A11 (mouse monoclonal; 1:1000; Santa Cruz Biotechnologies); anti-involucrin

(mouse monoclonal; 1:250; Santa Cruz Biotechnologies, CA, USA); TSG101 (mouse monoclonal; 1:1000; ThermoFisher Scientific; Waltham, MA, USA), calreticulin (rabbit polyclonal; 1:1000; Elabscience; Houston, TX, USA); anti-p-VEGFR2 (rabbit monoclonal; (Tyr951); 1:500; Cell Signaling Technology, Danvers, Massachusetts, USA); ERK (rabbit monoclonal; 1:1000; Cell Signaling Technology, Danvers, Massachusetts, USA); p-ERK (rabbit monoclonal; 1:1000; (Thr202/Tyr204); Cell Signaling Technology, Danvers, Massachusetts, USA), p38MAPK (rabbit monoclonal; 1:1000; Cell Signaling Technology, Danvers, Massachusetts, USA); p-HSP27 (rabbit monoclonal; S78; 1:250; Cell Signaling Technology, Danvers, Massachusetts, USA); FAK (rabbit monoclonal; 1:1000; Cell Signaling Technology, Danvers, Massachusetts, USA); p-FAK (rabbit monoclonal; (Tyr397) 1:1000; Cell Signaling Technology, Danvers, Massachusetts, USA); VEGF (rabbit polyclonal; 1:100; Santa Cruz Biotechnologies; Dallas, TX, USA); CD81 (mouse monoclonal; 1:500; BD Pharmingen, Franklin Lakes, NJ, USA); CD63 (mouse monoclonal; 1:500; BioLegend; San Diego, CA); GAPDH (rabbit monoclonal; 1:1000 Cell Signaling Technology, Danvers, Massachusetts, USA); β-actin (mouse monoclonal; 1:1000; Santa Cruz Biotechnologies; Dallas, TX, USA). The blots were exposed to Las4000 (GE Healthcare Life Sciences) and the relative band intensities were determined using ImageQuant software (GE Healthcare Life Sciences). Results were considered significant if $p < 0.01$.

6.5 Measurement of intracellular Ca^{2+} signalling

Intracellular Ca^{2+} concentrations [Ca^{2+}] were measured using the fluorescent indicator dye Fura 2-AM (Sigma Aldrich, St. Louis, MO, USA), the membrane-permeant acetoxymethyl ester form of Fura 2, as previously described [273]. Briefly, HaCaT cells (1×10^5/mL) were washed in (PBS) resuspended in 1 mL of Hank's balanced salt solution (HBSS, Thermo Fisher Scientific, Waltham, MA, USA) containing 5 µM Fura 2-AM and incubated for 45 min at 37 °C. After the incubation period, cells were washed with the same buffer to remove excess of Fura 2-AM and then incubated in 1 mL of buffer. Keratinocytes were then transferred to the spectrofluorimeter (Perkin-Elmer LS-55, Waltham, MA, USA). Treatments with ionomycin (1 mM; Sigma Aldrich, St. Louis, MO, USA), EDTA (15 mM, Sigma Aldrich, St. Louis, MO, USA), fMLP (50 nM; Sigma Aldrich, St. Louis, MO, USA), Ac2-26 (1 µM), BOC1 (100 µM), were carried out by adding the appropriate concentrations of each substance into the cuvette in Ca^{2+}-free HBSS/0.5 mM EDTA buffer. The excitation wavelength was alternated between 340 and 380 nm, and emission fluorescence was recorded at 515 nm. The fluorescence ratio was calculated as F340/F380 nm. Maximum and minimum [Ca^{2+}] were determined at the end of each experimental protocol by adding to the cells HBSS containing 1 mM ionomycin and 15 mM EDTA, respectively, according to the equation of Grynkiewicz [274].

6.6 siRNAs and transfection

The knockdown of SDC4 and ANXA1 proteins in HaCaT or HUVEC cells was performed using siRNAs targeting human SDC4 and ANXA1 proteins. All siRNAs were purchased from IDT (Integrated DNA Technologies Inc., Coralville, IA). The duplex sequences to target SDC4 were: (a) sense 5′-AGA UAA UAA AAC CUG GUA CUU UCT A-3′ and antisense 3′-UUU CUA UUA UUU UGG ACC AUG AAA GAU-5′; (b) sense 5′-CAA UGA GUU CUA CGC GUG AAG CUT G-3′ and antisense 3′-UGG UUA CUC AAG AUG CGC ACU UCG AAC-5′; (c) sense 5′-CCA AGA GAA UCU CAC CCG UUG AAG-3′ A and antisense 3′-GGG GUU CUC UUA GAG UGG GCA ACU UCU-5′. The duplex sequences to target ANXA1 were: (a) sense 5′-GCU AUG AUC AGA AGA CUU UAA UAA T-3′ and antisense 3′-UUC GAU ACU AGU CUU CUG AAA UUA AUA-5′; (b) sense 5′-GUU GUU UUA GCU CUG CUA AAA ACT C-3′ and antisense 3′-UCC AAC AAA AUC GAG ACG AUU UUU GAG-5′; (c) sense 5′-AAG UAC AGU AAG CAU GAC AUG AAC A-3′ and antisense 3′-GGU UCA UGU CAU UCG UAC UGU ACU UGU-5′. siRNA Oligo-Scrambled (Santa Cruz Biotechnology) was used as control at the same concentration. The cells were initially plated in media containing 10% FBS. After 24 h, the cells were washed once with PBS and transfected or not with siRNAs by Lipofectamine 2000 (ThermoFisher Scientific; Waltham, MA, USA) according to the manufacturer's instructions. The cells were processed for western blot analysis and confocal microscopy at 24 and 48 h after transfection. The administration of mesoglycan 300 mg/ml and/or VEGF 10ng/mL was performed 24 h after transfection.

6.7 *In vitro* wound-healing assay

HaCaT, BJ, HUVEC and MLEC cells were seeded in a 12-well plastic plate at 5×10^5 cells for well. After 24 h incubation, cells reached 100% confluency and a wound was produced at the center of the monolayer by gently scraping the cells with a sterile plastic p10 pipette tip to create a wound area of about 500 µm. After removing incubation medium and washing with PBS, cell cultures were incubated in presence of mesoglycan (0.3 mg/ml), siSDC4 (100 nM), siANXA1 siSDC4 (100 nM), EVs ctrl (20µg or $1x10^6$), EVs mesoglycan (20µg or $1x10^6$), Ac2-26 (1 µM; Tocris Bioscience, Bristol, UK), BOC1 (100 µM; Bachem AG, Bubendorf, Switzerland), VEGF (10ng/mL) or in growth medium as control. All experimental points were further treated with mitomycin C (10 µg/mL, Sigma Aldrich, St. Louis, MO, USA) to ensure the block of mitosis. The wounded cells were then incubated at 37 °C in a humidified and equilibrated (5% *v/v* CO_2) incubation chamber of an Integrated Live Cell Workstation Leica AF-6000 LX (Leica Microsystems, Wetzlar, Germany). A 10× phase contrast objective was used to record cell movements with a frequency of acquisition of 10 min on at least 10 different positions for each experimental condition. The migration rate of individual cells was determined by measuring the wound closure from the initial time to the selected time-points (bar of

distance tool, Leica ASF software, version Lite 2.3.5, Leica microsystem CMS Gmvh). For each wound 5 different positions were registered, and for each position 10 different cells were randomly selected to measure the migration distances.

6.8 Invasion assay

Cell invasiveness was studied using the Trans-well Cell Culture (12 mm diameter, 8.0-fim pore size) purchased from Corning Incorporated (New York, NY, USA), as reported in [272]. Briefly, the chambers were coated with Matrigel (Becton Dickinson Labware) that was diluted with 3 volumes of medium serum-free and stored at 37 °C until its gelation. Cells were plated in 350 µL of medium serum-free at a number of 9×10^4/insert in the upper chamber of the trans-well. 1,4 ml of MEM or EGM-2 with or without mesoglycan (0.3 mg/ml), siSDC4 (100 nM), siANXA1 siSDC4 (100 nM), EVs ctrl (20µg or $1x10^6$), EVs mesoglycan (20µg or $1x10^6$), Ac2-26 (1 µM; Tocris Bioscience, Bristol, UK), BOC1 (100 µM; Bachem AG, Bubendorf, Switzerland) were put in the lower chamber and the trans-well was left for 24 h at 37 °C in 5% CO2 -95% air humidified atmosphere. After that, the medium was aspirated, the filters were washed twice with PBS 1 × and fixed with 4% p-formaldehyde for 10 min, then with 100% methanol for 20 min. The filters so fixed, were stained with 0.5% crystal violet prepared from stock crystal violet (powder, Merck Chemicals) by distilled water and 20% methanol for 15 min. After that, the filters were washed again in PBS 1 × and cleaned with a cotton bud. The number of cells that had migrated to the lower surface was counted in 10 random fields using EVOS® light microscope (10 ×) (Life technologies Corporation).

6.9 Cytosol and membrane extracts

Compartmentalized protein extracts were obtained as reported in [275]. Briefly, HaCaT cells were washed twice with PBS, detached with trypsin-EDTA 1× in PBS, harvested in PBS and centrifuged for 5 min at 600*g* at 4°C. After that, the cells were lysed in 4 ml of buffer A (Tris HCl 20 mM, pH 7.4; sucrose 250 mM; DTT 1 mM; protease inhibitors, EDTA 1 mM in water; all from Sigma-Aldrich), sonicated (5 s pulse –9 s pause for 2 min, amplitude 40%) and then centrifuged at 4°C for 10 min, at 5,000*g*. The resulting supernatants were ultra-centrifuged for 1 hr at 100,000*g* at 4°C, until to obtain new supernatants corresponding to cytosol extracts. Each resultant pellet was dissolved in 4 ml of buffer A and ultra-centrifuged for 1 hr at 100,000*g* at 4°C. The pellets were then resuspended in 250 µl of buffer B (Tris HCl 20 mM, pH 7.4; DTT 1 mM; EDTA 1 mM; Triton X-100 1%, in water) and left overnight on orbital shaker at 4°C. Next, the solution was centrifuged for 30 min at 50,000*g* at 4°C: The supernatants represent membrane extracts.

6.10 Immunoprecipitation

For immunoprecipitation experiments, HaCaT cells were treated or not with sodium mesoglycan 300 μg/ml for 48 hr. After incubation, cell lysates were made by washing twice the cells with PBS and then solubilizing them in lysis buffer (50 mM Tris-HCl, 150 mM NaCl, 1% NP-40; all from Sigma-Aldrich) with Protease Inhibitor (Roche Life Sciences, Germany). An equal amount of each protein lysate (200 μg) was incubated with monoclonal anti-S100A11 (2 μg; mouse monoclonal; clone B5; sc-390250, Santa Cruz Biotechnologies) and polyclonal anti-ANXA1 (2 μg; rabbit polyclonal; 71–3,400; Invitrogen, Thermo Fisher Scientific) antibodies for 3 hr at RT, followed by 1 hr incubation with 35 μl of protein A-Sepharose beads (Sigma-Aldrich) previously treated with 1% (w/v in lysis buffer) bovine serum albumin (BSA; Sigma-Aldrich) and then equilibrated with lysis sample buffer according to the manufacturer's instructions. Mouse (IgGM; 2 μg) and rabbit (IgGR; 2 μg) IgGs (Sigma-Aldrich) were also used as controls. The beads were then washed, boiled, and the supernatants were used to immunoblot with antibodies against S100A11 (mouse monoclonal; 1:1,000; clone B5; sc-390250; Santa Cruz Biotechnologies) and ANXA1 (rabbit polyclonal; 1:100; 71–3,400; Invitrogen, Thermo Fisher Scientific) as previously described in Western blot Section. All experiments were performed in three independent experiments.

6.11 Field Emission-Scanning Electron Microscope (FE-SEM) Analysis

Sample morphology was analysed using a FE-SEM model LEO 1525 (Carl Zeiss SMTAG; Oberkochen, Germany). The EVs enriched in exosomes were fixed with 2% *v/v* p-formaldehyde and 1% *v/v*glutaraldehyde (Sigma-Aldrich; Saint Louis, MO, USA) in PBS. Next, a drop of the suspension was spread on a carbon tab placed on an aluminium stub (Agar Scientific; Stansted, UK) and left to dry in a stream of nitrogen for 25 min. Then, the dried samples were coated with gold (layer thickness 250 Å) using a sputter coater (model 108 A, Agar Scientific; Stansted, UK). Each analysis was performed in triplicate.

6.12 Dynamic Light Scattering (DLS) Analysis

The DLS technique was performed using a Zetasizer Nano S instrument (Worcestershire, UK) in order to obtain particle size distribution by number of the EVs. The DLS instrument works at 25 °C and is equipped with a 5.0 mW He-Ne laser operating at 633 nm with a scattering angle of 173°. Each measurement was repeated in triplicate.

6.13 EVs isolation

HUVEC cells (about 2×10^6 cells) were incubated for 24 hours in EGM-2 (DMEM, Euroclone, Milan, Italy) without FBS treated or not with mesoglycan (0.3 mg/ml). Then, the supernatant was centrifuged at 4,400x*g* at 4°C for 15 min to pellet death cells, followed by a second centrifugation at

13,000x*g* at 4°C for 2 min to remove apoptotic bodies. EVs were enriched by centrifuging at 20,000x*g* at 4°C for 30 min, the supernatant was removed, and pellets were re-suspended in the selected buffers. The buffer we chose for the resuspension was 100 µl PBS for the administration to cells and nanoparticle tracking analysis 30 µl RIPA lysis buffer to perform Bradford assay. All analyses were performed on fresh isolated fractions.

The enrichment of exosomes from cell culture supernatants has been performed as reported in [276]. HaCaT cells (about 8×10^7 cells) were incubated for 24 h in DMEM medium without FBS treated or not with mesoglycan (0.3 mg/mL). Conditioned medium (also reported as SS) was collected and centrifuged for 5 min at 300× *g* at room temperature (RT) to remove detached cells; the supernatant was transferred and centrifuged for 10 min at 2000× *g* at 4 °C to remove dead cells. The obtained supernatant was transferred and centrifuged at 10,000× *g* for 30 min at 4 °C to eliminate cell debris. Then, the cleared supernatant was transferred to ultracentrifuge tubes and centrifuged for 70 min at 100,000× *g* at 4 °C. Next, the supernatant was stored and used as EDS (EVs-depleted supernatant); the pellet was washed in PBS and re-ultracentrifuged at 100,000× *g* at 4 °C for 70 min. Finally, the supernatant was removed, and the pellet was resuspended. The buffer we selected for the resuspension was sterile bidistilled water with 5 mM EDTA, to avoid vesicles aggregation, for FE-SEM (Field Emission-Scanning Electron Microscope) and DLS (dynamic light scattering) analysis, 50 µL RIPA lysis buffer for Western blotting, or 200 µL PBS for the administration to cells. The normalization through Bradford assay has been performed using the correspondent amount of EVs lysed in RIPA buffer. This normalization has been important for us in order to administrate to cells the same amount of EVs (20 µg of proteins), derived from HaCaT treated with mesoglycan or not (EVs mesoglycan and EVs ctrl, respectively), on all the experimental points. All analyses were performed on fresh isolated fractions.

6.14 Gelatin gel zymography

Gelatinolytic activity was detected by SDS-PAGE zymography, as reported in [183]. Briefly, serum-free supernatant samples were analysed under non-reducing conditions without boiling, through a 10% SDS-polyacrylamide gel co-polymerized in the presence of gelatin 0.1% (Sigma-Aldrich). After the electrophoresis run, performed at 125 V, the proteins in the gel were renatured in a 2.5% Triton X-100 solution for 1 h. The gel was then incubated with 50 mM Tris–HCl, pH 7.8, 200 mM NaCl, 5 mM $CaCl_2$ and 5 µM $ZnCl_2$ at 37 °C for 48 h, which allows substrate degradation. Finally, the gels were stained with 0.5% Coomassie Brillant Blue R-250. Proteolytic bands were visualized by destaining with 10% methanol and 5% acetic acid.

6.15 Tube formation assay

A 24-well plate was coated with Matrigel (Becton Dickinson Labware, Franklin Lakes, NJ, USA) mixed to EGM-2 1:1 for HUVEC cells and MLEC medium 1:1 for MLEC WT and SDC4-KO on ice and incubated at 37 °C for 30 min to allow gelation to occur. The cells were seeded to the top of the gel at a density of 2×10^4 cells/well in presence or not of the treatments. Cells were incubated at 37 °C with 5% CO_2. After 12 h, pictures were captured using EVOS® light microscope (10 ×) (Life technologies Corporation, Carlsbad, CA, USA). The length of each tube was measured, and the number of branches was calculated using ImageJ (NIH, Bethesda, MD, USA) (Angiogenesis Analyzer for ImageJ) software.

6.16 Nanoparticle tracking analysis for sizing EVs

Approximately 0.5 ml of EVs (between 10^6 to 10^9 vesicles) in suspension were loaded onto the Nanosight NS300 with 488 nm scatter laser and high sensitivity camera (Malvern Instruments Ltd., Malvern, UK); five videos of 90 seconds each were recorded for each sample. Data analysis was performed with NTA2.1 software (Nanosight, Malvern, UK). Software settings for analysis were the following, Detection Threshold: 5–10; Blur: auto; Minimum expected particle size: 20 nm.

6.17 Excisional wound model

Female C57BL/6 (5 wk) mice were purchased from the Charles River Laboratories (Italy) and housed 5 per cage. All the procedures were performed in accordance with the local institutional guidelines for animal care established by Italian Health Ministry (authorization n. 489/2018-PR) and performed according to Italian law 26/2014. On the day of surgery, the hair on the back of each mouse was clipped, and the skin was wiped with ethanol. Mice were anesthetized by inhalation of isoflurane, and two 6-mm wounds were made using punch biopsies on their shaved dorsal skin. Around the wounds a sterile silicone sheet ring has been carefully placed previously treated with an instant-bonding adhesive (super attak, Loctite®; Henkel, Milan, Italy) and further fixed by surgical stitches (AgnTho´s AB; Lidingö, Sweden) (with the glue side down) so that the wound is centered within this created splint. On every mouse one wound was treated with a vehicle control (100 µl of PBS) and the other with mesoglycan (100 µl of mesoglycan 0.3 mg/ml). In total, the substances were administered every 48 hours to each mouse by topical application. The wound area was determined by taking daily digital pictures of the wounds. The mice were sacrificed after 10 days, and the size of wound area was recorded. The percentage of wound healing was based on changes in the same wound on the same mouse for indicated time points. Standardized photos for each wound were taken at the same distance between the camera and the pre-anesthetized mice. The photos were analysed using planimetry for objective measurement for the degree of wound healing [277]. Total pixels covering

unhealed areas have been drawn on digital images using a pattern overlay in ImageJ (ImageJ software, Wayne Rasband, National Institute of Health, Bethesda, MD, USA). The number of pixels covering the wound region on a given day was divided by the number of pixels scattered over the initial wound on day 0 to calculate a percentage of the closure. Percentage, rather than distance (e.g. mm) of wound closing, was determined from the estimated wound areas (pixel density).

6.18 Immunofluorescence on tissue section

Mice skin was harvested at about 50mm on the side of lesions including both of them for each sample biopsy, washed and fixed in a solution of p-formaldehyde. Then biopsies were incubated in a sucrose solution to guarantee the cryoprotection. The frozen sections were cut on a Leica CM 1950 cryostat at 5 μm, mounted directly on super frost slides (Thermo Fisher Scientific Inc. Waltham, MA, USA). The cryosections of frozen specimens cells were fixed in 4% paraformaldehyde, washed in PBS, and permeabilized in 0.5%Triton X-100 (5 minutes) and blocked in a blocking buffer containing 20% FBS and 0.05% Triton X-100 (30 minutes). The sections were then incubated O/N with primary antibodies in blocking buffer rabbit polyclonal anti-αSMA (1:100; Cusabio Life Science, College Park, MD, USA), anti-FAP-α (1:100; Santa Cruz Biotechnologies, Dallas, TX, USA), anti-CK6 (1:500; Flarebio Biotech LLC., Baltimore, MD, USA), anti-CK10 (1:500; Flarebio Biotech LLC., Baltimore, MD, USA), anti-CD31 (1:100; Biologend; San Diego, CA, USA) and anti-vimentin (1:250; Abcam, Cambrige, UK). The staining with conjugated anti-mouse and anti-rabbit antibodies and the nuclei, the confocal analysis and the quantification were performed as previously described.

6.19 Patients recruitment

Seven patients have been selected as affected by pressure ulcers in home wound care from almost three months. The lesions appeared cleansed, without any signs of bacterial infection, in phase of proliferative arrest from at least three weeks. This aspect becomes clinically evident, (no reduction of lesion area). All the pressure ulcers selected had to be overlapping for region (sacral), stage (III) and status (cleansed and/or tending towards wound bed sclerosis). The criteria for the exclusion were: neoplastic diseases; enteral and parenteral nutrition; albumin < 3.5 g/dl; lymphocytes <1500; infected lesion, other types of skin ulcers beside the pressure ones; no accurately performed mobilization of patient by nurses. The patients inserted in this study have suspended the previous medical treatment and have been medicated using the following method: cleansing with saline solution and povidoneiodine (50:50); Prisma® Skin as primary dressing; sterile gauze as secondary dressing; time of dressing change: 24h.

6.20 Skin biopsy collection

The area for the biopsies is identified in a not undermined region between 0.5 and 1 cm far from the lesion's edge. The biopsies have been performed at T0 and T14 (after 14 days from the beginning of the treatment). At T14 the tissues have been collected in a distant area from the previous point of biopsies at T0, on a parallel board at the lesion's edge between 1 and 2 cm. This procedure was used to avoid activity of tissue repair process after biopsy in that area. The biopsies have been performed with a punch of a diameter of 3.5 mm. At T0 and T14 a photo feature has been carried out to compare the histological data with the clinical ones. All the harvested samples have been analysed in double-blinded, without any clinical information about patients and experimental time.

6.21 H&E tissue staining

The harvested tissues were differently treated for H&E and IHC staining. In the first case, the samples were treated as reported in [20]. Briefly, they were fixed in a solution of formaldehyde 0.5% in PSB (Phosphate-Buffered Saline) 1x for 2 hours at 4°C. Then they were incubated O/N at 4°C in a sucrose solution (15% w/v in PBS 1x) to guarantee the cryoprotection. Next, the samples were included in OCT (Optimal Cutting Temperature; Sakura Finetek, Flemingweg, Netherlands) and stored at -80°C. The frozen tissue sections were cut on a microtome RM2125RT (Leica Microsystems, Wetzlar, Germany), mounted directly on super frost slides (Thermo Scientific, Waltham, MA), and processed for haematoxylin and eosin (H&E) staining. Briefly, cryostat sections were dehydrated for 5 minutes with cold acetone and then rehydrated. Next, slides were placed in haematoxylin stain for 9 minutes, rinsed in alcoholic acid, differentiated in 80% alcohol and stained with eosin for 2.5 minutes, rinsed in 95% ethanol, dehydrated with absolute ethanol and cleared in xylene or 4 minutes. The images were taken through the DIALUX 20 microscope (Leica Microsystems, Wetzlar, Germany) (10 and 25x). For quantitative analysis, H&E stained cells were counted using ImageJ software (NIH, Bethesda, MD, USA). A negative binomial model has been used to model counts as a function of treatment (T0 and T14) and interaction between treatment and patients, followed by ANOVA.

6.22 Immunohistochemical (IHC) staining

For IHC staining, sample was treated as reported above. All sections were fixed in 10% formalin, embedded in paraffin, and cut into 4 μm-thick slides. The slides were dewaxed, and the endogenous peroxidase activity was blocked by treatment with 3% hydrogen peroxide solution in methanol for 20 min. Epitope retrieval was performed by treating the slides with 10 mM sodium citrate buffer (pH 6.0) and heating in a microwave oven for two times at the high power for 6 min each. Non-specific binding was prevented by blocking with normal goat serum (1:10) for 10 min. The samples were

incubated with primary antibody anti-vimentin, CD4, CD8 (Roche, Ventana Medical Systems, Tucson, AZ) following the dilution suggested by the company, for 60 min at room temperature and with the appropriate secondary antibody at 37°C for 30 min followed by incubation with a 1:200 streptavidin-biotinperoxidase complex (Sigma-Aldrich, St. Louis, MO) for 30 min. Reactive products were visualized with 3,3'-diaminobenzidene (DAB) (Sigma-Aldrich, St. Louis, MO) as the chromogen, and the slides were counterstained with haematoxylin and coverslipped. Staining was performed on the Roche Ventana Medical Systems BenchMark ULTRA automated IHC platform using the ultraView Universal DAB Detection Kit (Roche, Ventana Medical Systems, Tucson, AZ). The images were taken through the DIALUX 20 microscope (Leica Biosystems, Wetzlar, Germany) (5, 10, 25 and 40X). For quantitative analysis, vimentin positive cells were counted using ImageJ software (NIH, Bethesda, MD, USA). A negative binomial model has been used to model counts as a function of treatment (T0 and T14) and interaction between treatment and patients, followed by ANOVA.

6.23 CCA solubility and Impregnation, PCL solubility, foaming and impregnation tests: Apparatus and Procedures

Sodium alginate (MW ≈ 240,000 Da, β-d-mannuronic/α-L-guluronic acid ratio 1:2) and calcium chloride ($CaCl_2$, purity ≥ 96 %) were bought from Sigma-Aldrich (Italy). Carbon dioxide (CO_2, purity 99 %) was purchased from Morlando Group S.R.L. (Italy). Ethanol (purity 99.9 %) was purchased from Carlo Erba (Italy). A laboratory water distiller, which was supplied by ISECO S.P.A. (St. Marcel, AO, Italy), was used to distill the water. The alcogels are placed in a stainless-steel cylindrical vessel with an internal volume of 500 mL; the $scCO_2$ is delivered through a high-pressure pump (Milton Roy, mod. Milroyal B, France), after being cooled thanks to a refrigerating bath. The operating pressure in the cylindrical vessel is regulated by a micrometric valve (Hoke, mod. 1315G4Y, Spartanburg, SC) and measured by a test gauge manometer (Salmoiraghi, model SC-3200, Italy). A proportional-integral-derivative (PID) controller (Watlow, mod. 93, USA), which is connected with electrically controlled thin bands, ensures the desired temperature. Downstream the micrometric valve, a collection second vessel, whose pressure was regulated by a backpressure valve (Tescom, model 26-1723-44, Italy), allows to recover the ethanol extracted from the alcogel pores. The CO_2 flow rate and the total quantity of CO_2 were respectively evaluated by a rotameter and a dry test meter located at the exit of the second vessel. First, a hydrogel was obtained by preparing a solution at 5 % w/w of sodium alginate in distilled water, which was stirred for about 24 h at 200 rpm and then poured into cylindrical molds. In order to promote the gelation, the samples were immersed in a coagulation bath of $CaCl_2$ (5 % w/w in distilled water) for about 24 h; in this way, sodium alginate was converted to calcium alginate. Then, Ca^{2+} residues were eliminated by washing the hydrogels

with distilled water. The second step was the attainment of an alcogel through a gradual replacement of the water filling the hydrogel pores by batch equilibration at room temperature with a series of ethanol baths lasting 24 h each, at increasing concentration of ethanol (30 %, 70 %, 90 % and two times 100 % v/v). Then, the aerogels were obtained by drying the alcogels using $scCO_2$: the samples were placed in the cylindrical vessel which was then filled with $scCO_2$ to reach the desired pressure (20 MPa) and temperature (35 °C); after, the drying was performed for 5 h using a $scCO_2$ flow rate of about 1 kg/h. Once the system was brought back at atmospheric pressure through a slow depressurization, the dried aerogels were recovered from the vessel.

High molecular weight polycaprolactone (PCL, average Mn ~ 80,000 by GPC) was bought from Sigma-Aldrich (Milan, Italy). Carbon dioxide (CO_2, purity 99%) was purchased from Morlando Group S.R.L. (Sant'Antimo-NA, Italy).

Experiments take place in an autoclave with a 100 mL internal volume, i.e., a stainless-steel cylinder (NWA GmbH, Germany) closed on the bottom and on the top with two finger tight clamps. The CO_2 is cooled before compression thanks to a refrigerating bath and then, it is fed by a diaphragm piston pump (Milton Roy, mod. Milroyal B, France). An impeller, which is mounted on the top cap and driven by a variable velocity electric motor, permits a homogeneous mixing in the autoclave. The operating pressure is measured by a digital gauge manometer (Parker, Minneapolis, MN). The thermal control into the autoclave is assured by a PID controller (Watlow, mod. 93, USA) connected with electrically controlled thin bands. At the exit of the autoclave, the CO_2 flow rate is measured by a rotameter. Depressurization is performed by a micrometric valve (Hoke, mod. 1315G4Y, Spartanburg, SC). The solubility of mesoglycan in $scCO_2$ was experimentally estimated in the range of pressure 12−18 MPa and at two temperatures (40 and 60 °C), according to a procedure set in previous papers [278]. A small stainless-steel cylinder containing a weighed amount of mesoglycan was wrapped with filter paper to avoid the drug entrainment and then, placed on the bottom of the autoclave. Once the autoclave was closed, it was heated up to the desired temperature, whereas the CO_2 was pumped up to the desired pressure. In order to ensure that the equilibrium conditions, the system was stored for 24 h under mechanical stirring. Then, CO_2 was slowly vented out (about 0.1 MPa/min). At the end of the experiment, the stainless-steel cylinder containing the not dissolved mesoglycan was weighed, so obtaining the amount of the dissolved mesoglycan by the weight difference. Solubility measurements were repeated in duplicate and the difference between the experiments was less than 2-3 %, probably due to the entrainment of drug through the filter paper during the depressurization. A static method [279] was used to perform the impregnation tests. The experimental data were obtained by charging a weighed amount of mesoglycan (about 10 mg) in a small container opened on the top, to allow its contact with $scCO_2$, and axially mounted on the

impeller. A weighed amount of aerogel (about 50 mg) or of PCL (70mg) were instead wrapped in a filter paper, to avoid its contact with the solid drug, and placed on the bottom of the autoclave. Finally, the autoclave was closed, and the CO_2 was slowly fed to the vessel, which was heated up to the desired temperature. Once the pressure of 18 MPa for CCA or 17 MPa for PCL was reached, the system was stored for a fixed time. Then, the CO_2 was vented out (constant flow rate of about 1 MPa/min) to reach the atmospheric conditions and to recover the loaded aerogel from the autoclave. The amount of CO_2 delivered to the autoclave was determined from the density value, calculated at the operating temperature and pressure by using the Bender equation of state. The amount of loaded mesoglycan was determined both from the weight increase of the sample after the experiment and by using UV/vis spectroscopy. The quantity of mesoglycan loaded on CAA was affected by both impregnation kinetics and thermodynamics. The study of the impregnation kinetics allows to determine the time required for the mesoglycan to reach the equilibrium concentration at the selected operating conditions. Fixing the working pressure at 18 MPa, the impregnation kinetics were investigated by measuring the amount of mesoglycan impregnated on CAA at different temperatures (40 and 60 °C) and varying the contact time between the mesoglycan dissolved in $scCO_2$ and the aerogel (from 2 to 24 h). Impregnation isotherms were determined to correlate the mesoglycan concentration in the $scCO_2$ to the mesoglycan concentration into the aerogel. Impregnation isotherms were studied at 40 °C/18 MPa and 60 °C/18 MPa, for a contact time of 24 h, by charging a different amount of mesoglycan in the vessel up to the saturated solubility of mesoglycan in $scCO_2$. Each experiment was performed in duplicate and the difference between the tests was less than 5 %, probably due to the possible entrainment of the material through the filter paper during depressurization and to the deposition of non-impregnated material on the aerogel surface. To prevent that the results are distorted by the residual amount of CO_2 adsorbed in the sample, the weighs were always carried out two hours after the end of each experiment. Each experiment was performed in duplicate; the difference between the tests was less than 5%, probably due to the possible entrainment of the material through the filter paper during depressurization and to the deposition of non-impregnated mesoglycan on the surface of foamed PCL.

6.24 Production of PCL film by compression molding

The pellets of PCL were dried for 2 h under vacuum at a temperature of 27 °C. The films (thickness of 100 μm) were obtained using a compression molding press (Model C, Fred S. Carver Inc., Menomonee Falls, WI, USA), adopting the following process conditions: (a) pre-heating at 120 °C for 5 min, (b) compression-molding at 150 bar for 2 min, and (c) cooling in air.

6.25 Analytical methods for samples' characterization

Sample structure was observed before and after impregnation by Field Emission Scanning Electron Microscopy (FESEM, mod. LEO 1525, Carl Zeiss SMT AG, Oberkochen, Germany). Small aerogel pieces were dispersed on a carbon tab stuck to an aluminum stub (Agar Scientific, United Kingdom). The samples were coated with gold-palladium (layer thickness 250 Å) using a sputter coater (mod. 108 A, Agar Scientific, Stansted, United Kingdom) in order to be conductive to get the FESEM images.

Drug loadings and dissolution tests were performed using an UV/vis spectrophotometer (model Cary 50, Varian, Palo Alto, CA, USA) at a wavelength of 206 nm. mesoglycan loadings were evaluated by placing each sample in a filter and, then, incubated in 250 mL of phosphate buffered saline solution (PBS) at slightly basic pH equal to 7.4; the system was continuously stirred at 150-200 rpm and 37 °C. The values of the absorbance were directly measured by the instrument each 0.3 min from time zero up to 100 min, every min in the range 101–1500 min, then every 5 min until the plateau value was reached. Drug loadings were determined considering the absorbance measured at the end of the release profiles, i.e., when all the mesoglycan was released from the CCA or the foamed PCL to the outer water phase. The absorbance was converted into mesoglycan concentration by using a calibration curve, in order to check the weight increase of the sample measured at the end of the impregnation experiments. Release tests were performed with the same procedure on samples containing an equivalent amount of mesoglycan of 20 mg, to do a proper comparison between the unprocessed mesoglycan and mesoglycan impregnated on CCA or foamed PCL. The dissolution profile, reported in this paper as the percentage of released mesoglycan *vs* the time, represents the average of three analyses.

6.26 *In vitro* assays to evaluate the CCA and PCL effects

For migration analysis using CCA the procedure was the same illustrated before for scratch wound healing assay. For the administration of the substances, after removing incubation medium and washing with PBS, cell cultures were incubated in the presence of powdered sodium MSG, CAA, MSG and CAA administered together as free drugs, and MSG impregnated on CAA, all of them at a final concentration of 0.3 mg/mL, and in growth medium as control.

For the evaluation of the effects of PCL the procedure was the same illustrated before for scratch wound healing assay, invasion assay and tube formation. For the administration of the substances: after removing incubation medium and washing with PBS, cell cultures were incubated (for migration and tube formation assay) in presence of powdered sodium mesoglycan at 50µg/mL and mesoglycan dissolved from PCL film, and harvested at 24, 48, and 72 h, all of them at a final concentration of 50

µg/mL, and in growth medium as control. Both powdered mesoglycan and mesoglycan deriving from PCL were sterilized by sterilizing filtration, through 0.22µm syringe filters.

For the invasion assay *in vitro* 1.4 mL of supplemented growth medium with or without sodium mesoglycan or PCL-derived mesoglycan at 24, 48, and 72 h were put in the lower chamber and the trans-well was left for 24 h at 37 °C in 5% CO2-95% air humidified atmosphere.

6.27 Statistical analysis

Data analyses and statistical evaluations were carried out using Microsoft Excel; the number of independent experiments and *p*-values are indicated in the figure legends. All results are the mean ± standard deviation of at least 3 experiments performed in triplicate. Statistical comparisons between the experimental points were made using two-tailed *t*-test comparing two variables. Differences were considered significant if $p < 0.05$, $p < 0.01$ and $p < 0.001$.

7.Results

7.1 Mesoglycan induces a change of localisation of SDC4 in keratinocytes

SDC4 is the fourth member of HSPGs, it is crucial during the wound healing process because mediates cell-cell and cell-matrix interactions through its HS chains. The latter can interplay with and modulate the function of several proteins, including those involved in cell migration and differentiation [280]. To verify if mesoglycan was able to activate SDC4 pathway we analysed SDC4 expression and localization at different time point. As reported in figure 7.1 A did not change the level expression of SDC4 after 5, 15, 30, 60 minutes and 48 hours of treatment with mesoglycan compared with the untreated control. On the contrary, as reported in figure 7.1 B (panels a-f), mesoglycan induces SDC4 sub-cellular localization at 5 minutes from treatment (Fig. 7.1 B panel b). Surprisingly, after 15 minutes of mesoglycan administration, SDC4 is massively localized in the nuclei and perinuclear areas and it persists up to 48 hours (Fig. 7.1 B panels c-f).

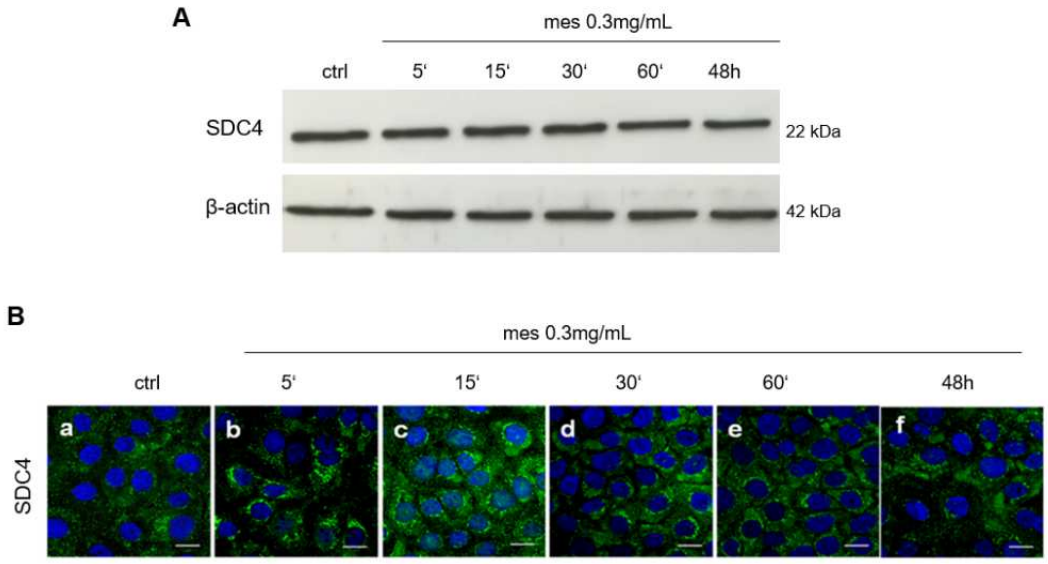

Fig. 7.1 (**A**) Western blot analysis of total protein extracts from control or mesoglycan (0.3 mg/ml; from 5 min up to 48 hr) HaCaT keratinocytes. Cropped blots from full-length gels are representative of $n = 3$ independent experiments with similar results using antibodies against SDC4. The blots were exposed to Las4000 (GE Healthcare Life Sciences) and normalized on β-actin levels. (**B**) Immunofluorescence analysis of mesoglycan treated (0.3 mg/ml; from 5 min up to 48 hr) HaCaT keratinocytes. The cells were fixed and labelled with antibody against SDC4. Magnification 63 × 1.4 NA. Bar = 20 μm. All images are representative fields of $n = 3$ experiments with similar results.

7.2 SDC4 is involved in motility and differentiation of HaCaT cells treated with mesoglycan

Cell migration requires the reorganization of the actin cytoskeleton, activation of integrins, formation of stress fibres and focal adhesions [281]. Migration and invasion assays were performed, to define the role of SDC4 in mediating mesoglycan effects on HaCaT cell motility. To evaluate the involvement of SDC4 pathway on keratinocytes migration promoted by mesoglycan, we utilised small interfering RNAs (siRNAs) against SDC4. As shown in figure 7.2 A-B for the motility and in figure 7.2 C-D for the invasion assay, functional experiments confirmed that both the processes were significantly affected by SDC4 loss of functions in mesoglycan treated keratinocytes.

Then, we evaluated if the inhibition of the SDC4 pathway altered mesoglycan effects on keratinocyte differentiation, another fundamental process [282] triggered by increased calcium influx. As shown in figure 7.2 E, the release of calcium from intracellular reserves, was measured using the fluorescent probe FURA-2 AM, we found a significant increase in calcium levels after treatment of mesoglycan. This intracellular calcium influx was not promoted in low levels of SDC4. Moreover, confocal microscopy analysis, observing typical markers of the early differentiation such as the expression of E-cadherin (Fig. 7.2 F, panels a-d), CK6 (Fig. 7.2 F, panels e-h) and CK10 (Fig. 7.2 F, panels i-l), established that this process triggered by mesoglycan was blocked by the inhibition of SDC4 pathway, through siSDC4s transfection. These results were confirmed by Western blot analysis (Fig. 7.2 G).

Therefore, SDC4 plays a decisive role in promoting the motility and differentiation of keratinocytes treated with mesoglycan.

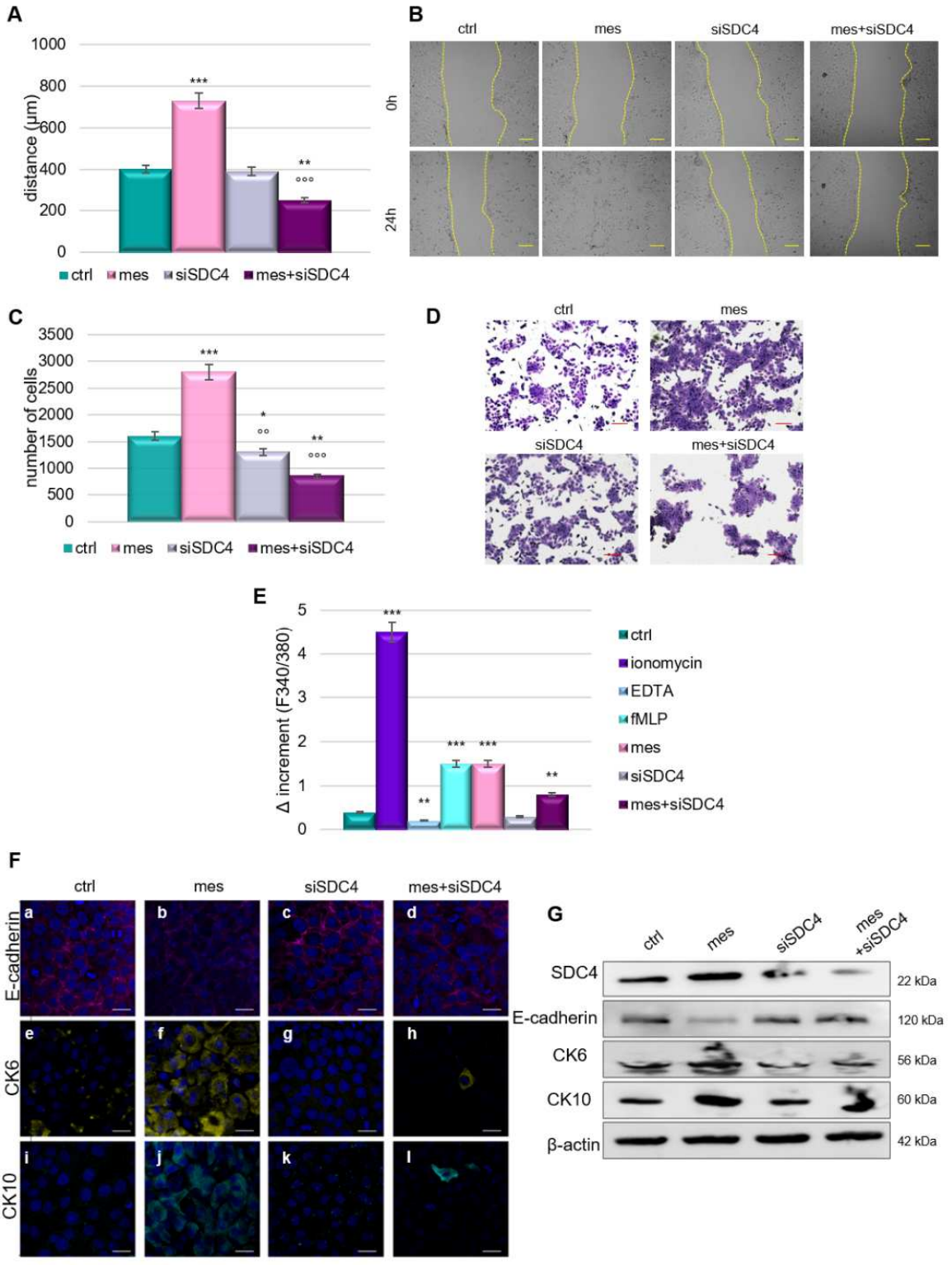

Fig. 7.2 (**A**) Analysis and (**B**) brightfield images of the Scratch Wound Healing Assay and on HaCaT cells treated or not with mesoglycan (0.3 mg/ml; 48 hr of treatment), siSDC4s (100 nM; 48 hr of treatment). The migration rate was determined by measuring the distances covered by individual cells from the initial time to the selected time-point (24 hr; bar of distance tool, Leica ASF software). The data are representative of $n = 3$ independent experiments ± SD. (**C**) Results and (**D**) brightfield images of the Invasion Assay on keratinocytes treated or not with mesoglycan (0.3 mg/ml; 48 hr of treatment), siSDC4s (100 nM; 48 hr of

treatment). The data represent mean cell counts of 15 separate fields per well ± SD of $n = 3$ independent experiments. *$p < 0.05$, **$p < 0.01$, and ***$p < 0.001$ *vs* controls; °°°$p < 0.001$ *vs* mesoglycan treated cells. (**E**) The histograms show the fluorescence ratio calculated as F340/F380 nm in absence of extracellular Ca^{2+}. Data are means ± SEM of three experiments with similar results. *$p < 0.05$, ** $p < 0.01$; *** $p < 0.001$ treated cells *vs* non treated control. (**F**) Immunofluorescence analysis of control, mesoglycan (0.3 mg/ml; 48 hr) and/or siSDC4 (100 nM; 72 hr) treated keratinocytes. After incubations, the cells were fixed and labelled with antibodies against E-cadherin (panels a–d), CK6 (panels e–h), and CK10 (panels i–l). Magnification 63 × 1.4 NA. Bar = 20 μm. All images are representative fields of $n = 5$ experiments with similar results. (**G**) Western blot analysis of total protein extracts from control, mesoglycan (0.3 mg/ml; 48 hr) and/or siSDC4 (100 nM; 72 hr) HaCaT keratinocytes. Cropped blots from full-length gels are representative of $n = 3$ independent experiments with similar results using antibodies against SDC4, E-cadherin, CK6, and CK10. The blots were exposed to Las4000 (GE Healthcare Life Sciences) and normalized on β-actin levels.

7.3 Mesoglycan activates SDC4 pathway in keratinocytes *in vitro*

It is known that there is a connection between SDC4 and PKCα activation and their membrane translocation [283]. Consequently, we investigate p-PKCα expression and localization after mesoglycan treatment in human keratinocytes. The GAGs mixture can activate PKCα inducing its phosphorylation from 5 to 60 minutes after the treatment (Fig. 7.3 A panels g-l).

This series of studies verified that mesoglycan did not substantially affect SDC4 expression (Fig. 7.3 B panel b; Fig. 7.3 C). Surprising, we shown that when SDC4 is knocked down, PKCα was less phosphorylated, losing its ability to translocate to cell periphery (Fig. 3B panel g), despite mesoglycan application (Fig. 7.3 B panel h). One of the proteins by which SDC4 triggers PKCα activation is the integrin β1, involved in the formation of focal adhesion and in cell migration [281]. Although mesoglycan activated integrin β1 membrane clustering (Fig. 7.3 B, panel j) this reaction was inhibited by SDC4 knockdown (Fig. 7.3 B, panels k-l). In addition, Western blot analysis revealed a mesoglycan-induced rise in integrin β1 expression, which returned to baseline levels when in HaCaT cells was reduced SDC4 (Fig. 7.3 C).

Once the migration signal was received, the cells developed focal complexes. The major focal adhesion adaptor protein paxillin, may be directly or indirectly phosphorylated by PKCα at adhesion sites to induce focal adhesion disassembly and cell migration [284]. Mesoglycan stimulated a strong thickening of paxillin expression in emerging adhesion sites (Fig. 7.3 B, panel n) whereas no phosphorylation signal was detected in untreated cells or cells treated with mesoglycan and siSDC4 (Fig. 7.3 B, panels m-p). Several kinases including PKCα, are able to phosphorylate ERM proteins (ezrin, radixin and moesin) to induce their translocation to sub-cellular structures such as cell

adhesion sites [285]. Notably, it was found that mesoglycan led ezrin membrane localization (Fig. 7.3 B, panel r) and this event was clearly reverted in SDC4 knock-down cells (Fig. 7.3 B, panels s). We also showed that mesoglycan induced a moderate increase of ezrin expression and that the treatment of keratinocytes with the siSDC4s reverted this occurrence (Fig. 7.3 C).

These results show how the SDC4 pathway is activated in mesoglycan-stimulated keratinocytes.

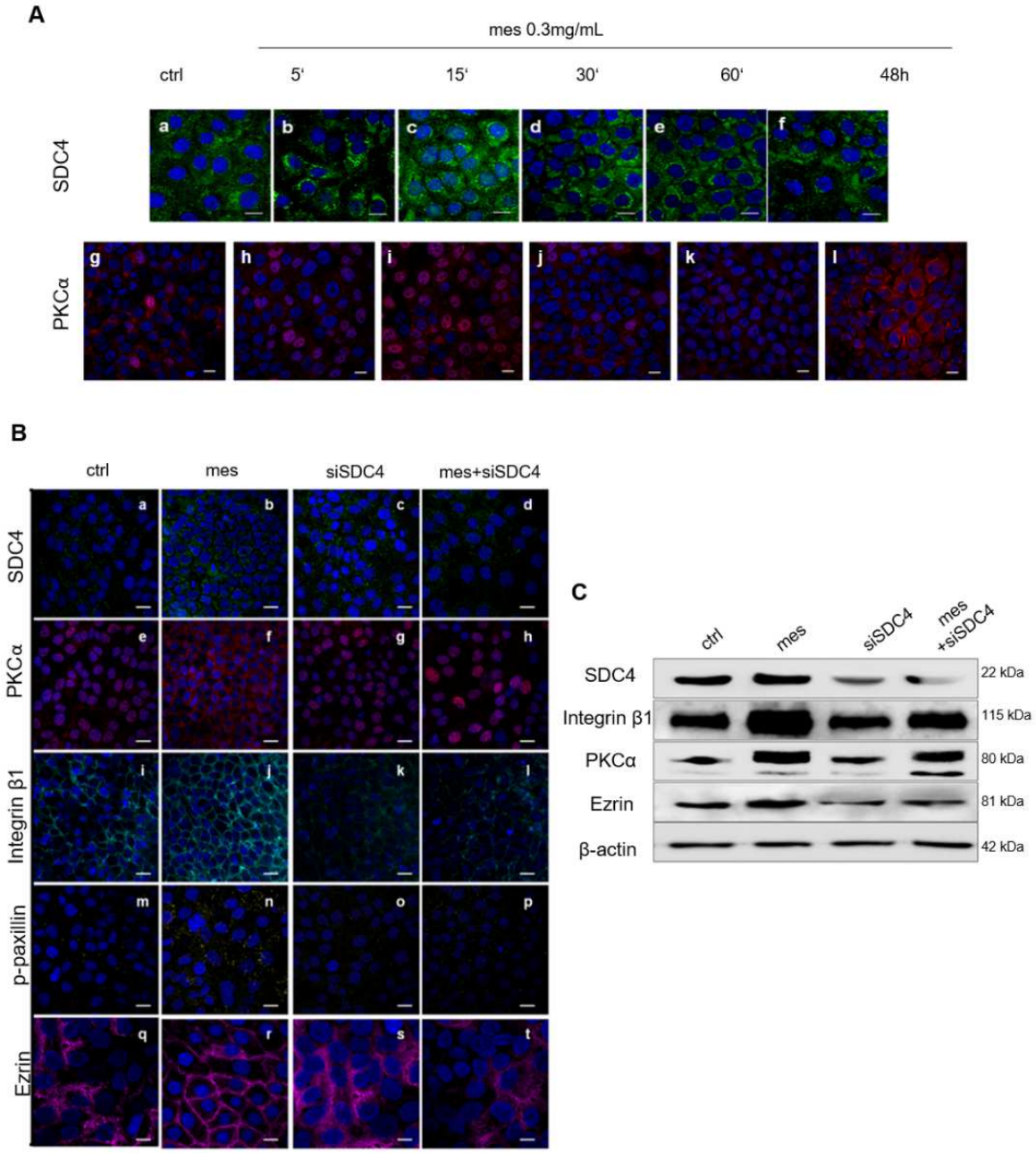

Fig. 7.3 (**A**) Immunofluorescence analysis of mesoglycan treated (0.3 mg/ml; from 5 min up to 48 hr) HaCaT keratinocytes. The cells were fixed and labelled with antibody against SDC4 and p-PKCα. Magnification 63 × 1.4 NA. Bar = 20 μm. All images are representative fields of *n* = 3 experiments with

similar results. (**B**) Immunofluorescence analysis of control, mesoglycan (0.3 mg/ml; 48 hr) and/or siSDC4 (100 nM; 72 hr) treated HaCaT cells. After incubations, the cells were fixed and labelled with antibodies against SDC4, p-PKCα (panels e–h), integrin β1 (panels i–l), p-paxillin (panels m–p) and ezrin (panels q–t). Magnification 63 × 1.4 NA. Bar = 20 μm (panels a–p) and 10 μm (panels q–t). All images are representative fields of $n = 5$ experiments with similar results. (**C**) Western blot analysis of total protein extracts from control, mesoglycan (0.3 mg/ml; 48 hr) and/or siSDC4 (100 nM; 72 hr) treated keratinocytes. Cropped blots from full-length gels are representative of $n = 3$ independent experiments with similar results using antibodies against SDC4, p-PKCα, integrin β1, and ezrin. The blots were exposed to Las4000 (GE Healthcare Life Sciences) and normalized on β-actin levels.

7.4 Mesoglycan promote the formation of the complex S100A11/ANXA1 via SDC4 activation

ANXA1 may be one of the central proteins of the mediation of keratinocyte dynamics, including cell migration [263], [265]. This protein was overexpressed and released by differentiating cells [262]. Knowing that mesoglycan promote HaCaT differentiation, we observed ANXA1 localization after the administration of this GAGs mixture. In figure 7.4 A (panels a-b) after 48 hours of mesoglycan stimulation, we observed a small increase in ANXA1 expression and its translocation to the inner cytoplasmic surface of the keratinocytes. These results were supported by Western blot analysis, which also revealed the release of ANXA1 in extracellular environments (Fig. 7.4 B, supernatants lanes) where the protein appeared at different molecular weights. During the differentiation of keratinocytes, ANXA1 creates a complex with the S100A11 protein, moving to the plasma membrane [286]. Thus, was performed a S100A11/ANXA1 co-precipitated experiments as reported in figure 7.4 C. This result suggested that mesoglycan treatment induced the formation of the S100A11/ANXA1 complex. To further confirm this data, we carried out the double staining confocal microscopy for ANXA1 and S100A11. We found that both ANXA1 (Fig. 7.4 D panels a-b) and S100A11 (Fig. 7.4 D panels e-f) after 48 hours of mesoglycan treatment translocated from the cytosol to the membrane. These two proteins seemed to mainly interact close to the plasma membranes (blue arrows in figure 7.4 D panel j). Instead, the inhibition of SDC4 pathway using siSDC4, reverted mesoglycan effects on this interaction (Fig. 7.4 D panel k-l). No significative differences were observed with respect to ANXA1 and S100A11 expression in keratinocytes treated with mesoglycan and/or siSDC4 (Fig. 7.4 E).

Hence, mesoglycan induces the formation of the ANXA1/S100A11 complex in keratinocytes.

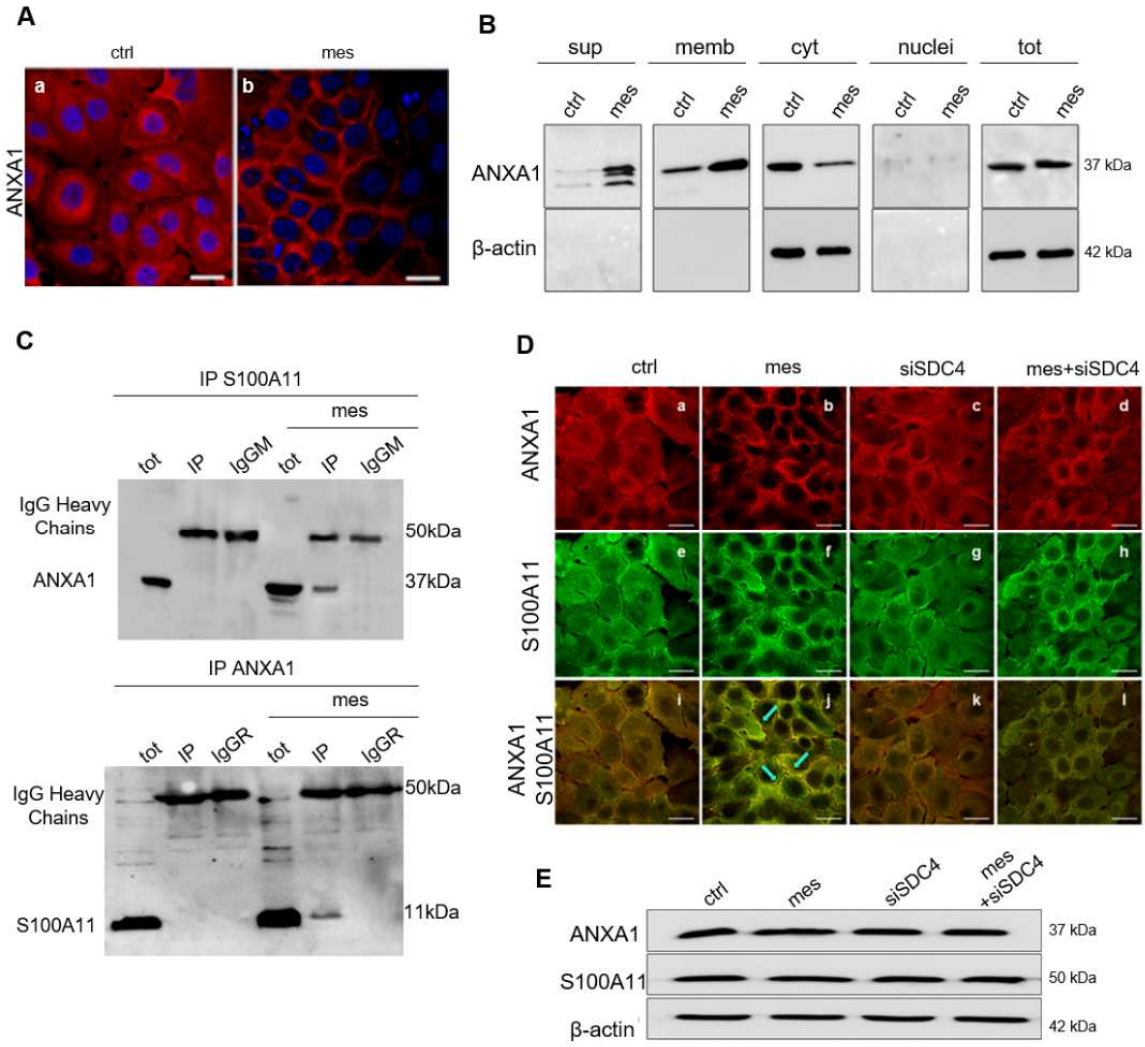

Fig. 7.4 (**A**) Immunofluorescence analysis of control and/or mesoglycan (0.3 mg/ml; 48 hr) treated HaCaT keratinocytes. After incubation, the cells were fixed and labelled with an antibody against ANXA1 and nuclei were stained using Hoechst 33342. Magnification 63 × 1.4 NA. Bar = 20 μm. All images are representative fields of n = 5 experiments with similar results. (**B**) Whole, membrane, cytosol, and extracellular expression of ANXA1 in HaCaT cells was analysed by Western blot with an anti-ANXA1 antibody. Protein extracts from cellular compartments were obtained as described in Materials and Methods Section. Cropped blots from full-length gels are shown. Protein normalization was performed on β-actin levels. (**C**) The detection of ANXA1/S100A11 complex was performed by immunoprecipitation experiments (IP). HaCaT cells were treated or not with mesoglycan (0.3 mg/ml; 48 hr) and cell lysates were made. An amount of 200 μg for each protein lysate was incubated with monoclonal anti-S100A11 (2 μg) or polyclonal anti-ANXA1 (2 μg) antibodies. Mouse (IgGM; 2 μg) and rabbit (IgGR; 2 μg) IgGs were also used as controls. The blots were incubated with antibodies against S100A11 (1:1,000) or ANXA1 (1:100). Blot images are representative of n = 3 independent experiments. (**D**) Immunofluorescence analysis of control and/or mesoglycan (0.3 mg/ml; 48 hr) treated HaCaT keratinocytes. After incubations, the cells were fixed

and labelled with an antibody against ANXA1 and S100A11. The light blue arrows point to ANXA1/S100A11 overlapping signals in the merged images (panels i–l). Magnification 63 × 1.4 NA. Bar = 20 μm. All images are representative fields of *n* = 5 experiments with similar results. (**E**) Cropped blots from full-length gels of Western blot analysis of ANXA1 and S100A11 expression in HaCaT cells treated or with mesoglycan (0.3 mg/ml; 48 hr) and/or siSDC4s (100 nM; 72 hr) to knock down SDC4 expression. Blot images are representative of *n* = 3 experiments with similar results.

7.5 Mesoglycan-activated SDC4 induces keratinocytes motility and differentiation in ANXA1-dependent manner

To understand the reason of the mobilization of ANXA1, we used siANXA1 transfection for 24 hours to knock down this protein, as reported in figure 7.5 A. Then, we performed a scratch wound healing assay and an invasion assay to study ANXA1 contribution in mesoglycan-induced motility. siANXA1s were able to considerably inhibit keratinocyte migration rate also in mesoglycan-treated cells (Fig. 7.5 B-C). Additionally, in figure 7.5 D-E is shown the significative inhibition of keratinocyte invasion following the treatment with siANXA1.

ANXA1 downregulation (Fig. 7.5 D panels c-d) was able to influence the differentiation process in keratinocytes. Indeed, cells treated with siANXA1 presented the arrest of E-cadherin clustering and its decrease (Fig. 7.5 D panels g-h). The loss presence of ANXA1 is able to reduce the expression of differentiation markers such as CK6 (Fig. 7.5 D panels k-l) and CK10 (Fig. 7.5 D panels o-p). These data are confirmed via western blot in figure 7.5 E.

These data therefore show us that mesoglycan - activated SDC4 induces keratinocyte migration and invasion in an ANXA1-dependent manner.

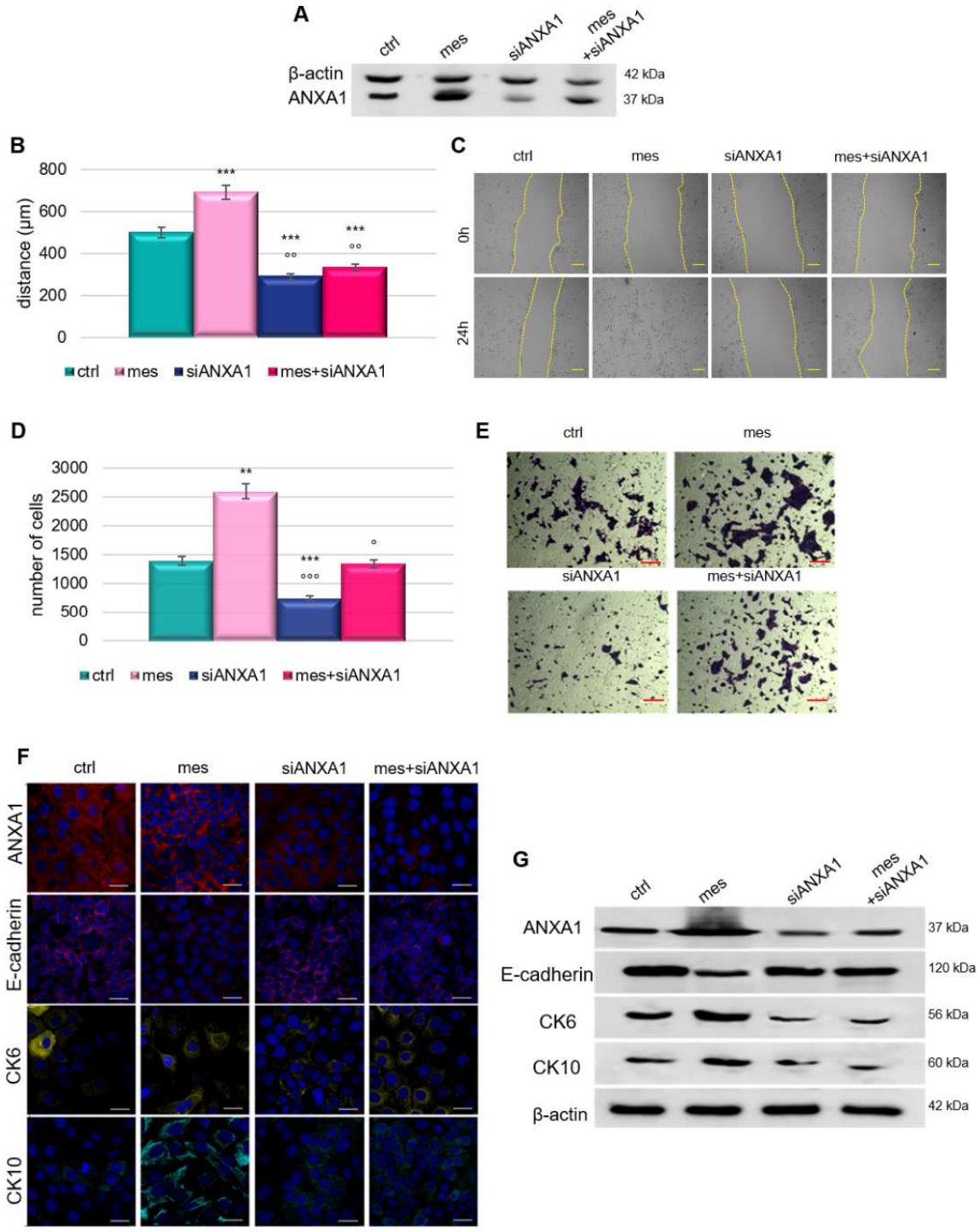

Fig. 7.5 (**A**) Western blot analysis of total protein extract from HaCaT keratinocytes treated or not with mesoglycan (0.3 mg/ml; 48 hr), and siANXA1s (100 nM; 72 hr). The shown blots are representative of $n = 3$ experiments with similar results. (**B**) Results from the Scratch Wound Healing Assay and (**C**) representative bright field images of HaCaT cells treated or not with mesoglycan (0.3 mg/ml; 48 hr), and siANXA1s (100 nM; 72 hr). ***$p < 0.001$ *vs* untreated controls; $^{\circ\circ}p < 0.01$ *vs* mesoglycan treated cells. The images were captured by Time Lapse microscope (Leica AF-6000 LX; Leica Microsystems). Magnification 10×. Bar = 100 μm. The migration rate was determined by measuring the distances covered by individual cells from the

initial time to the selected time points (bar of distance tool, Leica ASF software). The data are representative of $n = 3$ independent experiments ± SEM. (**D**) Results of the Invasion Assay (**E**) representative images of HaCaT cells treated or not with mesoglycan (0.3 mg/ml; 48 hr), and siANXA1s (100 nM; 72 hr). Magnification 20×. Bar = 150 μm. The data represent mean cell counts of 15 separate fields per well ± SD of $n = 3$ experiments. $^{**}p < 0.01$ and $^{***}p < 0.001$ *vs* untreated controls; $^{\circ}p < 0.05$ and $^{\circ\circ\circ}p < 0.001$ *vs* mesoglycan treated cells. (**F**) The immunofluorescence analysis of ANXA1 (panels a–d), E-cadherin (panels e–h), CK6 (panels i–l), and CK10 (panels m–p) protein expression and localization in HaCaT cells treated or not with mesoglycan (0.3 mg/ml; 48 hr) and/or siANXA1s (100 nM; 72 hr). Magnification 63 × 1.4 NA. Bar = 20 μm. All images are representative fields of $n = 3$ experiments with similar results. (**G**) After the selected times of treatment, the cells were harvested to obtain total protein extracts. Cropped blots from full-length gels are representative of $n = 3$ experiments with similar results using antibodies against ANXA1, E-cadherin, CK6, and CK10. The blots were exposed to Las4000 (GE Healthcare Life Sciences) and normalized on β-actin levels.

7.6 Keratinocytes release more vesicles following mesoglycan treatment

ANXA1 is involved in vesicle trafficking, mediating the interaction of vesicles with cytoplasmic machinery, for the production of extracellular vesicles (EVs), in particular exosomes [255]. Indeed, EVs pathway may represent the main mechanism of ANXA1 externalization, evolving through the exocytosis of microvesicles by fusion of multivesicular endosomes with the plasma membrane [287]. Thus, we purified EVs, enriched in exosomes, by supernatant of cells and analysed them by Field Emission Scanning Electron Microscopy (FE-SEM) and dynamic light-scattering (DLS). In the first case, we observed rounded particles ranging from 30 to 180 nm in diameter which presented the typical morphological features of exosomes (Fig. 7.6 A). Moreover, we found that keratinocytes secreted an increased amount of EVs when previously treated with mesoglycan. This result has been corroborated through DLS (Fig. 7.6 B), by which we estimated the EVs size distribution by number depending on the measurement of their diameter.

In order to confirm the enrichment in exosomes of the EVs isolated from HaCaT cells, Western blot analysis was conducted. Figure 7.6 C showed the presence of TSG101, frequently used as an exosome marker, exclusively in EVs fractions. Instead, calreticulin was present only in total cell lysates, while was absent in EVs fractions, because it is exposed on the surface of apoptotic cells and ends up in apoptotic bodies. Finally, the presence of ANXA1 was detected in total cell lysate, in conditioned medium (SS) and in EVs. Specifically, in SS (conditioned medium) and EVs, ANXA1 appeared both as full length protein (37 kDa) and in its cleaved form (33 kDa). Moreover, SS and EVs mesoglycan showed a larger amount of ANXA1 if compared to SS and EVs ctrl.

Hence, the mesoglycan stimulates the release of ANXA1-containing EVs from HUVEC cells.

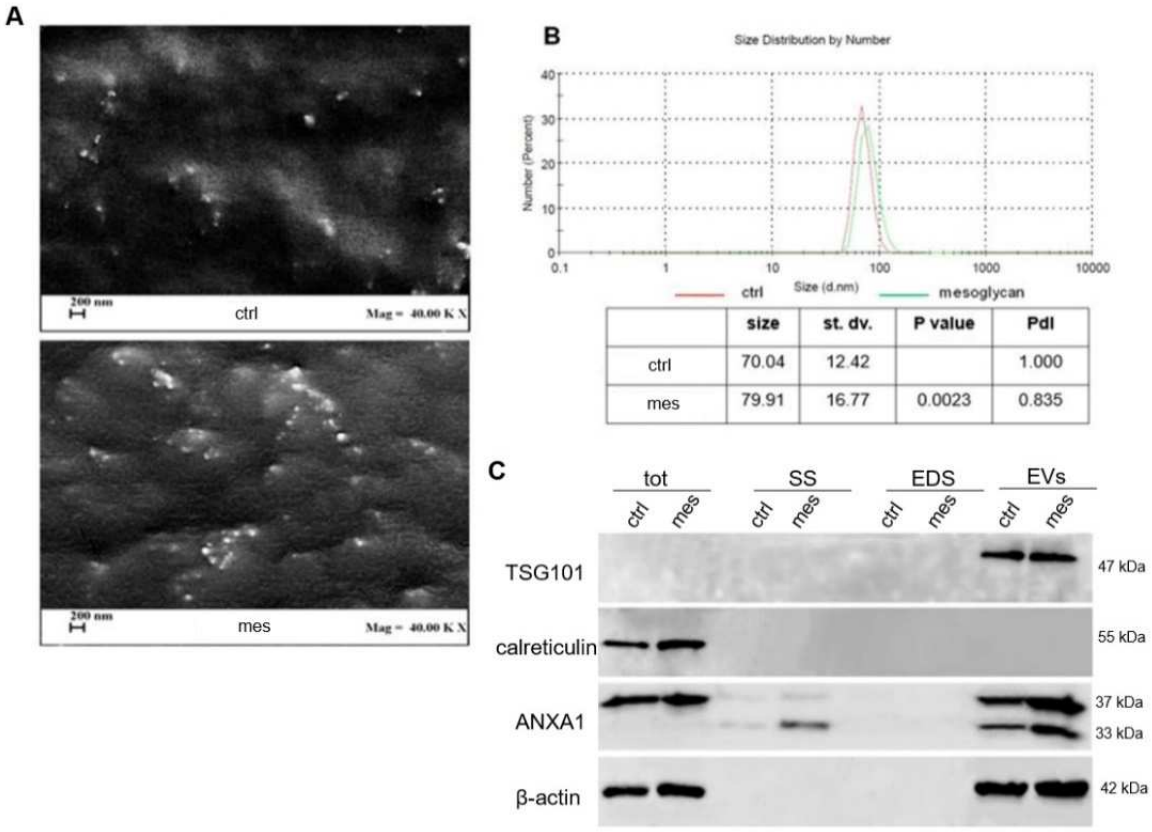

	size	st. dv.	P value	PdI
ctrl	70.04	12.42		1.000
mes	79.91	16.77	0.0023	0.835

Fig. 7.6 (**A**) EVs deriving from keratinocytes treated or not with mesoglycan (0.3 mg/mL) were imaged by Field Emission-Scanning Electron Microscope (FE-SEM). Magnitude = 40,000 KX (that is 40,000,000) and scale bar = 200 nm. (**B**) Characterization of the EVs size distributions was found by dynamic light scattering (DLS). The table reports the EVs mean size, standard deviation, *p* value, referring to EVs mesoglycan distribution *vs* EVs ctrl, and PdI. The experiments were performed in triplicate. (**C**) Western blot using antibodies against TSG101, calreticulin, and ANXA1 on protein content of total cell lysates, conditioned medium (SS), EV-depleted extracellular fractions (EDS) and EVs fractions extracted from keratinocytes treated or not with mesoglycan. Protein normalization and the check of the sample quality were performed on β-actin levels.

7.7 ANXA1 mimetic peptide induced the externalization and the secretion of ANXA1 promoting keratinocytes activation

Based on the previous results, we studied the possible role of the extracellular ANXA1 on keratinocytes. We used Ac2-26, the ANXA1 N-terminal mimetic peptide at the concentration of 1 μM. Immunofluorescence analysis reported in figure 7.7 A showed that in HaCaT cells treated with the peptide, ANXA1 translocated to the plasma membrane (Fig. 7.7 A panel b, white arrows)

compared to the untreated cells (Fig. 7.7 A panel a) where the signal was diffuse. This result was confirmed by western blot in figure 7.7 B. In addition to corroborate that, we observed that ANXA1 was moved to the plasma membrane in HaCaT cells treated with the mimetic peptide. Moreover, we found the presence of the protein at the two different molecular weights in the supernatant of keratinocytes treated with Ac-26. The localization of ANXA1 on cell surface and its externalization are two important event supporting cell motility [273]. The most of function of secreted ANXA1 are triggered through the activation of formyl peptide receptors (FPRs) [273], [288], [289]. We performed functional experiments on keratinocytes treated with Ac2-26 in presence or not of BOC1 at a concentration of 100 μM, as pan-antagonist of FPRs. Figure 7.7 C-D showed an increase of migration rate in cells treated with ANXA1 mimetic peptide, compared with the untreated cells. Instead, this motility stimulation appeared inhibited by BOC1. In a similar way, the invasive ability of HaCaT cells was positively influenced by Ac2-26, but in presence of BOC1 the number of the cells able to invade the coating of matrigel, was strongly reduced, as reported in figure 7.7 E-F. ANXA1-FPRs interaction caused several cellular response, such as ERK phosphorylation and the increase of intracellular calcium concentration [272] that are important for keratinocytes differentiation processes [290]. We incubated keratinocytes with the fluorescent calcium indicator FURA-2 AM before stimulation with ionomicyn (1 mM) as positive control, EDTA (15 mM) as a negative one, fMLP the natural FPR agonist (50 nM), Ac2-26 (1 μM), BOC1 (100 μM) and fMLP/BOC1 and Ac2-26/BOC1 together. The graph in figure 7.7 G showed that the treatment with fMLP and Ac2-26 increased intracellular calcium levels. On the contrary, was not observed calcium mobilization following the treatment with fMLP and/or Ac2-26 with BOC1. Moreover, in figure 7.7 H we observed via confocal microscopy that the administration of the ANXA1 mimetic peptide induced the increase of CK6 (panel b), CK10 (panel f) and involucrin (panel j). Simultaneously, E-cadherin localization disappeared from the cell edge when HaCaT cells were treated with Ac2-26 (Fig. 7.7 H panel n). Instead, no changes were observed in protein localization or signal intensity in treatment with BOC1 (Fig. 7.7 H panels c, g, k, o). Surprising, the effects of Ac2-26 were reverted by the co-presence of BOC1, inducing a midway phenotype between Ac2-26 and BOC1 alone (Fig. 7.7 H panels d, h, l, p).

Thus, Ac2-26, ANXA1 mimetic peptide stimulates keratinocyte motility and differentiation in an FPRs dependent manner.

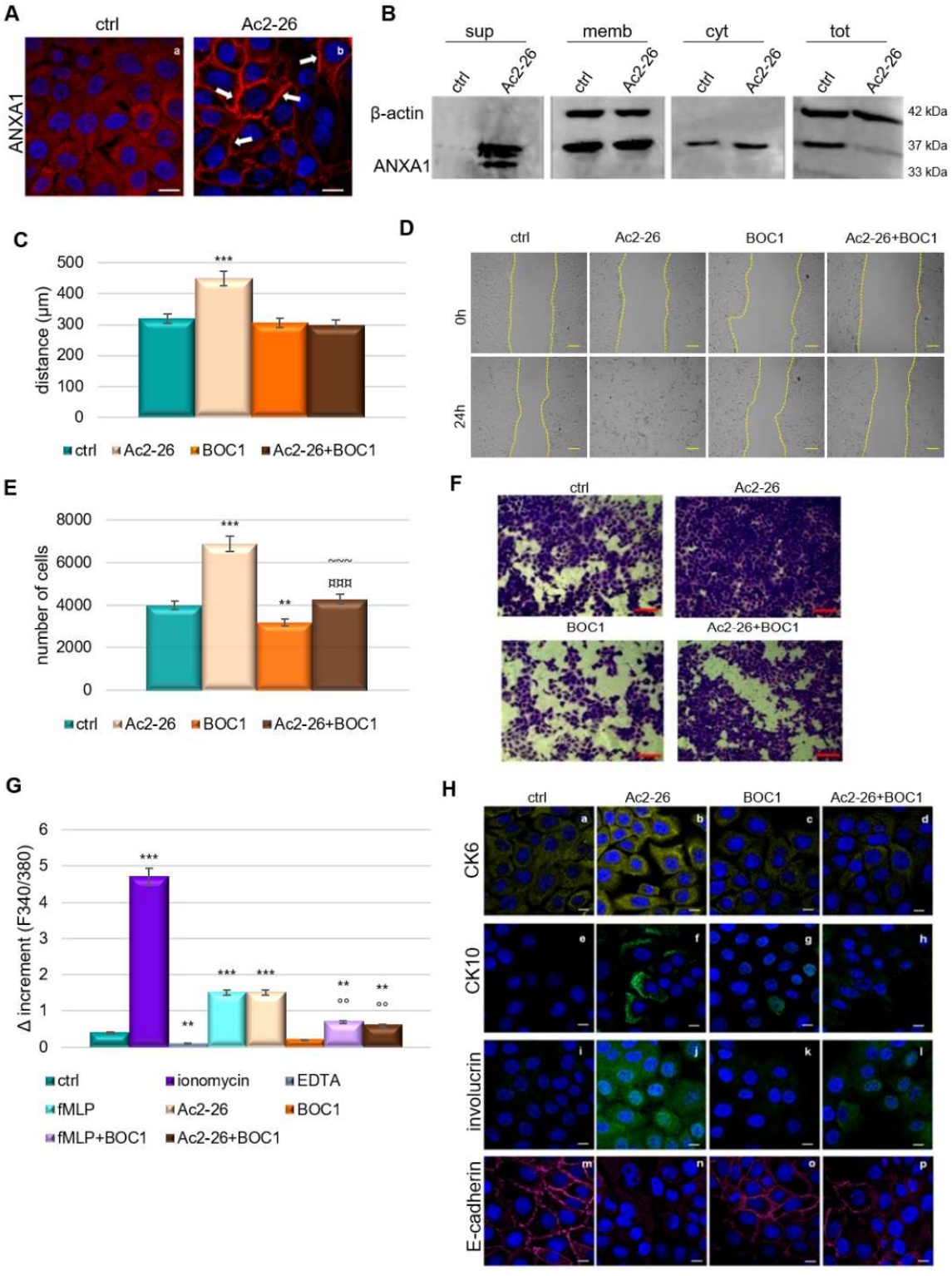

Fig. 7.7 (**A**) Immunofluorescence analysis to detect ANXA1 in keratinocytes not treated (panel a) and treated with Ac2-26 1 μM (panel b). Magnification 63 × 1.4 NA. Bar = 20 μm. (**B**) Extracellular, whole, membrane, and cytosol expression of ANXA1 in HaCaT cells treated or not with Ac2-26 1 μM was analysed by Western blot with an anti-ANXA1 antibody. Protein extracts from cellular compartments were obtained as described in Materials and Methods Section. Protein normalization and the check of the sample quality were performed on β-actin levels. The data shown are representative of three experiments with similar

results. (**C**) Analysis of the migration rate (**D**) and the representative images of HaCaT cells in the presence or not of Ac2-26 (1 μM) and BOC1 (100 μM). The migration rate was determined by measuring the wound closure by individual cells from the initial time (0 h) to the selected time-points (24 h) (bar of distance tool, Leica ASF software). Bar = 150 μm. (**E**) Analysis of invasion speed and (**F**) representative images of keratinocytes treated or not with Ac2-26 (1 μM) and BOC1 (100 μM). Magnification 20×. Bar = 50 μm. Data represent the mean cell counts of 10 separate fields per well. The data represent a mean of three independent experiments ± SEM, their statistical significance were evaluated using Student's *t*-test, assuming a 2-tailed distribution and unequal variance. ** $p < 0.01$; *** $p < 0.001$ for treated *vs* non treated cells; ~~~ $p < 0.001$ for Ac2-26+BOC1 *vs* Ac2-26; ¤¤¤ $p < 0.001$ for Ac2-26+Boc-1 *vs* BOC1. (**G**)The histograms show the fluorescence ratio calculated as F340/F380 nm in absence of extracellular Ca^{2+}. Data are means ± SEM of three experiments with similar results. ** $p < 0.01$; *** $p< 0.001$ treated cells *vs* non treated control; oo $p < 0.01$ fMLP + BOC1 and Ac2-26 + BOC1 *vs* fMLP and Ac2-26, respectively. (**H**) Immunofluorescence analysis to detect: CK6 (panels a–d), CK10 (panels e–h), involucrin (panels i–l), E-cadherin (panels m–p) treated or not with Ac2-26 with or without BOC1. Magnification 63 × 1.4 NA. Bar = 20 μm.

7.8 EVs-containing ANXA1 improved motility and differentiation of keratinocytes through FPRs

Based on the result obtained, we proceed with the study of the role of ANXA1 contained in EVs in motility and differentiation processes. The interaction of microvesicles with target cells triggers intracellular events that control a myriad of cellular responses, such as proliferation, survival, migration, adhesion, and differentiation [291]. In order to evaluate the autocrine effects of microvesicles isolated by HaCaT cells treated or not with mesoglycan, and the involvement of FPRs, migration and invasion assays by administering this EVs on the same keratinocytes were performed. As reported in figure 7.8 A-B, both types of EVs were able to increase the levels of keratinocyte migration, compared to untreated cells. Also, we found a significative reduction of keratinocyte migration rate in presence of the FPRs pan-antagonist, BOC1, even when this compound was administrated together with the two groups of EVs. In the same way, we found a significant increase of keratinocyte invasive speed in presence of EVs mesoglycan more than EVs ctrl, as reported in figure 7.8 C-D. On the contrary, in keratinocytes in presence of BOC1 was observed a reduction of invasive capability, even when the pan-antagonist was administrated with the two kinds of vesicles.

Moreover, the autocrine effect of ANXA1 as a component of EVs has been studied also for the differentiation process. Initially, we evaluated the release of calcium from intracellular reserves. By the fluorescent probe FURA-2 AM we found a significant increase in calcium levels in the cytosol of cells treated with EVs ctrl and much more in presence of EVs mesoglycan. We also assisted a notable

rescue when both EVs have been administrated together with BOC1 (Fig. 7.8 E). In addition, in presence of EVs ctrl and EVs mesoglycan, we investigated the increased expression of ANXA1 followed by its translocation to the cell surface (Fig. 7.8 F panels a–c) the rise in CK6 levels (panels g–i), CK10 (panels m–o), involucrin (panels s–u), and finally, the disorganization of E-cadherin away from the plasma membrane (panels y–a'). Not all these events occurred in presence of BOC1 (panels d, j, p, v, b'). Interestingly, the positive effect on differentiation was partly reversed when all groups of EVs were administered to keratinocytes with BOC1 (panels e, f for ANXA1, panels k, l for CK6, panels q, r for CK10, panels w, x for involucrin and panels c', d' for E-cadherin). Indeed, in this case, we found an intermediate phenotype between EV-treated cells and BOC1 alone.

Thus, these data showed us the significative involvement of ANXA1 contained in mesoglycan EVs in promoting keratinocyte activation in an FPRs dependent manner.

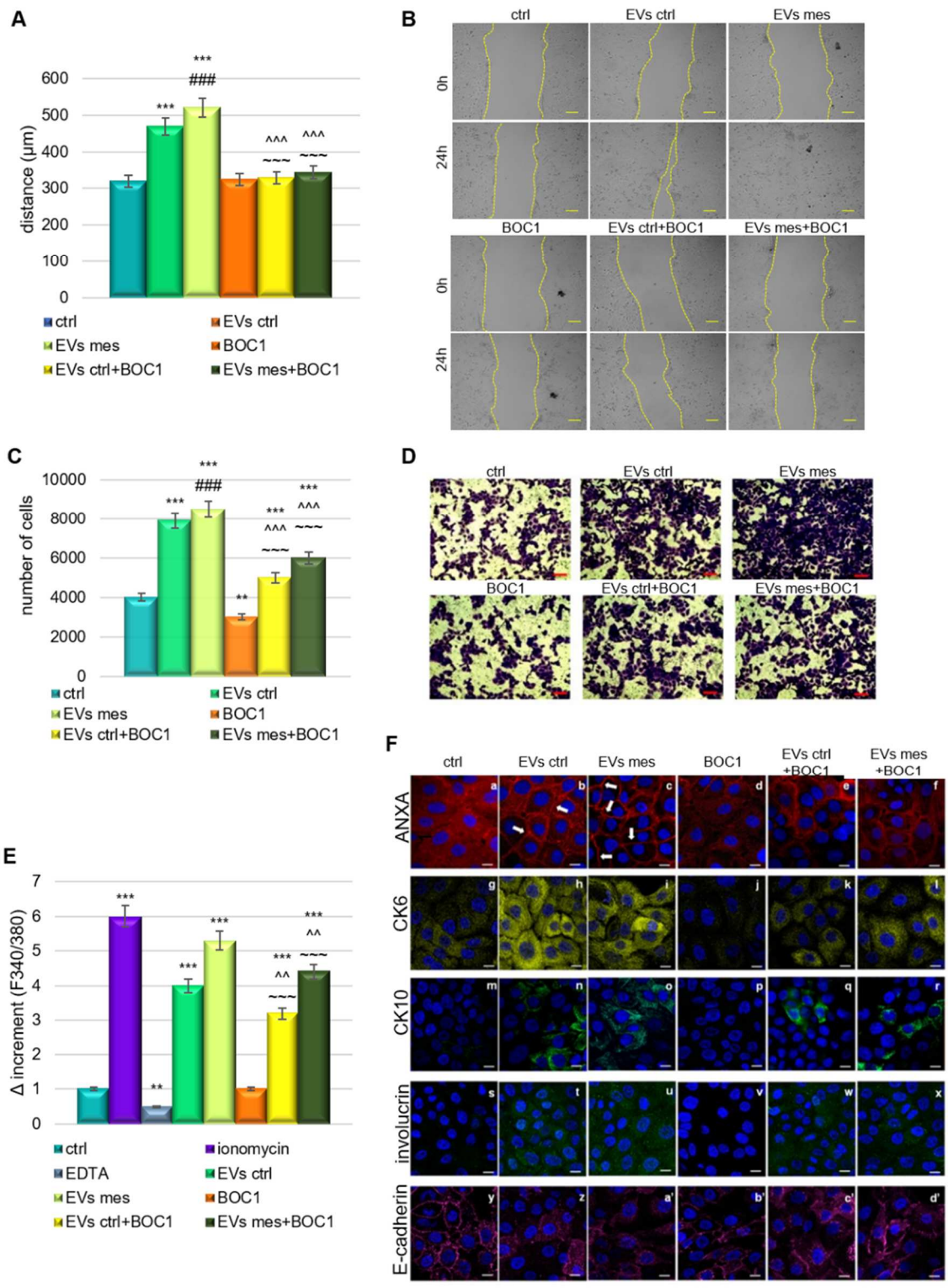

Fig. 7.8 (**A**) Analysis of the migration rate (**B**) and representative images of keratinocytes in presence or not of EVs ctrl, EVs mesoglycan and BOC1 (100 µM). The migration rate was determined by measuring the wound closure by individual cells from the initial time (0 h) to the selected time-points (24 h) (bar of distance tool, Leica ASF software). Bar = 150 µm. (**C**) Analysis and (**D**) representative images of invasion speed of keratinocytes treated or not with EVs ctrl, EVs mesoglycan and Boc-1 (100 µM). Data represent the mean cell counts of 10 separate fields per well ± SEM of 3 experiments with similar results. ** $p < 0.01$;

*** $p < 0.001$ treated cells *vs* non treated control; ### $p < 0.001$ EVs mesoglycan *vs* EVs ctrl; ^^^ $p < 0.001$ EVs ctrl + BOC1 or EVs mesoglycan + BOC1 vs EVs ctrl or EVs mesoglycan respectively; and ~~~ $p < 0.001$ EVs ctrl + BOC1 or EVs mesoglycan + BOC1 *vs* BOC1. Magnification 20×. Bar = 50 μm. (**E**) Effects of ionomicyn (1 mM), EDTA (15 mM), EVs ctrl (20 μg). EVs mesoglycan (20 μg) Boc-1 (100 μM), EVs ctrl+Boc-1 and EVs mesoglycan+BOC1 on the variation of intracellular Ca^{2+}levels in HaCaT cells. The histograms show the fluorescence ratio calculated as F340/F380 nm in absence of extracellular Ca^{2+}. Data are means ± SEM of three experiments with similar results. ** $p < 0.01$; *** $p < 0.001$ treated cells *vs* non treated control; ^^ $p < 0.01$ EVs ctrl + BOC1 or EVs mesoglycan + BOC1 *vs* EVs ctrl or EVs mesoglycan, respectively; ~~~ $p < 0.001$ EVs ctrl + BOC1 or EVs mesoglycan + BOC1 *vs* BOC1. (**F**) Immunofluorescence analysis to detect ANXA1 (panels a–f), CK6 (panels g–l), CK10 (panels m-r), involucrin (panels s–x) and E-cadherin (panels y-d') on keratinocytes treated or not with EVs ctrl, EVs mesoglycan and BOC1. Magnification 63 × 1.4 NA. Bar = 20 μm. The data are representative of three experiments with similar results.

7.9 EVs mesoglycan increased the motility of endothelial cells and fibroblasts

Once confirmed the autocrine effects of EVs mesoglycan on keratinocytes, our interest was to investigate their paracrine effects on human fibroblasts (BJ) and endothelial cells (HUVEC), two cell population involved in skin wound healing process.

As reported in figure 7.9 A-D the vesicles were able to promote the motility in both cell lines. Although EVs ctrl may stimulate major migration compared to untreated cells, but EVs mesoglycan are responsible for the complete closure of the wound for both endothelial cells and fibroblasts. Similarly, cell invasiveness is strongly affected by the presence of EVs (Fig. 7.9 E-H), particularly those isolated from mesoglycan-treated HaCaT cells. EVs released from keratinocytes have been shown to increase the rate of migration of fibroblasts presumably by activation of metalloproteases [158]. Based on this information, we performed a gel zymography observing the increase in matrix metalloproteinases-2 (MMP-2) secretion by BJ cells treated with vesicles in a time-dependent manner from 24 to 72 h (Fig. 7.9 I). It is know that endothelial cells treated with exogenous pro-MMP-2 generates a dose-dependent morphological change associated with an angiogenic reaction [292]. Moreover, once observed the positive effects of vesicles in promoting migration and invasion of endothelial cells, that are considered as preliminary stages of angiogenesis, we proceeded with the study with an *in vitro* formation of capillary-like structures assay. The figure 7. 9 J showed the evidence of EVs in promoting tube formation compared to untreated cells. In particular, EVs isolated from mesoglycan-treated keratinocytes stimulated HUVECs to arrange themselves in tubes longer

and more branched than the once produced by vesicles isolated from untreated keratinocytes (Fig. 7.9 K-L).

These functional data obtained encourage the paracrine role of vesicles isolated from mesoglycan treated keratinocytes.

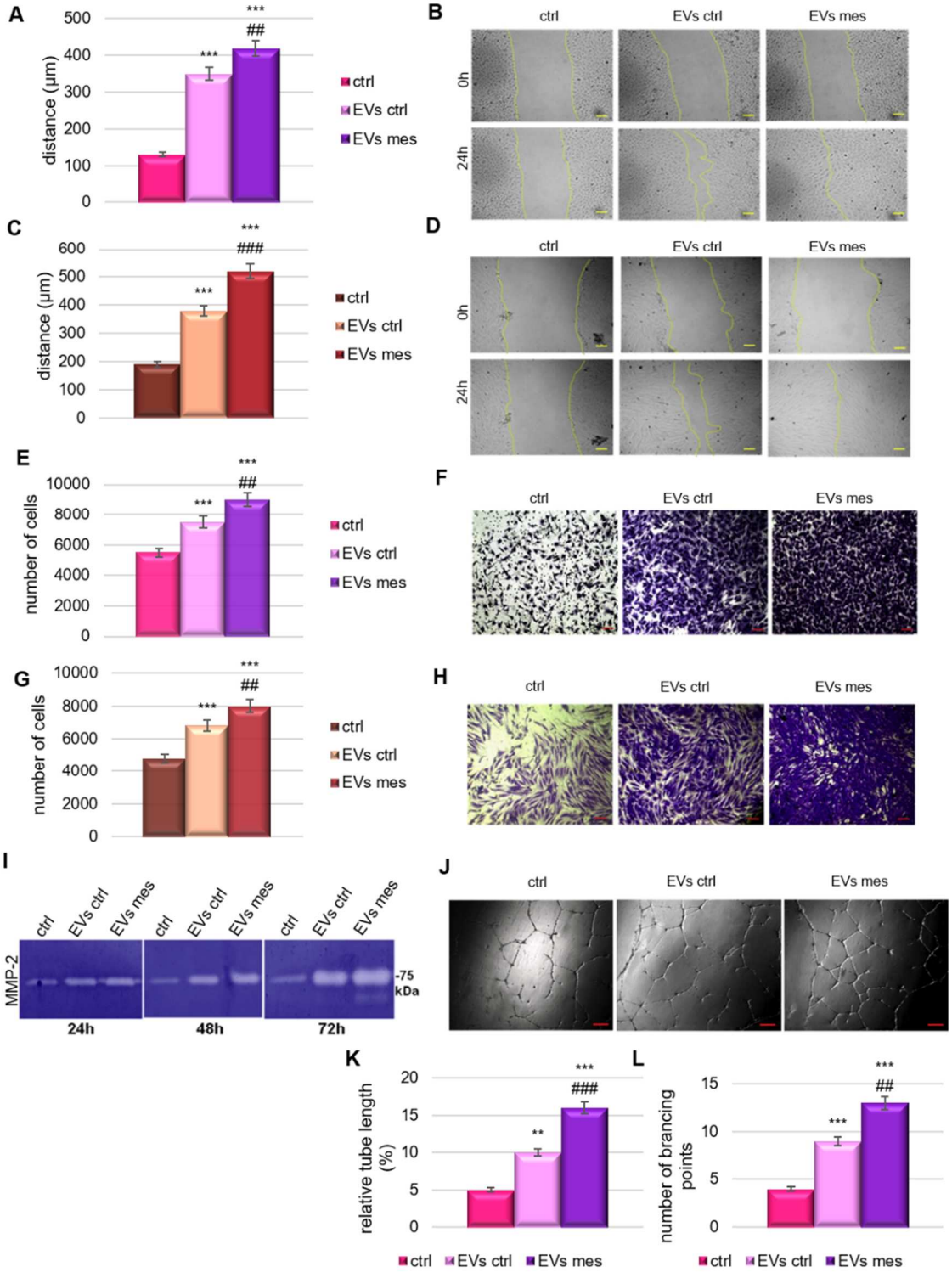

Fig. 7.9 (**A**) Histogram of the results of wound healing assay of HUVEC cells treated or not with EVs ctrl and EVs mesoglycan with the related bright field images (**B**). (**C**) Analysis of the migration rate of fibroblasts in presence or not of EVs ctrl and EVs mesoglycan and their related representative images (**D**). Magnification 10 ×. Bar = 150 μm. (**E**) Analysis of invasion speed of endothelial cells treated or not with EVs ctrl and EVs mesoglycan, and (**F**) its representative images of analysed fields of invasion assay. Magnification 10 ×. Bar = 50 μm. (**G**) Analysis of invasion rate of fibroblasts treated or not with EVs ctrl and EVs mesoglycan and relative bright field images (**H**). Magnification 20 ×. Bar = 50 μm. (**I**) Gelatin zymography showing the gelatinolytic activity of fibroblasts. Zymography was performed using 0.1% gelatin gel as described in Materials and methods followed by Coomassie blue staining. (**J**) Representative images of tube formation by HUVEC cells seeded for 12 h on matrigel and EBM2 1:1 and treated or not with EVs ctrl and EVs mesoglycan. Bar = 100 μm. Analysis of: (**K**) tube length and (**L**) number of branches calculated by ImageJ (Angiogenesis Analyzer tool) software. The data represent a mean of three independent experiments ±S.E.M., their statistical significance was evaluated using Student's t-test, assuming a 2-tailed distribution and unequal variance. ** $p < 0.01$; *** $p < 0.001$ for EVs ctrl and EVs mesoglycan *vs* non treated control; ## $p < 0.01$; ### $p < 0.001$ for EVs mesoglycan *vs* EVs ctrl.

7.10 EVs mesoglycan promoted fibroblast activation and Endothelial to mesenchymal transition

In order to confirm the functional effects observed on migration and invasion in response to the paracrine effects of keratinocytes EVs, we continued our studies observing the cytoskeletal organization of fibroblasts and EndMT of endothelial cells. A significant increase in well-organized stress F-actin fibers was observed in presence of EVs, especially EVs mesoglycan, as shown by phalloidin staining for immunofluorescence assay (Fig. 7.10 A panels a-c). BJ cells showed a basal high level of vimentin, which were not affected by the treatment of the two groups of EVs (Fig. 7.10 A panels d-f). However, observing this marker was revealed a major parallel structure of the fibroblasts and a slight elongation of the cellular body in presence of EVs ctrl and more EVs mesoglycan (Fig. 7.10 A panels e-f). This situation is much more evident in figure 7.10 A panels g-i, observing the expression of Fibroblast Activated Protein 1 (FAP1α). This protein is normally related to activated fibroblasts [293] and it seemed to be expressed in presence of EVs mesoglycan, as shown in figure 7.10 A panels i. A further essential function of fibroblasts is the formation of a new extracellular matrix (ECM) and collagen structures to support other cells, a crucial mechanism for the granulation tissue formation [292]. Therefore, we proceed observing the levels of collagen A1 (COL1A) in fibroblast treated or not with EVs ctrl and EVs mesoglycan. As shown in figure 7.10 A panels j-l, the levels of this protein were increased in presence of EVs, particularly the ones isolated from keratinocytes treated with mesoglycan, compared to untreated cells. Fibroblast growth factor

(FGF) stimulates several pathways involved in cell proliferation, migration and invasion [294]. We focused our attention on FGF-2 a potent chemiotactic factor for fibroblast and endothelial cells in wound healing and produced by fibroblasts [295]. Via immunofluorescence analysis we observed that EVs mesoglycan were able to increase FGF-2 signal in BJ cells compared with their basal expression in untreated fibroblast and in those treated with EVs ctrl (Fig. 7.10 A panels d-f).

On the other hand, once evaluated the functional aspects of migration and invasion, as two process of angiogenesis, we studied the EndMT through immunofluorescence microscopy. The first protein analysed was Vascular Endothelial (VE)-cadherin, a cell adhesion molecule [296]. There was a significative loss of its expression in presence of both the kinds of vesicles compared with the untreated control (Fig. 7.10 B panels a-c). Contrary, the fibronectin protein was strong expressed and structured in presence of the EVs (Fig. 7.10 B panels d-f) with an increased fluorescence intensity in panel f. FAPα is a pro-angiogenic factor in endothelial cells [297], and as shown in figure 7.10 B it is absent in untreated control (panel g) while it is detected in EVs treated cells, particularly EVs mesoglycan (panel i). Another marker for mesenchymal phenotype is α-smooth muscle actin (αSMA), a contractile filament protein, important for the development of the vessels [298]. The expression of this protein was increased in EVs treated cells, particularly in cells treated with EVs mesoglycan (Fig. 7.10 B panels k-l). Moreover, vascular endothelial growth factor (VEGF) is a pro-angiogenic factor also involved in maintenance of vessel homeostasis [297]. As reported in figure 7.10 B its expression appears perinuclear in untreated endothelial cells (panel m), with a cytoplasmic localization following the stimulation with EVs ctrl (panel n) and more evident with EVs mesoglycan (panel o).

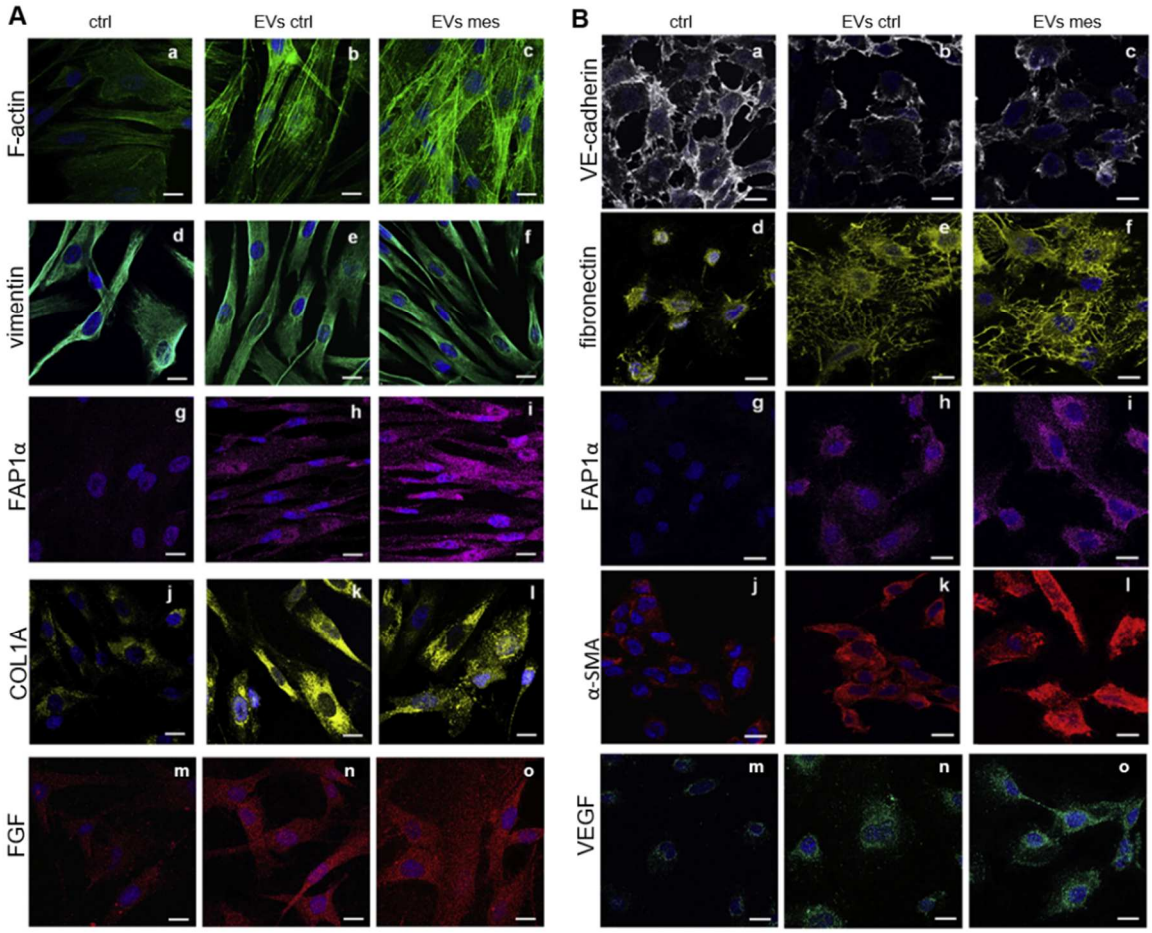

Fig. 7.10 (**A**) Immunofluorescence analysis on BJ cells to detect F-actin (panels a, b, c), vimentin (panels d, e, f), FAP1α (panels g, h, i), COL1A (panels j, k, l) and FGF (panels m,n,o) treated or not with EVs ctrl and EVs mesoglycan for 24 h. Bar = 50 μm. (**B**) Immunofluorescence analysis on HUVEC cells to detect VE-cadherin (panels a, b, c), fibronectin (panels d, e, f), FAP1α (panels g, h, i), α-SMA (panels j, k, l), VEGF (panels m, n, o) treated or not with EVs ctrl and EVs mesoglycan for 24 h. Nuclei were stained with Hoechst 33342 1:1000 for 30 min at room temperature (RT) in the dark. Magnification 63× 1.4 NA. Bar = 50 μm.

7.11 Mesoglycan-VEGF association promotes angiogenesis *in vitro* activating VEGFR2 pathway

Angiogenesis is the process that creates new blood vessels and plays a key role in wound repair [2]. Here, we tested the effect of mesoglycan and VEGFA, a potent angiogenic factor, alone and in combination on the migratory properties of HUVECs using a scratch wound assay. As expected, treatment with VEGFA or mesoglycan lead to increased EC migration. Surprisingly, this effect was increased further when both mesoglycan and VEGFA were used in combination (Fig. 7.11 A and B). We next evaluated the effects of mesoglycan and VEGFA on micro-capillary formation in response

to matrigel. In common with the scratch wound assays, both VEGFA and mesoglycan treatment lead to the formation of significantly longer and more branched tubules as compared with the untreated control. These parameters were enhanced further when treated with VEGFA and mesoglycan in combination, as shown in figure 7.11 C-E.

To explore the effect of mesoglycan and VEGFA in combination in stimulating angiogenesis, we explored the impact of these treatments on VEGFR2 signalling and effectors downstream of this receptor. Treatment of HUVECs with VEGFA and mesoglycan alone or in combination had no discernible effects on the expression levels of VEGFR2. Engagement of VEGRF2 with VEGFA leads to the phosphorylation of a number of Tyr residues in its cytoplasmic domain. Phosphorylation of Tyr951 is intimately associated with EC migration [8]. Phosphorylation of this residue was comparable to controls when HUVECs were treated with mesoglycan alone, however as expected VEGFA treatment resulted in an increase in phosphorylation of Tyr951 and this effect was even greater when mesoglycan and VEGFA were used in combination. Which is suggestive of a role for mesoglycan in promoting the interaction between VEGFA and VEGFR2.

We next looked at the phosphorylation status of several downstream kinases of VEGFR2 which are known to be phosphorylated in response to VEGFA. These included, ERK, 38 MAPK, pHSP27, and FAK. In all instances, phosphorylation was substantially more when mesoglycan and VEGFA were used in concert. As reported in the western blot in figure 7.11 F no significant difference appeared in Extracellular-signal-regulated kinases (ERK) expression between the treatments. In contrast, there was a positive regulation of p-ERK in HUVEC treated with mesoglycan and VEGFA separately, but particularly when these two components were co- administered. The same trend occurred for the expression levels of p38 mitogen-activated protein kinases (p38MAPK) and heat shock protein 27 phosphorylation (p-HSP27). p38MAPK-HSP27 signalling downstream VEGFA-VEGFR2 contributes to actin cytoskeleton reorganization and migration of endothelial cells to promote pro-angiogenic effects [18]. Focal adhesion kinase (FAK) and its phosphorylated form (p-FAK) are proteins downstream VEGFR2 pathway, involved focal adhesions and stress fiber development. The co-administration of mesoglycan and VEGF promoted higher expression levels of FAK, and this was also reflected in an increase in p-FAK. Interestingly, administration of VEGFA and Mesoglycan alone could promote this increase in FAK levels (Fig. 7.11 F).

Immunofluorescence analysis revealed that internalization of p-VEGFR2 after 24 hours of VEGFA treatment and this was enhanced by co-administration with mesoglycan (Fig. 7.11 G panels a-d). Loss of VE-cadherin is associated with VEGFA promoted EndMT [19] and we observed a substantial loss of VE-cadherin expression in HUVECS upon treatment with VEFA and mesoglycan (Fig. 7.11 G panels e-h). The corresponded to an increase in the formation of stress fibers observed

through the polymerization of F-actin (Fig. 7.11 G panels i-l) and FAK positive focal adhesions (Fig. 7.11 G panels m-p). These results suggested that mesoglycan and VEGFA in combination drive the formation of new vessels *in vitro* to a greater extent than when applied individually. Moreover, mesoglycan in concert with VEGFA leads to enhanced angiogenic responses and this is due to enhanced signalling through the VEGFA/VEGFR2 axis.

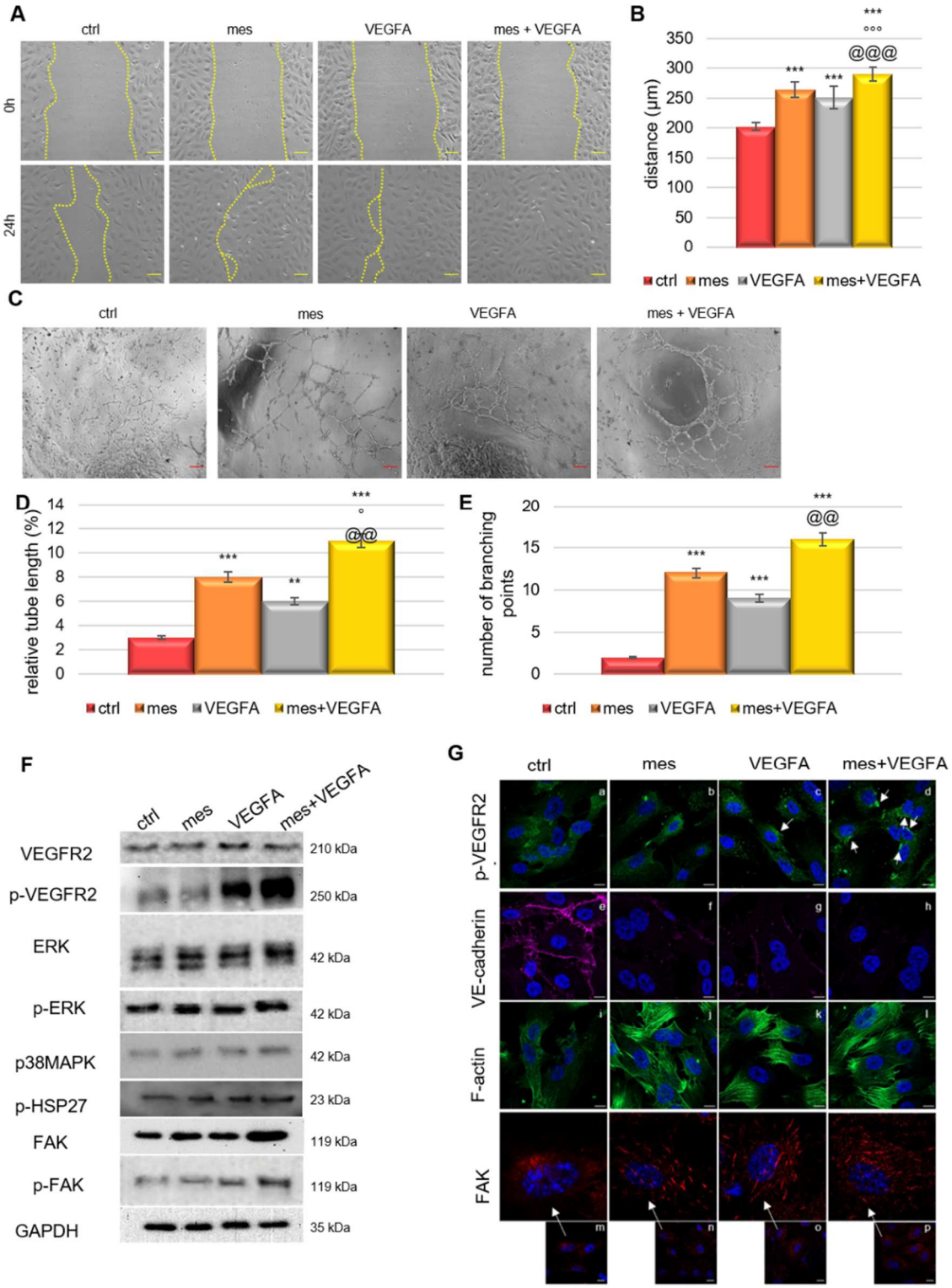

Fig. 7.11 (**A**)Representative images for migration assay and (**B**) analysis of HUVEC cells in presence or not of mesoglycan (0.3 mg/mL), VEGF (10ng/mL), mesoglycan (0.3 mg/mL) and VEGF (10ng/mL). The migration rate was determined by measuring the wound closure by individual cells from the initial time (0 h) to the selected time-points (24 h). Magnification 10 ×. Bar = 150 μm. (**C**) Representative images of tube formation by HUVEC cells seeded for 12 h on matrigel and EBM2 1:1 and in presence or not with mesoglycan (0.3 mg/mL), VEGF (10ng/mL), mesoglycan (0.3 mg/mL) and VEGF (10ng/mL). Analysis of (**D**) tube length and (**E**) number of branches calculated by ImageJ (Angiogenesis Analyzer tool) software. The data represent a mean of three independent experiments ± SEM, their statistical significance was evaluated using Student's *t*-test, assuming a 2-tailed distribution and unequal variance. ** $p < 0.01$; *** $p < 0.001$ for all treatments *vs* untreated cells. # $p < 0.05$; ### $p < 0.001$ for all treatments *vs* mesoglycan. @@ $p < 0.01$; @@@ $p < 0.001$ for all treatments *vs* VEGF. (**F**) Western blot analysis of total protein extracts from endothelial cells treated or not for 24 h with mesoglycan (0.3 mg/mL), VEGF (10ng/mL) and mesoglycan (0.3 mg/mL) and VEGF (10ng/mL) together. Cropped blots from full-length gels are representative of $n = 3$ independent experiments with similar results using antibodies against VEGFR2, p-VEGFR2, ERK, p-ERK, p38MAPK, p-HSP27, FAK, p-FAK and normalized with GAPDH. The blots were exposed to Las4000 (GE Healthcare Life Sciences). (**G**) Immunofluorescence analysis of HUVEC cells in presence or not of mesoglycan (0.3 mg/mL), VEGF (10ng/mL) and mesoglycan (0.3 mg/mL) and VEGF (10ng/mL) co-administrated. The cells were fixed and labelled with antibody against p-VEGFR2 (panels a-d), VE-cadherin (panels e-h), FAK (panels m-p) and with phalloidin (panels i-l). Nuclei were stained with Hoechst 33342 1:1000 for 30 min at room temperature (RT) in the dark. Magnification 63× 1.4 NA. Bar = 50 μm.

7.12 SDC4 is required for mesoglycan-VEGFA promoting angiogenesis *in vitro*

Our published study [14] describes how mesoglycan can stimulate syndecan-4 pathway and promote the migration in human keratinocytes during wound repair process.

Mice null for syndecan-4 exhibit wound defects, particularly in the formation of granulation tissue in which angiogenesis is impaired and in wound closure [20]. Based on this we speculated it may have a role in the synergistic effects of mesoglycan-VEGFA on angiogenesis.

We therefore performed scratch wound migration assays on primary mouse lung endothelial cells from WT and Sdc4-/- animals. WT MLECs had the same response profile we observed in HUVECs, in that co-administration of VEGFA and mesoglycan significantly increased EC migration.

In contrast, the absence of SDC4 lead to reduced EC migration in response to all treatments (Fig. 7.12 A-B), suggesting a role for this proteoglycan in both VEGFA and mesoglycan driven responses. These results were mirrored when tubule formation in response to matrigel was assayed. WT MLECs showed enhanced response to VEGFA and mesoglycan and this was enhanced when the two were combined. In all instances SDC4 showed a lack response (Fig. 7.12 C-E).

These results suggest that syndecan-4 may have a role in the pro-angiogenic pathways stimulated by VEGFA and mesoglycan.

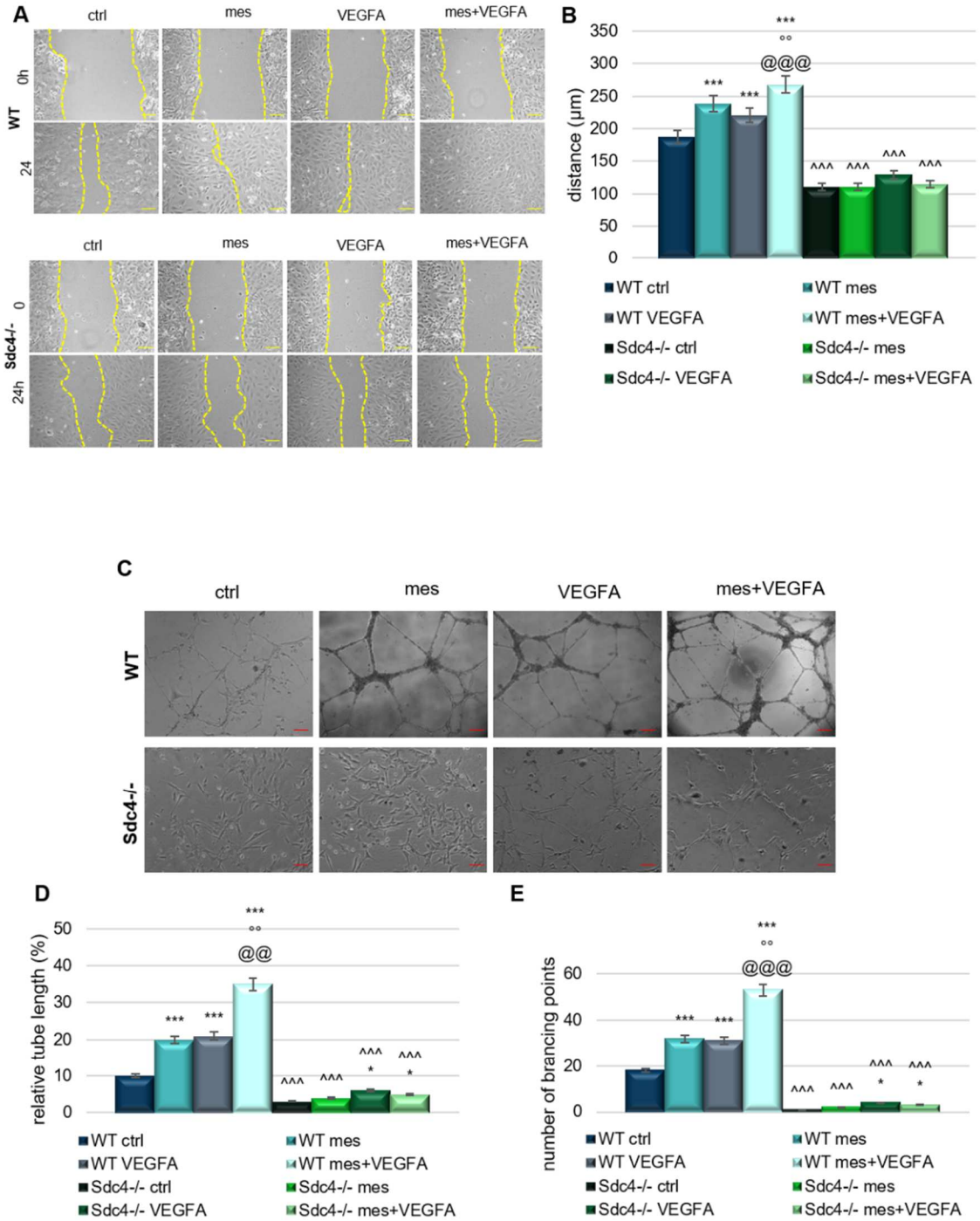

Fig. 7.12 (**A**)Representative images for migration assay of MLEC WT and *Sdc4-/-* and (**B**) analysis in presence or not of mesoglycan (0.3 mg/mL), VEGF (10ng/mL), mesoglycan (0.3 mg/mL) and VEGF (10ng/mL) co-administered. Magnification 10 ×. Bar = 150 µm. (**C**) Representative images of tube formation by MLEC WT and *Sdc4-/-* seeded for 12 h on matrigel and MLEC medium 1:1 and in presence or not

with mesoglycan (0.3 mg/mL), VEGF (10ng/mL), mesoglycan (0.3 mg/mL) and VEGF (10ng/mL) together. Analysis of (**D**) tube length and (**E**) number of branches calculated by ImageJ (Angiogenesis Analyzer tool) software. The data represent a mean of three independent experiments ± SEM, their statistical significance was evaluated using Student's *t*-test, assuming a 2-tailed distribution and unequal variance. ** $p < 0.01$; *** $p < 0.001$ for all treatments *vs* untreated cells. ## $p < 0.01$ for all treatments *vs* mesoglycan. @@ $p < 0.01$; @@@ $p < 0.001$ for all treatments *vs* VEGF. ^^^ $p < 0.001$ for *Sdc4*-/- treatment *vs* WT treatment.

7.13 SDC4 has a role in mesoglycan-VEGF-VEGFR2 pathway

Having confirmed the pro-angiogenic effects that mesoglycan-VEGFA exert on WT and not on Sdc4-/- MLECs we sort to determine whether genetic ablation of SDC4 had any impact on VEGFA/VEGFR2 signalling. WT and Sdc4-/- MLECs had equivalent levels of VEGFR2 regardless of the treatments. Additionally, measurement of Tyr951 phosphorylation on VEGFR2 in WT MLECs broadly reflected the situation observed on HUVECs in that VEGA treatment alone and in combination elicited more VEGFR2 phosphorylation. Levels of VEGFR2 phosphorylation was at a lower level in Sdc4-/- MLECs however VEGFA treatment did elicit a phosphorylation response. Of note combined treatment of Sdc4-/- MLECs with mesoglycan and VEGFA lead to a reduction in VEGFR2 phosphorylation. VEGFA alone or with mesoglycan administered to WT MLECs stimulated an increase in ERK and p-ERK levels. In Sdc4-/- MLECs, ERK levels of expression remained similar to the untreated control, while its phosphorylated form increased only in presence of VEGFA alone. In addition, increases in p38MAPK and p-HSP27 were not evident in Sdc4-/- cells, while in WT cells their phosphorylation increased following VEGFA and mesoglycan- VEGFA treatment in concert. FAK and p-FAK in WT MLECs appeared upregulate particularly after VEGFA and mesoglycan-VEGF treatment, on the contrary, MLEC Sdc4-/ did not show a significant alteration, except for VEGF (Fig. 7.13 A-B).

We next observed via confocal microscopy the localization of proteins involved in EndMT. For p-VEGFR2, WT cells presented the same trend previously observed in HUVECs. However, in Sdc4-/- cells the fluorescence intensity of p-VEGFR2 was lower than in WT cells (Fig. 7.13 C panels a-h) and its expression level increased only in presence of VEGFA (Figure 7.13 C panel g). VE-cadherin was clearly visible at the leading edge of WT MLECs only in the untreated control (Fig. 7.13 C panel i) and disappeared with all treatments (Fig. 7.13 C panels j-l). On the contrary, in Sdc4-/- MLECs, we found a slight decrease of this protein only in presence of VEGFA (Fig. 13 C panels m-p). Simultaneously, F-actin was not completely assembled in Sdc4-/- cells (Fig. 7.13 C panels u-x) as opposed to WT ones. Furthermore, in the latter, actin filaments appeared well organized with mesoglycan, VEGFA and mesoglycan- VEGFA treatments (Fig. 7.13 C panels r-t). Comparing FAK

expression between WT and Sdc4-/- EC, the reduction of focal adhesions was clearly visible in absence of the proteoglycan. FAK appeared as clusters at the boundary of WT MLECs treated with mesoglycan and VEGFA (Fig. 7.13 C panels z-a'), but particularly when combined (Fig. 7.13 C panel b'). In contrast, its expression in Sdc4-/- cells was similar to the untreated control of WT cells (Fig. 7.13 C panel c'), except for the treatments with VEGFA (Fig. 7.13 C panel e').

Taken together these results showed that mesoglycan act as a bridge among SDC4 and VEGFA-VEGFR2 pathway.

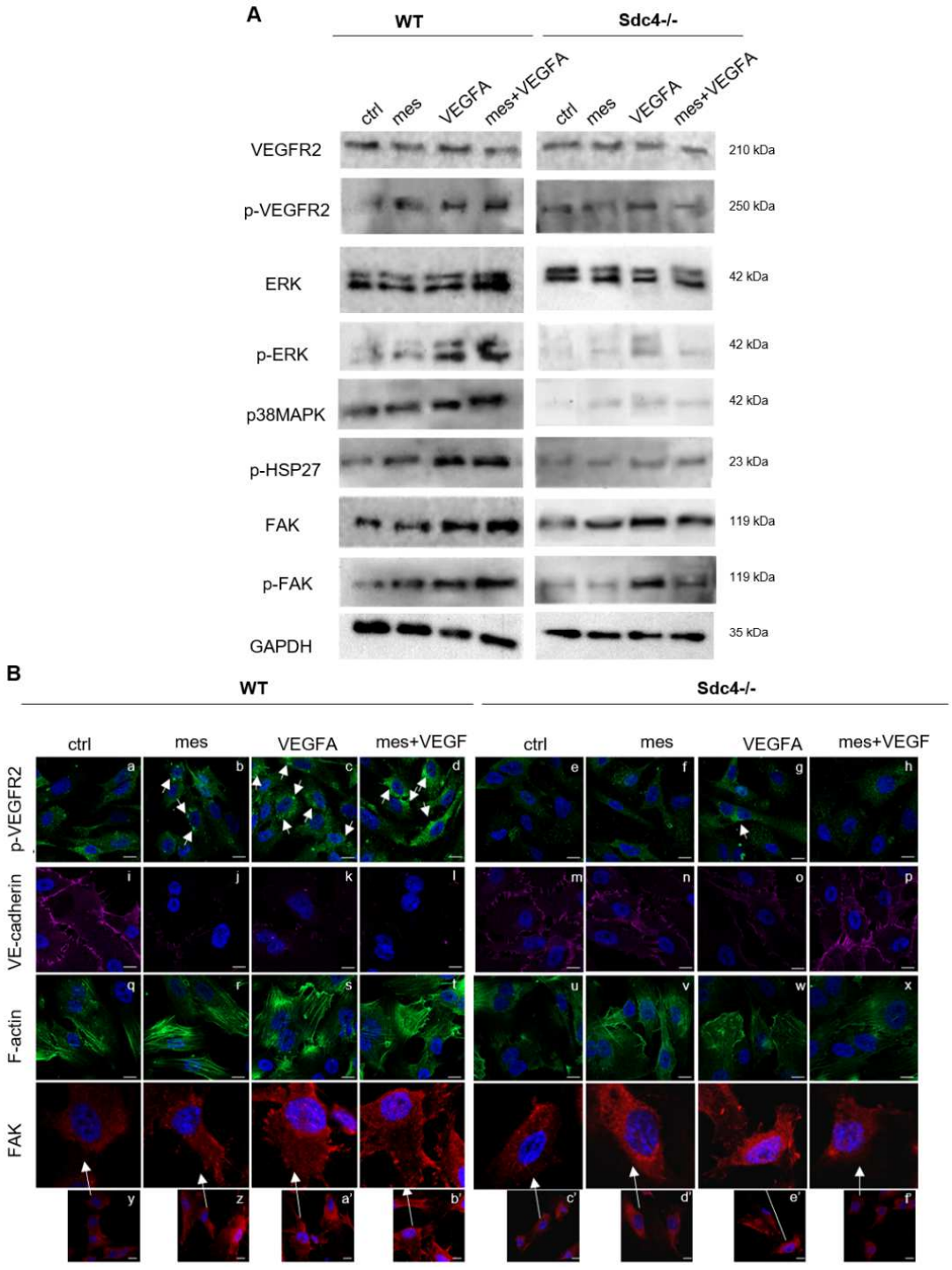

Fig. 7.13 (**A**) Western blot analysis of total protein extracts from MLEC WT and *Sdc4*-/- treated or not for 24 h with mesoglycan (0.3 mg/mL), VEGF (10ng/mL) and mesoglycan (0.3 mg/mL) and VEGF (10ng/mL) co-administered. Cropped blots from full-length gels are representative of n = 3 independent experiments with similar results using antibodies against VEGFR2, p-VEGFR2, ERK, p-ERK, p38MAPK, p-HSP27, FAK, p-FAK and normalized with GAPDH. The blots were exposed to Las4000 (GE Healthcare Life Sciences). (**B**) Immunofluorescence analysis of MLEC WT and SDC4-KO in presence or not of mesoglycan (0.3 mg/mL), VEGF (10ng/mL) and mesoglycan (0.3 mg/mL) and VEGF (10ng/mL) together. The cells were fixed and labelled with antibody against p-VEGFR2 (panels a-h), VE-cadherin (panels i-p), FAK (panels y-f') and with phalloidin (panels q-x). Nuclei were stained with Hoechst 33342 1:1000 for 30 min at room temperature (RT) in the dark. Magnification 63× 1.4 NA. Bar = 50 μm.

7.14 ANXA1 is the connection between SDC4 and VEGFR2

In order to better understand the connection, promoted by mesoglycan, between SDC4 and VEGFR2 in enhancing angiogenesis *in vitro*, we investigated the protein AnnexinA1 (ANXA1) as a key regulator of angiogenesis both in pathological and physiological environment [12, 15, 21].

Here, we found an increase of this protein in WT MLECs and HUVECs treated with mesoglycan, compared to Sdc4-/- cells that presented a small significant rise of ANXA1 only in VEGFA treatment (Fig. 7.14 A-B). Based on this, our strategy was to treat HUVECs with small interfering RNA (siRNA) against ANXA1 (siANXA1), by which we obtained a significant decrease in ANXA1, as reported in fig. 7.14 A-B. We next performed functional experiments on HUVECs using siANXA1 in presence or absence of mesoglycan, VEGFA and in combination. Interestingly, migration and micro-capillary formation *in vitro* were reduced when ANXA1 had been knocked down in HUVECs (Fig. 7.14 C-G).

We hypothesized that the increase of ANXA1 in HUVEC cells treated with mesoglycan was able to promote the subsequent externalization of VEGFA and facilitate the motility. We have revealed via Western blot the presence of VEGFA in HUVECs supernatant, particularly when treated with mesoglycan (Fig. 7.14 H). To validate the purity of the analysed supernatants, and the absence of cells, we used β-actin as a technical control.

Together, these results provide important insights into the role of ANXA1 as a mediator of angiogenesis promoted by the combination of mesoglycan and VEGFA.

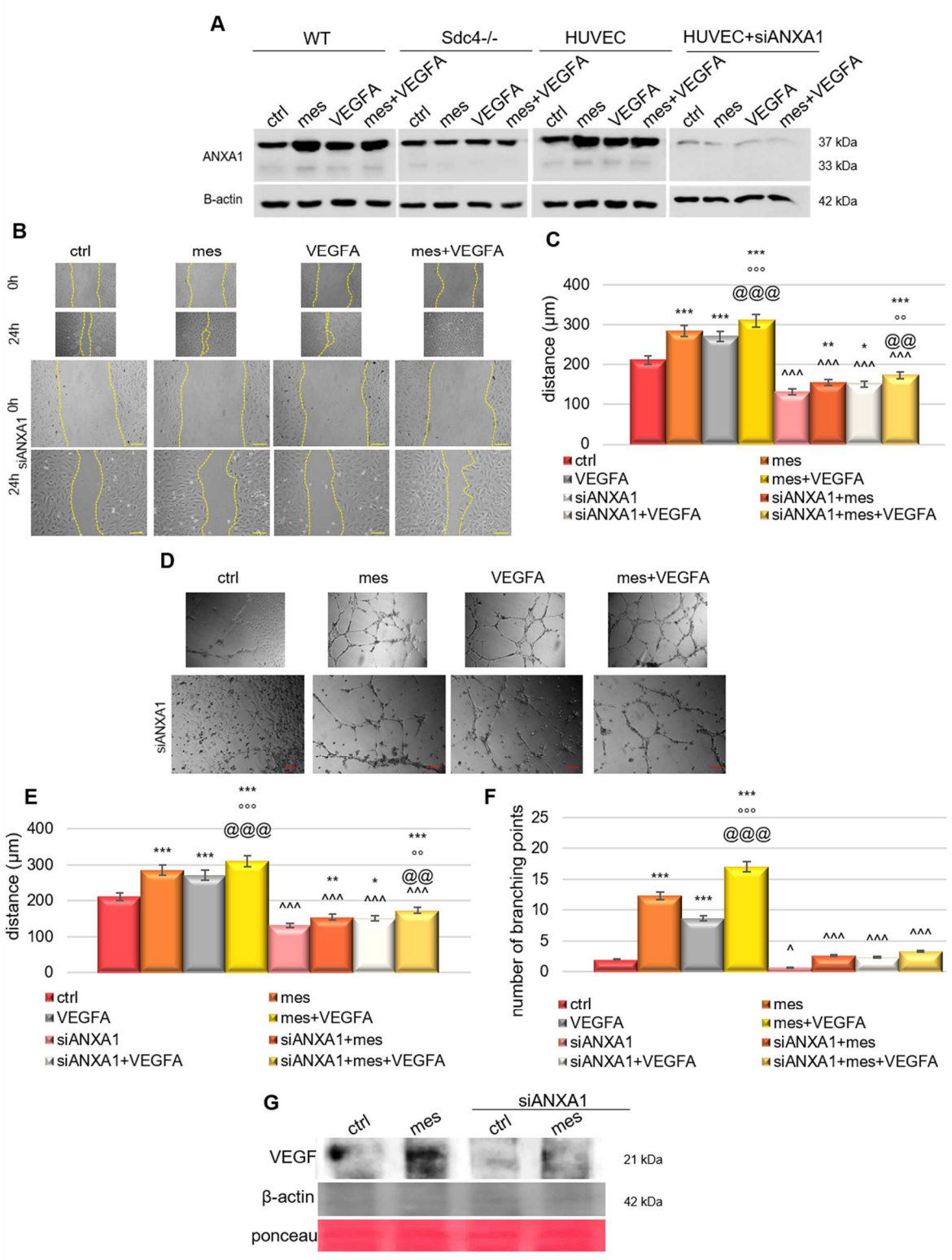

Fig. 7.14 (**A**) Western blot for ANXA1 of total protein extract from HUVEC cells treated or not with mesoglycan (0.3 mg/mL), VEGF (10ng/mL), mesoglycan (0.3 mg/mL) and VEGF (10ng/mL) together, HUVEC treated or not with siANXA1 (100 nM; 48hr) and/or mesoglycan (0.3 mg/mL; 24hr), VEGF (10ng/mL; 24hr), mesoglycan (0.3 mg/mL; 24hr) and VEGF (10ng/mL; 24hr) co-administered. The shown blots normalized using Beta-actin, are representative of $n = 3$ experiments with similar results. (**B**) Representative bright field images captured of HUVEC cells and (**C**) results from the Scratch Wound

Healing Assay at 0 and 24 hr from produced wounds treated or not with mesoglycan (0.3 mg/mL; 24hr), VEGF (10ng/mL; 24hr), mesoglycan (0.3 mg/mL; 24hr) and VEGF (10ng/mL; 24hr) together and/or with siANXA1(100 nM; 48hr). Magnification 10×. Bar = 100 μm. (**D**) Representative images of tube formation by HUVEC seeded for 12 h on matrigel and EBM2 medium 1:1 and in presence or not of mesoglycan (0.3 mg/mL; 24hr), VEGF (10ng/mL; 24hr), mesoglycan (0.3 mg/mL; 24hr) and VEGF (10ng/mL; 24hr) together and/or with siANXA1(100 nM; 48hr). Analysis of (**E**) tube length and (**F**) number of branches calculated by ImageJ (Angiogenesis Analyzer tool) software. The data represent a mean of three independent experiments ± SEM, their statistical significance was evaluated using Student's t-test, assuming a 2-tailed distribution and unequal variance. * $p < 0.05$; ** $p < 0.01$; *** $p < 0.001$ for all treatments *vs* untreated cells. # $p < 0.05$; ## $p < 0.01$; ### $p < 0.001$ for all treatments *vs* mesoglycan. @ $p < 0.05$; @@ $p < 0.01$; @@@ $p < 0.001$ for all treatments *vs* VEGF. ^^^ $p < 0.001$ for all siANXA1 treatment *vs* respective control. (**G**) Western blot for VEGF of supernatant from HUVEC cells treated or not with mesoglycan (0.3 mg/mL) and/or siANXA1. Protein normalization and the check of the sample quality were performed on β-actin and ponceau levels.

7.15 HUVEC cells treated with mesoglycan released EVs containing ANXA1

In our previous work we have shown that ANXA1 participates in extracellular vesicle (EVs) biogenesis and forms part of their cargo [12, 13]. We started out to observe whether mesoglycan stimulated the release of EVs containing ANXA1 from HUVECs. EVs isolated from HUVECs treated with mesoglycan (EVs mesoglycan) and from the same untreated cells (EVs ctrl) were purified through a serial centrifugation and their quantity and size were measured using nanoparticle tracking analysis. EVs mesoglycan (green line in figure 7.15A) showed a significant increase in number compared with EVs ctrl (red line in figure 7.15A). The range of the vesicles was from ~50 nm to 630 nm, with a majority of vesicles in the range of 80 to 150 nm for both the groups (Fig. 7.15 A). This enrichment of EVs between 80-150 nm corresponded with the subclass of nano-vesicles classed as exosomes. To confirm this data, we tested the two groups of vesicles by Western blot using CD63 and CD81 as specific exosomal markers [22]. As reported in figure 7.15 B, the expression of CD81 and CD63 was evident only in EV samples and not in HUVECs total lysates. Moreover, the amount of CD81 and CD63 was higher in EVs released in response to mesoglycan, supporting the previous analysis obtained via nanoparticle tracking analysis. We also observed the significant externalization of ANXA1 through EVs mesoglycan, particularly as cleaved form, compared with EVs ctrl (Fig. 7.15 B).

Therefore, mesoglycan promotes a consistent externalization of ANXA1 through EVs.

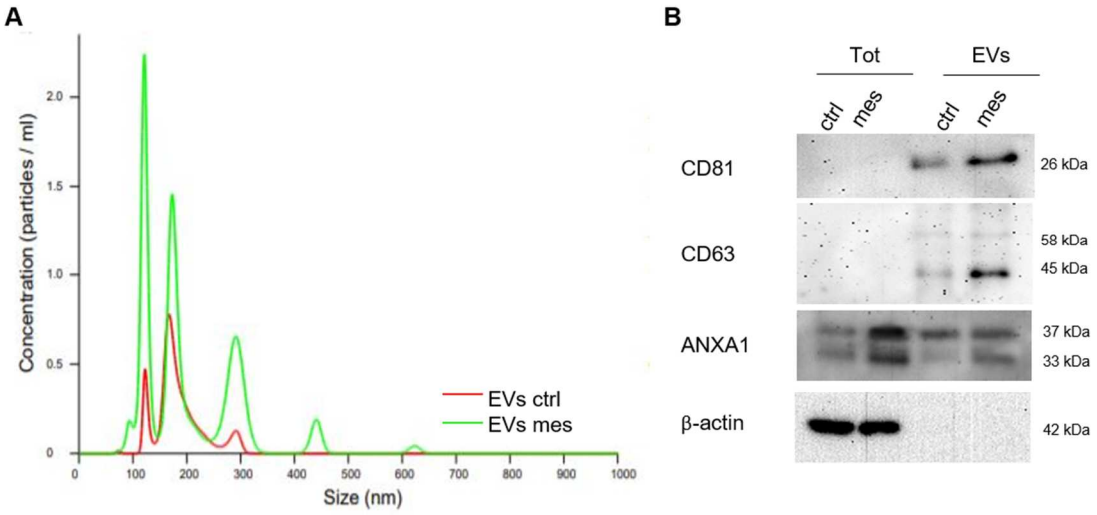

Fig. 7.15 (**A**) comparison of EVs released from HUVEC cells treated (green line) or not (red line) with mesoglycan (0.3 mg/mL) by Nanoparticle tracking analysis. (**B**) Western blot analysis of total protein extracts from HUVEC cells treated or not for 24 h with mesoglycan (0.3 mg/mL), their realised EVs. Cropped blots from full-length gels are representative of n = 3 independent experiments with similar results using antibodies against CD81, CD63, ANXA1 and normalized with β-actin. The blots were exposed to Las4000 (GE Healthcare Life Sciences).

7.16 EVs mesoglycan containing ANXA1 interacted with FPRs in autocrine manner promoting endothelial cell activation

In [299] we highlighted the autocrine loop ANXA1/EVs/FPRs induced by mesoglycan in keratinocytes. Based on this, we investigated the hypothetic role of the same loop in HUVECs in promoting angiogenesis. HUVEC migration was significantly enhanced with mesoglycan elicited EVs compared with the untreated control (Fig. 7.16 A-B). By utilizing BOC1 at a concentration of 100 μM to block both FPR1 and FPR2 (respectively receptors for and N-terminal mimetic peptide [23] and ANXA1 [24]), we studied the role of ANXA1 containing EVs. Surprisingly, in presence of BOC1 HUVEC cell motility was reduced.

We next evaluated the effects of ANXA1 in EVs promoting angiogenesis performing *in vitro* tests of capillary structures. As already seen for migration assay, also in this second process the ability of EVs to stimulate the formation of vessels was confirmed. Notably EVs mesoglycan promoted a significant number of branching points and the relative tube length compared to EVs ctrl and untreated control. On the contrary, by blocking FPRs these effects were reverted, although the same trend of the experimental points without BOC1 was maintained (Fig. 7.16 C-E).

After evaluating that EVs promoted functional effects on motility in autocrine ANXA1- FPRs dependent manner, we investigated EndMT process in absence of ANXA1 by confocal microscopy. First, we found that VE-cadherin expression was significantly reduced in HUVECs treated with EVs ctrl and EVs mesoglycan compared to the untreated control (Fig. 7.16 panels a-c). On the contrary, in presence of BOC1, this adhesion molecule was visible in the cell junctions, even in presence of the two groups of vesicles (Fig. 7.16 panels d-f). Based on the variation of HUVECs migration speed, we observed well organized stress fibers in cells treated with mesoglycan EVs (Fig. 7.16 panels g-i). This cytoskeletal reorganization was not observed when FPRs were blocked (Fig. 7.16 panels j-l). Moreover, the considerable presence of FAK clusters was influenced by the treatment with EVs. This phenomenon was greatly reduced following the addition of BOC1 (Fig. 7.16 panels s-x). The mesenchymal phenotype acquired by HUVECs is generally characterized by the secretion of ECM proteins such as fibronectin which supports the elongation of the vessels *in vitro* [25]. We found a strong and structured expression of fibronectin in presence of both types of EVs (Fig. 7.16 panels m-o). On the contrary, fluorescence intensity levels were significantly reduced when FPRs were blocked in HUVEC cells *in vitro* (Fig. 7.16 panels p-r).

The results in this section suggested that mesoglycan-induced ANXA1/EVs/FPRs loop promotes angiogenesis in HUVECs. Finally, EVs mesoglycan are able to enhance the angiogenesis on HUVECs promoting EndMT.

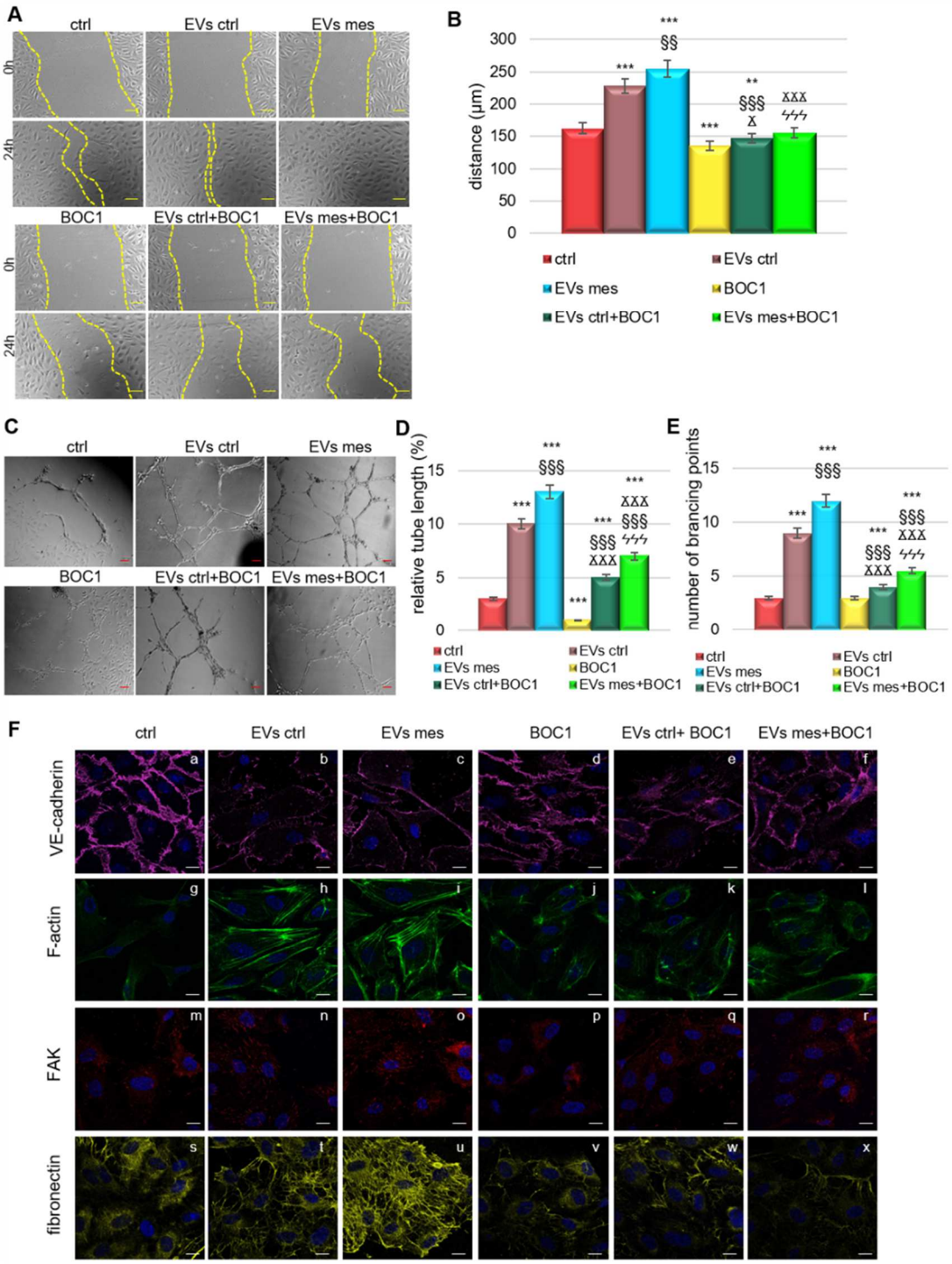

Fig. 7.16 (**A**)Bright field images and (**B**) histogram of wound healing assay of HUVEC cells treated or not with EVs ctrl ($1x10^6$), EVs mesoglycan ($1x10^6$), BOC1 (100 µM) and/or their association. (**C**) Representative images of analysed fields of tube formation assay by HUVEC seeded for 12 h on matrigel and EBM2 medium 1:1 and in presence or not of EVs ctrl ($1x10^6$), EVs mesoglycan ($1x10^6$) and/or BOC1 (100 µM). Magnification 20×. Bar = 150 µm. Analysis of (**D**) tube length and (**E**) number of branches calculated by ImageJ (Angiogenesis Analyzer tool) software. The data represent a mean of three independent experiments ± SEM, their statistical significance was evaluated using Student's t-test, assuming a 2-tailed distribution and unequal variance. ** $p < 0.01$; *** $p < 0.001$ for all treatments *vs* untreated cells. §§ p <

0.01; §§§ $p < 0.001$ for all treatment *vs* EVs ctrl. ϟϟϟ $p < 0.001$ for all treatments *vs* EVs mesoglycan. ΧΧΧ $p < 0.001$ for all treatment *vs* BOC1. (**F**) Immunofluorescence analysis of endothelial cells in presence or not of EVs ctrl ($1x10^6$), EVs mesoglycan ($1x10^6$), BOC1 (100 μM) and vesicles and BOC1 (100 μM) together. The cells were fixed and labelled with antibody against VE-cadherin (panels a-f), FAK (panels m-r), fibronectin (panels s-x) and with phalloidin (panels g-l). Nuclei were stained with Hoechst 33342 1:1000 for 30 min at room temperature (RT) in the dark. Magnification 63× 1.4 NA. Bar = 50 μm.

7.17 Mesoglycan enhanced cell recruitment in the wound areas *in vivo*

Following the evaluated the *in vitro* effects of mesoglycan on different cell types involved in wound repair, we proceeded our study on an *in vivo* system. We tested the effects of mesoglycan on C57BL/6 mice on which we created two interscapular skin wounds. For each mouse, one wound was treated with mesoglycan and the other with PBS as technical control. The interscapular wounds were performed according to the [300] protocol as reported in Material and methods section. The wounds were produced by the surgical removal of all skin layers (epidermis, dermis and subcutaneous fat) from the animal and silicone rubber rings were used to reduce the contraction of the wounds [301]. The wound bed easily accessed to apply topical drops of mesoglycan, or PBS have been recorded by photography for 10 days, in order to study the effects of the treatments on the repair process. As shown in figure 7.17 A, mice sacrificed after 10 days of treatment, respectively, shown a reduction in the wound diameter when treated with mesoglycan compared to control with PBS. The photos shown in figure 7.17 A showed a faster wound healing response and a subtle reduction of the injured area in presence of mesoglycan compared with the wounds treated with control PBS. Indeed, measuring the size of the area of the two different treated wounds after 10 days, did not appeared significative difference as reported in the graph in figure 7.17 A.

This has prompted our interest to investigate the presence of different cell type involved in wound repair in the injured site. Thus, we first confirmed the presence and the activation of keratinocytes through CK6 and CK10, that were among the earliest proteins to be expressed during the differentiation process. CK6 expression was significantly elevated in the damaged human epidermis and during epidermal regeneration, and this keratin had an important role on keratinocyte migration and differentiation during wound healing [301]. As reported in figure 7.17 B, the expression level of CK6 appeared only following the treatment of mesoglycan (panel b) and not in presence of control PBS (panel a). In the same way, CK10 expression was upregulated in epithelial layer of mesoglycan treated wounds (Fig. 7.17 B panel c) and not in PBS treated ones (Fig. 7.17 B pane d). FAPα is a member of group II integral serine proteases, its presence was typically attributed to reactive stromal fibroblasts [302]. In mice skin wounds treated with mesoglycan the level expression of FAPα in the

dermal section of mice biopsies were significant higher compared with the PBS treated wounds, as shown in figure 7.17 B panels e-f.

Vimentin has been shown to act as a signalling integrator for tissue regeneration and healing [303], It was a distinguishing feature of a resident mesenchymal "repair" cell population, to immediately migrate and populate from the edge of the wounded epithelium [304] and stimulate the ability of the cells to invade [305]. The biopsies of skin mice treated for 10 days with mesoglycan showed a significant high level of vimentin in the dermis, compared to the skin treated with PBS of control (Fig. 7.17 B, panels g-h).

In order to verify the presence of endothelial cells in biopsies of skin mice previously treated for 10 days with PBS or mesoglycan, we used the endothelial specific marker CD31. Immunofluorescence staining of blood vessels with CD31 appeared enhanced after the treatment with mesoglycan, appearing as diffusive spots in the dermis area (Fig. 7.17B, panel l), compared to the PBS treated once (Fig. 7.17 B, panel k).

These data showed that the cell activation in mice skin lesions is promoted by mesoglycan.

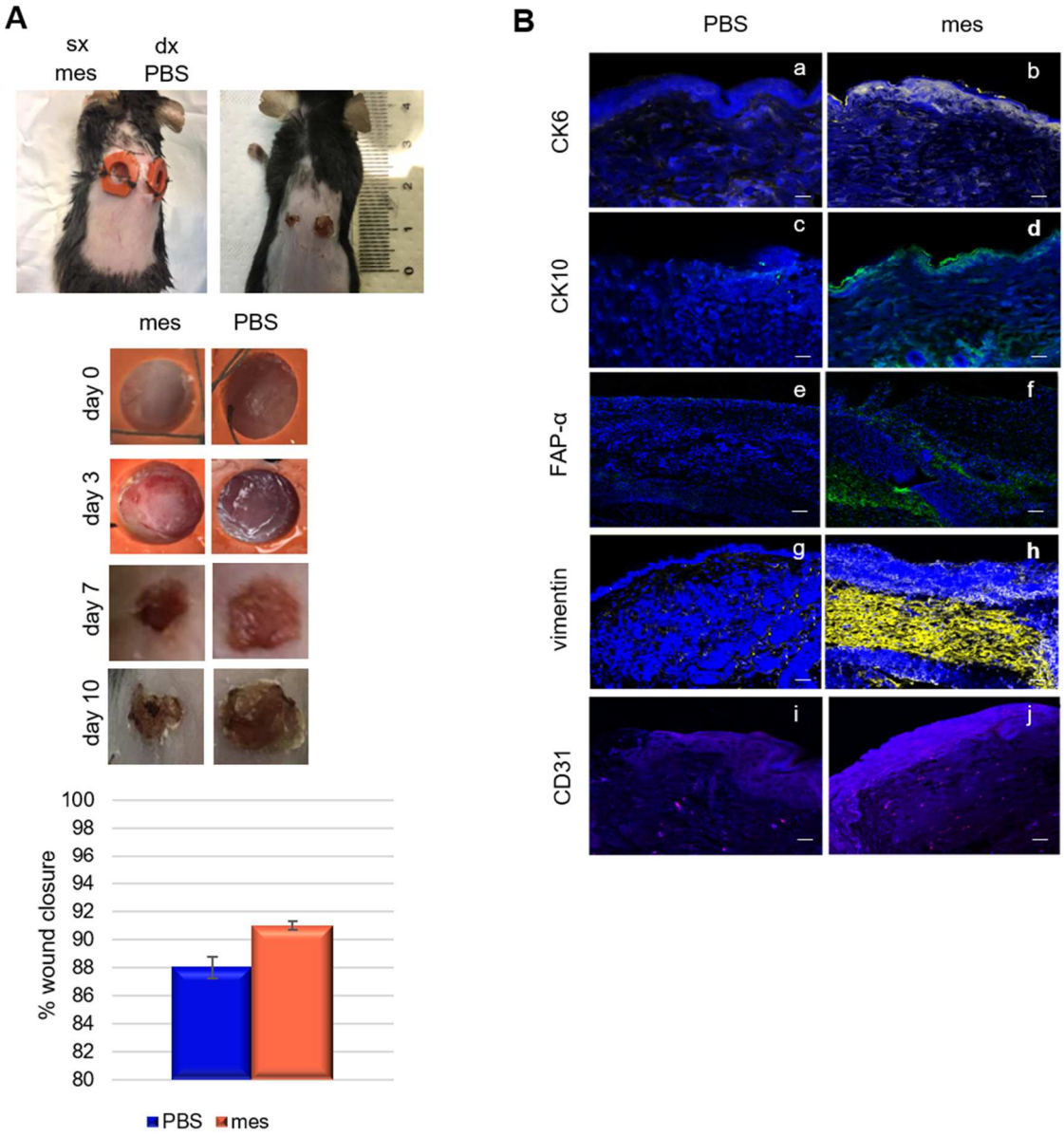

Fig. 7.17 (**A**)Skin wound created in female of C57BL/6 mice, representative photographs from wound showing the macroscopic wound closure on 0, 3, 7 or 10 days postinjury and relative graph of the closure percentage of intrascapular wounds on mice treated with PBS or mesoglycan, respectively. (**B**) Immunofluorescence analysis of skin biopsies of mice treated for 10 days with PBS or mesoglycan. The sections were fixed and labelled with antibody against CK6 (panels a-b), CK10 (panels c-d), FAP-α (panels e-f), vimentin (panels g-h) and CD31 (panels i-j). Nuclei were stained with Hoechst 33342 1:3000 for 120 min at room temperature (RT) in the dark.

7.18 Mesoglycan is able to recruit cells in wound area of patients skin lesions

Previous *in vitro* investigations showed that mesoglycan can enhance re-epithelialization and granulation processes, acting on human epidermal keratinocytes and dermal fibroblasts. Indeed, mesoglycan can induce a strong cytoskeletal reorganization to rise cell migration and invasion, two

key processes at the base of the re-epithelialization and granulation of wound healing. Particularly, fibroblast treated with mesoglycan exhibited the increase of FAP-α and a significant change in shape and orientation, two common features of reactive stromal fibroblasts [183].

Then, to confirm the results previously obtained *in vitro* and observed *in vivo* on mice, we continued the study with the treatment of pressure ulcers with mesoglycan contained in Prisma® Skin. This medical device is a water-soluble dressing with advanced-technology alginate on inert polyethylene terephthalate (PET) support material, including mainly the GAGs mixture and hyaluronic acid. The pressure ulcers, unlike the others, are mainly determined by immobility, regardless of the patient's clinical characteristics and somatic characteristics [306]. Pressure ulcers vary across different degrees of severity, which can be accurately assessed by considering topography, staging, and condition [307], according to international classifications. Taken together, these characteristics made pressure ulcers as a good clinical model for evaluating the effects of mesoglycan *in vivo*. In particular, seven patients affected by pressure ulcers have been selected as described in Materials and methods section and the proliferative arrest was the starting point for studying the activity of fibroblasts, highlighting the function of this device in the granulation phase of wound repair. All patients were in treatment for almost three months, in home care setting, with standard topical protocols that led slight improvements observed during this initial time, but in the following three weeks, the healing process appeared to be stationary and in absence of an evident inflammatory response. As reported in figure 7.18 A, we found no reduction of lesion area and appearance of the wound bed sclerosis. In order to corroborate this preliminary clinical observation and to define the experimental started point (T0) for the application of mesoglycan, we levelled the patients by a histological point of view, carrying out a H&E staining to highlight microscopic differences. The biopsies were made closely to the edge of the lesion because it is known that the process of wound repair starts from the perilesional edge in pressure ulcers of stage III [308]. As reported in figure 7.18 B, patients A-G presented a spread fibrosis component with a reduced presence of fibroblasts or other cell types, including cells of the inflammatory response (Fig. 7.18 B panels a-f). The patient G presented a moderate inflammation suggested by the presence of inflammatory infiltrates, moreover, we found fibroblasts on one side of the section (Fig. 7.18 B panel g, yellow arrow).

To further study the T0 we performed IHC analysis with anti-vimentin antibody to define the effective presence of fibroblasts as shown in figure 7.18 C panels (a-g), confirming the low level of their intervention in the wound area.

Established the characteristic of the T0 as experimental start point, the patients were treated for 14 days with Prisma® Skin containing mesoglycan, for the management of pressure ulcers, according to

the principles of the Wound Bed Preparation. To reduce the possibility of the emergence of general and local complications and to have a good clinical range of monitoring time useful for both the clinical and histological evaluations of cellular activity, we concentrated on a time range 0-14 days (T0-T14). In figure 7.18 D it is shown a photography reportage of the patients and their related wound diameter at T0 and T14, after treatment with Prisma® Skin containing mesoglycan. The pictures confirmed the modification of the wound bed which started to lose its sclerotic features, as a fundamental phase to trigger the following wound closure. Skin biopsies from patients A-I were collected after 14 days (T14) and stained with H&E just like earlier for the starting point (T0). Differently from T0 samples, histological analysis showed a relevant cell architecture (Fig. 7.18 E, panels h-n). Indeed, as shown in the graph in figure 7.18 G, at T14 there is a significant increase in the number of cells compared to T0 for all the patients analysed. This result confirmed that the treatment with Prisma® Skin significantly induced the recruitment of cells in wound areas. In the same way of before, to evaluate the presence of fibroblasts, we executed IHC analysis with anti-vimentin at T14 of patient's biopsies. After the treatment with mesoglycan contained in Prisma® Skin, we found a significant amount of vimentin signal, confirming the massive presence of fibroblasts (Fig. 7.18 F, panels h-n). The significant increase of vimentin in the analysed biopsies after 14 days of treatment with mesoglycan compared to T0, is reported in figure 7.18 H.

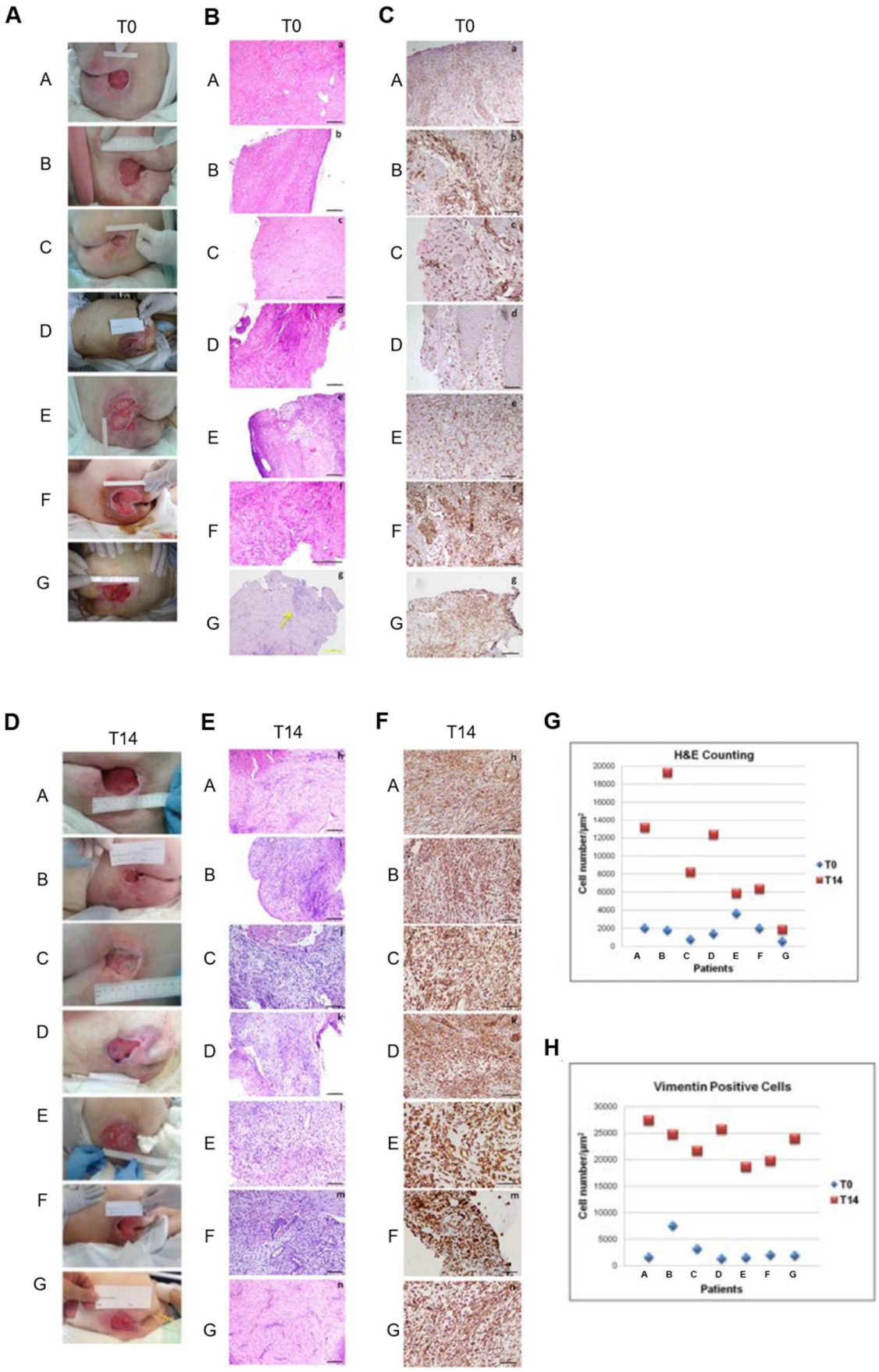

Fig. 7.18 Pictures showing a bedsore wound of patients A-G at T0 (**A**) and T14 (**D**), their tissue sections stained through H&E at T0 (**B**) and T14 (**E**) and the relative IHC staining for tissue sections for vimentin at

T0 (**C**) and T14 (**F**). (**G**) The number of cells per µm2 was counted in at least three fields from three different specimens for each patient. In the graph the average value is shown for patients at T0 (blue dots) and T14 (red square). A negative binomial model was used to model counts as a function of treatment (T0 and T14) and interaction between treatment and patients, followed by ANOVA. P value was < 2.2e-16 for treatment and < 2.2e-16 for the interaction. (**H**) The number of cells positive for vimentin per µm2 was counted in at least three fields from three different specimens for each patient. In the graph the average value is shown for patients at T0 (blue dots) and T14 (red square). A negative binomial model was used to model counts as a function of treatment (T0 and T14) and interaction between treatment and patients, followed by ANOVA. P value was < 2.2e-16 for treatment and < 2.2e-16 for the interaction treatment-patient.

7.19 Mesoglycan impregnated on calcium alginate aerogel using supercritical CO_2 to produce new topical formulation

Gauze, lint, plasters, bandages, and cotton wool are the products traditionally used for wound dressing and to protect them from contamination by pathogenic microorganisms.

Often these traditional dressings are used to absorb and drain exudates from the wound, therefore they require frequent changes to protect against maceration of healthy tissues, making them less convenient. Another disadvantage of traditional dressings is that they fail to provide the wound with a moist environment, which is useful for proper wound repair. Therefore, these have been replaced by modern dressings with more advanced formulations [309]. Modern dressings are not created only to cover the wound but have the aim of facilitating healing as well as preventing dehydration. These devices are generally made up of synthetic polymers and can be passive, interactive and bioactive products. Passive products are non-occlusive dressings used to cover the wound and restore its underlying function. Instead, interactive dressings are semi-occlusive or occlusive, available in the form of film, foam, hydrogel and hydrocolloid, which act as a barrier against the penetration of bacteria into the wound environment [309].

Alginate dressings are made from sodium and calcium salts and are highly absorbent. This high absorption capacity is obtained thanks to the formation of hydrophilic gel containing the drug, which reduces the exudates of the wound avoiding bacterial contamination and promote the healing. The use of alginate-based dressings ensures that its ions are exchanged with the blood to form a protective film [309].

Recently, an innovative technique for impregnating a drug in polymeric matrices involves the use of supercritical carbon dioxide ($scCO_2$). The $scCO_2$ acts both as a solvent to solubilize the active ingredient to be impregnated thanks to its high solvent power, and as a plasticizing and swelling agent for polymers enters a rapid penetration into the matrices [310].

In order to produce topical devices in the form of calcium alginate (CAA) aerogel containing mesoglycan, supercritical impregnation was investigated.

A hydrogel was initially prepared (5% w / w sodium alginate in distilled water, stirred for 24 hours at 200 rpm and then poured into cylindrical molds) and made to gel by immersion in a $CaCl_2$ coagulation bath (5% w/w in distilled water) for about 24 hours. In this process, sodium alginate was converted to calcium alginate. The hydrogel obtained was transformed into alcogel through a gradual replacement of the water contained in the pores of the hydrogel by means of a series of ethanol baths lasting 24 hours each, with an increasing concentration of ethanol (30%, 70%, 90% and twice 100% v/v). Finally, the conversion from alcogel to aerogel was obtained using $scCO_2$.

Figure 7.19 A panel a, shown the diagram of the instrument used to dry the alcolgels obtaining the aerogels used for the impregnation. The alcogels were placed in a stainless-steel cylinder, the $scCO_2$ was delivered by a high-pressure pump (20MPa), regulated by a pressure gauge, and after being cooled by a refrigerant bath. The temperature (35°C) instead was regulated by a proportional-integral-derivative (PID) regulator. The drying lasts 5 hours, using an $scCO_2$ flow rate of about 1 kg / h. Below the micrometric valve, there was a second collection vessel, which allowed to recover the ethanol extracted from the pores of the alcohol.

Finally, after the plant was brought back to atmospheric pressure by slow depressurization, the dried aerogels were recovered from the vessel.

Figure 7.19 A panel b showed a diagram of the instrument used to carry out the solubility and impregnation tests. It featured a cylindrical stainless-steel autoclave. The CO_2, once cooled thanks to a refrigerant bath, was fed into the system by a pump. Also in this case, the pressure was measured by a digital pressure gauge, while the temperature by a PID controller. At the exit of the autoclave there was a rotameter which measured the CO_2 output. The solubility of mesoglycan in $scCO_2$ was been experimentally estimated in the pressure range of 18 MPa and at two temperatures (40 and 60°C) in this way: the mesoglycan was wrapped in filter paper and placed on the bottom of the autoclave, closed the instrument and brought to the desired temperature and pressure of CO_2. Once the equilibrium was reached, the system was stored for 24 hours under mechanical stirring. At the end of the experiment, the CO_2 was removed, and the undissolved mesoglycan remained on the filter paper was weighed to obtain the precise amount of dissolved mesoglycan.

Once the conditions for the mesoglycan are established, we proceed with the impregnation tests. A static method was used for the impregnation. 10 mg of mesoglycan were placed in a small open top container to allow contact with $scCO_2$. Instead, 50 mg of aerogel were wrapped in a filter paper, to avoid its contact with the solid drug, and placed on the bottom of the autoclave. Finally, the autoclave was closed, and the CO_2 was slowly fed to the desired temperature. Once the pressure of

18MPa was reached, the system was stored for a specified time. Then, the CO_2 was discharged to reach atmospheric conditions and recover the loaded aerogel from the autoclave. The amount of mesoglycan loaded was determined by both the weight gain of the sample after the experiment and using UV/vis spectroscopy (data not shown).

By means of the FESEM analysis, the morphology of the CAA was analysed both before (Fig. 7.19 B panel a) and after (panel b) the mesoglycan impregnation. CAA alone was characterized by a nano-porous structure with an average pore size of approximately 100 nm (Fig. 7.19 B panel a). The presence of the ports was preserved after the mesoglycan impregnation (Fig. 7.19 B panel b).

To improve the healing process by interacting with the wound, the goal of new wound dressings was the release of bioactive molecules while maintaining the necessary favourable conditions for the restoration of skin integrity and homeostasis. Therefore, the release profile of mesoglycan impregnated on CAA was evaluated, at 18MPa and 60°C for an impregnation time equal to 24h, as shown in the graph in figure 7.19 C. At a physiological pH of 7.4, the release of mesoglycan was quick and complete.

Once we characterized the aerogel containing mesoglycan, we studied its effects on keratinocytes and fibroblasts, cellular lines that represent the main actors in the healing process of skin wounds. To understand the effects of mesoglycan released by CAA on the migration process, we performed functional *in vitro* wound healing assays to evaluate the migration process as reported in the Materials and Methods section. As reported in figure 7.19 D, the motility of HaCaT keratinocytes treated for 24 hours with mesoglycan on CAA resulted significantly increased (43%) both compared to mesoglycan and CAA analysed individually and compared to the untreated control. The same trend was observed on BJ fibroblasts, as reported in figure 7.19 E, in which the increased migration in presence of mesoglycan on CAA increases by 93% compared to mesoglycan alone and 56% more than by CAA alone and untreated cells.

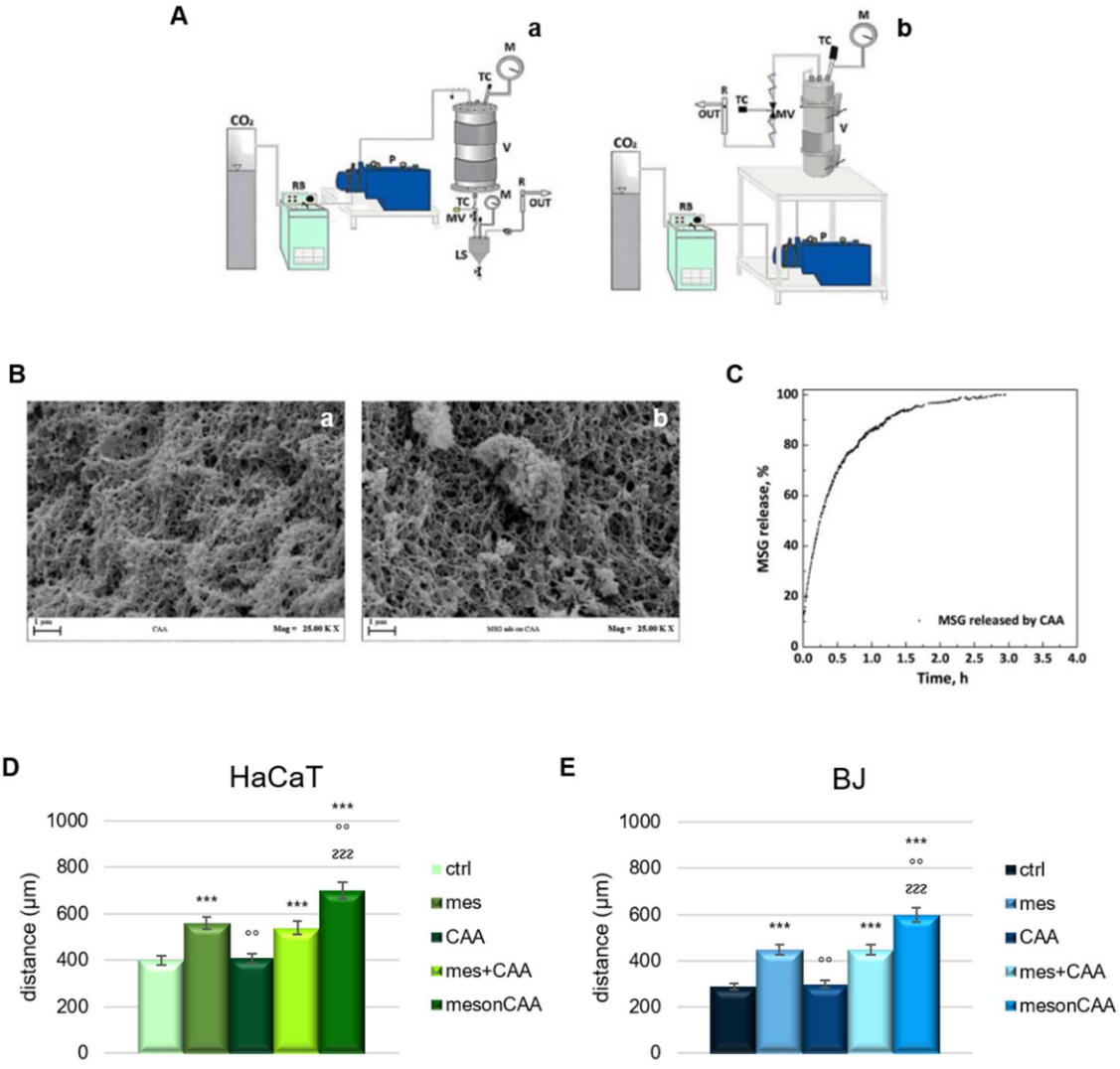

Fig. 7.19 (**A**) Sketches of the laboratory plants for (a) drying; (b) impregnation. CO_2: supply of carbon dioxide; RB: refrigerating bath; P: pump; V: vessel; MV: micrometric valve; LS: liquid separator; TC: thermocouple; M: manometer; R: rotameter. (**B**) FESEM images of (a) pure CAA after drying using $scCO_2$, (b) mesoglycan impregnated on CAA. (**C**) Dissolution profile of mesoglycan loaded on CAA. Evaluation of migration rate of human (**D**) keratinocytes and (**E**) fibroblasts in presence of pure mesoglycan, CAA, mesoglycan and CAA, and mesoglycan impregnated on CAA. The migration rate was determined by measuring the wound closure by individual cells from the initial time to the selected time-points (bar of distance tool, Leica ASF software). The data represent a mean of 3 independent experiments ± SEM, *** $p < 0.001$ *vs* not treated cells; °° $p < 0.01$ treated cells *vs* pure MSG; ƨƨƨ $p < 0.001$ treated cells mesoglycan on CAA *vs* CAA.

7.20 PCL/Mesoglycan obtained by supercritical foaming and impregnation promote the release of the drug in a controlled-time manner

Recent innovation for the treatment of cutaneous wounds is represented by foam dressings. These devices consist of a hydrophobic and hydrophilic foam. The hydrophobic properties of the external part of the device guarantee protection from liquids, at the same time favouring the exchange of gas and water vapor. In addition, the foam has the ability to drain and absorb wound fluids [311].

The use of polycaprolactone (PCL) seems to be particularly promising for the wound dressing, because of its biocompatibility and its capability to prolong the drug release.

After performing the same process described for the CCA, the mesoglycan was impregnated in the foamed PCL. The images in Figure 7.20 A showed the unprocessed PCL and following various mesoglycan adsorption times using scCO2. Particularly after 15 and 24 hours of adsorption, the PCL appeared as swollen sphere. By means of compression the PCL spheres were joined, forming films with a thickness of 100 µm. Following the mesoglycan impregnation at 35°C, 17 MPa for 24 h, a foam of 0.23 mg MSG / mgPCL was formed (Fig. 7.20 B). The morphology of the PCL was observed by FESEM analysis in absence of mesoglycan (Fig. 7.20 C panel a) was characterized by a porous structure. Instead, in presence of mesoglycan (Fig. 7.20 C panel b) the crystalline drug appeared in small needles that filled and covered the porosities of PCL.

Achieving a controlled release of mesoglycan overcomes the major problem of short residence times at the wound site [309]. The dissolution profiles of mesoglycan and mesoglycan impregnated on PCL were evaluated by miming physiological conditions, in PBS at pH 7.4. Their comparison was shown in the graph in figure 7.20 D. The pure mesoglycan was completely dissolved in less than an hour, while mesoglycan impregnated on PCL employed about 70 hours (about 3 days). After analysing the release of mesoglycan from PCL, we studied the effects on the activation of human keratinocytes, fibroblasts and endothelial cells as the main cell populations involved in the repair of skin wounds. We evaluated the migration process as a necessary first step for wound healing. In figure 7.20 E-G we evaluated the effect of the mesoglycan released by the PCL after 24, 48 and 72 hours. In all three experimental times the molecule was able to significantly increase the speed of migration on HaCaT, BJ and HUVEC cells. Indeed, the effects of the mesoglycan released by the PCL were compared with the untreated control and with the pure mesoglycan 50 µg/mL, confirming its positive effects. To further analyse the effects of mesoglycan released by PCL over an extended time, we evaluated the invasion capacity of all cell lines as reported in the Materials and Methods section. Cells acquired greater invasive capacity in presence of mesoglycan released from PCL from 24 to 72 h (Fig. 7.20 H-J) in a very similar way to pure mesoglycan. Another step necessary for effective wound healing is the angiogenesis process. Therefore, we focused on *in vitro* tubulogenesis using HUVEC

cells treated or not with pure 50 µg/mL pure mesoglycan and mesoglycan released from PCL foam at 24, 28 and 72 hours at a final concentration of 50 µg/mL. Figure 7.20 K-L showed that for all experimental times the mesoglycan derived from PCL induced a remarkable angiogenesis *in vitro* both by referring to the relative length of the tube and to the number of branching points reported in the relative histograms.

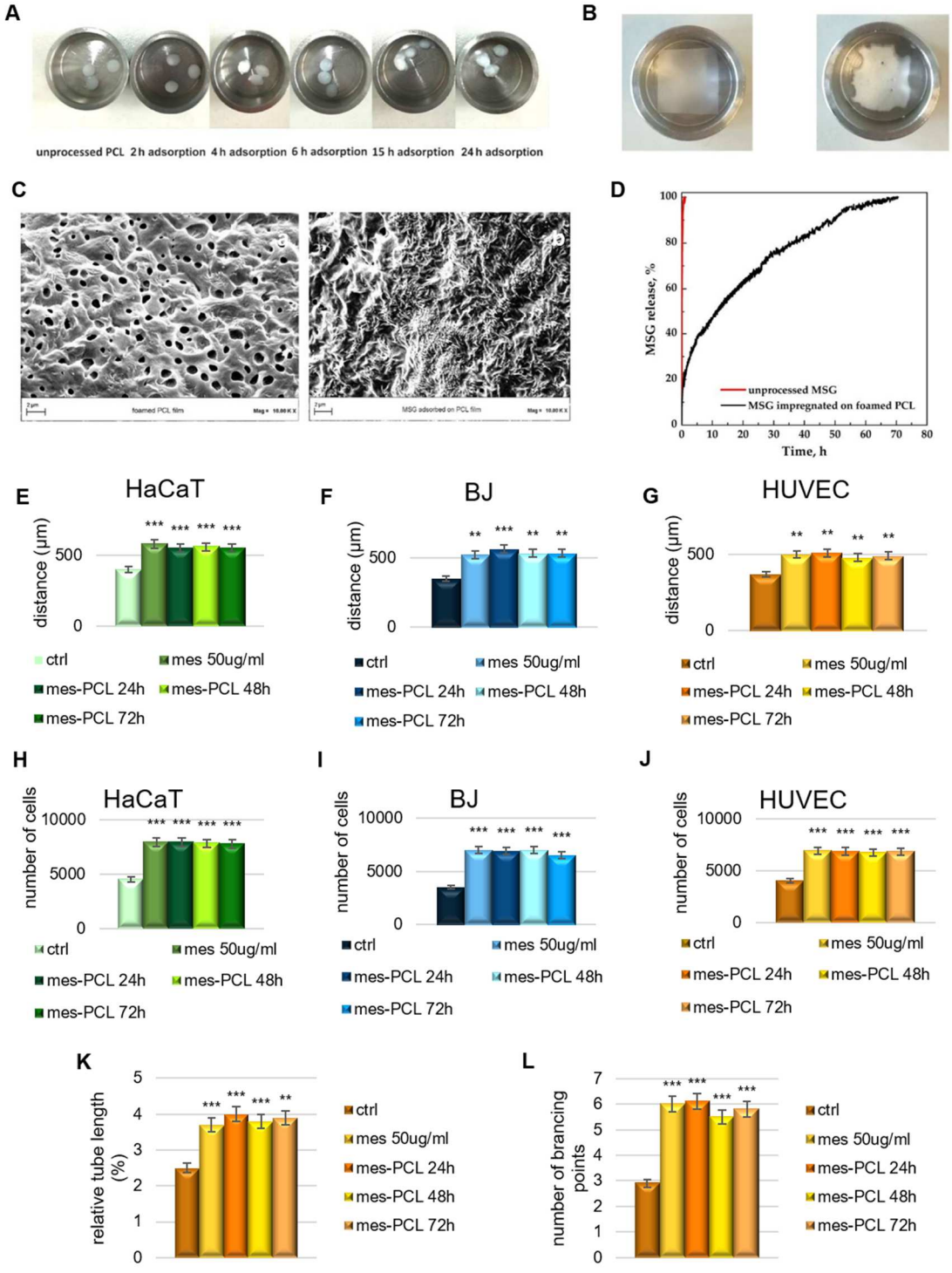

Fig. 7.20 (**A**) Photographs of (a) unprocessed polymer, and impregnated samples at 17 MPa and 35 °C for various contact time: (b) 2 h; (c) 4 h; (d) 6 h; (e) 15 h; (f) 24 h. (**B**) Unprocessed PCL film (a), and foamed PCL film after mesoglycan impregnation (b). (**C**) Field emission scanning electron microscopy (FESEM) images of (a) PCL film foamed by $scCO_2$, and (b) mesoglycan impregnated into/on foamed PCL film. (**D**) Dissolution tests of MSG in PBS at pH 7.4 and 37 °C. Histograms representing the analysis of *in vitro* wound-healing assay on HaCaT (**E**), BJ (**F**), and HUVEC (**G**) cells treated or not with pure mesoglycan, and PCL-derived mesoglycan harvested at 24, 48, and 72 h, all of them at a final concentration of 50 µg/mL. Invasion assay on HaCaT (**H**), BJ (**I**), and HUVEC (**J**) cells. Bar = 150 µm. Analysis of tube length (**K**) and number of branches (**L**)calculated by ImageJ (Angiogenesis Analyzer tool) software. Bar = 100µm. The values reported in the graphs are the mean ± SEM from three independent experiments performed in triplicates. Results appeared significant based on Student's t-test, assuming a 2-tailed distribution and unequal variance. *** $p < 0.001$ and ** $p < 0.01$ *vs* not treated cells.

8. Discussion

Wound healing mechanism is a cascade of concatenated and consequential cellular events that by convention are divided in four phases: haemostasis, inflammatory, proliferative, and remodelling. Reepithelialisation is the most critical step of the wound healing process belonging to the proliferative phase. A failure of this step can lead to a chronic non healing wounds, representing a significant clinical problem. This is the step on which a wound bed could be covered by the formation of a temporary ECM through the migration of cells from the edge of the wound, their proliferation and their differentiation favouring the formation of a new epithelium [312]. ECM proteins, such as GAGs and PGs, can mediate the reepithelialisation [313]. Recently, it is interesting to exploit these molecules as drugs to promote and facilitate the repair process of tissue damage.

Mesoglycan is a mixture of GAGs prescribed as fibrinolytic in clinical practice that supports the reepithelialisation promoting the activation of several cell types involved in skin repair such as keratinocytes, fibroblasts [183] and endothelial cells [271].

SDC4 is a main actor in cell adhesion to ECM as co-receptor [281] and its expression in human skin increase during the injury repair [231] and participate to the healing [232].

For the first time, we show a new molecular mechanism for mesoglycan, which can activate the SDC4 pathway and triggering the migration and differentiation of human keratinocytes.

We examined expression and localization of SDC4 at different times after administration of mesoglycan. SDC4 was massively located in the nuclei of the treated cells in the initial stages of keratinocyte activation (approximately 15 min after treatment), indicating that mesoglycan was able to induce SDC4 coreceptor activation. The nuclear localization of SDC4 is not yet fully understood, but it can increase in some cell populations under conditions associated with a wounded state. A hypothesized role for this nuclear localization is to act as a shuttle for nuclear Hp transport binding growth factors that could modulate cellular functions [314]. The same nuclear localization, 15 min after mesoglycan treatment, was observed for PKCα. The exact role of SDC4-dependent PKCα activation is still unclear, but their co-localisation in focal contacts indicates a probable role in cytoskeletal reorganization, stress fiber formation and cell spread [232]. The possibility that mesoglycan exercised its effects on keratinocytes through the SDC4/PKCα pathway was examined focusing on some PKCα target protein. We discovered that mesoglycan was able to cause the activation and aggregation of integrin β1 on the cell surface, activate paxillin phosphorylation, and induce ezrin translocation to the plasma membranes. All these events are identified as SDC4/PKCα-mediated during focal adhesion assembly and cell migration [281], [315], [316]. Mesoglycan actions on keratinocytes motility mediated by SDC4/PKCα were confirmed by the increase of cell migration

and invasion at 24 hours from treatment, these effects could be fully blocked by SDC4 knockdown, confirming the involvement of the co-receptor in mesoglycan supporting keratinocytes motility.

During the reepithelialisation process, the intracellular Ca^{2+} level modulates events such as keratinocyte migration, proliferation and differentiation [317]. While mesoglycan promotes the increase of intracellular Ca^{2+} concentrations, low levels of SDC4 were able to inhibit mesoglycan effects on Ca^{2+} homeostasis, confirming that the SDC4 co-receptor is a target of mesoglycan. Keratinocytes differentiation starts when the activated cells migrate from the basal layer to the surface of the skin. This event is followed changes in cell interactions that promote cell movements [318]. We also noted the presence of prominent E-cadherin clustering in the cell periphery, associated with the lack of basal cell interactions and the acquisition of a motile phenotype, which is a key event in the differentiation process. The induction of the differentiation program by mesoglycan was further confirmed via the analysis of the keratins CK6 and CK10. These two keratins were upregulated in mesoglycan treated cells. More interestingly, in SDC4 knockdown keratinocytes, mesoglycan effects on the PKCα pathway as well as on cell differentiation were almost nullified, suggesting that mesoglycan effects are mediated by SDC4. When basal keratinocytes undergo differentiation, they express characteristic genes. ANXA1 is one of the proteins identified as the actor of early keratinocyte differentiation [319]. Indeed, we found that mesoglycan promotes the increase in ANXA1 expression and its translocation to the plasma membrane with consequent secretion in extracellular environments. It is unclear how ANXA1 is externalized, one of the proposed mechanisms is that the S100A11 protein can function as a chaperone. In keratinocytes the increase in Ca^{2+} is sufficient to redistribute both S100A11 and ANXA1 to the plasma membrane [320]. We have shown that mesoglycan induces the formation of the ANXA1 / S100A11 complex on the plasma membrane of keratinocytes. The observed co-localization supports the idea that these Ca^{2+} binding proteins can form a membrane-associated complex in the early stages of the keratinocyte differentiation process [321]. This event is mediated by the activation of the SDC4 pathway, perhaps because HS has been implicated in mediating the attachment of proteins, and therefore of ANXA1, to cell surfaces [322]. Moreover, ANXA1 is implicated in cytoskeletal dynamics and cell motility [268], [273]. ANXA1 promotes motility of keratinocytes in terms of migration and invasion treated with mesoglycan. Indeed, these motility processes despite the presence of mesoglycan are significantly inhibited by the reduction of ANXA1. Furthermore, ANXA1 knockdown in keratinocytes significantly reduced the expression of the differentiation markers CK6 and CK10 and increased that of E-cadherin instead.

Thanks to this first data collection, we have uncovered a cascade of reactions triggered by mesoglycan inducing keratinocyte migration and differentiation through stimulation of the syndecan-

4 / PKC pathway. Furthermore, these effects are also due to the formation of the A1 / S100A11 complex (Fig.8.1).

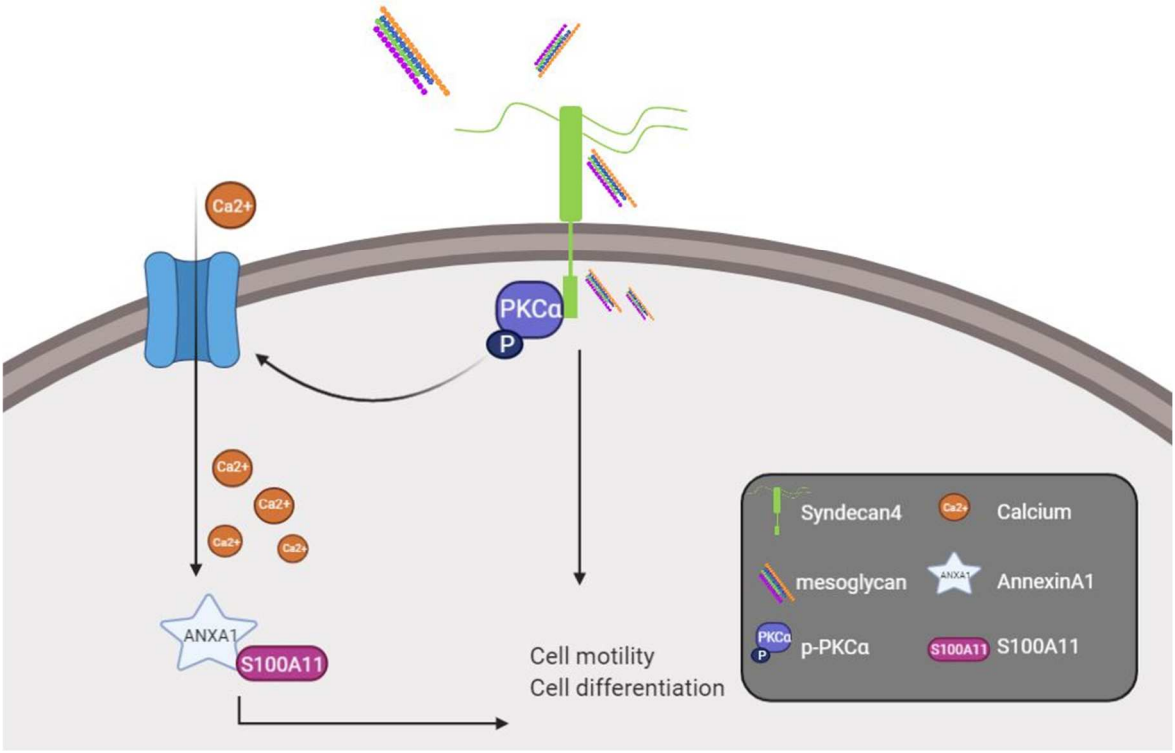

Fig. 8.1 Mesoglycan interacts with the SDC4 co-receptor which it promotes activation of PKCα. This activation is related to the entry of calcium into the cell. By interacting with calcium, the ANXA1 protein becomes available for binding with the sup partner S100A1. SDC4 / PKCα and ANXA1 / S100A11 promote keratinocyte activation by stimulating motility and differentiation.

Since mesoglycan induced ANXA1 translocation to the plasma membrane, followed by its secretion in extracellular environments [323] and knowing that ANXA1 is one of the proteins responsible of exosome formation and secretion [255], we analysed the presence of EVs in the supernatant of keratinocytes treated and not with the mixture of GAGs. We confirmed the involvement of mesoglycan and ANXA1 in promotion the exosome formation because keratinocytes treated for 24 hours with the GAGs released more EVs (EVs mesoglycan), enriched in exosomes, than the untreated keratinocytes (EVs ctrl). The higher presence of ANXA1 in EVs mesoglycan, confirmed the capability of mesoglycan to promote the externalization of this protein. Moreover, using ANXA1 mimetic peptide Ac2-26, we surprisingly observed that the protein triggers a positive loop allowing the further translocation of ANXA1 to the plasma membrane and its subsequent externalization.

ANXA1 could act in an autocrine or paracrine way through the possible interaction with the FPRs, triggering several biological effects as cell motility both in physiological and pathological systems [265], [273], [288], [324]. Moreover, FPRs are involved in keratinocytes activation [325], and several reports have shown that ANXA1-FPRs binding can promote positive effect on the resolution of wound injury [326]–[328]. Based on this, we proceed our studies confirming the autocrine role of extracellular ANXA1 contained in EVs on keratinocytes activation. Using BOC1 at a concentration of 100 µM to block FPR1 and FPR2 (respectively receptors for and N-terminal mimetic peptide [329] and ANXA1 [330]) EVs isolated from keratinocytes treated with mesoglycan (EVs mesoglycan) significantly intensified cell migration and invasion speed thanks to their ANXA1 content. In the same way, the vesiscles, particularly EVs mesoglycan, enhanced keratinocyte differentiation through the activation of FPR pathway in autocrine manner.

These data highlight for the first time a new mechanism of action through the formation of EVs that amplify the activity of mesoglycan. It results in the formation of an ANXA1 / EVs / FPRs axis that represents an autocrine loop that activates keratinocytes, a key event for wound repair (Fig. 8.2).

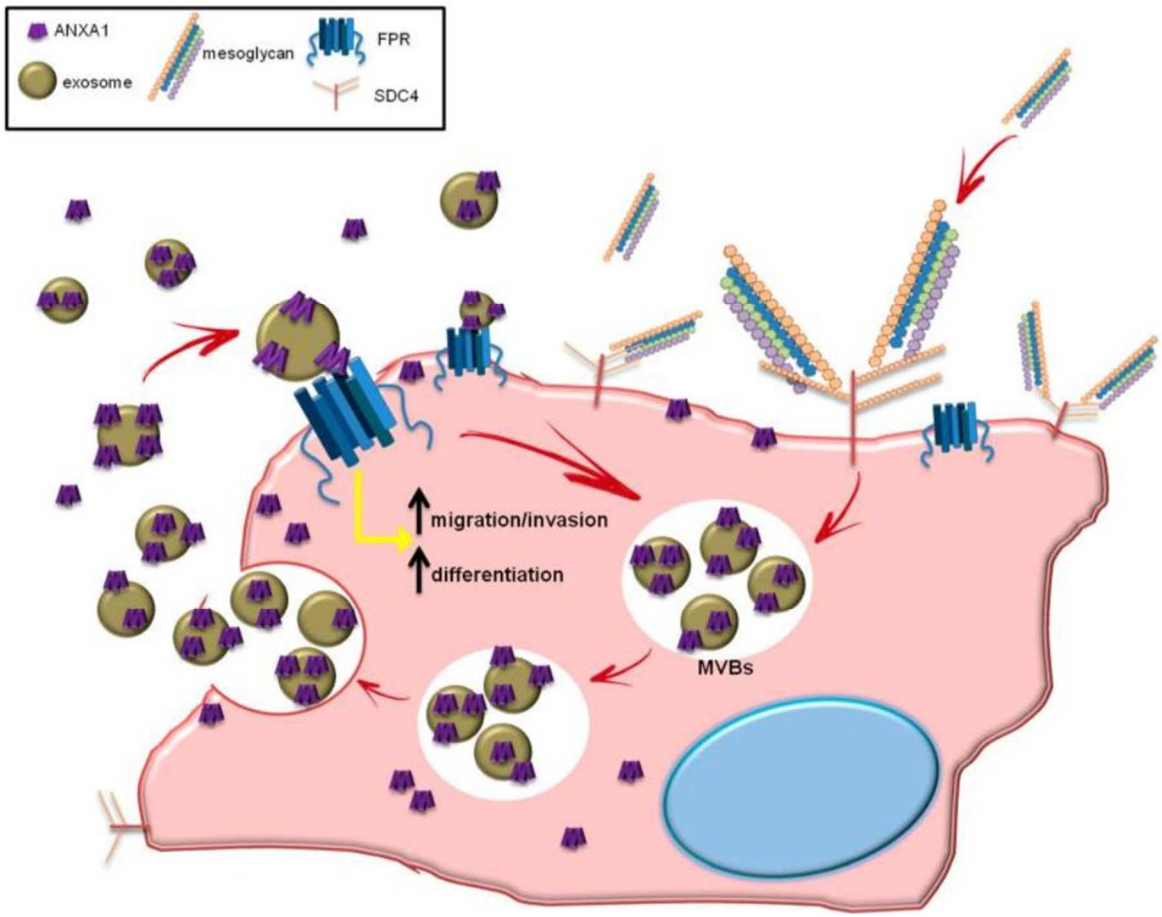

Fig. 8.2 Mesoglycan administered to keratinocytes interacts with SDC4 promoting the formation of multivesicular bodies (MVB) which are transported to the plasma membrane for the release of exosomes. Released EVs contain ANXA1 which interacts with FPRs to promote keratinocyte migration, invasion and differentiation. An internal loop promoted by ANXA1 is triggered which amplifies the process.

At the basis of effective wound healing there is continuous and reciprocal communication between epidermal and dermal cells. EVs can be critical actors in promoting this network, because they are involved in cell-cell and cell-matrix communication, both in physiological and pathological processes [331]. For this reason, we proceeded our study with the paracrine role of EVs isolated from HaCaT cells treated or not with mesoglycan in a specialized fibrovascular network formation, which affects fibroblasts and endothelial cells and is essential for the formation of the granulation tissue. Fibroblasts deposit a provisional matrix composed of GAGs, PGs, collagen and other ECM proteins. This matrix promotes cell motility and can facilitate the development and the growth of vessels [332]. EVs secreted by keratinocytes in presence of mesoglycan enhance the activation of human fibroblasts that lost their quiescent status to become proto-myofibroblasts. EVs promote a phenotype switch in fibroblasts, which is manifested by typical features including the development of a higher migration and invasion rate, but also by the well-organized re-arrangement of the cytoskeleton in parallel cell orientation observed by the expression of FAP1α and the production of collagen type I, that supports angiogenesis [333]. Moreover, the activation of endothelial cells by EVs mesoglycan from keratinocytes further supported the paracrine signalling with positive feedback. Endothelial cells in the process of angiogenesis arrange themselves in branched microvascular network and to do so they need the acquisition of a mesenchymal phenotype through the EndMT. This transition is characterized by the secretion of ECM proteins such as fibronectin [334], loss of adhesion molecules such as VE-cadherin [335], and organization of the cytoskeleton effected by α-SMA filaments [336], three events that are strongly promoted by mesoglycan EVs. Prior studies that have noted the importance of growth factors such as FGF and VEGF in the activation of fibroblasts and endothelial cells respectively [294], [295], [337]. Surprisingly, EVs mesoglycan isolated from keratinocytes stimulated a strong expression of FGF-2 in fibroblasts and VEGF in endothelial cells. This indicate that a cross-talk between the growth factors and the receptors/coreceptors among the parental and receiving cells can be established to facilitate the development of granulation tissue.

These collected data allow us for the first time that EVs deriving from keratinocytes, in particular those previously treated with mesoglycan, trigger a paracrine positive feedback able to further amplify the effects of mesoglycan. These vesicles are able to promote communication between cells and form an inter-cellular network essential for a correct re-epithelialization (Fig. 8.3).

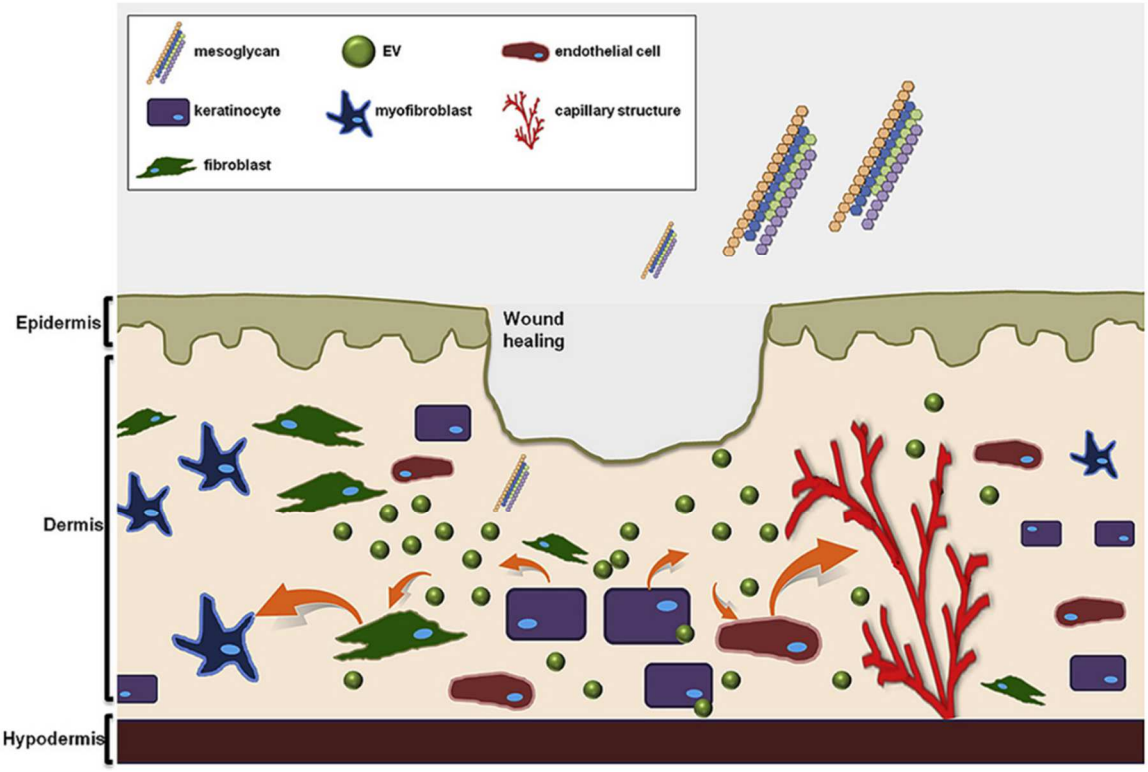

Fig.8.3 Mesoglycan administered to a skin wound stimulates the keratinocytes to produce EVs. These EVs act in a paracrine manner by promoting the switching of fibroblasts into proto-myofibroblasts and the formation of vessels from endothelial cells.

Numerous studies have explored the use of mesoglycan for treatment of vascular disease and its efficacious anti-thrombotic and fibrinolytic effects [26 - 28]. We have established the significant *in vitro* impact of mesoglycan in skin wound repair. Mesoglycan is a mixture of GAGs that activate several of the cell types involved in skin regeneration, these include keratinocytes, fibroblasts, and endothelial cells. Mesoglycan accelerates healing and promotes the formation of granulation tissue, stimulating migration and differentiation of keratinocytes, fibroblast activation and angiogenesis [1, 16].

In order to heal the wounds correctly, the formation of new blood vessels from the pre-existing vascular system is essential. Endothelial cells, after injury, are stimulated and activated by various pro-angiogenic factors, including VEGFA [5]. In healthy skin, this growth factor is not highly expressed, however, skin injury causes a marked VEGF increase with consequent angiogenesis [29].

In this study we demonstrate a synergistic effect between mesoglycan and VEGFA which enhances the pro-angiogenic stimuli necessary for wound repair. In HUVECs we found that administration of mesoglycan-VEGFA promotes EC migration, tube formation and sprouting

compared to a greater extent than the two components individually. The use of mesoglycan and VEGFA in combination also resulted significantly more stimulation of VEGFR2 related signalling pathways that promote angiogenic processes such as cell survival, vascular permeability, proliferation, cytoskeletal rearrangement and cell migration [8]. After the co-treatment mesoglycan-VEGFA phosphorylation of several proteins such as p-ERK, p38-MAPK and p-HSP27 is increased. These proteins are important for the actin polymerisation [18] and FAK activation necessary for focal adhesion turnover and regulation of migration [30] supporting cell motility.

Our previous studies have highlighted that the mechanism of action of mesoglycan on keratinocytes involves SDC4 [13, 14], a membrane proteoglycan that is also of significant importance in angiogenesis [20]. Endothelial cells from *Sdc4-/-* mice exhibited reduced cell migration as compared to WT supporting the hypothesis that it is involved in the pro- angiogenic effects elicited by the co-administration of mesoglycan-VEGFA *in vitro.* VEGFR2 phosphorylation in response to mesoglycan and VEGFA was considerably reduced, and analysis of downstream cellular events such as the redistribution of VE-cadherin [31], FAK activation [32] and cytoskeletal remodelling [33] revealed that these were also reduced. Interestingly mesoglycan alone cannot stimulate any of these pathways.

Prior studies have described the involvement of ANXA1 protein in promoting angiogenesis [11, 12, 21, 34], and we observed an increase of the level of this protein in cells treated with mesoglycan. Hence, to comprehend the role of ANXA1 in our system, we performed functional experiments on HUVEC cell motility by reducing the levels of available ANXA1 using siRNA. Our results showed that with low levels of the protein, endothelial cell motility and tube formation are not promoted, confirming the fundamental role of this protein in angiogenesis. Our previous studies have shown that keratinocytes treated with mesoglycan secreted a large amount of ANXA1 through EVs in the extracellular environment and promoted angiogenesis *in vitro* [13, 15]. Based on this we speculated that ANXA1+ EVs could be a link between SDC4 and VEGFR2. Indeed, treatment of endothelial cells with mesoglycan generated a greater number of ANXA1+ secreted vesicles as was the case with keratinocytes and we confirmed that this occurred FPRs. We assumed an interaction between ANXA1 and its receptor, just as already demonstrated [13]. This was later confirmed using BOC1 molecule as a pan-antagonist of FPRs [35]. Indeed, EVs containing ANXA1 can further promote the angiogenic effect of mesoglycan in an autocrine way, but in presence of BOC1, the effects on this process were not significant. This finding suggests, for the first time, that the interaction between vesicles and endothelial cells occurs through the ANXA1-FPRs interaction promoting motility and angiogenesis in an autocrine manner, following mesoglycan treatment.

ANXA1-FPR2 binding can control VEGFA secretion in uterine cells [9]. We analysed whether mesoglycan induced secretion of ANXA1 and its interaction with FPRs could promote the externalisation of VEGFA. Analysing via western blot the supernatant from HUVEC cells treated with mesoglycan, we observed the significant presence of VEGFA compared with the untreated cells. Moreover, this growth factor is not secreted in the absence of ANXA1, confirming the needs of this protein to promote the externalisation of VEGFA. The involvement of ANXA1 in VEGFA release was already demonstrated in another model. Indeed, cardiac macrophages from ANXA1-KO mice are unable to release VEGFA, instead, when these mice treated with ANXA1 showed high amounts of VEGFA released from cardiac macrophages [36].

Taken together, our data confirm the positive effects of mesoglycan on angiogenesis stimulation *in vitro* and allowed us to hypothesise a novel mesoglycan-promoted mechanism. We highlighted the ability of mesoglycan to trigger the activation of three different pathways that convey in HUVEC cells activation. (I) Mesoglycan interacts with the co-receptors SDC4 and stimulates the expression of EndMT markers, endothelial cell motility and the production of ANXA1-containing vesicles. (II) These vesicles are then externalised and interact in an autocrine manner with FPRs, amplifying the activation of endothelial cells. (III) The ANXA1-FPRs interaction results promoting the externalisation of VEGFA, which in turn stimulates the VEGR2 further supporting angiogenic processes (Fig. 8.4).

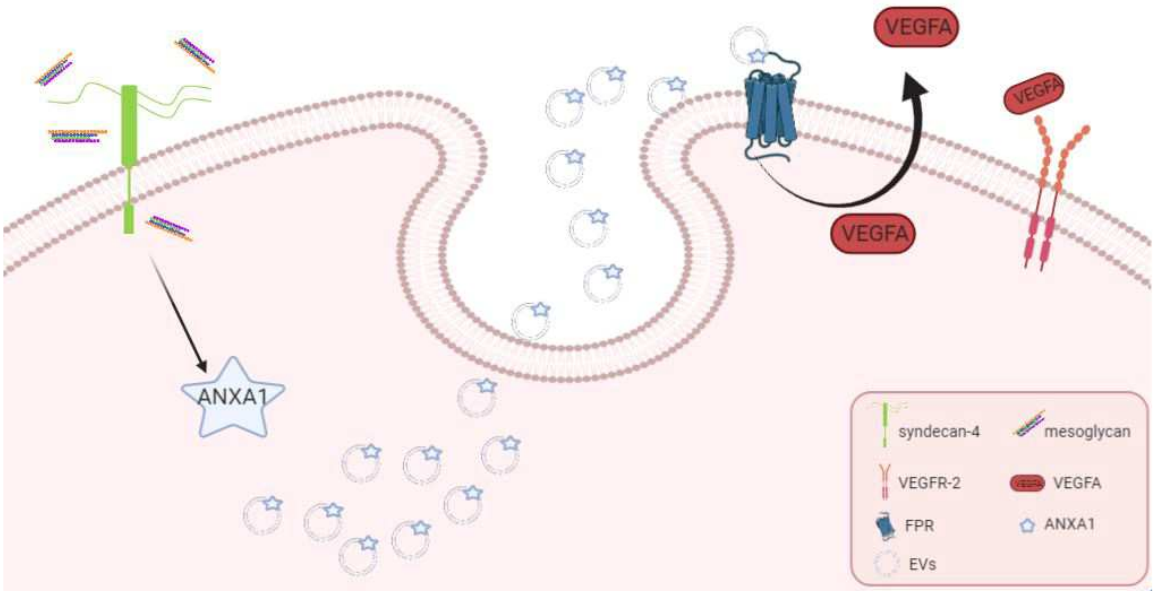

Fig. 8.4 Mesoglycan interacts with SDC4, this causes an increase in ANXA1, formation and secretion of vesicles containing this protein. ANXA1 released in EVs interacts with FPRs receptors in an autocrine

way. This interaction promotes the release of VEGFA, which binds VEGFR2 enhancing the pro-angiogenic activity in endothelial cells.

It is complex to reproduce perfectly *in vitro* the mechanism of tissue repair, for this resulted necessary the use of animal model. To ensure that the healing processes are as similar to human ones, it would be preferable to use a large animal model such as pigs but it can be complicated to house and is not always practical. For this, mouse model is the most used, as they are easy to handle, can be genetically manipulated and are affordable. Indeed, after anesthetizing C57BL/6 mice and shaving them, we used a sterile 4mm biopsy punch to generate a double wound at the level of the shoulder blades. However, mice have small bodies, they greatly differ in thickness and number of dermal and epidermal cells, but above all differences in physiology compared to humans, also due to the wound healing process that heals mainly by contraction, with the formation of an extensive subcutaneous striated muscle layer [338]. One strategy to prevent the contraction and make the mice as a good model for translational applications can be to use a splint. We used a silicone splint adequately adhered and anchored to the skin with sutures to ensure placement for both the wounds. The splints were daily monitored, and the wounds were photographed, measured, and treated with 100 µl of mesoglycan or with 100 µl of PBS as control. After 10 days of treatment, we found a slightly higher closure of the wounds treated with mesoglycan compared with the PBS treated ones. For this, the granulation tissue and re-epithelization processes were observed via confocal microscopy, to observe in the details if there were differences in cellular component between the two treatments. We found the significative presence of CK6, marker of hyperproliferation that was widely expressed throughout the epithelium only following mesoglycan treatment. The maturation-associated cytokeratin CK10 was detected only in mesoglycan treated wounds. This protein was not only an epidermal spinous-cell marker but also a terminal differentiation marker, which indicated the presence of mature tissue formation promoted by mesoglycan and not by the PBS of control.

Mesoglycan was able to promote the activation of fibroblasts in the dermis. FAPα is often used as a marker of differentiated fibroblasts [297] and it is expressed only in skin section of wound treated with mesoglycan. Moreover, vimentin is a protein involved in fibroblast proliferation, collagen accumulation, keratinocyte trans-differentiation, and re-epithelialisation [303] and appeared strong mainly in dermal compartments of skin biopsies of mice treated with mesoglycan. Finally, the observed specific marker for EC, CD31, showed its expression in wound skin biopsies particularly following the treatment with mesoglycan, compared with the counterpart treated with PBS, indicating the involvement of the mixture of GAGs in recruiting EC and stimulate angiogenesis.

With these findings we had the confirmation that although visually the two wounds seemed comparable, what changed was the significant presence of actively differentiating keratinocytes, activated fibroblasts and EC, which are the protagonists of the re-epithelialization, fibroplasia, and angiogenesis processes.

Analyses of mice wound healing treated with mesoglycan provided the broadest set of meaningful information, contributing to the knowledge of human wound healing and enabling us to translate the findings into human applications. Since there are different type of chronic wounds in human, we chose for the study patients in home wound care affected by pressure ulcers, whose etiopathogenesis is very simple and unambiguous. A recent challenge for the treatment of these lesions is represented by topical systems to be applied directly on chronic wounds, lesions and skin ulcers, in order to favour the formation of a protective barrier to ensure a favourable environment for the wound healing process and the formation of the tissues through a direct and immediate action. The patients were treated for 14 days with Prisma® Skin, the pharmaceutical dressing device developed by Mediolanum Farmaceutici s.p.a., consisting of a water-soluble and solid matrix, mainly composed of sodium alginate and hyaluronic acid, and mesoglycan. This device absorbs the exudates of the injured part and turns into a semi-solid of hydrogel type. We focused on the activity of fibroblasts, as the purpose of this type of dressings is to improve re-epithelialization, regenerating vital tissues and without scar formation. In order to have a good clinical range of time monitoring, useful for all clinical and histological evaluations of fibroblast activity, we focused on a time range of 0-14 days. H&E and IHC staining of patient biopsies at T0 demonstrated a lack of cell structure in the analysed tissues with a tendency to wound bed sclerosis. The decreased concentration of growth factors resulting from the reduction of cell migration could cause the absence of fibroblasts in the lesion area, consequently limiting the activity of fibroblasts to produce GAG and PG, with a relative reduction of angiogenesis [339]. After treating patients with Prisma® Skin, no significant wound closure was noted at T14. In the wound bed at T14 there was a significant number of migrated and well-oriented fibroblasts in the area, probably because they are ready to differentiate into myofibroblasts, as we have previously observed *in vitro* [183]. A plausible explanation for this might be that CS and DS could support the polymerisation of the collagen chain and interfere with the production of growth factors. HS can anchor to the surrounding ECM and release TGF-β and stimulate pro-angiogenesis effects. Finally, HS and HEP can protect the basic fibroblast growth factor (bFGF) and to stabilise its binding to the FGFR receptor [340]. Taken together, these results obtained *in vivo* reflected the translation of the previous data *in vitro*, confirming the activity of the mesoglycan on the fibroblasts, stimulating proliferation, migration, and invasive activity. These data suggested that Prisma® Skin applied for

14 days to patients suffering from pressure ulcers could induce an increase in proliferative activity in the wound bed, resulting in the formation of granulation tissue.

The use of alginate to convey mesoglycan is particularly promising thanks to its biodegradability, biocompatibility, and non-toxicity. To characterize the mesoglycan release kinetics from the alginate support, we realised the impregnation of the mixture of GAGs into porous polymer matrices using supercritical carbon dioxide (scCO2) is an innovative technique to produce pharmaceutical composite systems. The morphology of the created CCA after mesoglycan impregnation was characterised by FESEM, while the release of mesoglycan impregnated on CAA at 18 MPa and 60 °C was released through a dissolution tests at pH 7.4, as physiological condition. The support of CCA guarantees the complete release of mesoglycan in 3 hours, which is appropriate for an immediate and effective action on wounds. The effects of mesoglycan released by CAA on the cell migration was also analysed through a functional assay of *in vitro* wound healing. There was a 75% increase in distance travelled by mesoglycan-treated keratinocytes on CCA compared to single-component-treated or untreated cells. Similarly, in fibroblasts the migration capacity is increased by 93% in presence of mesoglycan released by the CCA against the mesoglycan and CCA analysed individually and untreated cells. these data confirm by confirming the pro-migratory role of the composite system produced and that the supercritical impregnation is suitable for obtaining systems loaded with mesoglycan to be applied on the skin for a correct regeneration of the epithelium and protection of the wound.

Long-term mesoglycan-based therapies could be useful to avoid the patient frequent dressing changes and repeated dosages that can induce side effects, ensuring correct re-epithelialization. A good option may be new drug-controlled wound dressings. The polymer carrier for achieving sustained release systems is a key choice. The use of polycaprolactone (PCL) guarantees a prolonged drug release and being biocompatible seems to be particularly advantageous [341], [342]. Among the categories of wound dressing, foam dressings are very beneficial as they are designed to absorb and prevent leakage of exudate while maintaining a moist wound surface. In semi-occlusive formulation thus allowing the exchange of gas and vapor [343]. Recently, the foaming conditions of the PCL granules have been optimized, showing that the best foaming of PCL was achieved at the temperature and pressure of 35°C and 17 MPa [344]. Based on this, we decided to develop a PCL/mesoglycan foaming to be applied as a topical prolonged release device on the wounds for a correct re-epithelialization process. Comparing the dissolution profiles in PBS at pH 7.4 we observe that the pure mesoglycan was completely dissolved in less than an hour, while when impregnated in PCL film it took about 70 hours. This is a successful result that delays the dissolution of the mesoglycan by 70 times, allowing a sustained release which overcomes the major problem of conventional wound care systems; that is, the short residence times in the wound site ensuring continuous treatment for a long

period of time [309]. To confirm the effectiveness of the mesoglycan released by the PCL foaming, we performed functional tests *in vitro* with mesoglycan previously released by the support for 24, 48 and 72 hours. These assays confirmed the positive and even more efficient effects of mesoglycan released by PCL compared to the pure mixture at the same final concentration in the three most abundant cell populations in damaged tissues: keratinocytes, fibroblasts, and endothelial cells. These data obtained *in vitro* encouraged the development of topical devices designed to release the active ingredients in a controlled manner, reducing the administration, ensuring wound protection and repair of tissue damage with regeneration of the epithelium.

These results raise the issue that mesoglycan, used for decades as a fibrinolytic, is able to promote wound healing process. In particular, it stimulates the formation of granulation tissue with consequent recruitment and activation of fibroblasts, keratinocytes and endothelial cells at the site of damage. Furthermore, this mixture of GAGs represents a new approach to the treatment of skin lesions, and its impregnation on PCL foaming could be a promising innovative prolonged release device.

Bibliography

[1] R. Nejati, D. Kovacic, and A. Slominski, 'Neuro-immune-endocrine functions of the skin: An overview', *Expert Review of Dermatology*, vol. 8, no. 6. NIH Public Access, pp. 581–583, 2013, doi: 10.1586/17469872.2013.856690.

[2] P. Rousselle, F. Braye, and G. Dayan, 'Re-epithelialization of adult skin wounds: Cellular mechanisms and therapeutic strategies', *Advanced Drug Delivery Reviews*, vol. 146. Elsevier B.V., pp. 344–365, Jun. 01, 2019, doi: 10.1016/j.addr.2018.06.019.

[3] T. S. Kupper and R. C. Fuhlbrigge, 'Immune surveillance in the skin: Mechanisms and clinical consequences', *Nature Reviews Immunology*, vol. 4, no. 3. Nature Publishing Group, pp. 211–222, 2004, doi: 10.1038/nri1310.

[4] C. Y. L. Chao and G. L. Y. Cheing, 'Microvascular dysfunction in diabetic foot disease and ulceration', *Diabetes. Metab. Res. Rev.*, vol. 25, no. 7, pp. 604–614, Oct. 2009, doi: 10.1002/dmrr.1004.

[5] J. S. Boateng, K. H. Matthews, H. N. E. Stevens, and G. M. Eccleston, 'Wound Healing Dressings and Drug Delivery Systems: A Review', *J. Pharm. Sci.*, vol. 97, no. 8, pp. 2892–2923, Aug. 2008, doi: 10.1002/jps.21210.

[6] M. C. Robson, D. L. Steed, and M. G. Franz, 'Wound healing: Biologic features and approaches to maximize healing trajectories', *Curr. Probl. Surg.*, vol. 38, no. 2, p. A1, Feb. 2001, doi: 10.1067/msg.2001.111167.

[7] T. N. Demidova-Rice, M. R. Hamblin, and I. M. Herman, 'Acute and impaired wound healing: Pathophysiology and current methods for drug delivery, part 1: Normal and chronic wounds: Biology, causes, and approaches to care', *Advances in Skin and Wound Care*, vol. 25, no. 7. NIH Public Access, pp. 304–314, Jul. 2012, doi: 10.1097/01.ASW.0000416006.55218.d0.

[8] L. Cañedo-Dorantes and M. Cañedo-Ayala, 'Skin Acute Wound Healing: A Comprehensive Review', *Int. J. Inflam.*, vol. 2019, 2019, doi: 10.1155/2019/3706315.

[9] A. Shai and S. Halevy, 'Direct triggers for ulceration in patients with venous insufficiency', *Int. J. Dermatol.*, vol. 44, no. 12, pp. 1006–1009, Dec. 2005, doi: 10.1111/j.1365-4632.2005.02317.x.

[10] R. Nunan, K. G. Harding, and P. Martin, 'Clinical challenges of chronic wounds: Searching for an optimal animal model to recapitulate their complexity', *DMM Dis. Model. Mech.*, vol. 7, no. 11, pp. 1205–1213, Nov. 2014, doi: 10.1242/dmm.016782.

[11] T. J. Shaw and P. Martin, 'Wound repair at a glance', *J. Cell Sci.*, vol. 122, no. 18, pp. 3209–3213, Sep. 2009, doi: 10.1242/jcs.031187.

[12] S.-H. Yun, E.-H. Sim, R.-Y. Goh, J.-I. Park, and J.-Y. Han, 'Platelet Activation: The Mechanisms and Potential Biomarkers', *Biomed Res. Int.*, vol. 2016, 2016, doi: 10.1155/2016/9060143.

[13] J. D. McFadyen and Z. S. Kaplan, 'Platelets are not just for clots', *Transfusion Medicine Reviews*, vol. 29, no. 2. W.B. Saunders, pp. 110–119, Apr. 01, 2015, doi: 10.1016/j.tmrv.2014.11.006.

[14] K. Broos, H. B. Feys, S. F. De Meyer, K. Vanhoorelbeke, and H. Deckmyn, 'Platelets at work in primary hemostasis', *Blood Rev.*, vol. 25, no. 4, pp. 155–167, Jul. 2011, doi: 10.1016/j.blre.2011.03.002.

[15] A. T. Nurden, P. Nurden, M. Sanchez, I. Andia, and E. Anitua, 'Platelets and wound healing', *Frontiers in Bioscience*, vol. 13, no. 9. pp. 3532–3548, 2008, doi: 10.2741/2947.

[16] B. Hinz, 'The role of myofibroblasts in wound healing', *Curr. Res. Transl. Med.*, vol. 64, no. 4, pp. 171–177, Oct. 2016, doi: 10.1016/j.retram.2016.09.003.

[17] P. Olczyk, Ł. Mencner, and K. Komosinska-Vassev, 'The Role of the Extracellular Matrix Components in Cutaneous Wound Healing', *Biomed Res. Int.*, vol. 2014, 2014, doi: 10.1155/2014/747584.

[18] W. F. Bahou and D. V. Gnatenko, 'Platelet transcriptome: The application of microarray analysis to platelets', *Seminars in Thrombosis and Hemostasis*, vol. 30, no. 4. Copyright © 2004 by Thieme Medical Publishers, Inc., 333 Seventh Avenue, New York, NY 10001, USA., pp. 473–484, Aug. 08, 2004, doi: 10.1055/s-2004-833482.

[19] N. Nami *et al.*, 'Crosstalk between platelets and PBMC: New evidence in wound healing', *Platelets*, vol. 27, no. 2, pp. 143–148, Feb. 2016, doi: 10.3109/09537104.2015.1048216.

[20] M. H. Kim *et al.*, 'Dynamics of neutrophil infiltration during cutaneous wound healing and infection using fluorescence imaging', *J. Invest. Dermatol.*, vol. 128, no. 7, pp. 1812–1820, 2008, doi: 10.1038/sj.jid.5701223.

[21] A. Ridiandries, J. T. M. Tan, and C. A. Bursill, 'The role of chemokines in wound healing', *International Journal of Molecular Sciences*, vol. 19, no. 10. MDPI AG, p. 3217, Oct. 18, 2018, doi: 10.3390/ijms19103217.

[22] S. A. Eming, T. Krieg, and J. M. Davidson, 'Inflammation in wound repair: Molecular and cellular mechanisms', *Journal of Investigative Dermatology*, vol. 127, no. 3. Nature Publishing Group, pp. 514–525, Mar. 01, 2007, doi: 10.1038/sj.jid.5700701.

[23] M. Schnoor, P. Alcaide, M.-B. Voisin, and J. D. Van Buul, 'Crossing the Vascular Wall: Common and Unique Mechanisms Exploited by Different Leukocyte Subsets during Extravasation', 2015, doi: 10.1155/2015/946509.

[24] K. Theilgaard-Mönch, S. Knudsen, P. Follin, and N. Borregaard, 'The Transcriptional Activation Program of Human Neutrophils in Skin Lesions Supports Their Important Role in Wound Healing', *J. Immunol.*, vol. 172, no. 12, pp. 7684–7693, Jun. 2004, doi: 10.4049/jimmunol.172.12.7684.

[25] T. Thuraisingam *et al.*, 'MAPKAPK-2 signaling is critical for cutaneous wound healing', *J. Invest. Dermatol.*, vol. 130, no. 1, pp. 278–286, Jan. 2010, doi: 10.1038/jid.2009.209.

[26] C. Auffray *et al.*, 'Monitoring of blood vessels and tissues by a population of monocytes with patrolling behavior', *Science (80-.).*, vol. 317, no. 5838, pp. 666–670, Aug. 2007, doi: 10.1126/science.1142883.

[27] F. Ginhoux, J. L. Schultze, P. J. Murray, J. Ochando, and S. K. Biswas, 'New insights into the multidimensional concept of macrophage ontogeny, activation and function', *Nature Immunology*, vol. 17, no. 1. Nature Publishing Group, pp. 34–40, Jan. 01, 2016, doi: 10.1038/ni.3324.

[28] M. P. Rodero and K. Khosrotehrani, 'Skin wound healing modulation by macrophages', *International Journal of Clinical and Experimental Pathology*, vol. 3, no. 7. e-Century Publishing Corporation, pp. 643–653, 2010.

[29] H. R. Jones, C. T. Robb, M. Perretti, and A. G. Rossi, 'The role of neutrophils in inflammation resolution', *Seminars in Immunology*, vol. 28, no. 2. Academic Press, pp. 137–145, Apr. 01, 2016, doi: 10.1016/j.smim.2016.03.007.

[30] J. Dalli and C. Serhan, 'Macrophage Proresolving Mediators-the When and Where', in *Myeloid Cells in Health and Disease*, Washington, DC, USA: ASM Press, 2017, pp. 367–383.

[31] A. Das, K. Ganesh, S. Khanna, C. K. Sen, and S. Roy, 'Engulfment of Apoptotic Cells by Macrophages: A Role of MicroRNA-21 in the Resolution of Wound Inflammation', *J. Immunol.*, vol. 192, no. 3, pp. 1120–1129, Feb. 2014, doi: 10.4049/jimmunol.1300613.

[32] A. Das *et al.*, 'Monocyte and Macrophage Plasticity in Tissue Repair and Regeneration', *American Journal of Pathology*, vol. 185, no. 10. Elsevier Inc., pp. 2596–2606, Oct. 01, 2015, doi: 10.1016/j.ajpath.2015.06.001.

[33] N. X. Landén, D. Li, and M. Ståhle, 'Transition from inflammation to proliferation: a critical step during wound healing', *Cellular and Molecular Life Sciences*, vol. 73, no. 20. Birkhauser Verlag AG, pp. 3861–3885, Oct. 01, 2016, doi: 10.1007/s00018-016-2268-0.

[34] T. A. Wynn and K. M. Vannella, 'Macrophages in Tissue Repair, Regeneration, and Fibrosis', *Immunity*, vol. 44, no. 3. Cell Press, pp. 450–462, Mar. 15, 2016, doi: 10.1016/j.immuni.2016.02.015.

[35] N. S. Greaves, K. J. Ashcroft, M. Baguneid, and A. Bayat, 'Current understanding of molecular

and cellular mechanisms in fibroplasia and angiogenesis during acute wound healing', *Journal of Dermatological Science*, vol. 72, no. 3. Elsevier, pp. 206–217, Dec. 01, 2013, doi: 10.1016/j.jdermsci.2013.07.008.

[36] M. P. Welch, G. F. Odland, and R. A. F. Clark, 'Temporal relationships of F-actin bundle formation, collagen and fibronectin matrix assembly, and fibronectin receptor expression to wound contraction', *J. Cell Biol.*, vol. 110, no. 1, pp. 133–145, 1990, doi: 10.1083/jcb.110.1.133.

[37] A. Desmouliere, M. Redard, I. Darby, and G. Gabbiani, 'Apoptosis mediates the decrease in cellularity during the transition between granulation tissue and scar', *Am. J. Pathol.*, vol. 146, no. 1, pp. 56–66, 1995.

[38] L. Rittié, 'Cellular mechanisms of skin repair in humans and other mammals', *Journal of Cell Communication and Signaling*, vol. 10, no. 2. Springer Netherlands, pp. 103–120, Jun. 01, 2016, doi: 10.1007/s12079-016-0330-1.

[39] M. I. Koster and D. R. Roop, 'Mechanisms Regulating Epithelial Stratification', *Annu. Rev. Cell Dev. Biol.*, vol. 23, no. 1, pp. 93–113, Nov. 2007, doi: 10.1146/annurev.cellbio.23.090506.123357.

[40] M. Koizumi, T. Matsuzaki, and S. Ihara, 'Expression of P-cadherin distinct from that of E-cadherin in re-epithelialization in neonatal rat skin', *Dev. Growth Differ.*, vol. 47, no. 2, pp. 75–85, Feb. 2005, doi: 10.1111/j.1440-169x.2004.00784.x.

[41] M. L. Usui, R. A. Underwood, J. N. Mansbridge, L. A. Muffley, W. G. Carter, and J. E. Olerud, 'Morphological evidence for the role of suprabasal keratinocytes in wound reepithelialization', *Wound Repair Regen.*, vol. 13, no. 5, pp. 468–479, Sep. 2005, doi: 10.1111/j.1067-1927.2005.00067.x.

[42] P. Rousselle, M. Montmasson, and C. Garnier, 'Extracellular matrix contribution to skin wound re-epithelialization', *Matrix Biology*, vol. 75–76. Elsevier B.V., pp. 12–26, Jan. 01, 2019, doi: 10.1016/j.matbio.2018.01.002.

[43] M. Kubo *et al.*, 'Fibrinogen and fibrin are anti-adhesive for keratinocytes: A mechanism for fibrin eschar slough during wound repair', *J. Invest. Dermatol.*, vol. 117, no. 6, pp. 1369–1381, Dec. 2001, doi: 10.1046/j.0022-202x.2001.01551.x.

[44] R. Grose *et al.*, 'A crucial role of β1 integrins for keratinocyte migration in vitro and during cutaneous wound repair', *Development*, vol. 129, no. 9. pp. 2303–2315, 2002.

[45] I. M. Freedberg, M. Tomic-Canic, M. Komine, and M. Blumenberg, 'Keratins and the keratinocyte activation cycle', *Journal of Investigative Dermatology*, vol. 116, no. 5. Elsevier, pp. 633–640, May 01, 2001, doi: 10.1046/j.1523-1747.2001.01327.x.

[46] S. Werner, T. Krieg, and H. Smola, 'Keratinocyte-fibroblast interactions in wound healing', *J. Invest. Dermatol.*, vol. 127, no. 5, pp. 998–1008, May 2007, doi: 10.1038/sj.jid.5700786.

[47] C. Murdoch, M. Muthana, and C. E. Lewis, 'Hypoxia Regulates Macrophage Functions in Inflammation', *J. Immunol.*, vol. 175, no. 10, pp. 6257–6263, Nov. 2005, doi: 10.4049/jimmunol.175.10.6257.

[48] D. Duscher *et al.*, 'Fibroblast-specific deletion of hypoxia inducible factor-1 critically impairs murine cutaneous neovascularization and wound healing', *Plast. Reconstr. Surg.*, vol. 136, no. 5, pp. 1004–1013, Oct. 2015, doi: 10.1097/PRS.0000000000001699.

[49] N. Skuli *et al.*, 'Endothelial HIF-2α regulates murine pathological angiogenesis and revascularization processes', *J. Clin. Invest.*, vol. 122, no. 4, pp. 1427–1443, Apr. 2012, doi: 10.1172/JCI57322.

[50] H. R. Rezvani *et al.*, 'Loss of epidermal hypoxia-inducible factor-1α accelerates epidermal aging and affects re-epithelialization in human and mouse', *J. Cell Sci.*, vol. 124, no. 24, pp. 4172–4183, Dec. 2011, doi: 10.1242/jcs.082370.

[51] G. Eelen, P. De Zeeuw, M. Simons, and P. Carmeliet, 'Endothelial cell metabolism in normal and diseased vasculature', *Circulation Research*, vol. 116, no. 7. Lippincott Williams and Wilkins, pp. 1231–1244, Mar. 27, 2015, doi: 10.1161/CIRCRESAHA.116.302855.

[52] M. E. Maragoudakis, N. E. Tsopanoglou, and P. Andriopoulou, 'Mechanism of thrombin-induced angiogenesis.', *Biochemical Society transactions*, vol. 30, no. 2. Portland Press, pp. 173–177, Apr. 01, 2002, doi: 10.1042/bst0300173.

[53] M. Nguyen, J. Arkell, and C. J. Jackson, 'Human endothelial gelatinases and angiogenesis', *International Journal of Biochemistry and Cell Biology*, vol. 33, no. 10. Pergamon, pp. 960–970, Oct. 01, 2001, doi: 10.1016/S1357-2725(01)00007-3.

[54] E. Hadjipanayi *et al.*, 'The Fibrin Matrix Regulates Angiogenic Responses within the Hemostatic Microenvironment through Biochemical Control', *PLoS One*, vol. 10, no. 8, p. e0135618, Aug. 2015, doi: 10.1371/journal.pone.0135618.

[55] M. Crowther, N. J. Brown, E. T. Bishop, and C. E. Lewis, 'Microenvironmental influence on macrophage regulation of angiogenesis in wounds and malignant tumors', *J. Leukoc. Biol.*, vol. 70, no. 4, pp. 478–490, Oct. 2001, doi: 10.1189/JLB.70.4.478.

[56] P. Carmeliet and R. K. Jain, 'Molecular mechanisms and clinical applications of angiogenesis', *Nature*, vol. 473, no. 7347. NIH Public Access, pp. 298–307, May 19, 2011, doi: 10.1038/nature10144.

[57] P. Carmeliet, 'Angiogenesis in health and disease', *Nature Medicine*, vol. 9, no. 6. Nature Publishing Group, pp. 653–660, Jun. 01, 2003, doi: 10.1038/nm0603-653.

[58] J. Li, J. Chen, and R. Kirsner, 'Pathophysiology of acute wound healing', *Clin. Dermatol.*, vol. 25, no. 1, pp. 9–18, Jan. 2007, doi: 10.1016/j.clindermatol.2006.09.007.

[59] M. Ngaage and M. Agius, 'The psychology of scars: a mini-review', 2018.

[60] F. Seyfarth, S. Schliemann, D. Antonov, and P. Elsner, 'Dry skin, barrier function, and irritant contact dermatitis in the elderly', *Clin. Dermatol.*, vol. 29, no. 1, pp. 31–36, Jan. 2011, doi: 10.1016/j.clindermatol.2010.07.004.

[61] S. Diridollou *et al.*, 'Skin ageing: Changes of physical properties of human skin in vivo', *Int. J. Cosmet. Sci.*, vol. 23, no. 6, pp. 353–362, 2001, doi: 10.1046/j.0412-5463.2001.00105.x.

[62] H. N. Wilkinson and M. J. Hardman, 'Wound senescence: A functional link between diabetes and ageing?', *Exp. Dermatol.*, p. exd.14082, Feb. 2020, doi: 10.1111/exd.14082.

[63] G. Nelson, O. Kucheryavenko, J. Wordsworth, and T. von Zglinicki, 'The senescent bystander effect is caused by ROS-activated NF-κB signalling', *Mech. Ageing Dev.*, vol. 170, pp. 30–36, Mar. 2018, doi: 10.1016/j.mad.2017.08.005.

[64] P. Lou, S. Liu, X. Xu, C. Pan, Y. Lu, and J. Liu, 'Extracellular vesicle-based therapeutics for the regeneration of chronic wounds: current knowledge and future perspectives', *Acta Biomaterialia*, vol. 119. Acta Materialia Inc, pp. 42–56, Jan. 01, 2020, doi: 10.1016/j.actbio.2020.11.001.

[65] S. L. Wong *et al.*, 'Diabetes primes neutrophils to undergo NETosis, which impairs wound healing', *Nat. Med.*, vol. 21, no. 7, pp. 815–819, Jul. 2015, doi: 10.1038/nm.3887.

[66] P. Bannon, S. Wood, T. Restivo, L. Campbell, M. J. Hardman, and K. A. Mace, 'Diabetes induces stable intrinsic changes to myeloid cells that contribute to chronic inflammation during wound healing in mice', *DMM Dis. Model. Mech.*, vol. 6, no. 6, pp. 1434–1447, Nov. 2013, doi: 10.1242/dmm.012237.

[67] A. Lecube, G. Pachón, J. Petriz, C. Hernández, and R. Simó, 'Phagocytic activity is impaired in type 2 diabetes mellitus and increases after metabolic improvement', *PLoS One*, vol. 6, no. 8, 2011, doi: 10.1371/journal.pone.0023366.

[68] S. Khanna *et al.*, 'Macrophage dysfunction impairs resolution of inflammation in the wounds of diabetic mice', *PLoS One*, vol. 5, no. 3, Mar. 2010, doi: 10.1371/journal.pone.0009539.

[69] O. Stojadinovic *et al.*, 'Molecular pathogenesis of chronic wounds: The role of β-catenin and c-myc in the inhibition of epithelialization and wound healing', *Am. J. Pathol.*, vol. 167, no. 1, pp. 59–69, 2005, doi: 10.1016/S0002-9440(10)62953-7.

[70] I. B. Wall *et al.*, 'Fibroblast dysfunction is a key factor in the non-healing of chronic venous leg ulcers', *J. Invest. Dermatol.*, vol. 128, no. 10, pp. 2526–2540, Oct. 2008, doi: 10.1038/jid.2008.114.

[71] G. Han and R. Ceilley, 'Chronic Wound Healing: A Review of Current Management and Treatments', *Advances in Therapy*, vol. 34, no. 3. Springer Healthcare, pp. 599–610, Mar. 01, 2017, doi: 10.1007/s12325-017-0478-y.

[72] A. Clinton and T. Carter, 'Chronic wound biofilms: Pathogenesis and potential therapies', *Lab Medicine*, vol. 46, no. 4. Oxford University Press, pp. 277–284, Nov. 01, 2015, doi: 10.1309/LMBNSWKUI4JPN7SO.

[73] U. Rowlatt, 'Intrauterine wound healing in a 20 week human fetus', *Virchows Arch. A Pathol. Anat. Histol.*, vol. 381, no. 3, pp. 353–361, Jan. 1979, doi: 10.1007/BF00432477.

[74] J. Hopkinson-Woolley, D. Hughes, S. Gordon, and P. Martin, 'Macrophage recruitment during limb development and wound healing in the embryonic and foetal mouse', *J. Cell Sci.*, vol. 107, no. 5, pp. 1159–1167, May 1994.

[75] N. A. Coolen, K. C. W. M. Schouten, E. Middelkoop, and M. M. W. Ulrich, 'Comparison between human fetal and adult skin', *Arch. Dermatol. Res.*, vol. 302, no. 1, pp. 47–55, 2010, doi: 10.1007/s00403-009-0989-8.

[76] K. W. Liechty, N. S. Adzick, and T. M. Crombleholme, 'Diminished interleukin 6 (IL-6) production during scarless human fetal wound repair', *Cytokine*, vol. 12, no. 6, pp. 671–676, Jun. 2000, doi: 10.1006/cyto.1999.0598.

[77] B. A. Mast, R. F. Diegelmann, T. M. Krummel, and I. K. Cohen, 'Hyaluronic Acid Modulates Proliferation, Collagen and Protein Synthesis of Cultured Fetal Fibroblasts', *Matrix*, vol. 13, no. 6, pp. 441–446, 1993, doi: 10.1016/S0934-8832(11)80110-1.

[78] L. Cuttle, M. Nataatmadja, J. F. Fraser, M. Kempf, R. M. Kimble, and M. T. Hayes, 'Collagen in the scarless fetal skin wound: Detection with Picrosirius-polarization', *Wound Repair Regen.*, vol. 13, no. 2, pp. 198–204, Mar. 2005, doi: 10.1111/j.1067-1927.2005.130211.x.

[79] S. O'Kane and M. W. Ferguson, 'Transforming growth factor beta s and wound healing.', *Int. J. Biochem. Cell Biol.*, vol. 29, no. 1, pp. 63–78, Jan. 1997, doi: 10.1016/s1357-2725(96)00120-3.

[80] R. Nieuwland and A. Sturk, 'Why do cells release vesicles?', *Thrombosis Research*, vol. 125, no. SUPPL. 1. Pergamon, pp. S49–S51, Apr. 01, 2010, doi: 10.1016/j.thromres.2010.01.037.

[81] E. van der Pol, A. N. Böing, P. Harrison, A. Sturk, and R. Nieuwland, 'Classification, functions, and clinical relevance of extracellular vesicles', *Pharmacol. Rev.*, vol. 64, no. 3, pp. 676–705, Jul. 2012, doi: 10.1124/pr.112.005983.

[82] B. Li, M. A. Antonyak, J. Zhang, and R. A. Cerione, 'RhoA triggers a specific signaling pathway that generates transforming microvesicles in cancer cells', *Oncogene*, vol. 31, no. 45, pp. 4740–4749, Nov. 2012, doi: 10.1038/onc.2011.636.

[83] L. Ma *et al.*, 'Discovery of the migrasome, an organelle mediating release of cytoplasmic contents during cell migration', *Cell Res.*, vol. 25, no. 1, pp. 24–38, Jan. 2015, doi: 10.1038/cr.2014.135.

[84] J. Kowal *et al.*, 'Proteomic comparison defines novel markers to characterize heterogeneous populations of extracellular vesicle subtypes', *Proc. Natl. Acad. Sci. U. S. A.*, vol. 113, no. 8, pp. E968–E977, Feb. 2016, doi: 10.1073/pnas.1521230113.

[85] H. Zhang *et al.*, 'Identification of distinct nanoparticles and subsets of extracellular vesicles by asymmetric flow field-flow fractionation', *Nat. Cell Biol.*, vol. 20, no. 3, pp. 332–343, Mar. 2018, doi: 10.1038/s41556-018-0040-4.

[86] S. T. Y. Chuo, J. C. Y. Chien, and C. P. K. Lai, 'Imaging extracellular vesicles: Current and emerging methods', *Journal of Biomedical Science*, vol. 25, no. 1. BioMed Central Ltd., p. 91, Dec. 24, 2018, doi: 10.1186/s12929-018-0494-5.

[87] S. J. Gould and G. Raposo, 'As we wait: Coping with an imperfect nomenclature for extracellular vesicles', *Journal of Extracellular Vesicles*, vol. 2, no. 1. Co-Action Publishing, 2013, doi: 10.3402/jev.v2i0.20389.

[88] D. Zabeo, A. Cvjetkovic, C. Lässer, M. Schorb, J. Lötvall, and J. L. Höög, 'Exosomes purified from a single cell type have diverse morphology', *J. Extracell. Vesicles*, vol. 6, no. 1, p. 1329476, Dec. 2017, doi: 10.1080/20013078.2017.1329476.

[89] J. L. Höög and J. Lötvall, 'Diversity of extracellular vesicles in human ejaculates revealed by cryo-electron microscopy', *J. Extracell. Vesicles*, vol. 4, no. 1, p. 28680, Jan. 2015, doi: 10.3402/jev.v4.28680.

[90] N. Arraud *et al.*, 'Extracellular vesicles from blood plasma: determination of their morphology, size, phenotype and concentration', *J. Thromb. Haemost.*, vol. 12, no. 5, pp. 614–627, May 2014, doi: 10.1111/jth.12554.

[91] C. Lässer, S. C. Jang, and J. Lötvall, 'Subpopulations of extracellular vesicles and their therapeutic potential', *Molecular Aspects of Medicine*, vol. 60. Elsevier Ltd, pp. 1–14, Apr. 01, 2018, doi: 10.1016/j.mam.2018.02.002.

[92] A. Piccin, W. G. Murphy, and O. P. Smith, 'Circulating microparticles: pathophysiology and clinical implications', *Blood Rev.*, vol. 21, no. 3, pp. 157–171, May 2007, doi: 10.1016/j.blre.2006.09.001.

[93] M. Colombo, G. Raposo, and C. Théry, 'Biogenesis, Secretion, and Intercellular Interactions of Exosomes and Other Extracellular Vesicles', *Annu. Rev. Cell Dev. Biol*, vol. 30, pp. 255–289, 2014, doi: 10.1146/annurev-cellbio-101512-122326.

[94] W. M. Henne, N. J. Buchkovich, and S. D. Emr, 'The ESCRT Pathway', *Developmental Cell*,

vol. 21, no. 1. Elsevier, pp. 77–91, Jul. 19, 2011, doi: 10.1016/j.devcel.2011.05.015.

[95] D. J. Gill *et al.*, 'Structural insight into the ESCRT-I/-II link and its role in MVB trafficking', *EMBO J.*, vol. 26, no. 2, pp. 600–612, Jan. 2007, doi: 10.1038/sj.emboj.7601501.

[96] S. Ghazi-Tabatabai *et al.*, 'Structure and Disassembly of Filaments Formed by the ESCRT-III Subunit Vps24', *Structure*, vol. 16, no. 9, pp. 1345–1356, Sep. 2008, doi: 10.1016/j.str.2008.06.010.

[97] M. F. Baietti *et al.*, 'Syndecan-syntenin-ALIX regulates the biogenesis of exosomes', *Nat. Cell Biol.*, vol. 14, no. 7, pp. 677–685, Jul. 2012, doi: 10.1038/ncb2502.

[98] S. Stuffers, C. Sem Wegner, H. Stenmark, and A. Brech, 'Multivesicular Endosome Biogenesis in the Absence of ESCRTs', *Traffic*, vol. 10, no. 7, pp. 925–937, Jul. 2009, doi: 10.1111/j.1600-0854.2009.00920.x.

[99] K. Trajkovic *et al.*, 'Ceramide triggers budding of exosome vesicles into multivesicular endosomes', *Science (80-.).*, vol. 319, no. 5867, pp. 1244–1247, Feb. 2008, doi: 10.1126/science.1153124.

[100] D. Perez-Hernandez *et al.*, 'The intracellular interactome of tetraspanin-enriched microdomains reveals their function as sorting machineries toward exosomes', *J. Biol. Chem.*, vol. 288, no. 17, pp. 11649–11661, Apr. 2013, doi: 10.1074/jbc.M112.445304.

[101] A. Chairoungdua, D. L. Smith, P. Pochard, M. Hull, and M. J. Caplan, 'Exosome release of β-catenin: A novel mechanism that antagonizes Wnt signaling', *J. Cell Biol.*, vol. 190, no. 6, pp. 1079–1091, Sep. 2010, doi: 10.1083/jcb.201002049.

[102] S. Charrin, S. Jouannet, C. Boucheix, and E. Rubinstein, 'Tetraspanins at a glance', *J. Cell Sci.*, vol. 127, no. 17, pp. 3641–3648, Sep. 2014, doi: 10.1242/jcs.154906.

[103] R. E. McConnell, J. N. Higginbotham, D. A. Shifrin, D. L. Tabb, R. J. Coffey, and M. J. Tyska, 'The enterocyte microvillus is a vesicle-generating organelle', *J. Cell Biol.*, vol. 185, no. 7, pp. 1285–1298, Jun. 2009, doi: 10.1083/jcb.200902147.

[104] M. Ostrowski *et al.*, 'Rab27a and Rab27b control different steps of the exosome secretion pathway', *Nat. Cell Biol.*, vol. 12, no. 1, pp. 19–30, Jan. 2010, doi: 10.1038/ncb2000.

[105] C. Hsu *et al.*, 'Regulation of exosome secretion by Rab35 and its GTPase-activating proteins TBC1D10A-C', *J. Cell Biol.*, vol. 189, no. 2, pp. 223–232, Apr. 2010, doi: 10.1083/jcb.200911018.

[106] A. Savina, M. Vidal, and M. I. Colombo, 'The exosome pathway in K562 cells is regulated by Rab11', *J. Cell Sci.*, vol. 115, no. 12, pp. 2505–2515, Jun. 2002.

[107] S. R. Pfeffer, 'Unsolved Mysteries in Membrane Traffic', *Annu. Rev. Biochem.*, vol. 76, no. 1, pp. 629–645, Jun. 2007, doi: 10.1146/annurev.biochem.76.061705.130002.

[108] N. P. Hessvik and A. Llorente, 'Current knowledge on exosome biogenesis and release', *Cellular and Molecular Life Sciences*, vol. 75, no. 2. Birkhauser Verlag AG, pp. 193–208, Jan. 01, 2018, doi: 10.1007/s00018-017-2595-9.

[109] J.-M. Pasquet, J. Dachary-Prigent, and A. T. Nurden, 'Calcium Influx is a Determining Factor of Calpain Activation and Microparticle Formation in Platelets', *Eur. J. Biochem.*, vol. 239, no. 3, pp. 647–654, Aug. 1996, doi: 10.1111/j.1432-1033.1996.0647u.x.

[110] Z. Andreu and M. Yáñez-Mó, 'Tetraspanins in extracellular vesicle formation and function', *Front. Immunol.*, vol. 5, no. SEP, 2014, doi: 10.3389/fimmu.2014.00442.

[111] C. Théry *et al.*, 'Proteomic Analysis of Dendritic Cell-Derived Exosomes: A Secreted Subcellular Compartment Distinct from Apoptotic Vesicles', *J. Immunol.*, vol. 166, no. 12, pp. 7309–7318, Jun. 2001, doi: 10.4049/jimmunol.166.12.7309.

[112] G. Palmisano *et al.*, 'Characterization of membrane-shed microvesicles from cytokine-stimulated β-cells using proteomics strategies', *Mol. Cell. Proteomics*, vol. 11, no. 8, pp. 230–243, Aug. 2012, doi: 10.1074/mcp.M111.012732.

[113] A. Sinha, V. Ignatchenko, A. Ignatchenko, S. Mejia-Guerrero, and T. Kislinger, 'In-depth proteomic analyses of ovarian cancer cell line exosomes reveals differential enrichment of functional categories compared to the NCI 60 proteome', *Biochem. Biophys. Res. Commun.*, vol. 445, no. 4, pp. 694–701, Mar. 2014, doi: 10.1016/j.bbrc.2013.12.070.

[114] M. Shimoda and R. Khokha, 'Proteolytic factors in exosomes', *Proteomics*, vol. 13, no. 10–11, pp. 1624–1636, May 2013, doi: 10.1002/pmic.201200458.

[115] K. Laulagnier *et al.*, 'Mast cell- and dendritic cell-derived display a specific lipid composition and an unusual membrane organization', *Biochem. J.*, vol. 380, no. 1, pp. 161–171, May 2004, doi: 10.1042/BJ20031594.

[116] X. Huang *et al.*, 'Characterization of human plasma-derived exosomal RNAs by deep sequencing', *BMC Genomics*, vol. 14, no. 1, p. 319, May 2013, doi: 10.1186/1471-2164-14-319.

[117] M. Mittelbrunn *et al.*, 'Unidirectional transfer of microRNA-loaded exosomes from T cells to antigen-presenting cells', *Nat. Commun.*, vol. 2, no. 1, p. 282, 2011, doi: 10.1038/ncomms1285.

[118] J. S. Redzic, L. Balaj, K. E. van der Vos, and X. O. Breakefield, 'Extracellular RNA mediates and marks cancer progression', *Seminars in Cancer Biology*, vol. 28. Academic Press, pp. 14–23, 2014, doi: 10.1016/j.semcancer.2014.04.010.

[119] B. K. Thakur *et al.*, 'Double-stranded DNA in exosomes: A novel biomarker in cancer detection', *Cell Research*, vol. 24, no. 6. Nature Publishing Group, pp. 766–769, 2014, doi:

10.1038/cr.2014.44.

[120] A. Hoshino *et al.*, 'Tumour exosome integrins determine organotropic metastasis', *Nature*, vol. 527, no. 7578, pp. 329–335, Nov. 2015, doi: 10.1038/nature15756.

[121] H. Valadi, K. Ekström, A. Bossios, M. Sjöstrand, J. J. Lee, and J. O. Lötvall, 'Exosome-mediated transfer of mRNAs and microRNAs is a novel mechanism of genetic exchange between cells', *Nat. Cell Biol.*, vol. 9, no. 6, pp. 654–659, Jun. 2007, doi: 10.1038/ncb1596.

[122] H. C. Christianson, K. J. Svensson, T. H. Van Kuppevelt, J. P. Li, and M. Belting, 'Cancer cell exosomes depend on cell-surface heparan sulfate proteoglycans for their internalization and functional activity', *Proc. Natl. Acad. Sci. U. S. A.*, vol. 110, no. 43, pp. 17380–17385, Oct. 2013, doi: 10.1073/pnas.1304266110.

[123] K. J. Svensson *et al.*, 'Exosome uptake depends on ERK1/2-heat shock protein 27 signaling and lipid raft-mediated endocytosis negatively regulated by caveolin-1', *J. Biol. Chem.*, vol. 288, no. 24, pp. 17713–17724, Jun. 2013, doi: 10.1074/jbc.M112.445403.

[124] S. Rana, S. Yue, D. Stadel, and M. Zöller, 'Toward tailored exosomes: The exosomal tetraspanin web contributes to target cell selection', *Int. J. Biochem. Cell Biol.*, vol. 44, no. 9, pp. 1574–1584, Sep. 2012, doi: 10.1016/j.biocel.2012.06.018.

[125] A. E. Morelli *et al.*, 'Endocytosis, intracellular sorting, and processing of exosomes by dendritic cells', *Blood*, vol. 104, no. 10, pp. 3257–3266, Nov. 2004, doi: 10.1182/blood-2004-03-0824.

[126] C. Escrevente, S. Keller, P. Altevogt, and J. Costa, 'Interaction and uptake of exosomes by ovarian cancer cells', *BMC Cancer*, vol. 11, p. 108, Mar. 2011, doi: 10.1186/1471-2407-11-108.

[127] A. Montecalvo *et al.*, 'Mechanism of transfer of functional microRNAs between mouse dendritic cells via exosomes', *Blood*, vol. 119, no. 3, pp. 756–766, Jan. 2012, doi: 10.1182/blood-2011-02-338004.

[128] D. Feng *et al.*, 'Cellular Internalization of Exosomes Occurs Through Phagocytosis', *Traffic*, vol. 11, no. 5, pp. 675–687, May 2010, doi: 10.1111/j.1600-0854.2010.01041.x.

[129] A. Nanbo, E. Kawanishi, R. Yoshida, and H. Yoshiyama, 'Exosomes Derived from Epstein-Barr Virus-Infected Cells Are Internalized via Caveola-Dependent Endocytosis and Promote Phenotypic Modulation in Target Cells', *J. Virol.*, vol. 87, no. 18, pp. 10334–10347, Sep. 2013, doi: 10.1128/jvi.01310-13.

[130] M. C. Kerr and R. D. Teasdale, 'Defining Macropinocytosis', *Traffic*, vol. 10, no. 4, pp. 364–371, Apr. 2009, doi: 10.1111/j.1600-0854.2009.00878.x.

[131] D. Fitzner *et al.*, 'Selective transfer of exosomes from oligodendrocytes to microglia by

macropinocytosis', *J. Cell Sci.*, vol. 124, no. 3, pp. 447–458, Feb. 2011, doi: 10.1242/jcs.074088.

[132] N. Izquierdo-Useros *et al.*, 'Capture and transfer of HIV-1 particles by mature dendritic cells converges with the exosome-dissemination pathway', *Blood*, vol. 113, no. 12, pp. 2732–2741, Mar. 2009, doi: 10.1182/blood-2008-05-158642.

[133] R. B. Koumangoye, A. M. Sakwe, J. S. Goodwin, T. Patel, and J. Ochieng, 'Detachment of breast tumor cells induces rapid secretion of exosomes which subsequently mediate cellular adhesion and spreading', *PLoS One*, vol. 6, no. 9, 2011, doi: 10.1371/journal.pone.0024234.

[134] I. Parolini *et al.*, 'Microenvironmental pH is a key factor for exosome traffic in tumor cells', *J. Biol. Chem.*, vol. 284, no. 49, pp. 34211–34222, Dec. 2009, doi: 10.1074/jbc.M109.041152.

[135] G. Camussi, M. C. Deregibus, S. Bruno, V. Cantaluppi, and L. Biancone, 'Exosomes/microvesicles as a mechanism of cell-to-cell communication', *Kidney International*, vol. 78, no. 9. Nature Publishing Group, pp. 838–848, Nov. 01, 2010, doi: 10.1038/ki.2010.278.

[136] J. Zhang *et al.*, 'Exosomes derived from human endothelial progenitor cells accelerate cutaneous wound healing by promoting angiogenesis through Erk1/2 signaling', *Int. J. Biol. Sci.*, vol. 12, no. 12, pp. 1472–1487, Nov. 2016, doi: 10.7150/ijbs.15514.

[137] S. Fang *et al.*, 'Umbilical Cord-Derived Mesenchymal Stem Cell-Derived Exosomal MicroRNAs Suppress Myofibroblast Differentiation by Inhibiting the Transforming Growth Factor-β/SMAD2 Pathway During Wound Healing', *Stem Cells Transl. Med.*, vol. 5, no. 10, pp. 1425–1439, Oct. 2016, doi: 10.5966/sctm.2015-0367.

[138] X. Li, C. Jiang, and J. Zhao, 'Human endothelial progenitor cells-derived exosomes accelerate cutaneous wound healing in diabetic rats by promoting endothelial function', *J. Diabetes Complications*, vol. 30, no. 6, pp. 986–992, Aug. 2016, doi: 10.1016/j.jdiacomp.2016.05.009.

[139] B. Zhang *et al.*, 'HucMSC-Exosome Mediated-Wnt4 Signaling Is Required for Cutaneous Wound Healing', *Stem Cells*, vol. 33, no. 7, pp. 2158–2168, Jul. 2015, doi: 10.1002/STEM.1771@10.1002/(ISSN)1549-4918.TOPTENARTICLESONTHEBIOLOGYOFEMBRYONICANDINDUCEDPLURIPOTENTSTEMCELLS.

[140] B. Zhao *et al.*, 'Exosomes derived from human amniotic epithelial cells accelerate wound healing and inhibit scar formation', *J. Mol. Histol.*, vol. 48, no. 2, pp. 121–132, Apr. 2017, doi: 10.1007/s10735-017-9711-x.

[141] X. Li *et al.*, 'Exosome Derived From Human Umbilical Cord Mesenchymal Stem Cell Mediates MiR-181c Attenuating Burn-induced Excessive Inflammation', *EBioMedicine*, vol.

8, pp. 72–82, Jun. 2016, doi: 10.1016/j.ebiom.2016.04.030.

[142] I. Del Conde, C. N. Shrimpton, P. Thiagarajan, and J. A. López, 'Tissue-factor-bearing microvesicles arise from lipid rafts and fuse with activated platelets to initiate coagulation', *Blood*, vol. 106, no. 5, pp. 1604–1611, Sep. 2005, doi: 10.1182/blood-2004-03-1095.

[143] E. Biro *et al.*, 'Human cell-derived microparticles promote thrombus formation in vivo in a tissue factor-dependent manner', *J. Thromb. Haemost.*, vol. 1, no. 12, pp. 2561–2568, Dec. 2003, doi: 10.1046/j.1538-7836.2003.00456.x.

[144] Y. C. Liu, X. B. Zou, Y. F. Chai, and Y. M. Yao, 'Macrophage polarization in inflammatory diseases', *International Journal of Biological Sciences*, vol. 10, no. 5. Ivyspring International Publisher, pp. 520–529, May 01, 2014, doi: 10.7150/ijbs.8879.

[145] D. Ti *et al.*, 'LPS-preconditioned mesenchymal stromal cells modify macrophage polarization for resolution of chronic inflammation via exosome-shuttled let-7b', *J. Transl. Med.*, vol. 13, no. 1, pp. 1–14, Sep. 2015, doi: 10.1186/s12967-015-0642-6.

[146] V. J. Moulin, D. Mayrand, H. Messier, M. C. Martinez, C. A. Lopez-Vallé, and H. Genest, 'Shedding of microparticles by myofibroblasts as mediator of cellular cross-talk during normal wound healing', *J. Cell. Physiol.*, vol. 225, no. 3, pp. 734–740, Dec. 2010, doi: 10.1002/jcp.22268.

[147] G. D. Sharma, J. He, and H. E. P. Bazan, 'p38 and ERK1/2 coordinate cellular migration and proliferation in epithelial wound healing. Evidence of cross-talk activation between map kinase cascades', *J. Biol. Chem.*, vol. 278, no. 24, pp. 21989–21997, Jun. 2003, doi: 10.1074/jbc.M302650200.

[148] S. Sano, K. S. Chan, and J. DiGiovanni, 'Impact of Stat3 activation upon skin biology: A dichotomy of its role between homeostasis and diseases', *Journal of Dermatological Science*, vol. 50, no. 1. Elsevier, pp. 1–14, Apr. 01, 2008, doi: 10.1016/j.jdermsci.2007.05.016.

[149] A. Shabbir, A. Cox, L. Rodriguez-Menocal, M. Salgado, and E. Van Badiavas, 'Mesenchymal Stem Cell Exosomes Induce Proliferation and Migration of Normal and Chronic Wound Fibroblasts, and Enhance Angiogenesis in Vitro', *Stem Cells Dev.*, vol. 24, no. 14, pp. 1635–1647, Jul. 2015, doi: 10.1089/scd.2014.0316.

[150] B. Zhang *et al.*, 'Human Umbilical Cord Mesenchymal Stem Cell Exosomes Enhance Angiogenesis Through the Wnt4/β-Catenin Pathway', *Stem Cells Transl. Med.*, vol. 4, no. 5, pp. 513–522, May 2015, doi: 10.5966/sctm.2014-0267.

[151] B. H. Sung, T. Ketova, D. Hoshino, A. Zijlstra, and A. M. Weaver, 'Directional cell movement through tissues is controlled by exosome secretion', *Nat. Commun.*, vol. 6, May 2015, doi: 10.1038/ncomms8164.

[152] J. W. Clancy *et al.*, 'Regulated delivery of molecular cargo to invasive tumour-derived microvesicles', *Nat. Commun.*, vol. 6, p. 6919, Apr. 2015, doi: 10.1038/ncomms7919.

[153] J. McCready, J. D. Sims, D. Chan, and D. G. Jay, 'Secretion of extracellular hsp90α via exosomes increases cancer cell motility: A role for plasminogen activation', *BMC Cancer*, vol. 10, p. 294, Jun. 2010, doi: 10.1186/1471-2407-10-294.

[154] R. Gastpar *et al.*, 'Heat shock protein 70 surface-positive tumor exosomes stimulate migratory and cytolytic activity of natural killer cells', *Cancer Res.*, vol. 65, no. 12, pp. 5238–5247, Jun. 2005, doi: 10.1158/0008-5472.CAN-04-3804.

[155] T. Nemoto, N. Sato, H. Iwanari, H. Yamashita, and T. Takagi, 'Domain structures and immunogenic regions of the 90-kDa heat-shock protein (HSP90). Probing with a library of anti-HSP90 monoclonal antibodies and limited proteolysis', *J. Biol. Chem.*, vol. 272, no. 42, pp. 26179–26187, Oct. 1997, doi: 10.1074/jbc.272.42.26179.

[156] C.-F. Cheng *et al.*, 'Transforming Growth Factor α (TGFα)-Stimulated Secretion of HSP90α: Using the Receptor LRP-1/CD91 To Promote Human Skin Cell Migration against a TGFβ-Rich Environment during Wound Healing', *Mol. Cell. Biol.*, vol. 28, no. 10, pp. 3344–3358, May 2008, doi: 10.1128/mcb.01287-07.

[157] L. Hu *et al.*, 'Exosomes derived from human adipose mensenchymal stem cells accelerates cutaneous wound healing via optimizing the characteristics of fibroblasts', *Sci. Rep.*, vol. 6, Sep. 2016, doi: 10.1038/srep32993.

[158] P. Huang *et al.*, 'Keratinocyte microvesicles regulate the expression of multiple genes in dermal fibroblasts', *J. Invest. Dermatol.*, vol. 135, no. 12, pp. 3051–3059, Dec. 2015, doi: 10.1038/jid.2015.320.

[159] J. Zhang *et al.*, 'Exosomes released from human induced pluripotent stem cells-derived MSCs facilitate cutaneous wound healing by promoting collagen synthesis and angiogenesis', *J. Transl. Med.*, vol. 13, no. 1, Feb. 2015, doi: 10.1186/s12967-015-0417-0.

[160] X. Liang, L. Zhang, S. Wang, Q. Han, and R. C. Zhao, 'Exosomes secreted by mesenchymal stem cells promote endothelial cell angiogenesis by transferring miR-125a', *J. Cell Sci.*, vol. 129, no. 11, pp. 2182–2189, Jun. 2016, doi: 10.1242/jcs.170373.

[161] H. K. Kim, K. S. Song, J.-H. Chung, K. R. Lee, and S.-N. Lee, 'Platelet microparticles induce angiogenesis in vitro', *Br. J. Haematol.*, vol. 124, no. 3, pp. 376–384, Feb. 2004, doi: 10.1046/j.1365-2141.2003.04773.x.

[162] A. Brill, O. Dashevsky, J. Rivo, Y. Gozal, and D. Varon, 'Platelet-derived microparticles induce angiogenesis and stimulate post-ischemic revascularization', *Cardiovasc. Res.*, vol. 67, no. 1, pp. 30–38, Jul. 2005, doi: 10.1016/j.cardiores.2005.04.007.

[163] G. Taraboletti, S. D'Ascenzo, P. Borsotti, R. Giavazzi, A. Pavan, and V. Dolo, 'Shedding of the matrix metalloproteinases MMP-2, MMP-9, and MT1-MMP as membrane vesicle-associated components by endothelial cells', *Am. J. Pathol.*, vol. 160, no. 2, pp. 673–680, Feb. 2002, doi: 10.1016/S0002-9440(10)64887-0.

[164] C. Yang *et al.*, 'Lymphocytic microparticles inhibit angiogenesis by stimulating oxidative stress and negatively regulating VEGF-induced pathways', *Am. J. Physiol. Integr. Comp. Physiol.*, vol. 294, no. 2, pp. R467–R476, Feb. 2008, doi: 10.1152/ajpregu.00432.2007.

[165] L. Chen *et al.*, 'Conditioned medium from hypoxic bone marrow-derived mesenchymal stem cells enhances wound healing in mice', *PLoS One*, vol. 9, no. 4, Apr. 2014, doi: 10.1371/journal.pone.0096161.

[166] S. Yamada and K. Sugahara, 'Potential Therapeutic Application of Chondroitin Sulfate/Dermatan Sulfate', *Curr. Drug Discov. Technol.*, vol. 5, no. 4, pp. 289–301, Dec. 2008, doi: 10.2174/157016308786733564.

[167] K. Sugahara, T. Mikami, T. Uyama, S. Mizuguchi, K. Nomura, and H. Kitagawa, 'Recent advances in the structural biology of chondroitin sulfate and dermatan sulfate', *Current Opinion in Structural Biology*, vol. 13, no. 5. Elsevier Ltd, pp. 612–620, Oct. 01, 2003, doi: 10.1016/j.sbi.2003.09.011.

[168] R. Sasisekharan and G. Venkataraman, 'Heparin and heparan sulfate: Biosynthesis, structure and function', *Current Opinion in Chemical Biology*, vol. 4, no. 6. Elsevier Ltd, pp. 626–631, 2000, doi: 10.1016/S1367-5931(00)00145-9.

[169] V. H. Pomin, 'Keratan sulfate: An up-to-date review', *International Journal of Biological Macromolecules*, vol. 72. Elsevier, pp. 282–289, Jan. 01, 2015, doi: 10.1016/j.ijbiomac.2014.08.029.

[170] A. Almond, 'Hyaluronan', *Cellular and Molecular Life Sciences*, vol. 64, no. 13. Cell Mol Life Sci, pp. 1591–1596, Jul. 2007, doi: 10.1007/s00018-007-7032-z.

[171] Y. Henrotin, M. Mathy, C. Sanchez, and C. Lambert, 'Chondroitin sulfate in the treatment of osteoarthritis: From in vitro studies to clinical recommendations', *Therapeutic Advances in Musculoskeletal Disease*, vol. 2, no. 6. SAGE Publications, pp. 335–348, 2010, doi: 10.1177/1759720X10383076.

[172] J. M. Trowbridge and R. L. Gallo, 'MINI REVIEW Dermatan sulfate: new functions from an old glycosaminoglycan', 2002.

[173] D. L. Rabenstein, 'Heparin and heparan sulfate: structure and function', 2002, doi: 10.1039/b100916h.

[174] J. L. Funderburgh, 'MINI REVIEW Keratan sulfate: structure, biosynthesis, and function',

2000.

[175] E. Papakonstantinou, M. Roth, and G. Karakiulakis, 'Hyaluronic acid: A key molecule in skin aging', *Dermato-Endocrinology*, vol. 4, no. 3. Landes Bioscience, p. 253, 2012, doi: 10.4161/derm.21923.

[176] F. Sasarman, C. Maftei, P. M. Campeau, C. Brunel-Guitton, G. A. Mitchell, and P. Allard, 'Biosynthesis of glycosaminoglycans: associated disorders and biochemical tests', *J. Inherit. Metab. Dis.*, vol. 39, no. 2, pp. 173–188, Mar. 2016, doi: 10.1007/s10545-015-9903-z.

[177] S. Mizumoto, S. Ikegawa, and K. Sugahara, 'Human genetic disorders caused by mutations in genes encoding biosynthetic enzymes for sulfated glycosaminoglycans', *J. Biol. Chem.*, vol. 288, no. 16, pp. 10953–10961, Apr. 2013, doi: 10.1074/jbc.R112.437038.

[178] S. Mizumoto, S. Yamada, and K. Sugahara, 'Human Genetic Disorders and Knockout Mice Deficient in Glycosaminoglycan', *Biomed Res. Int.*, vol. 2014, 2014, doi: 10.1155/2014/495764.

[179] J. L. Funderburgh, 'Keratan sulfate biosynthesis', *IUBMB Life*, vol. 54, no. 4. NIH Public Access, pp. 187–194, Oct. 01, 2002, doi: 10.1080/15216540214932.

[180] A. Tufano *et al.*, 'Mesoglycan: Clinical evidences for use in vascular diseases', *International Journal of Vascular Medicine*, vol. 2010. Hindawi Limited, 2010, doi: 10.1155/2010/390643.

[181] G. Derosa, A. D'Angelo, D. Romano, and P. Maffioli, 'Evaluation of the Effects of Mesoglycan on Some Markers of Endothelial Damage and Walking Distance in Diabetic Patients with Peripheral Arterial Disease', *Int. J. Mol. Sci.*, vol. 18, no. 3, Mar. 2017, doi: 10.3390/ijms18030572.

[182] S. F. Penc *et al.*, 'Dermatan sulfate released after injury is a potent promoter of fibroblast growth factor-2 function', *J. Biol. Chem.*, vol. 273, no. 43, pp. 28116–28121, Oct. 1998, doi: 10.1074/jbc.273.43.28116.

[183] R. Belvedere, V. Bizzarro, L. Parente, F. Petrella, and A. Petrella, 'Effects of Prisma® Skin dermal regeneration device containing glycosaminoglycans on human keratinocytes and fibroblasts', *Cell Adhes. Migr.*, vol. 12, no. 2, pp. 168–183, Mar. 2018, doi: 10.1080/19336918.2017.1340137.

[184] M. G. Rohani and W. C. Parks, 'Matrix remodeling by MMPs during wound repair', *Matrix Biology*, vol. 44–46. Elsevier, pp. 113–121, May 01, 2015, doi: 10.1016/j.matbio.2015.03.002.

[185] A. Jacinto, A. Martinez-Arias, and P. Martin, 'Mechanisms of epithelial fusion and repair', *Nature Cell Biology*, vol. 3, no. 5. Nat Cell Biol, 2001, doi: 10.1038/35074643.

[186] R. Knirsh *et al.*, 'Loss of E-cadherin-mediated cell-cell contacts activates a novel mechanism for up-regulation of the proto-oncogene c-jun', *Mol. Biol. Cell*, vol. 20, no. 7, pp. 2121–2129,

Apr. 2009, doi: 10.1091/mbc.E08-12-1196.

[187] D. Pokharel, M. P. Padula, J. F. Lu, R. Jaiswal, S. P. Djordjevic, and M. Bebawy, 'The role of CD44 and ERM proteins in expression and functionality of P-glycoprotein in breast cancer cells', *Molecules*, vol. 21, no. 3, Mar. 2016, doi: 10.3390/molecules21030290.

[188] K. Azuma *et al.*, 'Presence of α-smooth muscle actin-positive endothelial cells in the luminal surface of adult aorta', *Biochem. Biophys. Res. Commun.*, vol. 380, no. 3, pp. 620–626, Mar. 2009, doi: 10.1016/j.bbrc.2009.01.135.

[189] C. Giampietro *et al.*, 'Overlapping and divergent signaling pathways of N-cadherin and VE-cadherin in endothelial cells', *Blood*, vol. 119, no. 9, pp. 2159–2170, Mar. 2012, doi: 10.1182/blood-2011-09-381012.

[190] J. R. Couchman, 'Transmembrane Signaling Proteoglycans', *Annu. Rev. Cell Dev. Biol.*, vol. 26, no. 1, pp. 89–114, Nov. 2010, doi: 10.1146/annurev-cellbio-100109-104126.

[191] T. Manon-Jensen, Y. Itoh, and J. R. Couchman, 'Proteoglycans in health and disease: The multiple roles of syndecan shedding', *FEBS Journal*, vol. 277, no. 19. Blackwell Publishing Ltd, pp. 3876–3889, Oct. 01, 2010, doi: 10.1111/j.1742-4658.2010.07798.x.

[192] J. R. Couchman, S. Gopal, H. Ching Lim, S. Nørgaard, and H. A. Multhaupt, 'Syndecans: from peripheral coreceptors to mainstream regulators of cell behaviour', 2014, doi: 10.1111/iep.12112.

[193] S. S. Apte and W. C. Parks, 'Metalloproteinases: A parade of functions in matrix biology and an outlook for the future', *Matrix Biology*, vol. 44–46. Elsevier B.V., pp. 1–6, May 01, 2015, doi: 10.1016/j.matbio.2015.04.005.

[194] S. Weber and P. Saftig, 'Ectodomain shedding and ADAMs in development', *Development (Cambridge)*, vol. 139, no. 20. Oxford University Press for The Company of Biologists Limited, pp. 3693–3709, Oct. 15, 2012, doi: 10.1242/dev.076398.

[195] S. V. Subramanian, M. L. Fitzgerald, and M. Bernfield, 'Regulated shedding of syndecan-1 and -4 ectodomains by thrombin and growth factor receptor activation', *J. Biol. Chem.*, vol. 272, no. 23, pp. 14713–14720, Jun. 1997, doi: 10.1074/jbc.272.23.14713.

[196] S. Brule, N. Charnaux, A. Sutton, D. Ledoux, T. Chaigneau, and L. Gattegno, 'The shedding of syndecan-4 and syndecan-1 from HeLa cells and human primary macrophages is accelerated by SDF-1/CXCL12 and mediated by the matrix metalloproteinase-9', *Glycobiology*, vol. 16, no. 6, pp. 488–501, 2006, doi: 10.1093/glycob/cwj098.

[197] Y. Yang *et al.*, 'Heparanase enhances syndecan-1 shedding: A novel mechanism for stimulation of tumor growth and metastasis', *J. Biol. Chem.*, vol. 282, no. 18, pp. 13326–13333, May 2007, doi: 10.1074/jbc.M611259200.

[198] M. L. Fitzgerald, Z. Wang, P. W. Park, G. Murphy, and M. Bernfield, 'Shedding of syndecan-1 and -4 ectodomains is regulated by multiple signaling pathways and mediated by a TIMP-3-sensitive metalloproteinase', *J. Cell Biol.*, vol. 148, no. 4, pp. 811–824, Feb. 2000, doi: 10.1083/jcb.148.4.811.

[199] R. Steinfeld, H. Van Den Berghe, and G. David, 'Stimulation of fibroblast growth factor receptor-1 occupancy and signaling by cell surface-associated syndecans and glypican', *J. Cell Biol.*, vol. 133, no. 2, pp. 405–416, Apr. 1996, doi: 10.1083/jcb.133.2.405.

[200] V. Kainulainen, H. Wang, C. Schick, and M. Bernfield, 'Syndecans, heparan sulfate proteoglycans, maintain the proteolytic balance of acute wound fluids', *J. Biol. Chem.*, vol. 273, no. 19, pp. 11563–11569, May 1998, doi: 10.1074/jbc.273.19.11563.

[201] K. Elenius, S. Vainio, M. Laato, M. Salmivirta, I. Thesleff, and M. Jalkanen, 'Induced Expression of Syndecan in Healing Wounds'.

[202] P. Chen, L. E. Abacherli, S. T. Nadler, Y. Wang, Q. Li, and W. C. Parks, 'MMP7 shedding of syndecan-1 facilitates re-epithelialization by affecting α2β1 integrin activation', *PLoS One*, vol. 4, no. 8, Aug. 2009, doi: 10.1371/journal.pone.0006565.

[203] V. Elenius, M. Götte, O. Reizes, K. Elenius, and M. Bernfield, 'Inhibition by the soluble syndecan-1 ectodomains delays wound repair in mice overexpressing syndecan-1', *J. Biol. Chem.*, vol. 279, no. 40, pp. 41928–41935, Oct. 2004, doi: 10.1074/jbc.M404506200.

[204] S. Choi *et al.*, 'Transmembrane domain-induced oligomerization is crucial for the functions of syndecan-2 and syndecan-4', *J. Biol. Chem.*, vol. 280, no. 52, pp. 42573–42579, Dec. 2005, doi: 10.1074/jbc.M509238200.

[205] M. J. Kwon, J. Park, S. Jang, C. Y. Eom, and E. S. Oh, 'The conserved phenylalanine in the transmembrane domain enhances heteromeric interactions of syndecans', *J. Biol. Chem.*, vol. 291, no. 2, pp. 872–881, Jan. 2016, doi: 10.1074/jbc.M115.685040.

[206] F. Granés, C. Berndt, C. Roy, P. Mangeat, M. Reina, and S. Vilaró, 'Identification of a novel Ezrin-binding site in syndecan-2 cytoplasmic domain', *FEBS Lett.*, vol. 547, no. 1–3, pp. 212–216, Jul. 2003, doi: 10.1016/S0014-5793(03)00712-9.

[207] K. Chen and K. J. Williams, 'Molecular mediators for raft-dependent endocytosis of syndecan-1, a highly conserved, multifunctional receptor', *J. Biol. Chem.*, vol. 288, no. 20, pp. 13988–13999, May 2013, doi: 10.1074/jbc.M112.444737.

[208] U. J. R. N. V. S. Granés F, 'Ezrin links syndecan-2 to the cytoskeleton', *J. Cell Sci.*, vol. 113, pp. 1267–1276, Mar. 2000.

[209] S. S. , L. S. H. . D. F. , L. D. and G. P. F. Baciu P. C., 'Syndesmos, a protein that interacts with the cytoplasmic domain of syndecan-4, mediates cell spreading and actin cytoskeletal

organization', *J. Cell Sci.* , vol. 113, pp. 315–324, Jan. 2000.

[210] A. C. Rapraeger, 'Syndecan-regulated receptor signaling', *Journal of Cell Biology*, vol. 149, no. 5. The Rockefeller University Press, pp. 995–997, May 29, 2000, doi: 10.1083/jcb.149.5.995.

[211] A. P. Gilmore and K. Burridge, 'Regulation of vinculin binding to talin and actin by phosphatidylinositol-4-5-bisphosphate', *Nature*, vol. 381, no. 6582, pp. 531–535, 1996, doi: 10.1038/381531a0.

[212] S. Wennström *et al.*, 'Activation of phosphoinositide 3-kinase is required for PDGF-stimulated membrane ruffling', *Curr. Biol.*, vol. 4, no. 5, pp. 385–393, May 1994, doi: 10.1016/S0960-9822(00)00087-7.

[213] P. R. Sheperd, B. J. Reaves, and H. W. Davidson, 'Phosphoinositide 3-kinases and membrane traffic', *Trends in Cell Biology*, vol. 6, no. 3. Elsevier Ltd, pp. 92–97, Mar. 01, 1996, doi: 10.1016/0962-8924(96)80998-6.

[214] N. Divecha and R. F. Irvine, 'Phospholipid Signaling Review', 1995.

[215] M. H. Lee and R. M. Bell, 'Mechanism of Protein Kinase C Activation by Phosphatidylinositol 4,5-Bisphosphate', *Biochemistry*, vol. 30, no. 4, pp. 1041–1049, Jan. 1991, doi: 10.1021/bi00218a023.

[216] E. S. Oh, A. Woods, and J. R. Couchman, 'Syndecan-4 proteoglycan regulates the distribution and activity of protein kinase C', *J. Biol. Chem.*, vol. 272, no. 13, pp. 8133–8136, Mar. 1997, doi: 10.1074/jbc.272.13.8133.

[217] M. Sheng and C. Sala, 'PDZ Domains and the Organization of Supramolecular Complexes', *Annu. Rev. Neurosci.*, vol. 24, no. 1, pp. 1–29, Mar. 2001, doi: 10.1146/annurev.neuro.24.1.1.

[218] J. J. Grootjans *et al.*, 'Syntenin, a PDZ protein that binds syndecan cytoplasmic domains', *Proc. Natl. Acad. Sci. U. S. A.*, vol. 94, no. 25, pp. 13683–13688, Dec. 1997, doi: 10.1073/pnas.94.25.13683.

[219] P. Zimmermann *et al.*, 'Syndecan recyling is controlled by syntenin-PIP2 interaction and Arf6', *Dev. Cell*, vol. 9, no. 3, pp. 377–388, Sep. 2005, doi: 10.1016/j.devcel.2005.07.011.

[220] A. R. Cohen, D. F. Wood, S. M. Marfatia, Z. Walther, A. H. Chishti, and J. M. Anderson, 'Human CASK/LIN-2 binds syndecan-2 and protein 4.1 and Localizes to the basolateral membrane of epithelial cells', *J. Cell Biol.*, vol. 142, no. 1, pp. 129–138, Jul. 1998, doi: 10.1083/jcb.142.1.129.

[221] A. Horowitz and M. Simons, 'Regulation of syndecan-4 phosphorylation in vivo', *J. Biol. Chem.*, vol. 273, no. 18, pp. 10914–10918, May 1998, doi: 10.1074/jbc.273.18.10914.

[222] W. A. . F. A. . C. G. J. . G. J. T. , C. J. R. Longley R.L., 'Control of morphology, cytoskeleton

and migration by syndecan-4', *J. Cell Sci.*, vol. 112, pp. 3421–3431, 1999, doi: 10.1083/jcb.109.2.863.

[223] D. L. M. Beauvais, B. J. Burbach, and A. C. Rapraeger, 'The syndecan-1 ectodomain regulates αvβ3 integrin activily in human mammary carcinoma cells', *J. Cell Biol.*, vol. 167, no. 1, pp. 171–181, Oct. 2004, doi: 10.1083/jcb.200404171.

[224] K. J. McQuade, D. L. M. Beauvais, B. J. Burbach, and A. C. Rapraeger, 'Syndecan-1 regulates αvβ5 integrin activity in B82L fibroblasts', *J. Cell Sci.*, vol. 119, no. 12, pp. 2445–2456, Jun. 2006, doi: 10.1242/jcs.02970.

[225] K. Hozumi, N. Suzuki, P. K. Nielsen, M. Nomizu, and Y. Yamada, 'Laminin α1 chain LG4 module promotes cell attachment through syndecans and cell spreading through integrin α2β1', *J. Biol. Chem.*, vol. 281, no. 43, pp. 32929–32940, Oct. 2006, doi: 10.1074/jbc.M605708200.

[226] T. Ogawa, Y. Tsubota, J. Hashimoto, Y. Kariya, and K. Miyazaki, 'The short arm of laminin γ2 chain of laminin-5 (laminin-332) binds syndecan-1 and regulates cellular adhesion and migration by suppressing phosphorylation of integrin β4 chain', *Mol. Biol. Cell*, vol. 18, no. 5, pp. 1621–1633, May 2007, doi: 10.1091/mbc.E06-09-0806.

[227] S. Saoncella *et al.*, 'Syndecan-4 signals cooperatively with integrins in a Rho-dependent manner in the assembly of focal adhesions and actin stress fibers', *Proc. Natl. Acad. Sci. U. S. A.*, vol. 96, no. 6, pp. 2805–2810, Mar. 1999, doi: 10.1073/pnas.96.6.2805.

[228] Z. Mostafavi-Pour, J. A. Askari, S. J. Parkinson, P. J. Parker, T. T. C. Ng, and M. J. Humphries, 'Integrin-specific signaling pathways controlling focal adhesion formation and cell migration', *J. Cell Biol.*, vol. 161, no. 1, pp. 155–167, Apr. 2003, doi: 10.1083/jcb.200210176.

[229] M. D. Bass, M. R. Morgan, K. A. Roach, J. Settleman, A. B. Goryachev, and M. J. Humphries, 'p190RhoGAP is the convergence point of adhesion signals from α5β1 integrin and syndecan-4', *J. Cell Biol.*, vol. 181, no. 6, pp. 1013–1026, Jun. 2008, doi: 10.1083/jcb.200711129.

[230] V. F. Fiore, L. Ju, Y. Chen, C. Zhu, and T. H. Barker, 'Dynamic catch of a Thy-1-α5 β1 +syndecan-4 trimolecular complex', *Nat. Commun.*, vol. 5, 2014, doi: 10.1038/ncomms5886.

[231] R. Gallo, C. Kim, R. Kokenyesi, N. S. Adzick, and M. Bernfield, 'Syndecans-1 and -4 are induced during wound repair of neonatal but not fetal skin', *J. Invest. Dermatol.*, vol. 107, no. 5, pp. 676–683, 1996, doi: 10.1111/1523-1747.ep12365571.

[232] F. Echtermeyer *et al.*, 'Delayed wound repair and impaired angiogenesis in mice lacking syndecan-4', *J. Clin. Invest.*, vol. 107, no. 2, p. R9, 2001, doi: 10.1172/JCI10559.

[233] V. Gerke and S. E. Moss, 'Annexins: From structure to function', *Physiological Reviews*, vol. 82, no. 2. American Physiological Society, pp. 331–371, 2002, doi: 10.1152/physrev.00030.2001.

[234] M. Mirsaeidi, S. Gidfar, A. Vu, and D. Schraufnagel, 'Annexins family: Insights into their functions and potential role in pathogenesis of sarcoidosis', *Journal of Translational Medicine*, vol. 14, no. 1. BioMed Central Ltd., 2016, doi: 10.1186/s12967-016-0843-7.

[235] K. Monastyrskaya, E. B. Babiychuk, A. Hostettler, U. Rescher, and A. Draeger, 'Annexins as intracellular calcium sensors', *Cell Calcium*, vol. 41, no. 3, pp. 207–219, 2007, doi: 10.1016/j.ceca.2006.06.008.

[236] S. Liemann and A. Lewit-Bentley, 'Annexins: a novel family of calcium- and membrane-binding proteins in search of a function', *Structure*, vol. 3, no. 3, pp. 233–237, 1995, doi: 10.1016/S0969-2126(01)00152-6.

[237] X. Weng, H. Luecke, I. S. Song, D. S. Kang, S. -H Kim, and R. Huber, 'Crystal structure of human annexin I at 2.5 Å resolution', *Protein Sci.*, vol. 2, no. 3, pp. 448–458, 1993, doi: 10.1002/pro.5560020317.

[238] V. Gerke, C. E. Creutz, and S. E. Moss, 'Annexins: Linking Ca2+ signalling to membrane dynamics', *Nature Reviews Molecular Cell Biology*, vol. 6, no. 6. Nat Rev Mol Cell Biol, pp. 449–461, Jun. 2005, doi: 10.1038/nrm1661.

[239] A. Rosengarth, V. Gerke, and H. Luecke, 'X-ray structure of full-length annexin 1 and implications for membrane aggregation', *J. Mol. Biol.*, vol. 306, no. 3, pp. 489–498, Feb. 2001, doi: 10.1006/jmbi.2000.4423.

[240] L. H. K. Lim and S. Pervaiz, 'Annexin 1: the new face of an old molecule', *FASEB J.*, vol. 21, no. 4, pp. 968–975, Apr. 2007, doi: 10.1096/fj.06-7464rev.

[241] L. C. Alldridge and C. E. Bryant, 'Annexin 1 regulates cell proliferation by disruption of cell morphology and inhibition of cyclin D1 expression through sustained activation of the ERK1/2 MAPK signal', *Exp. Cell Res.*, vol. 290, no. 1, pp. 93–107, Oct. 2003, doi: 10.1016/S0014-4827(03)00310-0.

[242] F. D'Acquisto, M. Perretti, and R. J. Flower, 'Annexin-A1: A pivotal regulator of the innate and adaptive immune systems', *British Journal of Pharmacology*, vol. 155, no. 2. Br J Pharmacol, pp. 152–169, Sep. 2008, doi: 10.1038/bjp.2008.252.

[243] U. Rescher and V. Gerke, 'Annexins - Unique membrane binding proteins with diverse functions', *Journal of Cell Science*, vol. 117, no. 13. J Cell Sci, pp. 2631–2639, Jun. 01, 2004, doi: 10.1242/jcs.01245.

[244] M. Perretti and E. Solito, 'Annexin 1 and neutrophil apoptosis', in *Biochemical Society Transactions*, Jun. 2004, vol. 32, no. 3, pp. 507–510, doi: 10.1042/BST0320507.

[245] C. D. John, H. C. Christian, J. F. Morris, R. J. Flower, E. Solito, and J. C. Buckingham, 'Annexin 1 and the regulation of endocrine function', *Trends in Endocrinology and*

Metabolism, vol. 15, no. 3. Trends Endocrinol Metab, pp. 103–109, Apr. 2004, doi: 10.1016/j.tem.2004.02.001.

[246] H. H. Gerdes, 'Membrane traffic in the secretory pathway', *Cellular and Molecular Life Sciences*, vol. 65, no. 18. Cell Mol Life Sci, pp. 2779–2780, Sep. 2008, doi: 10.1007/s00018-008-8348-z.

[247] B. P. Wallner *et al.*, 'Cloning and expression of human lipocortin, a phospholipase A2 inhibitor with potential anti-inflammatory activity', *Nature*, vol. 320, no. 6057, pp. 77–81, 1986, doi: 10.1038/320077a0.

[248] P. Christman, J. Callaway, J. Fallon, J. Jones, and H. T. Haigler, 'Selective secretion of annexin 1, a protein without a signal sequence, by the human prostate gland', *J. Biol. Chem.*, vol. 266, no. 4, pp. 2499–2507, 1991.

[249] A. A. Aderem, K. A. Albert, M. M. Keum, J. K. T. Wang, P. Greengard, and Z. A. Cohn, 'Stimulus-dependent myristoylation of a major substrate for protein kinase C', *Nature*, vol. 332, no. 6162, pp. 362–364, 1988, doi: 10.1038/332362a0.

[250] S. Omer, D. Meredith, J. F. Morris, and H. C. Christian, 'Evidence for the role of adenosine 5′-triphosphate-binding cassette (ABC)-A1 in the externalization of annexin 1 from pituitary folliculostellate cells and ABCA1-transfected cell models', *Endocrinology*, vol. 147, no. 7, pp. 3219–3227, 2006, doi: 10.1210/en.2006-0099.

[251] H. S. Euzger, R. J. Flower, N. J. Goulding, and M. Perretti, 'Differential modulation of annexin I binding sites on monocytes and neutrophils', *Mediators Inflamm.*, vol. 8, no. 1, pp. 53–62, 1999, doi: 10.1080/09629359990720.

[252] J. Dalli, L. V. Norling, D. Renshaw, D. Cooper, K. Y. Leung, and M. Perretti, 'Annexin 1 mediates the rapid anti-inflammatory effects of neutrophil-derived microparticles', *Blood*, vol. 112, no. 6, pp. 2512–2519, Sep. 2008, doi: 10.1182/blood-2008-02-140533.

[253] G. Raposo and W. Stoorvogel, 'Extracellular vesicles: Exosomes, microvesicles, and friends', *Journal of Cell Biology*, vol. 200, no. 4. J Cell Biol, pp. 373–383, Feb. 2013, doi: 10.1083/jcb.201211138.

[254] G. Leoni *et al.*, 'Annexin A1'containing extracellular vesicles and polymeric nanoparticles promote epithelial wound repair', *J. Clin. Invest.*, vol. 125, no. 3, pp. 1215–1227, Mar. 2015, doi: 10.1172/JCI76693.

[255] E. Pessolano *et al.*, 'Annexin A1 may induce pancreatic cancer progression as a key player of extracellular vesicles effects as evidenced in the in vitro MIA PaCa-2 model system', *Int. J. Mol. Sci.*, vol. 19, no. 12, Dec. 2018, doi: 10.3390/ijms19123878.

[256] J. Skog *et al.*, 'Glioblastoma microvesicles transport RNA and proteins that promote tumour

growth and provide diagnostic biomarkers', *Nat. Cell Biol.*, vol. 10, no. 12, pp. 1470–1476, 2008, doi: 10.1038/ncb1800.

[257] E. Solito, C. De Coupade, L. Parente, R. J. Flower, and F. Russo-Marie, 'Human annexin 1 is highly expressed during the differentiation of the epithelial cell line A 549: Involvement of nuclear factor interleukin 6 in phorbol ester induction of annexin 1', *Cell Growth Differ.*, vol. 9, no. 4, pp. 327–336, Apr. 1998, Accessed: Nov. 26, 2020. [Online]. Available: https://europepmc.org/article/med/9563852.

[258] A. Petrella *et al.*, 'Annexin-1 downregulation in thyroid cancer correlates to the degree of tumor differentiation', *Cancer Biol. Ther.*, vol. 5, no. 6, pp. 643–647, 2006, doi: 10.4161/cbt.5.6.2700.

[259] P. Wong and P. A. Coulombe, 'Loss of keratin 6 (K6) proteins reveals a function for intermediate filaments during wound repair', *J. Cell Biol.*, vol. 163, no. 2, pp. 327–337, Oct. 2003, doi: 10.1083/jcb.200305032.

[260] A. L. Cheng *et al.*, 'Identification of novel nasopharyngeal carcinoma biomarkers by laser capture microdissection and proteomic analysis', *Clin. Cancer Res.*, vol. 14, no. 2, pp. 435–445, Jan. 2008, doi: 10.1158/1078-0432.CCR-07-1215.

[261] G. Yu *et al.*, 'Tissue microarray analysis reveals strong clinical evidence for a close association between loss of annexin A1 expression and nodal metastasis in gastric cancer', *Clin. Exp. Metastasis*, vol. 25, no. 7, pp. 695–702, Nov. 2008, doi: 10.1007/s10585-008-9178-y.

[262] V. Bizzarro *et al.*, 'Role of annexin A1 in mouse myoblast cell differentiation', *J. Cell. Physiol.*, vol. 224, no. 3, pp. 757–765, Sep. 2010, doi: 10.1002/jcp.22178.

[263] A. S. P. Ma and L. J. Ozers, 'Annexins I and II show differences in subcellular localization and differentiation related changes in human epidermal keratinocytes', *Arch. Dermatol. Res.*, vol. 288, no. 10, pp. 596–603, 1996, doi: 10.1007/BF02505262.

[264] N. A. Robinson, S. Lapic, J. F. Welter, and R. L. Eckert, 'S100A11, S100A10, annexin I, desmosomal proteins, small proline-rich proteins, plasminogen activator inhibitor-2, and involucrin are components of the cornified envelope of cultured human epidermal keratinocytes', *J. Biol. Chem.*, vol. 272, no. 18, pp. 12035–12046, May 1997, doi: 10.1074/jbc.272.18.12035.

[265] B. A. Babbin *et al.*, 'Annexin I regulates SKCO-15 cell invasion by signaling through formyl peptide receptors', *J. Biol. Chem.*, vol. 281, no. 28, pp. 19588–19599, Jul. 2006, doi: 10.1074/jbc.M513025200.

[266] F. Rondepierre *et al.*, 'Proteomic studies of B16 lines: Involvement of Annexin A1 in melanoma dissemination', *Biochim. Biophys. Acta - Proteins Proteomics*, vol. 1794, no. 1, pp.

61–69, Jan. 2009, doi: 10.1016/j.bbapap.2008.09.014.

[267] M. Okano *et al.*, 'Upregulated Annexin A1 promotes cellular invasion in triple-negative breast cancer', *Oncol. Rep.*, vol. 33, no. 3, pp. 1064–1070, Mar. 2015, doi: 10.3892/or.2015.3720.

[268] R. Belvedere, V. Bizzarro, G. Forte, F. Dal Piaz, L. Parente, and A. Petrella, 'Annexin A1 contributes to pancreatic cancer cell phenotype, behaviour and metastatic potential independently of Formyl Peptide Receptor pathway', *Sci. Rep.*, vol. 6, Jul. 2016, doi: 10.1038/srep29660.

[269] Y. Fang *et al.*, 'Knockdown of ANXA1 suppresses the biological behavior of human NSCLC cells in vitro', *Mol. Med. Rep.*, vol. 13, no. 5, pp. 3858–3866, May 2016, doi: 10.3892/mmr.2016.5022.

[270] G. Han *et al.*, 'Effect of Annexin A1 gene on the proliferation and invasion of esophageal squamous cell carcinoma cells and its regulatory mechanisms', *Int. J. Mol. Med.*, vol. 39, no. 2, pp. 357–363, Feb. 2017, doi: 10.3892/ijmm.2016.2840.

[271] R. Belvedere, V. Bizzarro, L. Parente, F. Petrella, and A. Petrella, 'The pharmaceutical device prisma® skin promotes in vitro angiogenesis through endothelial to mesenchymal transition during skin wound healing', *Int. J. Mol. Sci.*, vol. 18, no. 8, Aug. 2017, doi: 10.3390/ijms18081614.

[272] R. Belvedere *et al.*, 'Role of intracellular and extracellular annexin A1 in migration and invasion of human pancreatic carcinoma cells', *BMC Cancer*, vol. 14, no. 1, 2014, doi: 10.1186/1471-2407-14-961.

[273] V. Bizzarro *et al.*, 'Annexin A1 N-Terminal Derived Peptide Ac2-26 Stimulates Fibroblast Migration in High Glucose Conditions', *PLoS One*, vol. 7, no. 9, Sep. 2012, doi: 10.1371/journal.pone.0045639.

[274] G. Grynkiewicz, M. Poenie, and R. Tsien, 'A new generation of Ca2+ indicators with greatly improved fluorescence properties - PubMed', *J Biol Chem.*, vol. 260, no. 6, pp. 3440–50, Mar. 1985, Accessed: Dec. 04, 2020. [Online]. Available: https://pubmed.ncbi.nlm.nih.gov/3838314/.

[275] V. Bizzarro, R. Belvedere, V. Migliaro, E. Romano, L. Parente, and A. Petrella, 'Hypoxia regulates ANXA1 expression to support prostate cancer cell invasion and aggressiveness', *Cell Adhes. Migr.*, vol. 11, no. 3, pp. 247–260, May 2017, doi: 10.1080/19336918.2016.1259056.

[276] C. Théry, L. Zitvogel, and S. Amigorena, 'Exosomes: Composition, biogenesis and function', *Nature Reviews Immunology*, vol. 2, no. 8. European Association for Cardio-Thoracic Surgery, pp. 569–579, 2002, doi: 10.1038/nri855.

[277] D. T. Woodley *et al.*, 'Intravenously injected human fibroblasts home to skin wounds, deliver

type VII collagen, and promote wound healing', *Mol. Ther.*, vol. 15, no. 3, pp. 628–635, Mar. 2007, doi: 10.1038/sj.mt.6300041.

[278] G. Caputo, M. Scognamiglio, and I. De Marco, 'Nimesulide adsorbed on silica aerogel using supercritical carbon dioxide', *Chem. Eng. Res. Des.*, vol. 90, no. 8, pp. 1082–1089, Aug. 2012, doi: 10.1016/j.cherd.2011.11.011.

[279] Y. Zhang, D. Kang, M. Aindow, and C. Erkey, 'Preparation and characterization of ruthenium/carbon aerogel nanocomposites via a supercritical fluid route', *J. Phys. Chem. B*, vol. 109, no. 7, pp. 2617–2624, Feb. 2005, doi: 10.1021/jp0467595.

[280] J. Salbach *et al.*, 'Regenerative potential of glycosaminoglycans for skin and bone', *Journal of Molecular Medicine*, vol. 90, no. 6. J Mol Med (Berl), pp. 625–635, Jun. 2012, doi: 10.1007/s00109-011-0843-2.

[281] C. K. Thodeti *et al.*, 'ADAM12/syndecan-4 signaling promotes β1 integrin-dependent cell spreading through protein kinase Cα and RhoA', *J. Biol. Chem.*, vol. 278, no. 11, pp. 9576–9584, Mar. 2003, doi: 10.1074/jbc.M208937200.

[282] T. C. Wikramanayake, O. Stojadinovic, and M. Tomic-Canic, 'Epidermal Differentiation in Barrier Maintenance and Wound Healing', *Adv. Wound Care*, vol. 3, no. 3, pp. 272–280, Mar. 2014, doi: 10.1089/wound.2013.0503.

[283] E. S. Oh, A. Woods, S. T. Lim, A. W. Theibert, and J. R. Couchman, 'Syndecan-4 proteoglycan cytoplasmic domain and phosphatidylinositol 4,5- bisphosphate coordinately regulate protein kinase C activity', *J. Biol. Chem.*, vol. 273, no. 17, pp. 10624–10629, Apr. 1998, doi: 10.1074/jbc.273.17.10624.

[284] C. L. Tu, W. Chang, Z. Xie, and D. D. Bikle, 'Inactivation of the calcium sensing receptor inhibits E-cadherin-mediated cell-cell adhesion and calcium-induced differentiation in human epidermal keratinocytes', *J. Biol. Chem.*, vol. 283, no. 6, pp. 3519–3528, Feb. 2008, doi: 10.1074/jbc.M708318200.

[285] S. Prag *et al.*, 'Activated ezrin promotes cell migration through recruitment of the GEF Dbl to lipid rafts and preferential downstream activation of Cdc42', *Mol. Biol. Cell*, vol. 18, no. 8, pp. 2935–2948, Aug. 2007, doi: 10.1091/mbc.E06-11-1031.

[286] S. Réty *et al.*, 'Structural basis of the Ca2+-dependent association between S100C (S100A11) and its target, the N-terminal part of annexin I', *Structure*, vol. 8, no. 2, pp. 175–184, Feb. 2000, doi: 10.1016/S0969-2126(00)00093-9.

[287] Z. Boudhraa, B. Bouchon, C. Viallard, M. D'Incan, and F. Degoul, 'Annexin A1 localization and its relevance to cancer', *Clin. Sci.*, vol. 130, no. 4, pp. 205–220, 2016, doi: 10.1042/CS20150415.

[288] V. Bizzarro, R. Belvedere, F. Dal Piaz, L. Parente, and A. Petrella, 'Annexin A1 Induces Skeletal Muscle Cell Migration Acting through Formyl Peptide Receptors', *PLoS One*, vol. 7, no. 10, Oct. 2012, doi: 10.1371/journal.pone.0048246.

[289] V. Bizzarro *et al.*, 'Annexin A1 is involved in the acquisition and maintenance of a stem cell-like/aggressive phenotype in prostate cancer cells with acquired resistance to zoledronic acid', *Oncotarget*, vol. 6, no. 28, pp. 25076–25092, 2015, doi: 10.18632/oncotarget.4725.

[290] A. B. G. Lansdown, 'Calcium: A potential central regulator in wound healing in the skin', *Wound Repair and Regeneration*, vol. 10, no. 5. Wound Repair Regen, pp. 271–285, 2002, doi: 10.1046/j.1524-475X.2002.10502.x.

[291] A. Laberge, S. Arif, and V. J. Moulin, 'Microvesicles: Intercellular messengers in cutaneous wound healing', *Journal of Cellular Physiology*, vol. 233, no. 8. Wiley-Liss Inc., pp. 5550–5563, Aug. 01, 2018, doi: 10.1002/jcp.26426.

[292] H. W. Schnaper *et al.*, 'Type IV collagenase(s) and TIMPs modulate endothelial cell morphogenesis in vitro', *J. Cell. Physiol.*, vol. 156, no. 2, pp. 235–246, 1993, doi: 10.1002/jcp.1041560204.

[293] T. Kelly, Y. Huang, A. E. Simms, and A. Mazur, 'Fibroblast Activation Protein-α. A Key Modulator of the Microenvironment in Multiple Pathologies', in *International Review of Cell and Molecular Biology*, vol. 297, Elsevier Inc., 2012, pp. 83–116.

[294] Y. R. Yun *et al.*, 'Fibroblast growth factors: Biology, function, and application for tissue regeneration', *Journal of Tissue Engineering*, vol. 1, no. 1. J Tissue Eng, pp. 1–18, 2010, doi: 10.4061/2010/218142.

[295] S. Ortega, M. Ittmann, S. H. Tsang, M. Ehrlich, and C. Basilico, 'Neuronal defects and delayed wound healing in mice lacking fibroblast growth factor 2', *Proc. Natl. Acad. Sci. U. S. A.*, vol. 95, no. 10, pp. 5672–5677, May 1998, doi: 10.1073/pnas.95.10.5672.

[296] M. G. Lampugnani and E. Dejana, 'Interendothelial junctions: Structure, signalling and functional roles', *Curr. Opin. Cell Biol.*, vol. 9, no. 5, pp. 674–682, Oct. 1997, doi: 10.1016/S0955-0674(97)80121-4.

[297] M. M. Koczorowska *et al.*, 'Fibroblast activation protein-α, a stromal cell surface protease, shapes key features of cancer associated fibroblasts through proteome and degradome alterations', *Mol. Oncol.*, vol. 10, no. 1, pp. 40–58, Jan. 2016, doi: 10.1016/j.molonc.2015.08.001.

[298] G. Bergers and S. Song, 'The role of pericytes in blood-vessel formation and maintenance', *Neuro-Oncology*, vol. 7, no. 4. Neuro Oncol, pp. 452–464, Oct. 2005, doi: 10.1215/S1152851705000232.

[299] Pessolano *et al.*, 'Annexin A1 Contained in Extracellular Vesicles Promotes the Activation of Keratinocytes by Mesoglycan Effects: An Autocrine Loop Through FPRs', *Cells*, vol. 8, no. 7, p. 753, Jul. 2019, doi: 10.3390/cells8070753.

[300] X. Wang, J. Ge, E. E. Tredget, and Y. Wu, 'The mouse excisional wound splinting model, including applications for stem cell transplantation', *Nat. Protoc.*, vol. 8, no. 2, pp. 302–309, Feb. 2013, doi: 10.1038/nprot.2013.002.

[301] N. T. Meier *et al.*, 'Thyrotropin-releasing hormone (TRH) promotes wound re-epithelialisation in frog and human skin.', *PLoS One*, vol. 8, no. 9, 2013, doi: 10.1371/journal.pone.0073596.

[302] M. J. Scanlan *et al.*, 'Molecular cloning of fibroblast activation protein α, a member of the serine protease family selectively expressed in stromal fibroblasts of epithelial cancers', *Proc. Natl. Acad. Sci. U. S. A.*, vol. 91, no. 12, pp. 5657–5661, Jun. 1994, doi: 10.1073/pnas.91.12.5657.

[303] F. Cheng *et al.*, 'Vimentin coordinates fibroblast proliferation and keratinocyte differentiation in wound healing via TGF-β-Slug signaling', *Proc. Natl. Acad. Sci. U. S. A.*, vol. 113, no. 30, pp. E4320–E4327, Jul. 2016, doi: 10.1073/pnas.1519197113.

[304] J. L. Walker *et al.*, 'Unique precursors for the mesenchymal cells involved in injury response and fibrosis', *Proc. Natl. Acad. Sci. U. S. A.*, vol. 107, no. 31, pp. 13730–13735, Aug. 2010, doi: 10.1073/pnas.0910382107.

[305] B. M. Bleaken, A. S. Menko, and J. L. Walker, 'Cells activated for wound repair have the potential to direct collective invasion of an epithelium', *Mol. Biol. Cell*, vol. 27, no. 3, pp. 451–465, Feb. 2016, doi: 10.1091/mbc.E15-09-0615.

[306] M. Lindgren, M. Unosson, M. Fredrikson, and A. C. Ek, 'Immobility - A major risk factor for development of pressure ulcers among adult hospitalized patients: A prospective study', *Scand. J. Caring Sci.*, vol. 18, no. 1, pp. 57–64, Mar. 2004, doi: 10.1046/j.0283-9318.2003.00250.x.

[307] A. Rego, 'Pressure ulcers or moisture lesions: The theatre perspective', *Journal of Perioperative Practice*, vol. 26, no. 4. Association for Perioperative Practice, pp. 84–89, Apr. 01, 2016, doi: 10.1177/175045891602600405.

[308] S. Bhattacharya and R. Mishra, 'Pressure ulcers: Current understanding and newer modalities of treatment', *Indian Journal of Plastic Surgery*, vol. 48, no. 1. Medknow Publications, pp. 4–16, Jan. 01, 2015, doi: 10.4103/0970-0358.155260.

[309] J. S. Boateng, K. H. Matthews, H. N. E. Stevens, and G. M. Eccleston, 'Wound healing dressings and drug delivery systems: A review', *Journal of Pharmaceutical Sciences*, vol. 97, no. 8. John Wiley and Sons Inc., pp. 2892–2923, 2008, doi: 10.1002/jps.21210.

[310] G. Tkalec, M. Pantić, Z. Novak, and Ž. Knez, 'Supercritical impregnation of drugs and supercritical fluid deposition of metals into aerogels', *Journal of Materials Science*, vol. 50, no. 1. Kluwer Academic Publishers, pp. 1–12, Oct. 02, 2015, doi: 10.1007/s10853-014-8626-0.

[311] M. Ramos-E-Silva and M. C. Ribeiro de Castro, 'New dressings, including tissue-engineered living skin', *Clin. Dermatol.*, vol. 20, no. 6, pp. 715–723, 2002, doi: 10.1016/S0738-081X(02)00298-5.

[312] E. A. O'Toole, 'Extracellular matrix and keratinocyte migration', *Clinical and Experimental Dermatology*, vol. 26, no. 6. Clin Exp Dermatol, pp. 525–530, 2001, doi: 10.1046/j.1365-2230.2001.00891.x.

[313] F. M. Watt and H. Fujiwara, 'Cell-extracellular matrix interactions in normal and diseased skin', *Cold Spring Harb. Perspect. Biol.*, vol. 3, no. 4, pp. 1–14, 2011, doi: 10.1101/cshperspect.a005124.

[314] I. Kovalszky, A. Hjerpe, and K. Dobra, 'Nuclear translocation of heparan sulfate proteoglycans and their functional significance', *Biochimica et Biophysica Acta - General Subjects*, vol. 1840, no. 8. Elsevier, pp. 2491–2497, 2014, doi: 10.1016/j.bbagen.2014.04.015.

[315] T. Ng *et al.*, 'Ezrin is a downstream effector of trafficking PKC-integrin complexes involved in the control of cell motility', *EMBO J.*, vol. 20, no. 11, pp. 2723–2741, Jun. 2001, doi: 10.1093/emboj/20.11.2723.

[316] A. Woods and J. R. Couchman, 'Syndecan-4 and focal adhesion function', *Current Opinion in Cell Biology*, vol. 13, no. 5. Curr Opin Cell Biol, pp. 578–583, 2001, doi: 10.1016/S0955-0674(00)00254-4.

[317] A. B. G. Lansdown, 'Calcium: A potential central regulator in wound healing in the skin', *Wound Repair and Regeneration*, vol. 10, no. 5. Wound Repair Regen, pp. 271–285, 2002, doi: 10.1046/j.1524-475X.2002.10502.x.

[318] D. W. Owens, V. G. Brunton, E. K. Parkinson, and M. C. Frame, 'E-cadherin at the cell periphery is a determinant of keratinocyte differentiation in vitro', *Biochem. Biophys. Res. Commun.*, vol. 269, no. 2, pp. 369–376, Mar. 2000, doi: 10.1006/bbrc.2000.2292.

[319] S. E. Moss and R. O. Morgan, 'The annexins', *Genome Biology*, vol. 5, no. 4. Genome Biol, 2004, doi: 10.1186/gb-2004-5-4-219.

[320] M. Sakaguchi and N. H. Huh, 'S100A11, a dual growth regulator of epidermal keratinocytes', *Amino Acids*, vol. 41, no. 4. Amino Acids, pp. 797–807, Oct. 2011, doi: 10.1007/s00726-010-0747-4.

[321] A. M. Broome and R. L. Eckert, 'Microtubule-Dependent Redistribution of a Cytoplasmic

Cornified Envelope Precursor', *J. Invest. Dermatol.*, vol. 122, no. 1, pp. 29–38, Jan. 2004, doi: 10.1046/j.0022-202X.2003.22105.x.

[322] T. Horlacher *et al.*, 'Characterization of annexin A1 glycan binding reveals binding to highly sulfated glycans with preference for highly sulfated heparan sulfate and heparin', *Biochemistry*, vol. 50, no. 13, pp. 2650–2659, Apr. 2011, doi: 10.1021/bi101121a.

[323] V. Bizzarro *et al.*, 'Mesoglycan induces keratinocyte activation by triggering syndecan-4 pathway and the formation of the annexin A1/S100A11 complex', *J. Cell. Physiol.*, vol. 234, no. 11, pp. 20174–20192, Nov. 2019, doi: 10.1002/jcp.28618.

[324] M. Perretti, 'The annexin 1 receptor(s): Is the plot unravelling?', *Trends in Pharmacological Sciences*, vol. 24, no. 11. Elsevier Ltd, pp. 574–579, 2003, doi: 10.1016/j.tips.2003.09.010.

[325] N. Yu *et al.*, 'Serum amyloid A, an acute phase protein, stimulates proliferative and proinflammatory responses of keratinocytes', *Cell Prolif.*, vol. 50, no. 3, Jun. 2017, doi: 10.1111/cpr.12320.

[326] G. Leoni and A. Nusrat, 'Annexin A1: Shifting the balance towards resolution and repair', *Biological Chemistry*, vol. 397, no. 10. Walter de Gruyter GmbH, pp. 971–979, Oct. 01, 2016, doi: 10.1515/hsz-2016-0180.

[327] G. Leoni *et al.*, 'Annexin A1, formyl peptide receptor, and NOX1 orchestrate epithelial repair', *J. Clin. Invest.*, vol. 123, no. 1, pp. 443–454, Jan. 2013, doi: 10.1172/JCI65831.

[328] P. Del Gaudio *et al.*, 'Evaluation of in situ injectable hydrogels as controlled release device for ANXA1 derived peptide in wound healing', *Carbohydr. Polym.*, vol. 115, pp. 629–633, Jan. 2015, doi: 10.1016/j.carbpol.2014.09.040.

[329] A. Walther, K. Riehemann, and V. Gerke, 'A novel ligand of the formyl peptide receptor: Annexin I regulates neutrophil extravasation by interacting with FPR', *Mol. Cell*, vol. 5, no. 5, pp. 831–840, 2000, doi: 10.1016/S1097-2765(00)80323-8.

[330] M. Perretti *et al.*, 'Endogenous lipid- and peptide-derived anti-inflammatory pathways generated with glucocorticoid and aspirin treatment activate the lipoxin A4 receptor', *Nat. Med.*, vol. 8, no. 11, pp. 1296–1302, Nov. 2002, doi: 10.1038/nm786.

[331] M. Mittelbrunn and F. Sánchez-Madrid, 'Intercellular communication: Diverse structures for exchange of genetic information', *Nature Reviews Molecular Cell Biology*, vol. 13, no. 5. Nature Publishing Group, pp. 328–335, May 18, 2012, doi: 10.1038/nrm3335.

[332] S. A. Eming, B. Brachvogel, T. Odorisio, and M. Koch, 'Regulation of angiogenesis: Wound healing as a model', *Prog. Histochem. Cytochem.*, vol. 42, no. 3, pp. 115–170, Dec. 2007, doi: 10.1016/j.proghi.2007.06.001.

[333] T. Twardowski, A. Fertala, J. Orgel, and J. San Antonio, 'Type I Collagen and Collagen

Mimetics as Angiogenesis Promoting Superpolymers', *Curr. Pharm. Des.*, vol. 13, no. 35, pp. 3608–3621, Nov. 2007, doi: 10.2174/138161207782794176.

[334] R. F. Nicosia, E. Bonanno, and M. Smith, 'Fibronectin promotes the elongation of microvessels during angiogenesis in vitro', *J. Cell. Physiol.*, vol. 154, no. 3, pp. 654–661, Mar. 1993, doi: 10.1002/jcp.1041540325.

[335] D. Vestweber, 'VE-cadherin: The major endothelial adhesion molecule controlling cellular junctions and blood vessel formation', *Arteriosclerosis, Thrombosis, and Vascular Biology*, vol. 28, no. 2. Arterioscler Thromb Vasc Biol, pp. 223–232, Feb. 2008, doi: 10.1161/ATVBAHA.107.158014.

[336] X. Lu, J. Dunn, A. M. Dickinson, J. I. Gillespie, and S. V. Baudouin, 'Smooth muscle α-actin expression in endothelial cells derived from CD34+ human cord blood cells', *Stem Cells Dev.*, vol. 13, no. 5, pp. 521–527, Oct. 2004, doi: 10.1089/scd.2004.13.521.

[337] S. Cébe-Suarez, A. Zehnder-Fjällman, and K. Ballmer-Hofer, 'The role of VEGF receptors in angiogenesis; complex partnerships', *Cellular and Molecular Life Sciences*, vol. 63, no. 5. Cell Mol Life Sci, pp. 601–615, Mar. 2006, doi: 10.1007/s00018-005-5426-3.

[338] V. W. Wong, M. Sorkin, J. P. Glotzbach, and G. C. Longaker, Michael T. Gurtner, 'Surgical approaches to create murine models of human wound healing', *Journal of Biomedicine and Biotechnology*, vol. 2011. J Biomed Biotechnol, 2011, doi: 10.1155/2011/969618.

[339] N. N. Nissen, R. Shankar, R. L. Gamelli, A. Singh, and L. A. Dipietro, 'Heparin and heparan sulphate protect basic fibroblast growth factor from non-enzymic glycosylation', *Biochem. J.*, vol. 338, no. 3, pp. 637–642, Mar. 1999, doi: 10.1042/0264-6021:3380637.

[340] L. Pellegrini, D. F. Burke, F. Von Delft, B. Mulloy, and T. L. Blundell, 'Crystal structure of fibroblast growth factor receptor ectodomain bound to ligand and heparin', *Nature*, vol. 407, no. 6807, pp. 1029–1034, Oct. 2000, doi: 10.1038/35039551.

[341] A. Rai, S. Senapati, S. K. Saraf, and P. Maiti, 'Biodegradable poly(ϵ-caprolactone) as a controlled drug delivery vehicle of vancomycin for the treatment of MRSA infection', *J. Mater. Chem. B*, vol. 4, no. 30, pp. 5151–5160, Jul. 2016, doi: 10.1039/c6tb01623e.

[342] M. V. Natu *et al.*, 'A poly(ε-caprolactone) device for sustained release of an anti-glaucoma drug', *Biomed. Mater.*, vol. 6, no. 2, 2011, doi: 10.1088/1748-6041/6/2/025003.

[343] L. Bullough, S. Johnson, and R. Forder, 'Evaluation of a foam dressing for acute and chronic wound exudate management', *Br. J. Community Nurs.*, vol. 20, pp. S17–S24, Sep. 2015, doi: 10.12968/bjcn.2015.20.Sup9.S17.

[344] R. Campardelli, P. Franco, E. Reverchon, and I. De Marco, 'Polycaprolactone/nimesulide patches obtained by a one-step supercritical foaming + impregnation process', *J. Supercrit.*

Fluids, vol. 146, pp. 47–54, Apr. 2019, doi: 10.1016/j.supflu.2019.01.008.